Lithospheric structure of the western Betic Cordillera and its foreland: implications in the recent tectonic evolution

ANA RUIZ CONSTÁN

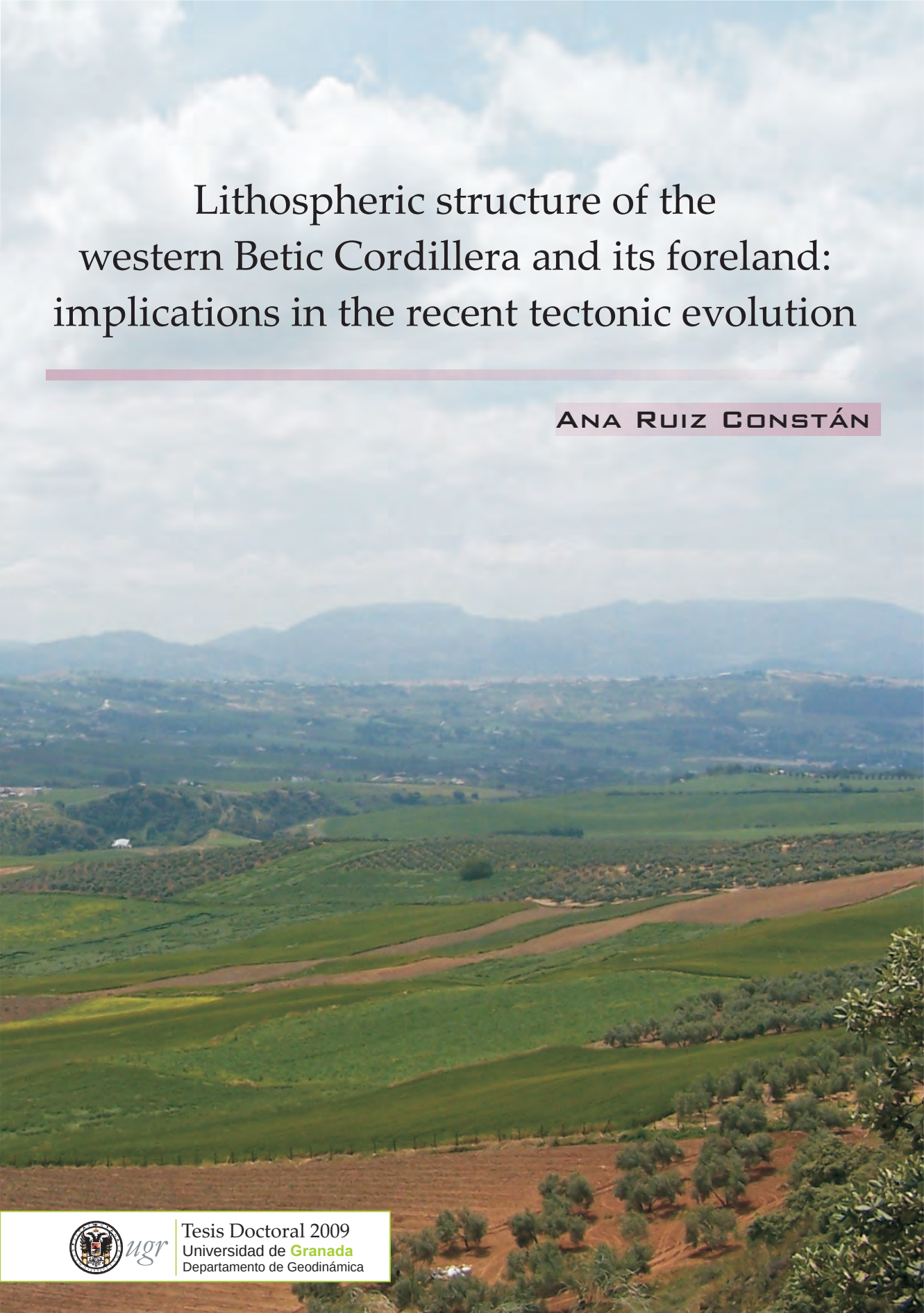

Tesis Doctoral 2009
Universidad de Granada
Departamento de Geodinámica

Departamento de Geodinámica
Universidad de Granada

Universidad de Granada

Jesús Galindo Zaldívar, Catedrático de Geodinámica Interna de la Universidad de Granada.

HACE CONSTAR:

Que la presente memoria titulada **"Lithospheric structure of the western Betic Cordillera and its foreland: implications in the recent tectonic evolution"** ha sido realizada bajo mi dirección por Ana Ruiz Constán y cumple las suficientes condiciones para que su autora pueda optar al grado de Doctor en Ciencias Geológicas.

Granada, Noviembre 2009

Vº Bº del Director

Fdo. Jesús Galindo Zaldívar **Fdo. Ana Ruiz Constán**

Pisé las piedras,
las modelé con sol
y con tristeza. Supe
que había allí un secreto
de paz, un corazón
latiendo para mí.

José Hierro

A Náussica y Migue

NOTA: *Las erratas son las últimas en abandonar el barco. Si encuentras alguna, sáltala.*

AGRADECIMIENTOS:

Este trabajo ha sido posible gracias a una beca de Formación de Profesorado Universitario concedida por el Ministerio de Educación y Ciencia, a los medios materiales del Grupo de investigación RNM-149 y del Departamento de Geodinámica de la Universidad de Granada y a los proyectos TOPO-IBERIA CONSOLIDER-INGENIO CICYT BTE2003-01699, CSD2006-00041 y CGL 2006-06001.

Además, me gustaría aprovechar estas líneas para expresar mi gratitud a todas las personas que, de una forma u otra, han contribuido a la realización de esta Tesis.

En primer lugar, dar las gracias a Jesús Galindo por su disponibilidad, orientación, apoyo y ánimo siempre que han sido necesarios. Es un privilegio poder trabajar con él, tanto a nivel personal como científico.

A los compañeros del Departamento de Geodinámica por sus ánimos y ayuda. En especial a Paco Lodeiro, Fernando Simancas y Manuel López Chicano por su buena disposición que siempre me ha facilitado el trabajo.

A todos los investigadores con los que he tenido la suerte de trabajar y compartir salidas de campo: Carlos Sanz, Ángel Carlos, Jose Miguel Azañón, Curro, Daniel Stich, Pepe Morales, Wiebke Heise y Fernando Monteiro Santos.

A Jorge Arzate, que se equivocó de lugar para pasar su año sabático. Su dominio de la azada, conocimiento del método y su conversación amena facilitaron la adquisición de gran parte de los datos que aquí se presentan.

A Jaume Pous, por su disponibilidad a la hora de resolver mis numerosas dudas sobre el método magnetotelúrico y su ayuda en la adquisición.

A Carlos Marín y Eva Asensio por su ayuda en la adquisición de los datos magnetotelúricos.

A Dickson Cunningham y a los miembros del Departamento de Geología de la Universidad de Leicester (Reino Unido) por su estupenda acogida. En especial, a Jawad que sin conocerme, prácticamente me adoptó.

A Emanuele Tondi y Luigi Piccardi por mostrarme la geología de los Apeninos centrales.

A los dueños y trabajadores de las fincas de Cádiz, Córdoba, Málaga y Sevilla en las que he instalado los equipos, así como a los Guardas de los Parques Naturales de Sierra de las Nieves, Sierra Norte de Sevilla y Hornachuelos, por su buena disposición e interés.

A Nemesio Heredia, porque con su buen humor y sus innumerables historias contribuyó a hacer de la primera campaña antártica una experiencia inolvidable.

A Jean Sanders, por su ayuda en la revisión y mejora del manuscrito en inglés.

A mis compañeros de la becariera de Geodinámica, es una suerte poder trabajar rodeada de amigos: A Pedro, porque gracias a él empecé este camino que también él pronto culminará. A Vicente, por su ánimo indestructible y por aguantarme durante la maquetación de esta tesis, gracias. A Silvia, la alegría de la becariera. A Carlos, motrileño adoptivo al que ya se le ha contagiado el carácter socarrón. A Farida, agradable compañía de las jornadas de campo y a Fermín, compañero de los primeros años ahora en tierras lejanas. Además, a todos los becarios "vecinos" con los que siempre es estupendo cruzarse (Marta, Pili, Jose Alberto, Chema, Vero, Ana Luque, Annika, Maja, Jose María, Idael, Iñaki, ...) y a los no becarios (Antonio Acosta, Patricia Ruano y Paco Lobo).

Quiero mencionar especialmente a mi amigo Antonio Pedrera, inmejorable compañía durante estos cuatro años, ha sido un placer compartir este trayecto con él.

A mis amigos no relacionados con la investigación, por estar siempre ahí: Ángela, Elo, Alberto, Francisco, Esther, María, Vane, Gloria, Pepi, Bego y Rafa, entre otros. Especialmente a Bea, a la que espero tener siempre cerca.

A mi familia, por su cariño y su comprensión. A mi madre, por estar siempre, incluso cuando aún no se lo he pedido. A mi padre, por contagiarme su pasión por los libros; a Dari, siempre pendiente de lo que le hace falta a "la niña"; a la abuela Carmen, por animarme a seguir los estudios que ella no pudo terminar; y a Marita, por su cariño y estupendos guisos.

Finalmente, a Miguel, porque a su lado la vida es fácil.

Abstract

The western Betic Cordillera is a region of great interest for recent tectonic studies due to its location in the westernmost part of the Gibraltar Arc, a key area for understanding the evolution of the westernmost Mediterranean in the framework of Eurasian-African plate interaction. This study surrounds the analysis of two complete transects crossing the main geological domains (from the Internal Zones, across the External Zones and the Guadalquivir Basin, up to the Iberian Massif foreland) together with additional detailed research of the mountain front (Morón de la Frontera-Puebla de Cazalla area), the largest intramontane outcrop of neogene sediments (Ronda Basin), and other seismogenic regions (Malaga intermediate seismicity and Cañete la Real area).

Geological and geophysical research efforts have been combined to determine the geometry of lithospheric structures and their recent activity. Long-period magnetotelluric results provide the first electrical anisotropy data of the western Mediterranean mantle. Geoelectrical analysis of the uppermost mantle establishes nearly orthogonal strikes below the Betic Cordillera (N-S) and the Iberian Massif (E-W). However, at deeper mantle levels, the strike remains constant in a N-S direction for all the stations in both geological domains.

Broadband magnetotelluric data afford additional constraints to the lithospheric structure. The crustal resistivity image reveals a deep conductive southward dipping body at midcrustal levels beneath the southern part of the profile. The shape of the body points to a continuation of the continental Iberian Massif crust below the western Betic Cordillera and its prolongation below the northern Alborán Sea, as supported by gravity data and seismicity distribution.

Furthermore, analysis of the earthquake focal mechanisms provides information about the present day stress in the area and its relation to the main structures, which may be complemented by the study of brittle deformations. There is a regional NW-SE maximum compressional stress field, with variable plunge due to the locally dominant structures: northwestward in deeper levels of mountain front, then becoming southeastward along the intermediate seismogenic zone of the Alborán Sea, parallel to the continental subducting slab. Earthquake thrust fault focal mechanisms evidence that the northwesternmost mountain front is the only one to remain active in the arched Betic Cordillera, owing to its favourable orientation with respect to the present-day convergence of the Eurasian-African plates. The active tectonic structures are partitioned, thus indicating NW-SE oriented compression and thrusting at depth, extension at surface, and the presence of transfer faults with opposite kinematics at the northeastern boundary. They produce local perturbation of the stress field in terms of NE-SW compression or apparently inconsistent NNE-SSW and WNW-ESE

compressions associated with NW-SE oriented transfer faults.

In this context, the Neogene Ronda basin underwent recent uplift and northwestward transport and may represent a piggy-back basin. The basin was slightly deformed since the Late Miocene by folds with nearly orthogonal axes, no dominant vergence and box geometries, related to the location of plastic low-density Triassic rocks.

Although many geodynamic models have been proposed for the recent evolution of this region, the new data gathered together here would seem to favour the presence of an eastward dipping subduction zone-rollback model occurring during the Early-Middle Miocene evolution of the Betic-Rif-Alborán area. At present, deformation at mountain front propagates southwards up to the continental subducting slab in the Alborán Sea, which may represent the last active remaining segment of the inherited Miocene subduction.

Resumen

La Cordillera Bética occidental es una región de gran interés para los estudios de tectónica reciente, ya que se sitúa en la parte noroccidental del Arco de Gibraltar, y permite comprender la evolución del Mediterráneo occidental en el marco de la interacción entre las placas Euroasiática y Africana. Se han estudiado dos transversales completas que atraviesan los principales dominios geológicos, desde las Zonas Internas, a través de las Zonas Externas, Cuenca del Guadalquivir y hasta el Macizo Ibérico. Se han analizado en detalle algunos sectores: el frente montañoso (Morón de la Frontera-Puebla de Cazalla), la mayor cuenca Neógena intramontañosa (Cuenca de Ronda) y otras zonas sismogénicas (Cañete la Real y zona de sismicidad intermedia de Málaga).

Con la finalidad de determinar la geometría de las estructuras litosféricas y su actividad reciente se han combinado distintas técnicas geológicas y geofísicas. Los resultados obtenidos a partir de los sondeos magnetotelúricos de largo periodo proporcionan la primera información acerca de las direcciones de anisotropía eléctrica del manto en el Mediterráneo occidental. La parte superior del manto litosférico está caracterizada por direcciones casi ortogonales bajo la Cordillera Bética (N-S) y el Macizo Ibérico (E-O). Sin embargo, a niveles más profundos del manto, el strike permanece constante en una dirección N-S para todas las estaciones de ambos dominios geológicos.

Los datos proporcionados por los sondeos magnetotelúricos de banda ancha permiten precisar la estructura litosférica. La imagen de resistividad de la corteza revela la existencia de un cuerpo conductor que buza hacia el SE, a niveles medios de la corteza, bajo la parte sur del perfil. La forma del cuerpo refleja la continuación de la corteza continental del Macizo Ibérico bajo la Cordillera Bética occidental y su prolongación bajo el Mar de Alborán. Esta geometría también está sustentada por datos gravimétricos y de distribución de la sismicidad.

Además, el análisis de mecanismos focales de terremotos, que proporciona información sobre los esfuerzos actuales en el área, ha sido complementado mediante el estudio geológico de campo de las deformaciones frágiles. Se ha determinado un esfuerzo compresivo NO-SE, con inclinación variable, condicionado por las estructuras locales dominantes: hacia el NO bajo el frente montañoso y hacia el SE en la zona de sismicidad intermedia del Mar de Alborán, paralelo al buzamiento de la laja que subduce. Los mecanismos focales de falla inversa evidencian que el frente montañoso noroccidental es el único que permanece activo en la Cordillera Bética,

debido a su orientación favorable respecto a la convergencia actual de las placas Euroasiática y Africana. Las estructuras tectónicas activas indican una partición de la deformación, con compresión NO-SE y cabalgamientos en profundidad, extensión en superficie y la existencia de fallas de transferencia con cinemáticas opuestas en el borde NE de la cuña. Esto produce perturbaciones locales con compresiones NE-SO y compresiones aparentemente inconsistentes (NNE-SSO y ONO-ESE) asociadas a fallas de transferencia NO-SE.

En este contexto, la cuenca neógena de Ronda se elevó y fue transportada hacia el NO como una cuenca de tipo *piggy-back*. Desde el Mioceno superior, la cuenca ha sido ligeramente deformada mediante pliegues con ejes casi ortogonales, sin vergencia definida y geometrías en caja, relacionados con la acumulación de rocas triásicas de comportamiento plástico y baja densidad.

Aunque se han propuesto diferentes modelos geodinámicos para explicar la evolución reciente de la Cordillera Bético-Rifeña y Mar de Alborán, los nuevos datos parecen favorecer los modelos de subducción hacia el E con *rollback* durante el Mioceno inferior-medio. En la actualidad, la deformación en el frente montañoso está localizada en el segmento noroccidental del Arco de Gibraltar y se propaga hacia el sur, bajo el Mar de Alborán, mediante la zona de subducción continental, que representa el único segmento activo heredado de la subducción miocena.

PART I

PART II

PART I

1

Introduction

The Betic-Rif Cordillera, located at the western end of the Mediterranean Sea (Fig. 1-1), forms an arc-shaped mountain belt that surrounds the Alborán Sea. This orogen formed since the Neogene in a general setting of Eurasian-African NW-SE (Dewey et al., 1989; Rosenbaum et al., 2002) plate convergence comprising a wide area of oblique convergence with distributed deformation. The Iberian Massif, the stable foreland of the Betic Cordillera, crops out northwards and forms part of the Variscan belt of central Europe that resulted from the late Paleozoic collision of Gondwana and Laurasia.

The Gibraltar Arc region, comprising the Betic-Rif Cordillera and the Alborán Basin, has undergone a polyphasic evolution with successive compressional and extensional deformations, some of them simultaneous. Geological and geophysical data acquired in the past years have been focused on elucidating the mechanisms responsible for the orogen´s tectonic evolution, provoking much controversy among

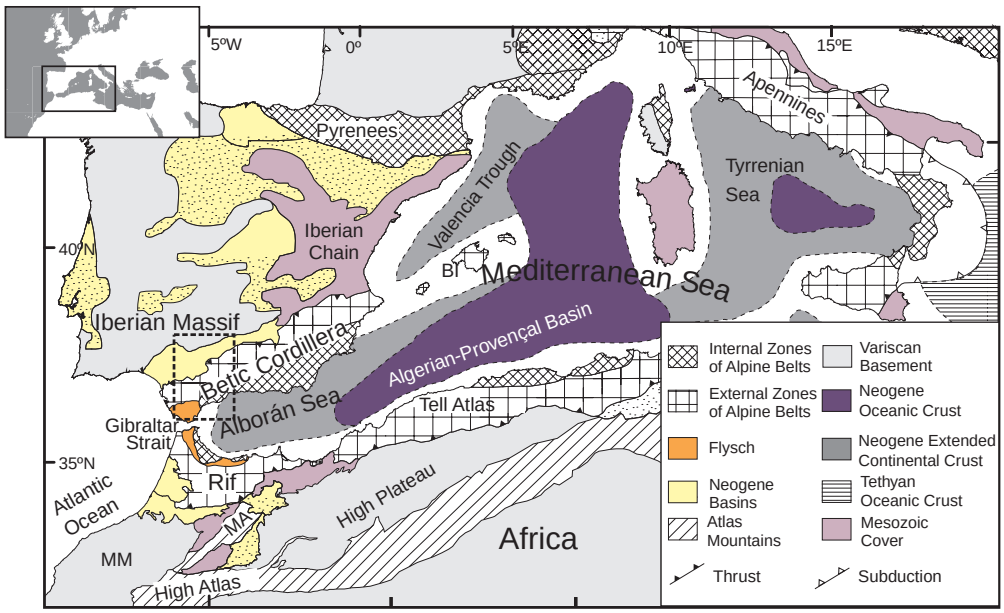

Figure 1-1. *Map showing the principal tectonic features of the western Mediterranean Sea (modified from Calvert et al., 2000b); MM: Moroccan Meseta; MA: Middle Atlas. The study area is marked.*

Earth researchers. Two main hypotheses have been proposed: models associated with detachment and/or delamination of subcontinental lithosphere beneath the Alborán Sea; and models involving subduction associated with slab roll-back and/or detachment of the subducted slab.

This Ph. D. Thesis presents new geological and geophysical data on the western sector of the Betic Cordillera and the southern outcrops of the SW Iberian Massif, which constitute a key area for determining the recent evolution of the Gibraltar Arc. The study surrounds the analysis of two complete transects crossing the main geological domains and additional detailed research in key sectors. New magnetotelluric and gravity data together with seismicity distribution provide additional constraints for the lithospheric structure. In addition, the analysis of earthquake focal mechanisms (from the shallow seismicity of Morón de la Frontera/Cañete la Real area up to the intermediate seismicity at the Málaga coast, Fig. 1-2) provides information about the present day stress state in the area and its relation to the outcropping structures. Finally, the research looks into the recent and active geological structures located at the western mountain front of the Betic Cordillera (Morón de la Frontera-Puebla de Cazalla area) and the Ronda Basin, constituting the largest intramontane outcrop of neogene sediments.

1.1. Geographical setting

The study area is located in the southern Iberian Peninsula (Fig. 1-2a) and focuses on two complete transects running from the Málaga coast, crossing the Guadalquivir Basin, up to the Iberian Massif (Sierra Morena). In addition, detailed studies are developed in three sectors crossed by the transects (Fig. 1-2b).

The first transect (from San Pedro de Alcántara to the south and Castilblanco de los Arroyos in the north) extends inside the coordinates 6-5º W longitude and 37.40-36.30º N latitude, crossing the provinces of Málaga, Cádiz and Sevilla with an approximate NW-SE trend. The second transect (from Coin in the southern end to Fuente Obejuna in the northern extremity) is located to the east of the first, between the coordinates longitude 5.25-4.45º W and latitude 38.15- 36.35º N; it roughly runs NNW-SSE through the provinces of Málaga, Sevilla and Córdoba.

Other key sectors have been studied in detail in order to analyse the lateral extension of main structures evidenced along the transects of the Cordillera. The Ronda Depression is the most important Neogene sedimentary basin in western Betics and is placed to the north of the Sierra de las Nieves. The Cañete la Real area is contiguous to the Ronda Basin and also lies northward of the Sierra de las Nieves. Finally, the Morón de la Frontera-Puebla de Cazalla area is situated at the northwesternmost reliefs of the Betic Cordillera, at the boundary with the Guadalquivir Basin.

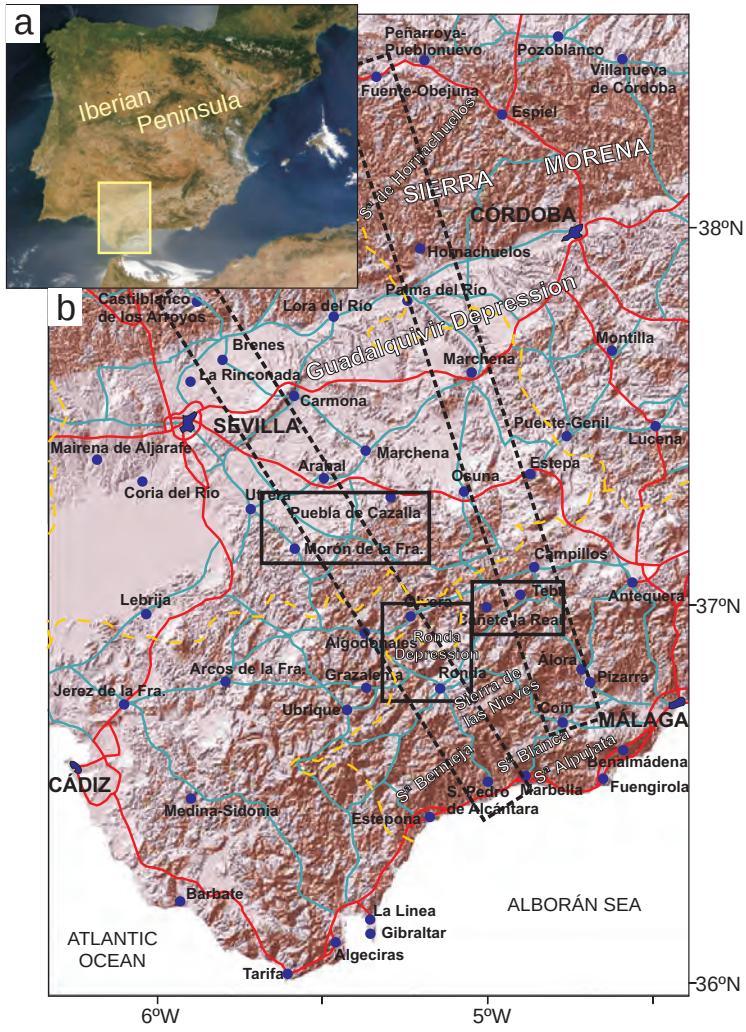

Figure 1-2. *Geographical setting of the study area:* **a)** *The study area is located in the Southern part of the Iberian Peninsula;* **b)** *Detailed geographical location of the main study transects (dashed black lines), and sectors (black solid lines) including access roads from major villages (red and blue lines), province boundaries (in yellow) and main geographical features (white).*

1.2. Geological setting

The Betic-Rif Cordillera is formed by the relative motion of the Eurasian and African plates. It is located between the Iberian Massif —which represents the South Iberian paleomargin— and the Moroccan Meseta and Middle Atlas, corresponding to the African paleomargin. The Betic Cordillera is the northern branch of the arcuate orogen that continues through the Gibraltar Strait in the Rif Cordillera (Fig. 1-3). The

Alborán Sea Neogene extensional basin is located at present at the inner part of this orogen. The development of this structure on the Eurasian–African plate boundary is a consequence of the westward displacement of the Internal Zones (Alborán Domain) due to the progressive opening of the Algero-Balearic Basin during the Oligocene and Early Miocene (Dewey et al., 1989; Rosenbaum et al., 2004), which rotated and deformed the External Zones (South Iberian Domain) and the Flysch.

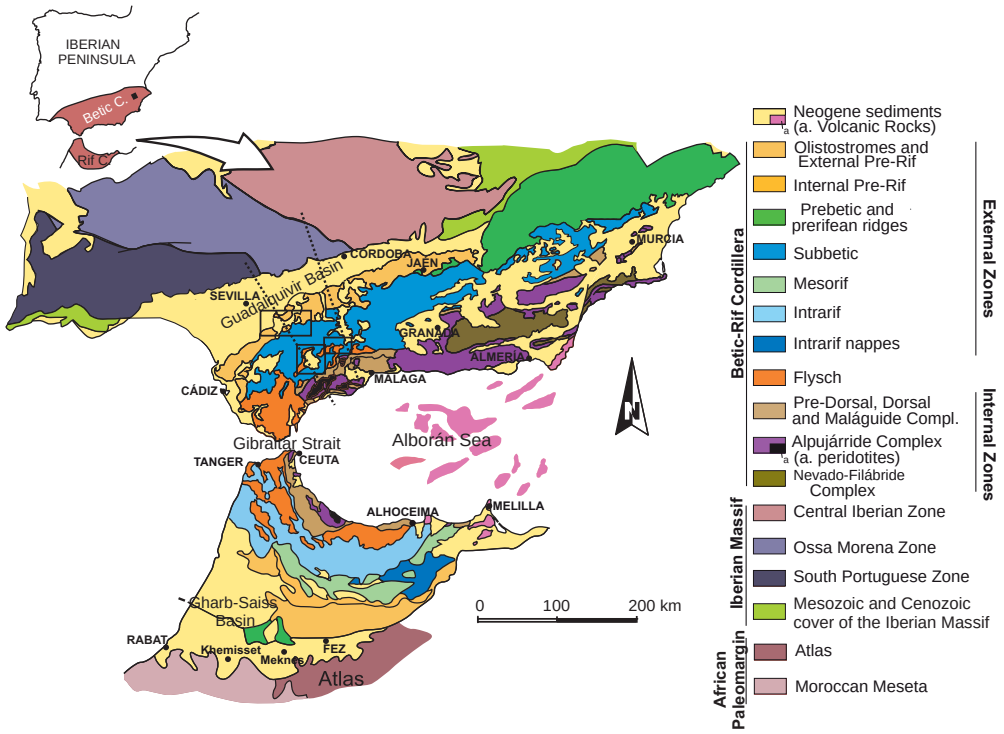

Figure 1-3. *Geological map of the Betic-Rif Cordillera and the SW Iberian Massif (modified from Ruano, 2003 and Pedrera, 2009). The study area is marked in the western Betic Cordillera.*

The great extension and complexity of the study area has led very numerous authors to get involved in studies of the geological and geophysical features of the region. In the next section, I describe some of the most relevant geological studies and previous geophysical data. Due to the huge area analyzed, this section cannot aspire to be an exhaustive revision, but simply expound the most relevant previous findings in relation to the new data presented in this Ph. D. Thesis.

1.2.1. Iberian Massif

The Iberian Massif is the most extensive outcrop in westernmost Europe of the Variscan belt that resulted from the Late Paleozoic collision of Gondwana and Laurasia.

Its division into several zones based on stratigraphic, structural, metamorphic, and magmatic criteria was first accomplished by Lotze, 1945. Nowadays, the main features of this division are still acceptable, though with several modifications (Julivert et al., 1974; Farias et al., 1987). The six zones from north to south are (Fig. 1-4a): Cantabrian, West Asturian-Leonese, Galicia-Tras-Os Montes, Central Iberian, Ossa-Morena and the South Portuguese Zone. In the study area —the SW part of the Iberian Massif— only three of these zones separated by suture-type contacts crop out: the South Portuguese Zone (SPZ), the Ossa Morena Zone (OMZ), and the Central Iberian Zone (CIZ).

The general structural vergence of the three tectonic complexes is to the SW (Fig. 1-4b). The SPZ, the southernmost outcrop of the Iberian Massif, is a foreland with Devonian and Carboniferous rocks affected by folds and thrusts (Oliveira, 1990). The Ossa Morena Zone and the CIZ constitute the internal zones of the orogen and are made up of Precambrian to Devonian preorogenic rocks affected by Late Palaeozoic metamorphism and ductile deformation (Simancas et al., 2001). Both boundaries of the OMZ continental block are interpreted as sutures corresponding to oceanic domains (Simancas et al., 2002). The SPZ/OMZ contact is held to be a suture of the Variscan orogen due to the existence of basic igneous rocks with oceanic affinity, namely the Beja-Acebuches amphibolites (Bard, 1977; Dupuy et al., 1979; Munhá, 1986) and

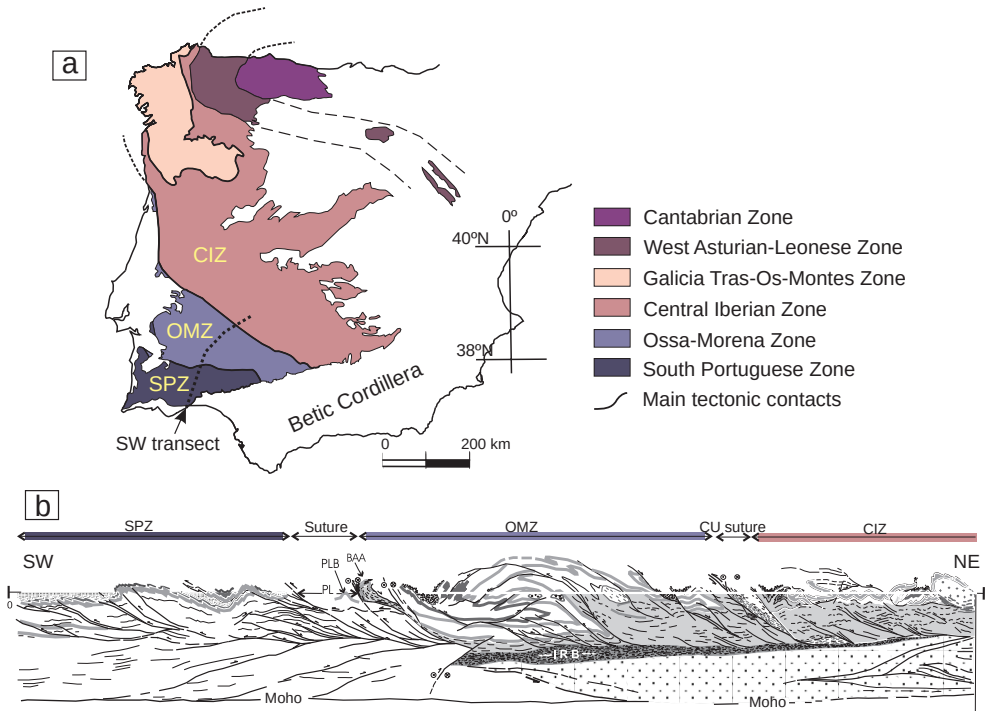

Figure 1-4. a) *Zones and sutures of the Iberian Massif;* **b)** *Crustal architecture of Southwest Iberia (modified from Simancas et al., 2003).*

the basalts included in the Pulo do Lobo Unit (Munhá, 1983). Additional important features of this contact are the lack of high pressure rocks (Bard, 1977) and the constant tectonic vergence to the SW at both sides of the contact (Crespo-Blanc and Orozco, 1991). The suture condition of the OMZ/CIZ contact, forming a wide deformation zone called Central Unit, was based on its metamorphic and tectonic evolution (Burg et al., 1981; Matte, 1986; Azor et al., 1994; Azor et al., 2003). This is further supported by the change in structural vergence (Simancas et al., 2001) and by the stratigraphic and palaeontological differences between the sequences to the NE and to the SW of this boundary (Robardet, 1976; Robardet and Gutiérrez Marco, 1990). The sediments of the Neogene Guadalquivir foreland Basin, to the south, unconformably overlie the Iberian Massif metamorphic complexes.

1.2.2. Betic Cordillera

In this section, the tectonic complexes that crop out in the western transect of the Betic Cordillera are broadly described (Fig. 1-5), including External Zones, Flysch and Internal Zones.

A) External Zones (South Iberian Domain)

The External Zones constitute the deformed cover of the South Iberian paleomargin. They are made up of sedimentary non-metamorphosed rocks, the Late Triassic being represented by claystones with gypsum and fine-grained sandstones (Keuper facies), and the Jurassic to Neogene sequences by carbonate rocks. The different paleogeographic units were deformed during intracontinental collision in the Miocene, forming a thin-skinned fold-and-thrust belt (Sanz de Galdeano and Vera, 1992; Lonergan and White, 1997). From the earliest studies (Blumenthal, 1927; Fallot, 1948), the External Zones have been differentiated in the Prebetic and Subbetic domains based on their tectonic, stratigraphic and paleogeographic features.

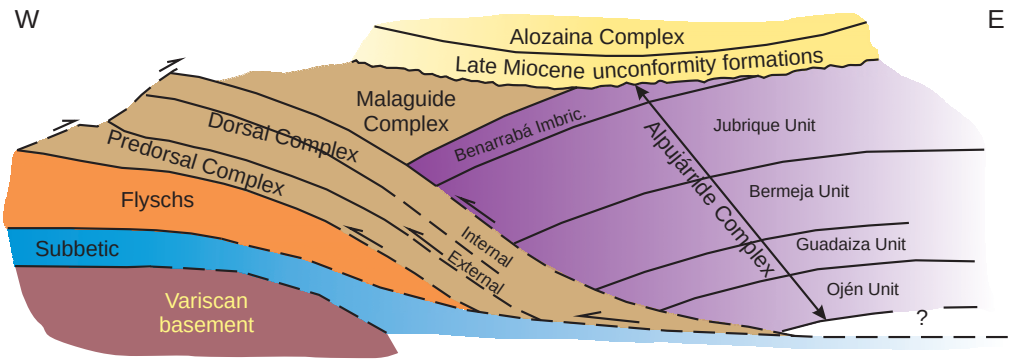

Figure 1-5. *Main tectonic complexes cropping out in western Betics (modified from Balanyá and García-Dueñas, 1991). Colour legend as in Figure 1-3.*

The Prebetic Zone crops out eastwards of the study area (Fig. 1-3) and is characterized by para-autochthonous shallow-water carbonate facies with terrigenous continental deposits (García-Hernández et al., 1980; Vera, 1988) showing a typical imbricate thrust system. The Subbetic Zone is constituted by allocthonous pelagic units detached from their Hercynian basement and intensively deformed during the Early to Middle Miocene. The Subbetic Zone has been differentiated into ‘‘structured’’ and ‘‘chaotic’’ Subbetics (Vera, 2004). The first of these could be subdivided into External, Median and Internal (or Penibetic; Fig. 1-6) zones on the basis of paleogeographic criteria and their position with respect to the emerged Variscan basement. The fold and thrust trend within the structured Subbetic Zone is mainly NE-SW to ENE-WSW. The complex structure of the chaotic Subbetic is mainly conditioned by the more intense deformation of the Jurassic-Cretaceous carbonate sequences located on the plastic Triassic rocks at the base of the stratigraphic series, especially the Keuper evaporites. These rocks acted as decollement levels during nappe emplacement, and were also subjected to tectonically induced diapirism since the Middle Miocene. Both Subbetic types widely crop out in the studied area and constitute the basement of the Ronda Basin.

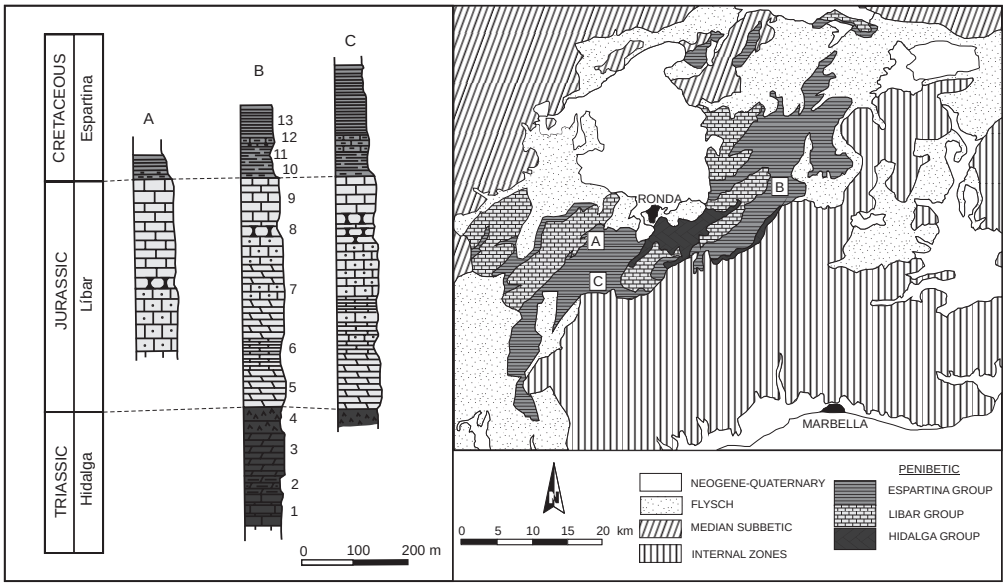

Figure 1-6. *Geological map and stratigraphic columns of the Penibetic (Internal Subbetic) in several locations near the Ronda Basin (A: Hacho de Montejaque; B: Sierra Blanquilla and C: Panderón-Jarastepar; modified from Martín-Algarra, 1987 and Balanyá and García-Dueñas, 1991). Legend: 1, dark limestones with marly levels; 2, dolostones and dolomitic marls; 3, dolostones; 4, clays and marls with gypsum; 5, massive and crystalized dolostones; 6, limestones; 7, oolitic limestones; 8, massive and crystalized dolostones; 9, pelagic oolitic limestones; 10, grey and white marls; 11, grey and white marly limestones; 12, limestones and marly limestones with silex; 13, limestones, marly limestones and marls.*

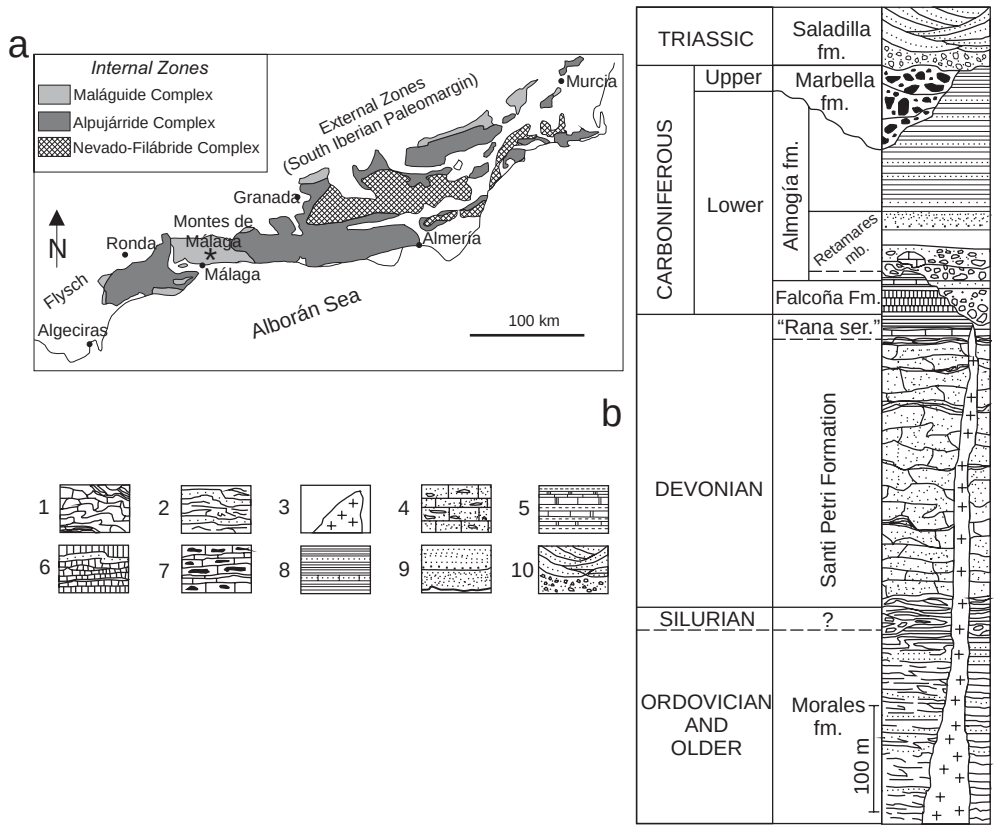

Figure 1-7. a) *Geological map of the Betic Cordillera Internal Zones (modified from Martín-Martín et al., 2006);* **b)** *Stratigraphy of the Maláguide Complex in the Montes de Malaga. Lithology (modified from O´Dogherty et al., 2000); 1: warped, fine-grained calcareous turbidites, slates and greywackes (Santi Petri formation). 2: greenish (locally reddish) greywackes and slates (Rana series). 3: Early Miocene mafic subvolcanic rocks. 4: thin-bedded turbiditic limestones and pebbly mudstones with limestone clast (top of Santi Petri formation). 5: grey to reddish-brownish well-bedded siliceous mudstones. 6: radiolarian cherts (lower member, Falcoña formation), with greywacke intercalations. 7: conodont-bearing limestones, sometimes with chert (upper member, Falcoña formation). 8: olive-green shales with some fine-grained and thin greywacke and sandy calcarenite beds. 9: medium- to coarse-grained greywackes (Retamares member). 10: red sandstones and conglomerates (Saladilla formation).*

B) Flysch

The Flysch Units are comprised of a stack of nappes, consisting of siliciclastic sediments of Cretaceous to Early Miocene age, not affected by alpine metamorphism, deposited in an attenuated continental lithosphere or oceanic setting (Durand-Delga et al., 2000) surrounding the Internal Zones. The westward motion of continental

metamorphic rocks of the Internal Zones produced the deformation and emplacement of the sedimentary infill of the Flysch Trough during the Miocene. The Flysch constitutes an inactive accretionary prism that crops out in the western Betics with a N–S structural trend (Luján et al., 2003) and extends between Ronda and Granada along the Internal/ External Zone boundary, in a WNW–ESE direction (Fig. 1-3). The Aljibe thrust is the main tectonic unit of the Flysch Complex (Didon et al., 1973). The Paleogene sequence of the unit comprises claystones and intercalations of calcareous limestones, while the Neogene sequence is made up of a characteristic quartzite formation with minor marly levels.

C) Internal Zones (Alborán Domain)

The Internal Zones consist of several frontal imbricated units that mainly crop out in the western and central Betics (Dorsal, Pre-Dorsal and Alozaina), plus three main stacked metamorphic complexes that, in ascending order, are the Nevado–Filábride, Alpujárride and Maláguide. These complexes have been distinguished according to lithological and metamorphic evolution criteria. The latter is only weakly affected by Alpine metamorphism; in contrast, the two lower nappe complexes record intense polyphase deformation including Alpine high-pressure metamorphism. The radiometric dates constraining the high-pressure metamorphism in the Nevado–Filábride Complex indicate that convergence began at about 51 Ma (Monié et al., 1991), although earlier dates have also been suggested (De Jong, 1991). A sharp decompression in the metamorphic P–T path of the Nevado–Filábride and Alpujárride complexes (Vissers, 1981; Gómez-Pugnaire and Fernández-Soler, 1987; Bakker et al., 1989; García-Casco and Torres-Roldán, 1996) suggests rock exhumation due to crustal-scale extension during the Early and Middle Miocene (Monié et al., 1991; García-Dueñas et al., 1992; Watts et al., 1993). The common tectonic evolution of the three main complexes began in the Early-Middle Miocene, when the whole domain was displaced westwards. The frontal units and the upper metamorphic complexes crop out in the studied sector, while the lowermost Nevado-Filábride Complex is only identified in the central and eastern Betics.

Predorsal and Alozaina Complexes

These units, Aquitanian-Burdigalian in age, are recognized exclusively along the Internal Zones front (Durand-Delga, 1972). The Predorsal unit is tectonically placed below the Flysch units and over the Dorsal Complex, and consists of clays and sandstones. Outcrops of the same rocks but with a different tectonic position, lying unconformably over the Alpujárride and Maláguide Complexes, have been referred to as the Alozaina Complex (Balanyá and García-Dueñas 1986).

Dorsal Complex

The Dorsal Complex, usually linked to the Maláguide Complex, is divided into two main domains, the Internal and the External. The Internal Dorsal is directly related to the Maláguide, forming part of its Mesozoic cover, while the External Dorsal extends as far as the Predorsal and the Flysch. It is made up of thinned carbonate cover units (Trias-Oligocene) and is tectonically placed below the Alpujárride and Maláguide Complexes and over the Predorsal and the Flysch units. It has a complex structure and discontinuous outcrops. The lithological sequence is diverse, but could be divided in three groups (Martín-Algarra, 1987): 1) The Internal Dorsal, with a similar sequence to the Maláguide cover; 2) De las Nieves Unit, characterized by a Triassic carbonatic member, a pelagic Liassic member and a post-Liassic one (although this unit is affected by metamorphism, the absence of key mineral assemblages does not allow for accurate determination of its characteristics); and 3) External Dorsal, characterized by Jurassic-Cretaceous sequences similar to the Subbetic.

Maláguide Complex

The Maláguide is the uppermost metamorphic Complex of the Internal Zones and tectonically overlies the Alpujárride Complex (Fig 1-5). It is constituted by a thick, weakly metamorphic to non-metamorphic Palaeozoic basement (Chalouan and Michard, 1990; Lonergan, 1993), unconformably covered by continental red beds of Triassic age and by a thin, stratigraphically incomplete, shallow marine to hemipelagic Jurassic to Aquitanian succession (Martin-Algarra, 1987). The Palaeozoic basement consists essentially of slates and greywackes with intercalations of conglomerate, chert and pelagic limestones.

In the Montes de Málaga (Fig. 1-7; O'Dogherty et al., 2000) the following lithostratigraphical units crop out, from bottom to top: Morales, Santi Petri, Falcoña, Almogía, Marbella and Saladilla formations. The Morales formation is the lowest unit and is constituted by a thick succession of pre-Silurian phyllitic slates and fine-grained greywackes. The Santi Petri formation is a thick strongly folded succession of fine-grained calcareous turbidites, greywackes and slates of probable Devonian age. In the study region, the Morales and, locally, the Santi Petri and Falcoña formations were intruded by Early Miocene arc-tholeiitic mafic dykes (Torres- Roldán et al., 1986). The Santi Petri formation is overlain by the Falcoña formation, a thin succession of cherts developed from underlying pelitic sediments ('Rana Series') followed by conodont-bearing limestones. The Santi Petri formation is overlain by the Almogía formation, a thick turbiditic succession of greywackes and shales that contains, in its lower part, conglomerates and coarse-grained sandstones (Retamares member) that may locally cut by erosion the underlying formations. Thick and very coarse-grained conglomerate lenses of the overlying Marbella formation locally cut the Almogía formation. Finally, the Saladilla formation comprises red sandstones and conglomerates of Triassic age.

Alpujárride Complex

The Alpujárride Complex, located below the Maláguide Complex, is thrusted over the frontal units in the western Betics, while it overlies the Nevado-Filábride Complex in the eastern Betics. The Alpujárride is formed by a succession starting in the Palaeozoic and up to the Triassic (Delgado et al., 1981; Martín and Braga, 1987; Tubía et al., 1992). The rocks show variable metamorphic grade, from upper amphibolite to granulite facies at the bottom of certain units, to low metamorphic grade at the top (Cuevas, 1990; Azañón et al., 1994, 1997).

There is no consensus at to the delimitation and nomenclature of the units that constitute the Alpujárride Complex, although a broad division could be established taking into account the rock sequences: the Lower, Middle and Upper Alpujárride Units (Aldaya et al., 1979; Martín-Algarra, 1987; Azañón et al., 2002). The Upper Alpujárride units comprise a more complete sequence, which from top to bottom includes: 1) Middle-Upper Triassic marbles, 2) Permo-Triassic metapelites without graphite, quartzites, carbonates and gypsum, 3) Paleozoic metapelites with graphite and quartzites and 4) gneiss above peridotites. The Intermediate Alpujárride is composed by the three uppermost levels of the sequence, while the Lower Alpujárride units comprise just the two uppermost levels.

In western Betics (Fig. 1-8) we may differentiate, in ascending order, the following units (Torres-Roldán 1979, Tubía 1985, Balanyá and García-Dueñas, 1991, Sanz de Galdeano y Andreo 1995; Balanyá et al., 1997):

a) Los Reales nappe (Upper Alpujárride):

-Bermeja unit: It is a thick slice of peridotites (mainly lherzolites) from the lithospheric mantle and associated mafic rocks. These rocks crop out in three sectors of the Betic Cordillera: Sierra Bermeja, Sierra Alpujata and the Carratraca Massif; yet together they are called the Ronda Peridotites (Tubía, 1988). Porfiroclastic textures are the most common, although milonitic textures are also relevant, associated with the hangingwall and footwall of the slice. The foliation and banding of the peridotites are frequently cut by acid dikes. They are 4.5 kilometres thick in Sierra Bermeja.

-Jubrique Unit: It constitutes the most complete Alpujárride sequence of the crust and is made up of gneiss, schists, phyllites and carbonates. It is situated below the Maláguide Complex and its maximum thickness is 5 kilometres. The lithologic contact between the Jubrique units and the peridotites occurs within the Bermeja-Jubrique shear zone (Balanyá and García-Dueñas, 1991).

-Benarrabá Imbrications: a number of imbrications that repeat the upper part of the Jubrique sequence (schist and carbonates). Thickness locally reaches 1.5 kilometres.

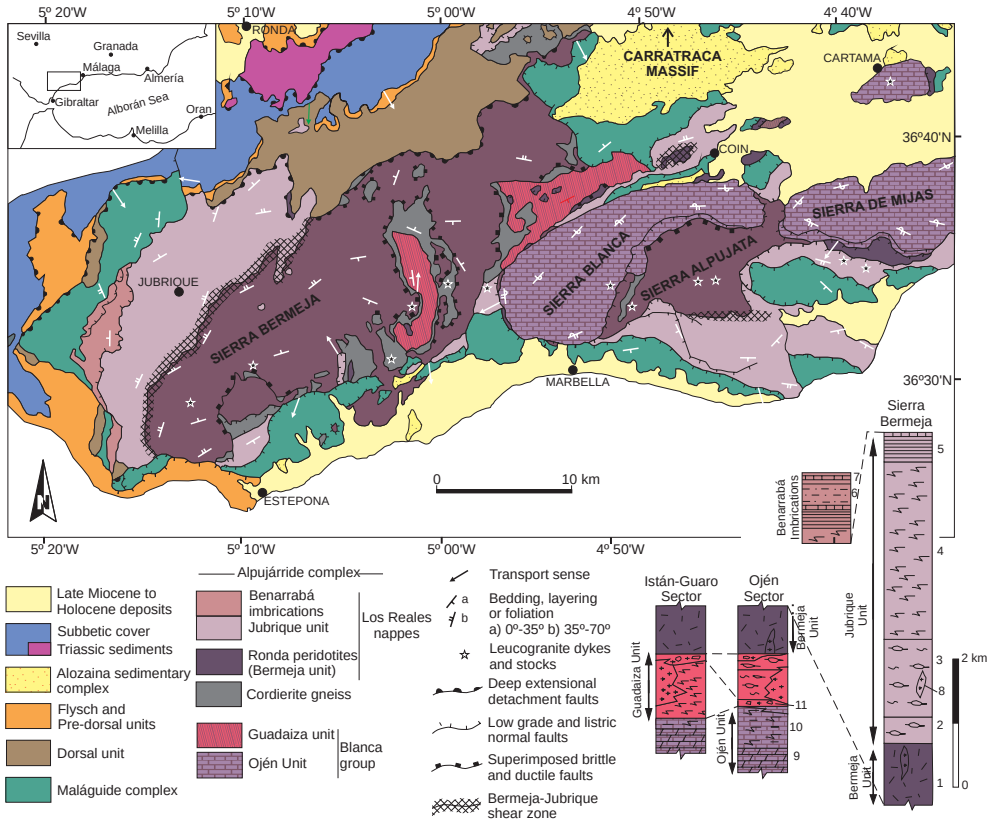

Figure 1-8. *Tectonic units of the Internal Zones in the western Betic Cordillera and representative lithologic columns of several sectors (modified from Balanyá and García-Dueñas, 1991 and Balanyá et al., 1997). Legend: 1. peridotites, 2. garnet gneiss; 3. migmatite gneiss; 4. dark schists; 5. phyllites and schists; 6. quarzites; 7. recrystalized limestones and dolostones; 8. leucogranites; 9. marbles; 10. schists and amphibolites 11. gneiss.*

b) Blanca Group (Intermediate Alpujárride):

This group comprises all the rocks below the peridotites, and is divided into two units:

-Ojén Unit: It is made up of garnet and migmatite gneisses, schist and amphibolites with intercalated marbles. It shows prominent north vergent overturned and recumbent folds at Sierra Blanca and Sierra de Mijas. The minimum thickness of the unit is 2 kilometres.

-Guadaiza Unit: The lithology and metamorphic grade are similar to the lower part of the Alpujárride. There is no evidence to establish its thickness and polarity. Medium-grade graphitic schists belonging to the Guadaiza unit crop out below the Ronda peridotite unit in several tectonic windows.

1.2.3. Neogene Basins

During the Early-Middle Miocene, sedimentation in the Betic Cordillera took place in an incipient Guadalquivir foreland Basin (called as North Betic Strait; Sanz de Galdeano and Vera, 1992) and the intramontane basins formed due to the emplacement of the Internal Zones to the west. As the result of eustatic and tectonic processes, these basins became dismembered. In a second stage of convergence between Eurasia and Africa, Late Miocene-Quaternary, the Neogene basins develop indiscriminantly over the Internal Zones, the External Zones or along the boundary between the two domains. The sedimentary basins that crop out in the study area, and will be described in this section, are the Guadalquivir foreland Basin and the Ronda Basin.

A) Guadalquivir foreland Basin

The Neogene Guadalquivir Basin, located in the southern part of the Iberian Peninsula, has an asymmetric geometry limited by the Iberian Massif to the north and the Betic Cordillera to the south (Fig. 1-9a). It was formed due to the load of the Betic reliefs over the Variscan basement. The sedimentary infill, mainly marine and of clastic nature, is Langhian-Pliocene in age. In its northern part, it autochthonous sediments crop out, while the southern border is made up of chaotic allocthonous sediments from the Subbetic. The northern boundary and basement of the basin are constituted by Paleozoic

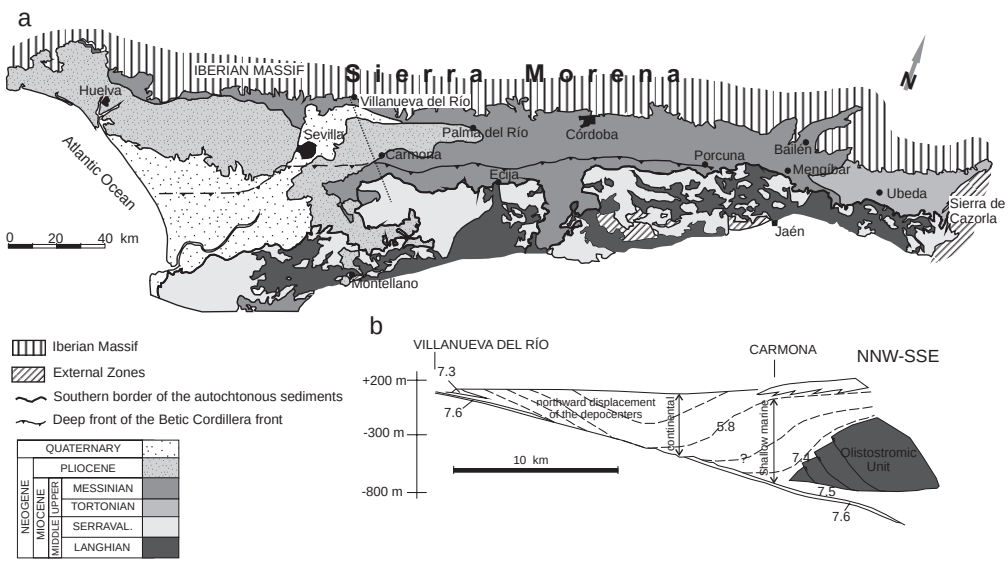

Figure 1-9. a) *Geological sketch of the Guadalquivir Basin (Modified from Roldán, 1995) and* **b)** *Cross-section of the western Guadalquivir Basin (modified from García-Castellanos et al., 2002 and Vera et al., 2004).*

and Mesozoic rocks of Sierra Morena (passive boundary), while the southern border is not well defined and constitutes the active boundary of the basin. The sedimentary infill shows progradation toward the WSW after the Messinian (Sierro et al., 1996; Vera et al., 2004; Fig. 1-9b), reflecting the present direction of sediment transport, whereas before this period the sedimentary units show small lateral variations along the strike of the basin (Berástegui et al., 1998). The sedimentary infill of the basin could be divided into six depositional sequences (Roldán, 1995):

Upper Langhian- Lower to Middle Serravallian Unit

Although it has been called the Olistostromic Unit (Roldán, 1988), the unit in question could also comprise previous denominations such as: Nummulítico de Morón (Calderón y Arana, 1890), Trías de Antequera (Staub, 1926), Manto de Carmona (Perconig, 1960-62), Unidad de Paterna (Chauve, 1963), Manto de Cambil (Fontbote, 1964) or Arcillas con bloques (Bourgois, 1978). It consists of clastic sediments deformed due to gravitational processes involving rocks coming from the External Zones at the southern border of the basin. It mainly comprises clays, marls, red sandstones, gypsum and dolostones of Triassic age, marly limestones of Cretaceous age and marls of Early to Middle Miocene. Because of its plastic nature, the internal structure is quite complex; structures range from kilometre-wide sheets to centimetre- or decimetre-sized blocks can be found interbedded within marlstones. At a mesoscopic scale, the structure of the Triassic rocks is characterized by multiple decollement tectonics, disharmonic folding, shear fabrics, and gypsum veins (Flinch, 1993). Poor surface exposure and a complex deformation impede establishment of an accurate stratigraphy of this allochthonous unit.

The unit is located at the southern part of the Guadalquivir Basin, close to the boundary of the Betic Cordillera, below the most recent sedimentary infill, which lies unconformably. In the studied area, it crops out in the Morón de la Frontera sector. Seismic reflection profiles have shown that the olistostromic unit overlies the Iberian Massif and exhibits northwards nappe stack geometry, also called Manto Bético (Roldán and Rodríguez-Fernández, 1991).

Upper Serravallian- Lower Tortonian Unit

This unit lies unconformably over the Olistostromic Unit or over the External Zones, and is equivalent to the upper part of the Atlántida Group (Martínez del Olmo et al., 1984). Its geometry is associated to piggy-back basins formed over a mobile substratum constituted by N-vergent thrusts of the External Zones. It shows high facies variability and geographical disconnection between the eastern and western sectors. Prevailing in the east are algal limestones, calcarenites and white marls, while in the western sector sands and sandstones with marls predominate (Castro del Río Unit; Roldán, 1988) along with white marls containing levels of calcareous sandstones (also called Albarizas or Moronitas). Within the study area, these sediments crop out in the Puebla de Cazalla sector.

Upper Tortonian Unit

This unit is equivalent to the lower part of the Bética Group (Martínez del Olmo et al., 1984). In the northern part of the basin it is constituted by limestones, sands, conglomerates and calcarenites, yet in the axial and southern parts of the basin it comprises yellow sandstones and blue marls. This unit does not crop out in the study area.

Messinian Unit

This unit corresponds to the upper part of the Bética Group (Martínez del Olmo et al., 1984). The outcrops of the northern border of the basin consist of red conglomerates with pebbles of different nature (quartzites, shales, limestones), while the southern border is constituted by sands, yellow silts and blue marls.

Upper Messinian- Lower Pliocene Unit

This unit is equivalent to the Andalucía Group of Martínez del Olmo et al. (1984). The prevailing lithologies are calcarenites and sands with alternating marls deposited in a shallow platform environment. It is well represented in the study area between the towns of Carmona- El Coronil- El Arahal.

Pliocene Unit

This unit extends from Carmona to Huelva and is equivalent to the Marismas Group (Martínez del Olmo et al., 1984). In the study area, it lies unconformably over the previous units. The prevailing lithology is a rhythmic succession of yellow sandstones and marls.

B) Ronda Basin

The Ronda Basin is the main Neogene outcrop of the western Betic Cordillera. It is located at the boundary between the last "structured" Internal Subbetic units —to the south— and the Flysch and Subbetic Chaotic Complexes to the north. The sedimentary sequence of the basin is Late Miocene in age (Fig. 1-10). Whereas in other sectors of the Subbetic the marine sedimentation ends at Late Tortonian, in the Ronda Basin it remains up to Late Messinian. Even though Chapter 7 contains a brief description of the Neogene sequence of the basin, it is best to introduce it here. Several formations have been differentiated (Serrano, 1980; Rodríguez-Fernández, 1982):

Gastor Formation (Early Tortonian)

This formation lies in unconformity over the Triassic rocks of the Subbetic Chaotic Complexes and below the marls of the Mina Formation. It reaches a thickness of 500 m thick, and from bottom to top contains: yellow sands with conglomerate levels, alternations of marls, sands and sandstones with massive strata, and conglomerates and sands with trough-cross-bedding or horizontal lamination (Fig. 1-11a). These sediments crop out in the NW border of the depression and were deposited on a deltaic fan environment prograding to the SE.

Tajo Formation (Late Tortonian)

This formation comprises conglomerates with limestone, dolostone and sandstone pebbles coming from the Subbetic and Flysch units located southwards of the depression. It shows a deltaic morphology with a maximum thickness of 150 m, but it thins toward the south until disappearing. The unit does not contain autochthonous fauna, although due to its stratigraphic position it could be attributed to the lower part of the Late Tortonian (Serrano, 1979) or previous to the Late Tortonian (Rodríguez-Fernández, 1982). These sediments crop out to the south of the town of Ronda, unconformably over the Flysch and conformably below the calcarenitic member of the Setenil Formation (Fig. 1-11b).

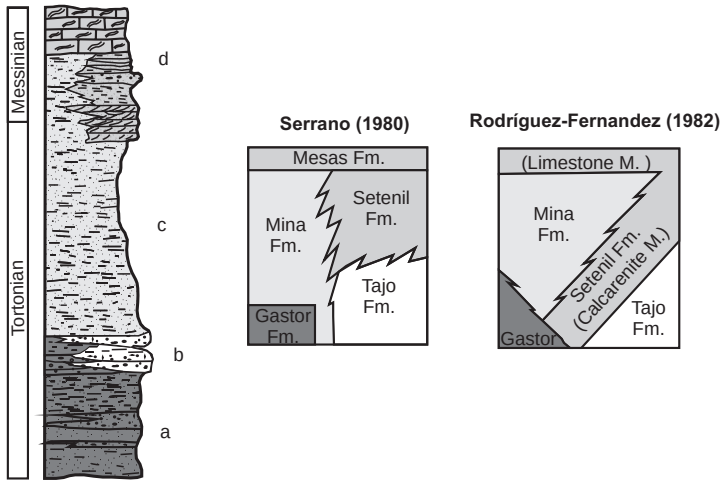

Figure 1-10. *Stratigraphic column type of the Ronda Basin (modified from Del Olmo Sanz et al., 1990) and lithostratigraphic divisions proposed by Serrano (1980) and Rodríguez-Fernández (1982). Legend: a) Gastor Formation: Sands, silts and conglomerates; b) Tajo formation: Conglomerates with silex, marble, limestone, dolostone and calcarenite pebbles; c) Mina Formation: Silts, clays and white marls; d) Setenil Formation: Calcarenites, sands and silts (Calcarenitic Member) and algal limestones (Limestone Member).*

The Mina Formation is constituted by marls and sandy silts deposited in a shallow non-coastal environmental medium (Figure 1-12a). The planktonic foraminifera, involved in the abundant marly levels, date the formation as Early Tortonian-Late Messinian; the other formations being dated by stratigraphic correlation. Its thickness is 800 meters; and it is well exposed in the western half of the basin, where it lies in conformity over the Gastor Formation.

Setenil Formation (Late Tortonian-Late Messinian)

This formation could be divided in two different members (Rodríguez-Fernández, 1982): a Limestone Member (equivalent to the Mesas Formation; Serrano, 1979) and a Calcarenite Member. It crops out in the entire depression except for the NW sector. Its thickness reaches 200 m and it lies directly upon the basement of the basin or over the Mina Formation (Fig. 1-12b).

Calcarenite Member: It comprises conglomerates and bioclastic calcarenites with cross-bedding that thins toward the basin edges. Frequently present is a conglomerate at the base of the sequence. At the boundaries of the basin, the calcarenite member lies in unconformity over the basement or over the Tajo Formation. The sedimentary

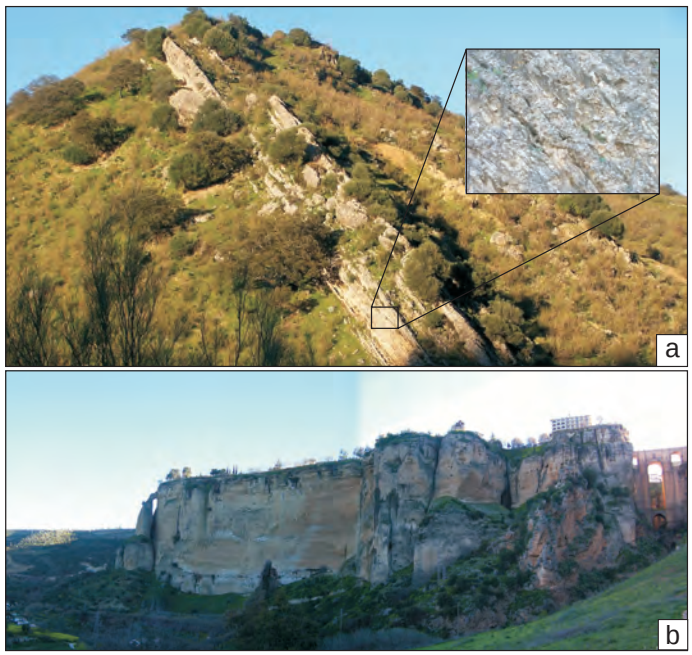

Figure 1-11. *Lower formations of the sedimentary infill of the Ronda Basin* **a)** *Early Tortonian conglomerates of the Gastor Formation;* **b)** *Late Tortonian conglomerates of the Tajo Formation.*

environment was near the coastline and has undergone depth variations. It is Late Tortonian-Late Messinian in age. The Sierra de Sanguijuela and Sierra de las Salinas determined a high in the basin ground that may condition the facies change of the Calcarenite Member to the Mina Formation.

Limestone Member: It is equivalent to the Mesas Formation (Serrano, 1979) and lies over the Calcarenite Member. It crops out at the middle part of the basin over the Mina Formation marls. It has a tabular geometry and 40 m in thickness, and is made up of algal limestones with slivers of ostreid, gasteropod and equinid. It is Upper Messinian in age, as determined by its stratigraphic position. The deposit would have occured in a shallow marine environment.

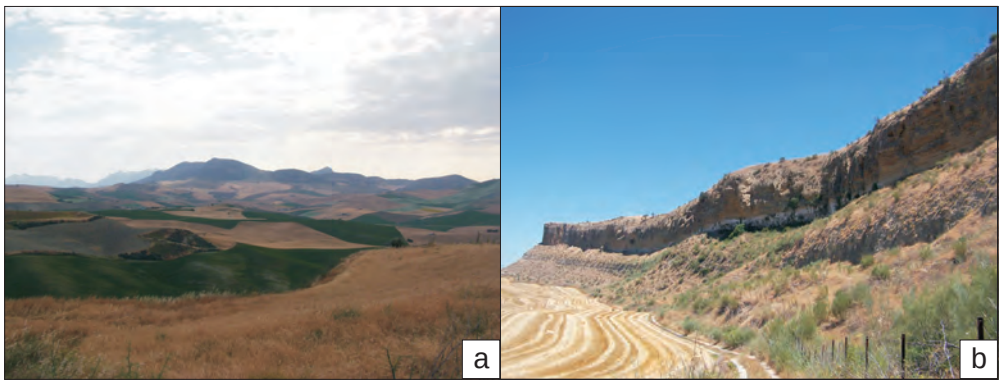

Figure 1-12. *Upper formations of the sedimentary infill of the Ronda Basin;* **a)** *Lower Tortonian –Upper Messinian marls of the Mina Formation;* **b)** *Upper Tortonian-Upper Messinian calcarenites of the Setenil Formation.*

1.3. Previous geophysical studies

In this section, I enumerate the main regional geophysical data acquired up to now in the Betic Cordillera and the southern Iberian Massif, and partially in the northern Alborán Sea. The aim of this section is to summarize our present day state of knowledge in order to highlight and frame the new geophysical data acquired in the context of this Ph. D. Thesis.

1.3.1. Gravity research

The administrative centre responsible for gravity measurements in Spain has traditionally been the Instituto Geográfico Nacional (I.G.N.). They gathered the gravity data used to perform the 1:1.000.000 free air and Bouguer anomaly maps (I.G.N., 1976), which reveal a good correlation between the geology and the gravity anomalies

(Fig. 1-13). The Bouguer anomaly of the Iberian Peninsula shows a mainly negative character, related to the relative low density of the thick continental crust, with the values generally nearing zero at the coast. The gravity minima are mostly found in the alpine belts and in the Iberian Cordillera. Indeed, the minima are located at the southeastern part of the Iberian Peninsula, related to the Betic Cordillera.

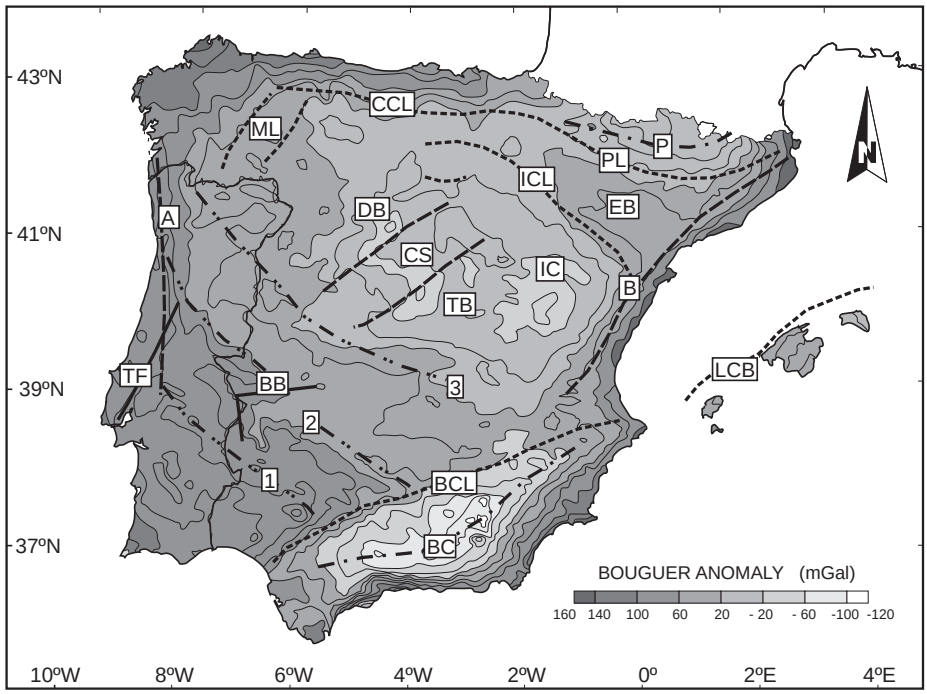

Figure 1-13. *The 1:1,000,000 Bouguer anomaly map of Spain (from IGN, 1976) with the main geologic features superimposed. Abbreviations from north to south: P: Pyrenees, PL: Pyrenees southern limit; CCL: Cordillera Cantábrica southern limit; ML: Montes de León; EB: Ebro Basin; DB: Duero Basin; TB: Tajo Basin; CS: Central System; 1, 2 and 3: gravity gradients associated with the Iberian Massif; CI: Iberian Cordillera; CIL: Iberian Cordillera northern limit; A and B: gravity gradients subparallel to the Atlantic and the Eastern coasts; TF: Tajo fault; BB: Badajoz Basin; CBL: Betic Cordillera northern limit; BC: Betic Cordillera.*

The Betic Cordillera minimum is placed at the boundary between the Internal and the External Zones, and extends from the Gulf of Cadiz to the Balearic Islands. It is due to the regional thickening of the crust and to the local presence of low density sediments in the Guadix-Baza, Granada and Guadalquivir basins. The gravity values show a steeper increase from the coast towards the Alborán Sea (Casas and Carbó, 1990), revealing the southward thinning of the crust (Torné and Banda, 1992). Positive values detected at the Málaga coast are related to the presence of basic rocks (Ronda peridotites). However, the anomaly is placed southward of the peridotitic outcrops,

pointing to the existence of deeper basic bodies (Torné et al., 1992). In the study region, the Bouguer anomaly approaches zero values close to the northern boundary of the Guadalquivir Basin. To the north, the SW Iberian Massif shows slightly negative to positive Bouguer anomaly values. The NW-SE trend of the gravity anomalies at the southern Iberian Massif (Fig. 1-13, 1 and 2) is related to the boundaries between the SPZ/OMZ and the OMZ/CIZ , as a consequence of the different crustal nature of the three domains. The northern gradient (Fig. 1-13, 3) is placed at the Central Iberian Zone but its origin is not quite clear.

Regional gravity analysis together with other geophysical constraints, such as refraction seismic data, would appear to be an appropriate tool for determining the crustal thickness of the region and to propose complete crustal sections that reflect the transition between the different geological domains (Fig. 1-14; Gaibar-Puertas, 1973; Hatzfeld, 1976; Suriñach and Udías, 1978; Bonini et al., 1973; Casas and Carbó, 1990; Torné and Banda, 1992; Galindo-Zaldívar et al., 1998; Torné et al., 2000; Sánchez Jiménez, 2003). Studies developed in the Betic Cordillera reveal that the crust thins from 32-38 km below the Internal Zones to 15–22 km beneath the Alborán Sea, depending on the analyzed transect (Torné and Banda, 1992). On the SW Iberian Massif, gravity data reveal a NE-SW gradient, with nearly zero values at the Ossa Morena Zone and positive values at the South Portuguese Zone. In this setting a constant Moho depth around 33-34 km has been proposed in both domains (Sánchez Jiménez, 2003), but revealing that

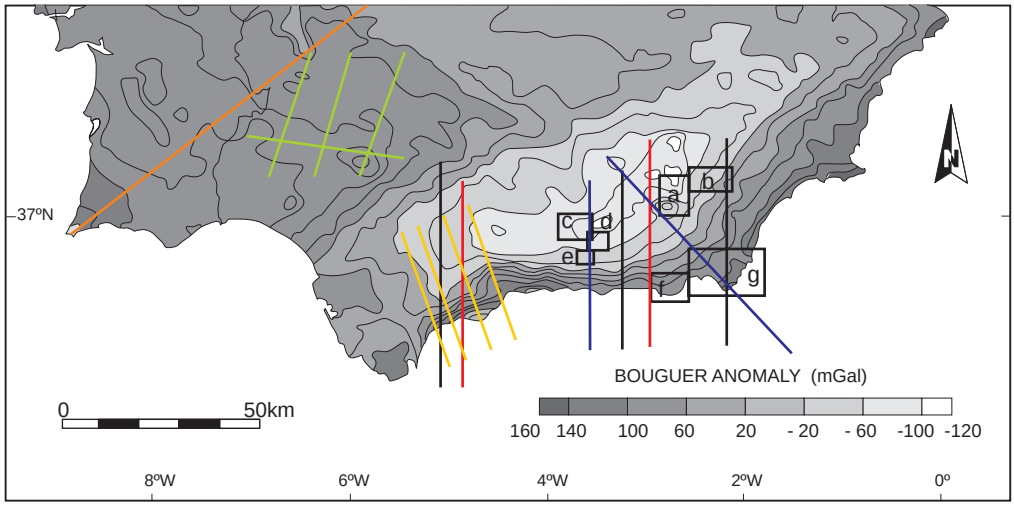

Figure 1-14. *Detail of the southern part of the 1:1,000,000 Bouguer anomaly map of Spain (IGN, 1976) with the gravity studies carried out in the area. The boxes mark the local gravity surveys performed in the basins (a: Alfaro et al., 2007; b: Pedrera et al., 2009;c: Jiménez-Pintor et al., 2002; d: Ruiz-Constán et al., 2005; e: Delgado et al., 2002; f: Marín-Lechado et al., 2007; g: Pedrera et al., 2006). The lines mark the regional transects (black: Casas et al., 1990; red: Bonini et al., 1973; blue: Torné and Banda, 1992; yellow: Torné et al., 1992; green: Sánchez Jiménez, 2003; orange: Fernàndez et al., 2004).*

the three layers forming the Variscan crust show noticeable thickness variations along the Ossa Morena and South Portuguese Zones (Fernàndez et al., 2004).

In addition to the regional features, several detailed gravity surveys have been performed to better establish the geometry of the main Neogene sedimentary basins and the relationship between the main depocentres and the faults (Fig. 1-14; Delgado et al., 2002; Jiménez-Pintor et al., 2002; Ruiz-Constán et al., 2005; Pedrera et al., 2006; Alfaro et al., 2007; Marín-Lechado et al., 2007). These studies have been basically carried out in the central and eastern Betic Cordillera, the western part remaining poorly known.

1.3.2. Magnetic research

The aeromagnetic map of the Iberian Peninsula (Ardizone et al., 1989) was developed from 10 km spacing fly lines with a mean barometric altitude of 3000 m. It shows the total magnetic field intensity anomalies related to regional structures, but has insufficient resolution for the study of bodies smaller than 10 km (Fig. 1-15).

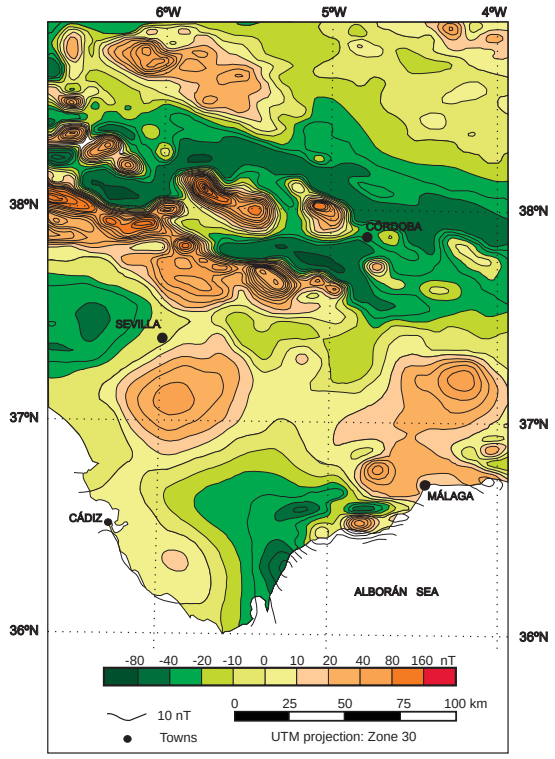

Figure 1-15. *Southwestern detail of the aeromagnetic map of Spain.*

The most important feature of the Iberian Massif is constituted by a WNW-ESE band of magnetic anomalies that has been interpreted as basic igneous rocks of the Ossa Morena Zone. In the Iberian Massif, the anomalies are high gradient dipoles that become progressively smooth toward the Betics with the same trend. This feature evidences the continuity of the basic rocks of the Iberian Massif beneath the Betic Cordillera, confirming the existence of a variscan basement in depth (Bohoyo et al., 2000). Another important feature is the high gradient dipole at the coastline that may be caused by the southward continuity of the outcropping peridotite bodies of Sierra Bermeja (Socías et al., 1991).

1.3.3. Seismic research

Since the 70s, in the Iberian Massif and the Betic Cordillera several controlled-source seismic experiments have been performed with the aim of determining the deep structure and the geometry and depth of the Moho (Fig.1-16). These data give a broad idea of the lithospheric structure, although geophysical studies based on other properties of the rocks would contribute to a more detailed analysis.

A) Deep seismic refraction

The first deep seismic studies carried out in the Iberian Massif established the Moho depth around 31-34 kilometres and revealed that the main characteristic of the Iberian Massif crust is its well developed layered structure, with clearly defined upper, middle and lower crusts (Córdoba et al., 1988; Suriñach and Vegas, 1988; Banda et al., 1993). In the late 1980s, deep seismic refraction profiles (ILIHA DSS Group, 1993) also provided relevant information about the crustal and upper mantle structure beneath Iberia, including evidences of the presence of seismic anisotropy in the uppermost mantle up to at least 90 km in depth. Recent studies (Flecha et al., 2009) reveal that the crust has a strongly heterogeneous nature, with a layered mafic intrusion at middle crustal levels and a laterally heterogeneous Moho below the South Portuguese, Ossa Morena and Central Iberian tectonic complexes.

The highest crustal thickness in the Betic Cordillera (37-38 km) was obtained under the large kilometric folds of the Internal Zones and decreases to 23-25 km along the south and southeast coast of the Iberian peninsula —except in the area close to the Gibraltar arc, characterized by 28-31 km in thickness (Banda and Ansorge, 1980; Medialdea et al., 1986; Barranco et al., 1990). In addition, the profiles located in the Betic Cordillera reveal the presence of crustal detachment levels that probably separate the upper crust, corresponding to outcropping rocks, from the lower crust (Banda and Ansorge, 1980; Banda et al., 1993). The continental crust gets thinner below the Alborán Sea, reaching 16 km in its central part (Hatzfeld, 1976; WGDSSAS-1974, 1978; Suriñach and Vegas, 1993). SW of Málaga seismic data evidence an anomalous structure that could be explained by a thin crust, a massive presence of peridotites or

a combination of both features (Banda et al., 1993). The low P and S spread velocities noticed in the upper mantle of the Alborán Sea (Hatzfeld and Ben Sari, 1977; Suriñach and Vegas, 1993) together with the high regional heat flow values (Polyak et al., 1996) suggest the existence of an anomalous mantle in this region (Hatzfeld, 1976).

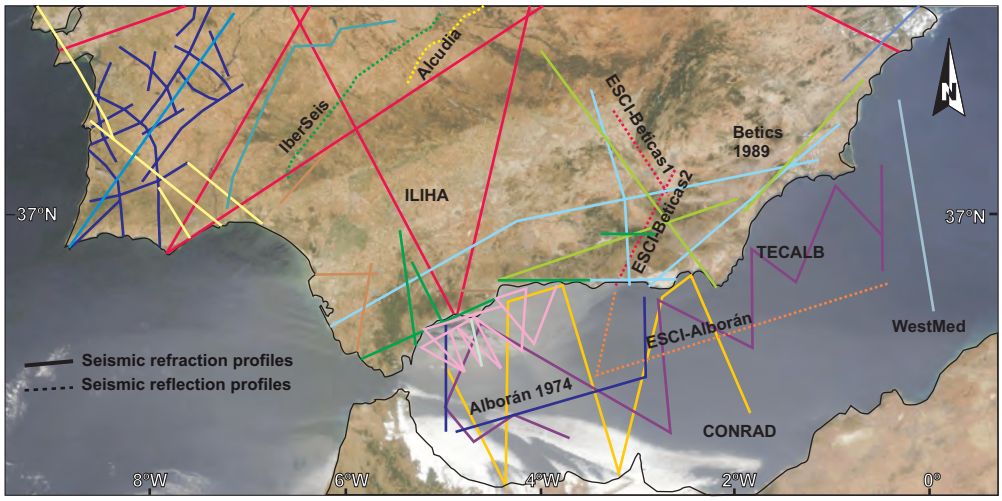

Figure 1-16. *Location of the refraction/wide-angle reflection and deep multichannel reflection profiles beneath the southern part of the Iberian Peninsula and the Alborán Sea (modified from Díaz and Gallart, 2009). Different colours show each main survey.*

B) Deep seismic reflection

The IBERSEIS deep seismic reflection profile (Simancas et al., 2003; Carbonell et al., 2004) provides a high-resolution image of the SW Iberian Massif using both multichannel and wide-angle methods. These data revealed a reflective body (Iberian Reflective Body, IRB), which has been proposed to be related to the high concentrations of mineral deposits present mainly in the Ossa Morena Zone (Casquet et al., 2001; Tornos et al., 2001; Carbonell et al., 2004). The IRB also coincides with a high velocity zone observed in the refraction seismic profile (Palomeras et al., 2009). Recently, the ALCUDIA profile (Martí and the Alcudia Team, 2009) extends the IBERSEIS line to the Northeast.

During the early 1990s, the ESCI-Béticas and ESCI-Alborán deep seismic reflection profiles were carried out to study the main features of the deep crustal structure of the eastern Betic Cordillera and the Alborán Sea. The ESCI-Béticas 1 extends from the Guadalquivir foreland Basin to the Guadix-Baza Basin, while the ESCI-Béticas 2 cuts across the Internal Zones of the Betic Cordillera (García-Dueñas et al., 1994; Galindo-Zaldívar et al., 1997). These data point to the absence of a differentiated

lower crust beneath the External Betics; yet an upper crust nearly transparent till 15-20 km, and a very reflective lower crust could be identified at the Internal Zones, clearly different from the three-layer model of the Iberian Massif crust. A distinct reflection at 11 s two-way travel-time has been interpreted as a horizontal Moho. Its flat geometry bears no correlation with the kilometric-scale folds that produced the main topographic features observed at surface (Weijermars et al., 1985). Other horizontal reflectors could be related to crustal detachment levels. The crustal thickness is of about 35 km at the Betic Cordillera and has an abrupt transition up to 15 km in the central Alborán Sea. Two seismic profiles were acquired offshore, one continuing the trace of the ESCI-Béticas 2 up to the northern part of the Alborán Sea (ESCI-Alborán 1), and the other connecting the Alborán Sea with the Algero-Balear Basin (ESCI-Alborán 2; Booth-Rea et al., 2007).

C) Seismic tomography

In the last decade or so, several authors have inverted the delay-times of local and teleseismic earthquakes to advance our knowledge of both the crust (Carbonell et al., 1998; Dañobeitia et al., 1998) and the upper mantle (Blanco and Spakman, 1993; Serrano et al., 1998; Morales et al., 1999; Gurría and Mezcua, 2000) of the Iberian Massif, Betic Cordillera and the Alborán Sea (Fig. 1-17). The different hypotheses invoked to explain the detected anomalies serve to highlight the complex tectonic setting of the region.

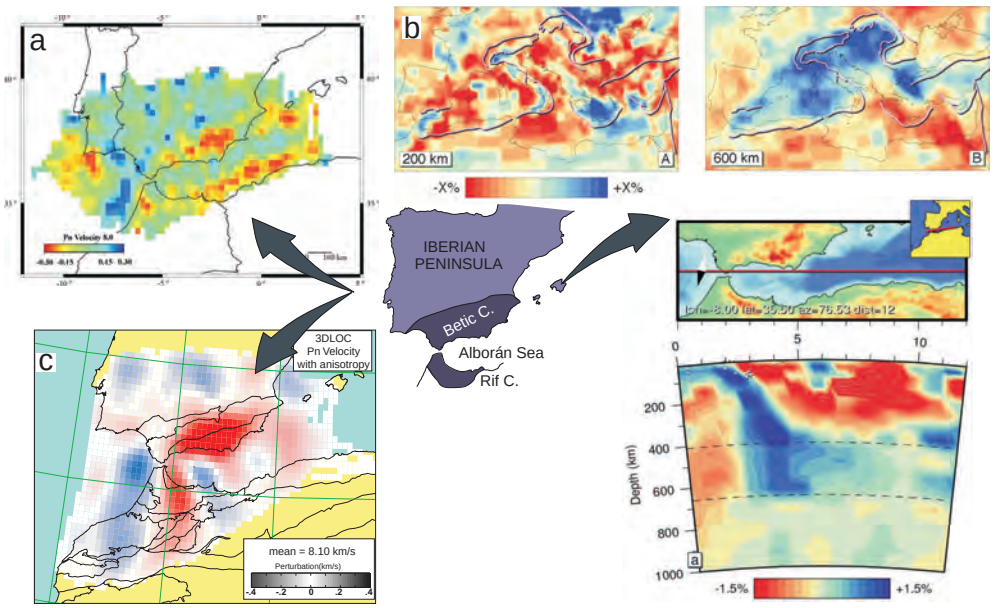

Figure 1-17. *Seismic tomography images of the western Mediterranean;* **a)** *Serrano et al., 2005;* **b)** *Spakman and Wortel, 2004;* **c)** *Calvert et al., 2000b. Red and blue indicate low and high velocity, respectively.*

Blanco and Spakman (1993) found a positive anomaly between 200 and 700 km depth below the Betic-Alborán region. The anomalous body was interpreted as a subducted lithospheric slab (Spakman, 1993; Gutscher et al., 2002; Spakman and Wortel, 2004) probably detached from the surface due to the presence of an aseismic zone in the uppermost mantle. The same finding has been supported by subsequent tomographies (Bijwaard et al., 1998; Calvert et al., 2000a), although with a different geodynamic significance, related to a delaminated lithospheric mantle block (Calvert et al., 2000b; Seber et al., 2006). The anomaly is also corroborated by the presence of very deep seismicity below the central Betics (~600 km, Buforn et al., 1991), but its origin remains a matter of debate.

Seismic tomography data of the Malaga region (Serrano et al., 1998; Morales et al., 1999) reveal the existence of a low-velocity anomaly in the upper mantle beneath the Betic Cordillera and the northern margin of the Alborán Sea that may be explained by the continental subduction of the Iberian Massif to the SSE. This setting could also explain the intermediate seismicity of the region (30<h<110 km).

D) Seismicity distribution, earthquake focal mechanisms and present-day stresses

The interaction between the Eurasian and African plates results in a complex region that corresponds to the transition from an oceanic boundary (between the Azores Islands and the Gorringe Bank), to a continental boundary that becomes more diffuse and constitutes a wider area of deformation, including the Betic-Rif Cordillera and extending to the western part of Algeria (Tell mountains). The distribution of seismicity in this region is irregular; its detailed features will be described in chapter 5 in order to avoid repetition in this section.

Earthquake focal mechanism studies carried out in the area have revealed a complex seismotectonic pattern (Fig. 1-18). The different regional fault sets have variable activity under a scenario of changing regional and local stress fields related to the irregularity of the plate boundary zone (Grimison and Chen, 1986; Galindo-Zaldívar et al., 1993; Buforn et al., 1995; Morel and Meghraoui, 1996; Henares et al., 2003; Stich et al., 2003; Buforn et al., 2004; Stich et al., 2006; De Vicente et al., 2007). Several roughly homogeneous zones may be considered taking into account the shallow seismicity:

(A) The Atlantic zone shows E–W striking faults with dextral strike-slip mechanisms and NE–SW thrusts (Morel and Meghraoui, 1996; Ribeiro et al., 1996). It shows a transpressive stress field, with subhorizontal NW–SE compression and minor E–W extension. The σ_1 axis is perpendicular to the major neotectonic lineaments, and subparallel to the regional NNW–SSE direction of plate convergence;

(B) The central Betics also show a complex seismotectonic pattern with predominant normal faulting, and seismicity is mostly related to the formation of

Neogene–Quaternary intramountain basins (Morales et al., 1990; Galindo-Zaldívar et al., 1999; Muñoz et al., 2002; Stich et al., 2003; Martínez-Martínez et al., 2006). This zone is characterized by an extensional stress field, with near-vertical compression (σ_1 axis) and near-horizontal ENE-WSW extension (σ_3 axis). In addition, several very deep earthquakes (>600 km) below the Granada region show a stress pattern with main stress axes plunging about 45º. This feature has been correlated with older oceanic crust subduction processes (Buforn et al., 1997 and 2004; Blanco and Spakman, 1993).

(C) In the eastern Betics and the Alborán Sea, strike-slip and normal faulting prevail, suggesting extensional tectonics in the context of Eurasian-African plate convergence (Mezcua and Rueda, 1997; Bezzeghoud and Buforn, 1999; Stich et al., 2003). Seismicity is consistent with a regional transtensional stress field having nearly N–S average compression and NE-SW extension;

(D) The Rif region exhibits a complex seismotectonic pattern that includes E–W and NE–SW fault planes with sinistral strike-slip mechanisms (Morel and Meghraoui, 1996; Stich et al., 2003). It shows a strike-slip to transtensional stress field, similar to the one observed in the eastern Betics, with average compression oriented NNW-SSE;

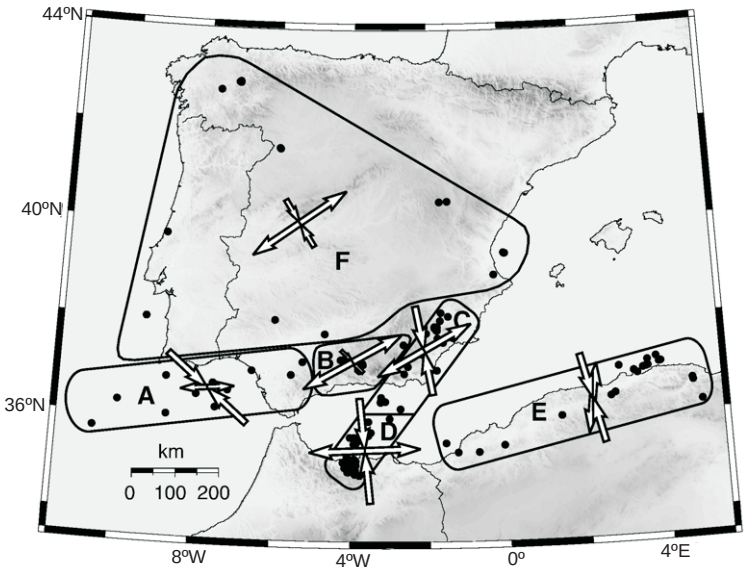

Figure 1-18. *Regional average stress tensors for different domains (white arrows) and the distribution of seismicity over the Iberia–Africa plate boundary (plotted as black dots) from Stich et al. (2006)*

(E) Northern Algeria is characterized by predominantly reverse faulting in a compressive stress field with NNW–SSE compression (Stich et al., 2006);

(F) Finally, mechanisms from the Iberian Massif point to a horizontal NE-SW extensional axis and NNW-SSE compressional axis, suggesting a mixture of extensional and strike-slip regimes in the area (Stich et al., 2006).

In addition, intermediate earthquakes are concentrated in the western Betics at 4.5°W (40-120 km depth) within a zone trending southward from the Spanish coast into the Alborán Sea (Seber et al., 1996; Buforn et al., 1997; Morales et al., 1997). The stress pattern shows nearly vertical dip slip faulting with varying strike, suggesting a dominance of buoyancy forces over lateral tectonic forces at upper mantle depths (Buforn and Coca, 2002; Buforn et al., 2004; Stich et al. 2006). The existence of intermediate seismicity may be explained by the existence of a seismogenic block, of approximate dimensions 200-km long, 150-km deep and 50-km wide, on the eastern side of the Gibraltar Strait (Buforn et al., 2004).

1.3.4. Magnetotelluric research

In the southern Iberian Massif several broadband magnetotelluric (BBMT) surveys (Fig. 1-19) have been carried out both in Portugal (Monteiro Santos et al., 1999, 2002; Almeida et al., 2001, 2005) and in Spain (Pous et al., 2004; Muñoz et al., 2005). Monteiro Santos et al. (1999) detected a highly conductive zone (1-10 Ω m) at the lower crust of the Ossa Morena Zone (20-27 km). This conductor body was related to granulitic basement rocks with the presence of interconnected films of graphite (Almeida et al., 2005). The same layer, extending along the whole Ossa Morena Zone, was also detected by Pous et al. (2004) on the Spanish side, and its top was observed to spatially correlate with a broad reflector (IRB) observed by the IBERSEIS deep seismic reflection profile (Simancas et al., 2003). Other midcrustal conductive bodies in the Ossa Morena Zone are correlated with the main thrust zones and related to the interconnected graphite formed during Variscan shearing processes (Monteiro Santos et al., 2002). One of these zones corresponds to the SPZ/OMZ contact and the other to the OMZ/CIZ contact (Almeida et al., 2001; Muñoz et al., 2005). Several high-resistivity bodies found in the upper crust are related to Paleozoic series and probably to some unexposed plutons in the South Portuguese and the Ossa Morena Zones. In the Central Iberian Zone, a high-resistivity body extending to the whole crust is correlated with extensive late Variscan granite intrusions (Pous et al., 2004). In addition, the resistivity distribution below 30 km depth at the Ossa Morena and South Portuguese Zones (Monteiro Santos et al., 1999) indicates a quite uniform upper mantle (200-400 Ω m). Finally, a 3D model including all the previous MT data was put forth (Muñoz et al., 2008). Just recently, a long-period magnetotelluric (LPMT) survey was performed in the Iberian Peninsula (Pous et al., 2009).

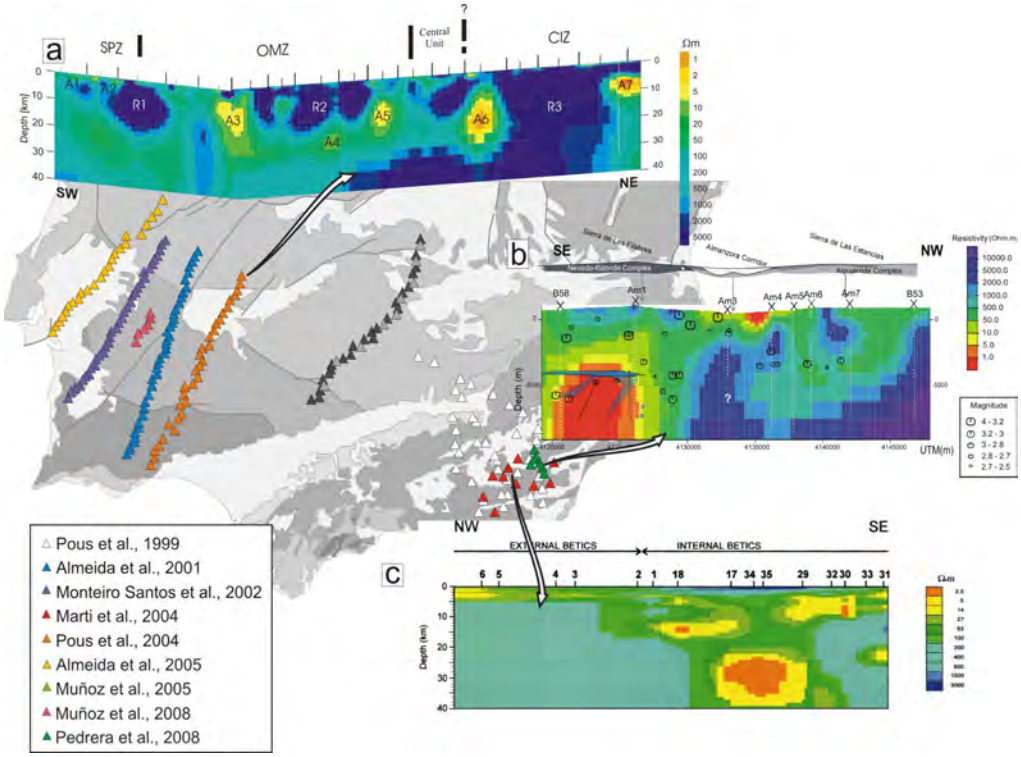

Figure 1-19. *Location of the magnetotelluric research performed in the Betic Cordillera and SW Iberian Massif (triangles represent MT sites); Two-dimensional electrical resistivity models of several transects from* **a)** *Pous et al. (2004),* **b)** *Pedrera et al. (2009) and,* **c)** *Pous et al. (1999).*

Southwards, in the Betic Cordillera, BBMT studies are scarce and only focused in its eastern part (Fig. 1-19). The first MT research (Pous et al., 1999) was a NW-SE transect from the Guadalquivir Basin, crossing the External Zones and reaching the Internal Zones of the Cordillera. The 2D model revealed a large conductive body at lower crustal depths, beneath the Internal Zones, that was interpreted as partial melting. A study of the geoelectric dimensionality based on the rotational invariants of the magnetotelluric tensor (Martí et al., 2004) was carried out at the same transect including new sites located within the Iberian Massif. A 3-D model of the crust reveals a shallow conductive body under Sierra de Los Filabres that possibly corresponds to basic igneous rocks (Martí et al., 2006). Finally, a detailed study of the upper crustal structure of the Sierra de los Filabres-Sierra de las Estancias (Pedrera et al., 2009), including geological field data and several geophysical methods, reveals the location of a conductive basic rock body at 4 to 9 km depth that has been related to the nucleation and development of the Sierra de Los Filabres antiform. West of the Granada Basin there is a lack in magnetotelluric data, so that further work must be tackled to better understand the geodynamic evolution of this zone.

1.3.5. Heat flow

Data acquired in the southern Iberian Peninsula (Fig. 1-20) revealed that the surface heat flow clearly varies from the Iberian mainland (65 ± 10 mW/m^2) to the Atlantic and the Mediterranean margins, where the heat flow reaches minimum (40-50 mW/m^2) and maximum values (80-100 mW/m^2), respectively (Fernández et al., 1998). The central and western Betics are characterized by low heat flow values (60 mW/m^2), whereas eastward and along the northern margin of the Alborán Sea, surface heat flow increases, reaching intermediate values (80–90 mW/m^2). At the Alborán Sea, a remarkable increasing trend in heat flow patterns exists from the western (69 ± 6 mW/m^2) to the eastern (124 ± 8 mW/m^2) part of the basin (Polyak et al., 1996). In the Rif Cordillera, values range from 50 to 90 mW/m^2, and heat flow values around 60 mW/m^2 are attained in the stable basement of the Meseta (Rimi and Lucazeau, 1987; Rimi et al., 1998). Over the Gulf of Cadiz prism, heat flow decreases systematically towards the east (from 57 mW/m^2 to unusually low values of 45 mW/m^2; Grevemeyer et al., 2009).

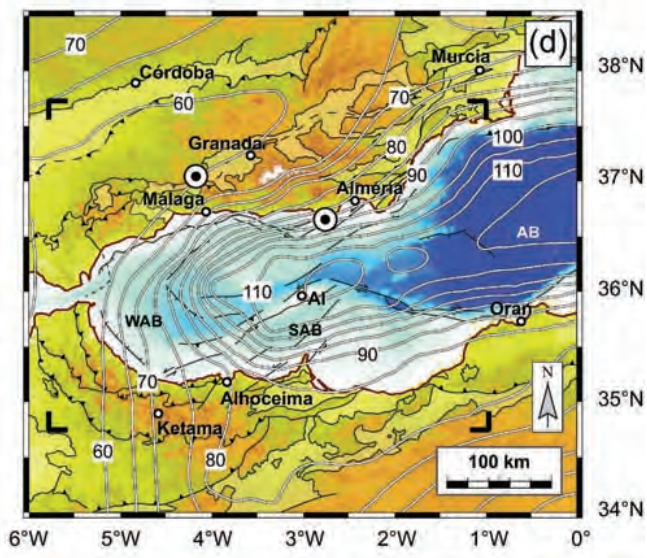

Figure 1-20. *Regional heat flow pattern modified from Fernández-Ibáñez and Soto, (2008) (in mW/m^2) and based on Fernàndez et al., 1998, Rimi et al., 1998, Polyak et al., 1996 and Pollack et al., 1993.*

Combining heat-flow, heat-production and elevation data it is possible to deduce the lithospheric structure of a region. The Iberian mainland is characterized by a lithospheric thickness of 110 ± 5 km that is maintained across the West Atlantic margin. Meanwhile, towards the Mediterranean margin the lithospheric thickness decreases down to 60-40 km (Fernàndez et al., 1998). In the Alborán Sea, an abrupt decrease in the

lithospheric thickness occurs from the western (50-90 km) to the eastern Alborán Basin (Polyak et al., 1996). Based on this approach, it is inferred that the crustal thickness should be about 14-16 km in the western Alborán Basin and between 11.5 and 14.5 km in the eastern Alborán Basin. Recent studies in the Cadiz Gulf (Grevemeyer et al. 2009) interpret the new heat flow data consistent with the prediction of heat flow derived from a finite element thermal model of an east-dipping subduction zone (Thiebot and Gutscher, 2006).

1.3.6. Rheological models

Fernández-Ibáñez and Soto (2008) modeled the rheology of the crust based on the crustal seismicity and additional geophysical data. Crustal yield strength and depth of the brittle-ductile transition zone (BDT) describe the curvature of the Gibraltar Arc with maximum depths of 12–9 km, and shallowing eastward in the Betics and Rif to 6–5 km in depth (Fig. 1-21). Maximum earthquake concentrations are immediately above or within the BDT zone (~16%), decreasing exponentially below this zone. Although 60% of the seismicity occurs in the brittle upper crust, there are also numerous events located below the BDT, in the ductile part of the lithosphere. They interpret the BDT as a decoupling horizon within the crust, capable of localizing strain and developing major detachment faults that condition the present-day deformation partitioning.

1.4. Geodetic studies

Continuously recording GPS observations in the last decades have made it possible to calculate the Euler vectors for relative motion of the Eurasian and African plates (DeMets et al., 1994; Sella et al., 2002; Calais et al., 2003; McClusky et al., 2003; Serpelloni et al., 2007). The geodetically derived models differ significantly in their proposed relative displacements due to the different determination of the rotation pole, although all of them predict a roughly northwest displacement of Africa with respect to Eurasia of 4-5 mm/a (Fig. 1-22). Moreover, GPS results are different than geological models, such as the NUVEL-1A, based primarily on the analysis of magnetic anomalies and transform fault orientations for a 3 Ma average. It could be observed that GPS data imply a more westward motion of Africa relative to Eurasia than the NUVEL-1A model, and slower convergence velocities. Calais et al. (2003) interpreted these discrepancies as possible changes in the last 3 Ma of Eurasia-Africa relative motion.

Recent densification of local GPS networks in Morocco and Spain has allowed deformation rates in the Gibraltar Arc area to be calculated (Stich et al., 2006; Fadil et al., 2006). These results are scarce, still have large errors and differ considerably from the global geodetic models owing to the scarce number of stations and the short recording period. However, they do constitute an approach for constraining the deformation due to regional and local structures in the Betic-Rif Cordillera. Results of both studies show remarkable differences in direction and magnitude between velocity vectors calculated for the same stations. Fadil et al. (2006) point out that surface deformation in Morocco

is roughly related to southward motion of the Rif relative to stable Africa (~3 mm/a), approximately normal to the direction of Eurasian-African convergence. Stich et al. (2006) estimate that ~ 2 mm/a of Eurasian-African plate convergence are currently accommodated in the Moroccan Atlas, and ~ 2 mm/a at the SW-Iberian margin, while Alborán extension can be quantified as ~ 2.5 mm/a along a NE-SW direction.

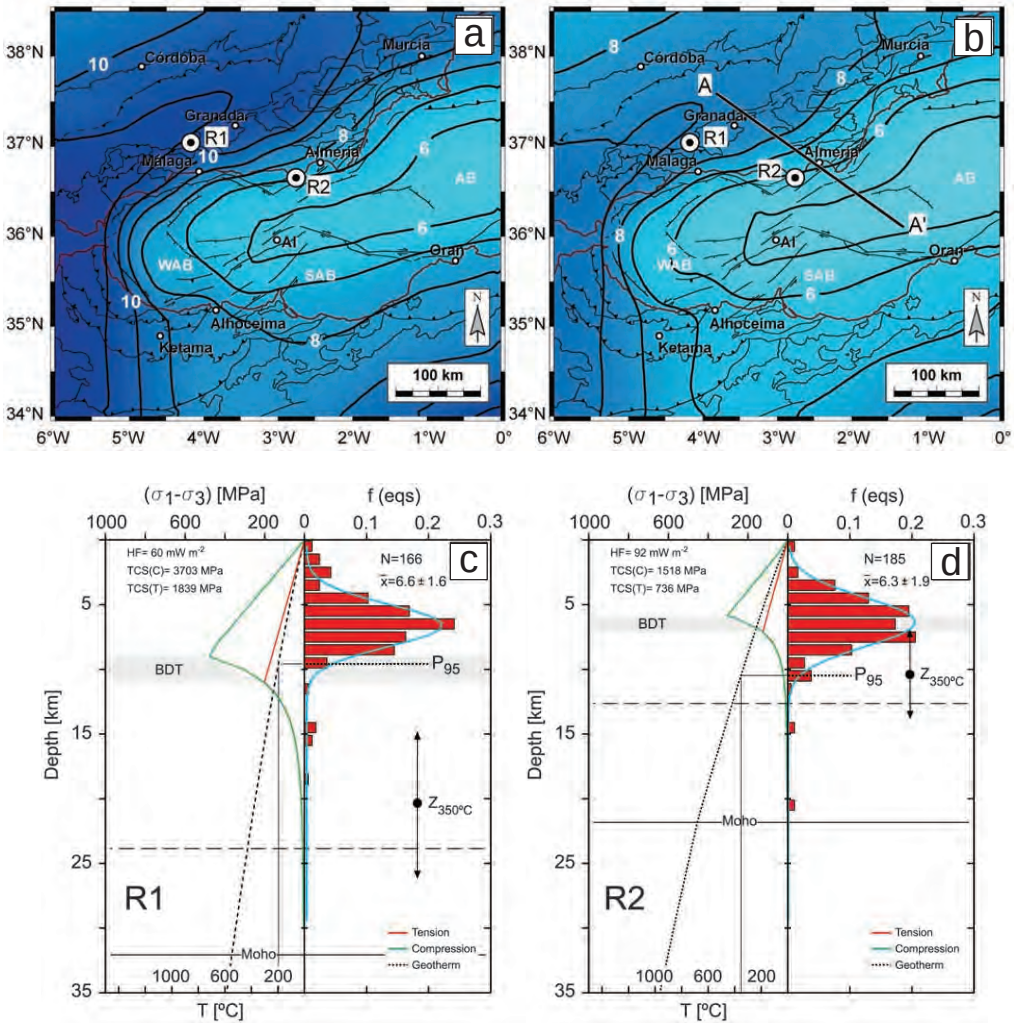

Figure 1-21. *Depth of the brittle-ductile transition (km) in the Gibraltar Arc under* **a)** *tension and* **b)** *compression; AI, Alborán Island; AB, Algerian Basin; SAB, South Alborán Basin; and WAB, West Alborán Basin. Rheological profiles and focal depth distribution of seismic events in;* **c)** *central Betics, and* **d)** *the northern margin of the Alborán Sea. The statistical distribution with the best fit (Gaussian) is also shown. P95 shows 95% of seismicity. Depths of the 250ºC, 350ºC, and 450ºC isotherms are indicated by the vertical arrows (from Fernández-Ibáñez et al., 2008).*

Based on these data, several authors have framed their results in the general geodynamical models proposed for the western Mediterranean until now. Serpelloni et al. (2007) remark that GPS data across the Gibraltar Arc support the hypothesis that eastward slab rollback is mostly slowed down or stopped because no significant but coherent deformation is occurring between the stations located on both sides of Morocco and Iberia. Fadil et al. (2006) observed southward displacement of stations in Morocco and suggested that it could be explained by the delamination and southward rollback of the African lithospheric mantle under the Alborán and Rif Cordillera.

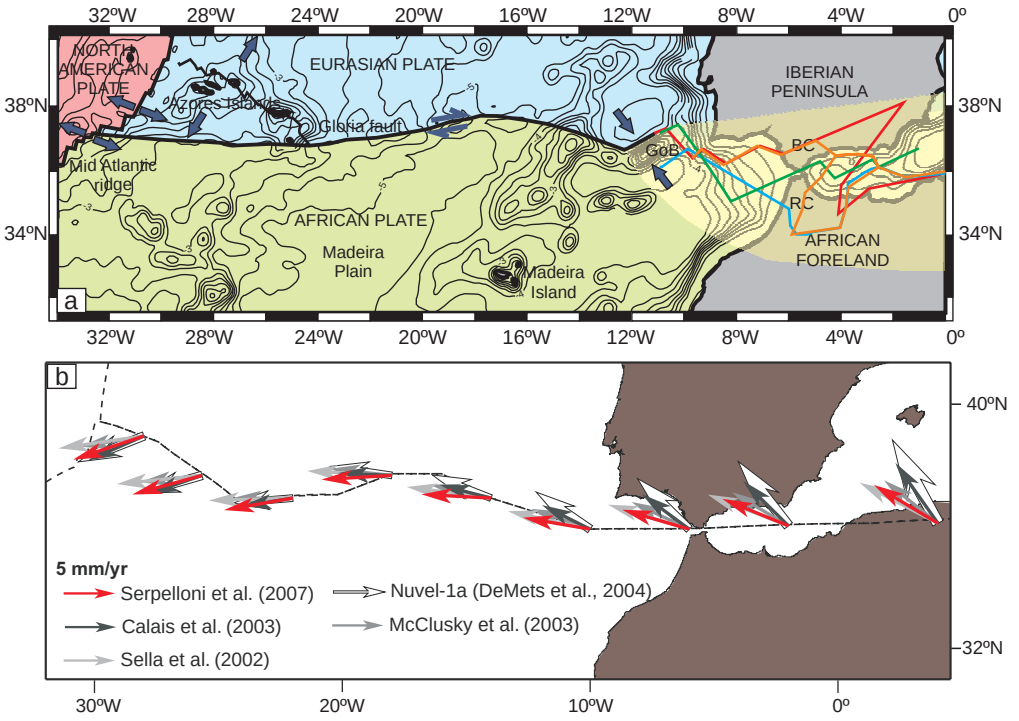

Figure 1-22. *Eurasian-African relative plate motion in western Mediterranean and Atlantic Ocean.* **a)** *Eurasian-African plate boundary sketch. Several proposed plate boundaries at the Gibraltar Arc are drawn (Klitgord and Schouten, 1986; Bird, 2003; Gutscher, 2004; Fadil et al., 2006); GoB: Gorringe Bank; BC: Betic Cordillera; RC: Rif Cordillera;* **b)** *Eurasia-Africa kinematic boundary conditions predicted by geologically and some geodetically derived relative Euler poles, along a simplified plate boundary (dashed line). Arrows show the displacement vectors and rates (in mm/a) of the African plate with respect to the Eurasia plate, modified from Serpelloni et al. (2007).*

1.5. Recent tectonic evolution of the Gibraltar Arc

Since the 1970s, a variety of geodynamic models have been proposed to shed light on the development and evolution of the Gibraltar Arc (Fig. 1-23). Till now, this matter remains controversial due to the progressive inclusion in the debate of new geological and geophysical data, including: (1) distribution, age and nature of the neogene volcanism; (2) occurrence of intermediate and very deep seismicity; (3) diffuse plate boundary with distributed deformation; (4) coeval thrusting on three sides of mountain fronts of the External Zones (Betics, Gibraltar Arc, Rif) and extension in the Internal zone (Alborán Sea and surrounding areas); and (5) location of deep seismic anomalous bodies.

The earliest models (Fig. 1-23a) tried to explain the arched geometry of the orogen and the fold-and-thrust-belt structure of the External Zones based on the westward emplacement of a rigid microplate constituted by the Internal Zones of the Cordillera (Alborán Domain) over the South Iberian and North Africa paleomargins (Andrieux et al., 1971; Andrieux and Mattauer, 1973). The tectonic escape of the Alborán microplate was explained as a consequence of the irregularities between the plate's boundaries (Tapponier, 1977), and was the mechanism invoked by later authors to explain the development of roughly E-W dextral strike-slip faults in the Betic Cordillera and sinistral strike-slip faults in the Rif (Bourgois, 1978; Sanz de Galdeano, 1983; Leblanc and Olivier, 1984; Bouillin et al., 1986, Martín-Algarra, 1987; Durand-Delga and Olivier, 1988; Dewey et al., 1989).

The presence of the Alborán Sea extensional basin in the inner part of a compressional orogenic belt was initially attributed to mantle diapir rising, radial emplacement of gravitational nappes, and subsequent cooling and thinning at the Alborán Sea (Fig. 1-23b; Cloetingh and Nieuwland, 1985; Weijermars et al., 1985). A diapiric intrusion is also the mechanism initially proposed to explain the emplacement of the Ronda peridotites (Bonini et al., 1973; Loomis, 1975). During the 80s, a reinterpretation of the thrust contacts between the main metamorphic complexes of the Internal Zones (Egeler and Simon, 1969) as low-angle normal faults (Aldaya et al., 1984; Galindo-Zaldívar, 1986; García-Dueñas and Balanyá, 1986; Galindo-Zaldívar et al., 1989; Platt and Vissers, 1989) implied the consideration of the Alborán domain as a tectonic wedge with a basal thrust (Gibraltar thrust) and extensional tectonics at the rear during its emplacement to the west (Balanyá and García-Dueñas, 1987; Jabaloy et al., 1992).

The advance of geophysical methods in the 90s, above all the seismic tomography studies, provided new constraints to the former models and gave rise to new hypotheses that could be clustered in three groups:

(1) Models associated with detachment and/or delamination of subcontinental lithosphere beneath the Alborán Sea

These models explain the simultaneity of shortening within the External Zones and extension in the Internal Zones through the removal and assimilation of the thickened lithospheric root of the orogen due to Late Oligocene-Early Miocene convective processes (Fig. 1-23c; Houseman et al., 1981; Platt and Vissers, 1989) or by lithospheric delamination (Fig. 1-23d; Docherty and Banda, 1995; García-Dueñas et al., 1992; Seber et al., 1996) provoking collapse and radial extension of the crust. In the former hypothesis the convection occurs below a fixed depocentre, whereas in the latter it would occur beneath a depocentre that migrates toward the western Alborán Sea. Seismic tomography data (Calvert et al., 2000a) reveal two high velocity bodies dipping to the SE beneath the Alborán Basin at intermediate (60-400 km) and very deep levels (570-650 km), a finding that has been related to the existence of a delaminated lithosphere.

(2) Models involving subduction associated with slab roll-back and/or detachment of the subducted slab

Numerous and contradictory subduction models with different geometry and polarity have been proposed for the Miocene evolution of the Betic-Rif Cordillera. The first models suggested a northward dipping subduction zone (Araña and Vegas, 1974; De Jong, 1991 and 1993; Wortel and Spakman, 1992; Zeck et al., 1992). Torres Roldán et al. (1986) proposed the existence of a double oceanic crust subduction zone active up to the Late Miocene. Chalouan et al. (2001) and Chalouan and Michard (2004) also supported two variables for the double-polarity subduction based on the different ages attributed to the metamorphism. An eastward dipping subduction with subsequent slab-rollback to the west has been widely proposed, fundamentally based in tomographic studies (Fig. 1-23e; Blanco and Spakman, 1993; Duggen et al., 2004b, 2005; Morley, 1993; Royden, 1993; Lonergan and White, 1997; Hoernle et al., 1999; Gutscher et al., 2002; Gill et al. 2004; Spakman and Wortel, 2004; Thiebot and Gutscher, 2006). Blanco and Spakman (1993) also described the break-off of the slab and its sinking into the astenosphere based on a positive seismic velocity anomaly between 200 and 650 km and in the existence of very deep earthquakes (Buforn et al., 1991). Later, Zeck (1996) supported the previous model by isotopic thermometers and palaentological data. In addition, a southward dipping continental subduction of the Iberian Massif below the Málaga region has been proposed based on the intermediate seismicity distribution, stress state and seismic tomography of the crust and the upper mantle of southern Iberia (Serrano et al., 1998; Morales et al. 1999).

(3) Subduction and delamination: a hypothesis combining both mechanisms

This model was proposed to explain the geochemical evolution of the Neogene magmatism of the region. The roll-back of an E-dipping Miocene subduction beneath

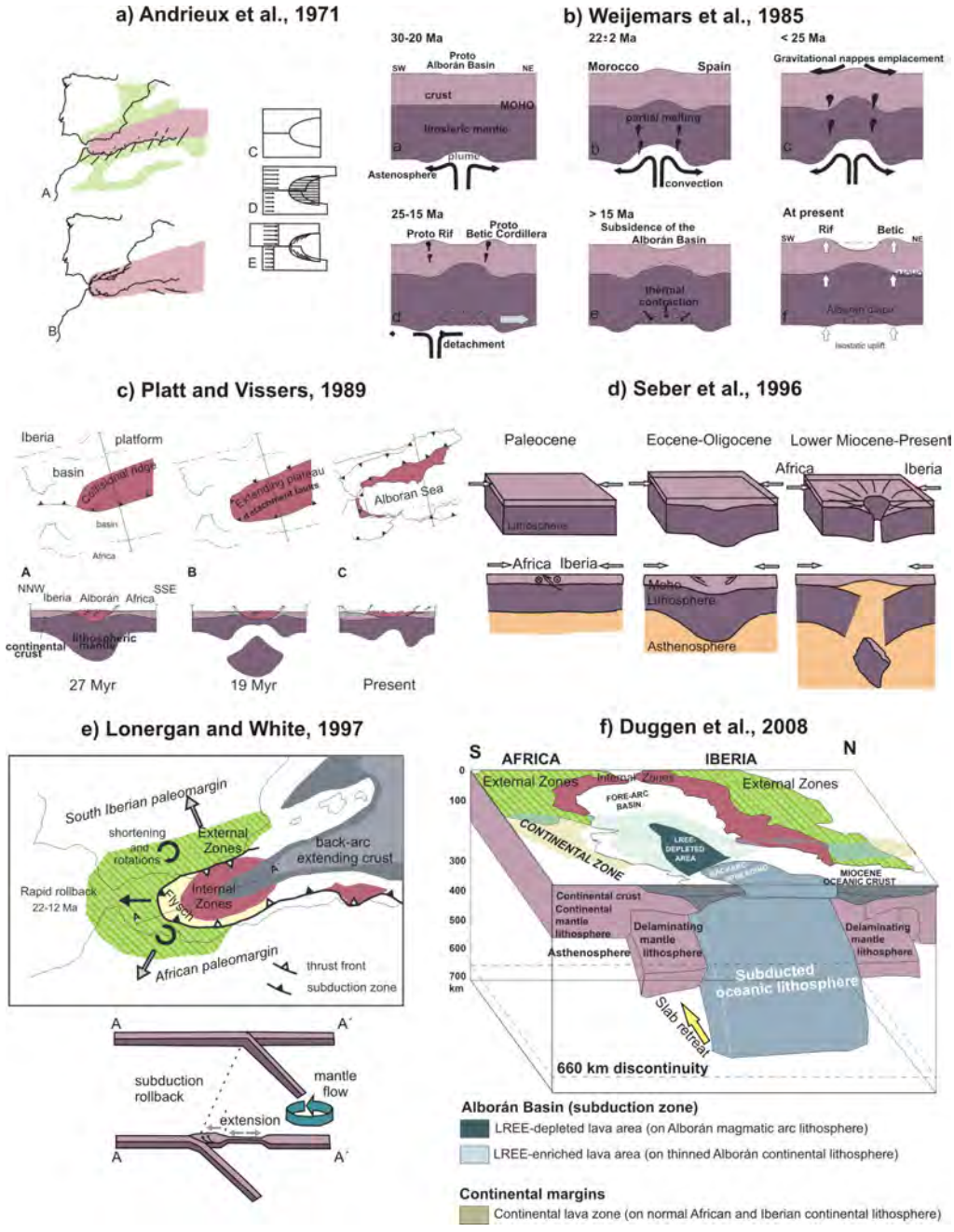

Figure 1-23. *Outline of the main geodynamic models proposed for the Betic-Rif Cordillera evolution.*

the Alborán Basin could be the engine that provoked Late Miocene delamination of subcontinental lithosphere beneath the continental margins of Iberia and Africa (Fig. 1-23f; Duggen et al., 2004a, 2008; Martínez-Martínez, 2006). The upwelling of sub-lithospheric mantle beneath these margins replaced the delaminating subcontinental lithospheric mantle.

In this framework, the lack of detailed deep geophysical data does not allow to constrain and choose among the wide variety of proposed models. Most of the present-day discussions are based on incomplete datasets that are taken into account for very controversial and even contradictory interpretations. Thus, the acquisition of new geological and geophysical observations is essential to focus discussion and determine the geodynamic evolution model for this complex plate boundary.

2

Aims

The western Betic Cordillera is an area of great interest for recent tectonic studies due to its location in the westernmost part of the Gibraltar Arc, a key area for our understanding of the evolution of the westernmost Mediterranean, within the framework of Eurasian- African plate interaction. The limited volume of geophysical research and detailed studies of recent and active structures comes to contrast with the amount of traditionally developed research regarding alpine tectonics, sedimentology, hydrogeology and stratigraphy. Up to now, gravity studies were limited to broad descriptions of the lithospheric structure of the Cordillera since there were no detailed gravity data for the zone. On the other hand, magnetotelluric surveys have thus far been restricted to uncovering the crustal structure in the eastern Betics. Furthermore, the lack of good outcrops is an important factor that has highly conditioned the development of recent tectonic studies.

The main aim of this Ph. D. Thesis is to contribute to the general body of knowledge of the western Betic Cordillera, concerning its evolution, deep structure and recent tectonics. This study is focused in the following aspects:

▪ Providing the first electrical anisotropy data of the upper mantle of the western Mediterranean, as measured through long-period magnetotelluric research, and comparing these data with previous seismic anisotropy studies of Pn and SKS shear wave splitting.

▪ Enhancing our knowledge of the crustal structure of the western Betic Cordillera on the basis of new and previously acquired geophysical data (gravity, broadband magnetotelluric results and seismicity). These deep data may contribute to an understanding of the recent evolution of the Betic mountain range in the context of the formation of the Gibraltar Arc.

▪ Establishing the stresses acting in the region during Neogene and Quaternary times through analysis of microfaults and earthquake focal mechanisms. They are related to the activity and main features of the seismogenic zones.

▪ Describing new morphologic, seismologic and tectonic evidence of recent and present-day deformation in the northwestern front of the Betic Cordillera in order to assess its activity.

▪ Describing in detail the recent structures (folds and faults) that deform the Ronda Basin, the most important Neogene sedimentary basin in the western Betics.

▪ Determining the deep geometry and nature of the basement below the Ronda Basin, using gravity data, in order to discuss the role of the basement´s nature on the reactivation of previous folds.

3

Methodology

The combination of geological and geophysical methods provides optimal results in the analysis of complex tectonic regions. While geological methods allow for direct observation of tectonic structures at surface and can reveal their shallow geometry and activity, geophysical methods serve to constrain their continuity in deep levels and evidence the main features of covered structures.

3.1. Geological Methods

A great variety of geological methods are used during field work. They are described in each one of the chapters in part II. For the sake of convenience, however, a brief description of the main techniques is included in this section.

3.1.1. Field geological studies

In order to constrain the main features of recent tectonic deformation of the studied transects within the western Betic Cordillera, I focus on the geological field research involving the most recent rocks, which include the Neogene and Quaternary sedimentary infill of the Ronda basin and the southern border of the Guadalquivir basin. Additional field observations were undertaken to improve the interpretation of the geophysical data obtained along these transects, that include a large number of tectonic units. I fundamentally took into account the recentmost folds, faults and joints that deform these sediments. The structures that conditioned the position and geometry of the basement rocks below the Neogene and Quaternary infill were also analyzed. The MAGNA (1:50.000) geological maps, in combination with later geological studies developed in the region, constitute a valuable base for geological field work: identifying the main structures is an initial step for the development of more detailed studies. The MAGNA maps that cover the studied area are: Carmona-985 (Roldan García, 1988); Marchena-1004 (Pignatelli García et al., 1977); Morón de la Frontera-1021 (Martín Serrano, 1986); Olvera-1036 (Cano Medina, 1990); Teba-1037 (Cruz San Julián, 1990); Ubrique-1050 (Moreno Serrano et al., 1990); Ronda-1051 (del Olmo Sanz et al., 1990). It is necessary to bear in mind the difficulties surrounding structural field work in the Guadalquivir basin due to the lack of good outcrops, the flat topography and regionally intensive agriculture. In many cases it may be complicated to discern the lateral continuity of lithological contacts, folds and faults, making necessary some additional analysis of aerial photographs and satellite images.

The most accurate study of folds was carried out in the Ronda Basin, where metric-scale up to kilometric-size folds deform the sedimentary infill and the basement units. It was necessary take into account the existence of different scale cross-bedding in Late Tortonian-Late Messinian calcarenites, which at some points impeded determination of the strata orientation in small outcrops, and may have led to an incorrect fold reconstruction.

The analysis of fractures includes faults and joints. Faults are scarce in recent rocks of the studied transects, and their orientation has been characterized in order to determine the paleostresses, established in outcrops with many and well exposed faults. Field work was aimed to determine their main features: fault surface geometry (strike, dip) and kinematic characteristics, including the trend of motion (striae, fault grooves) and the movement sense (step asymmetry on the fault plane, trails, cataclastic foliations and Riedel faults). The joint attitude was also determined as complementary evidence for stress field determination.

3.1.2. Paleostress determination

Paleostress determination through the analysis of microfaults was performed in reduced outcrops with a great deal of striated fault surfaces (Fig. 3-1). When possible, the fault kinematics should be determined along with the superposition and reactivation of different fault planes.

Fig. 3-1. *Striae and grooves on a mineralised fault plane.*

In this Ph. D. Thesis, the paleostress field was determined using the Search Grid Method (Galindo-Zaldívar and González-Lodeiro, 1988). This method is based upon analysis of the microfault planes and orientation of the striae from both known and

unknown regimes, and provides data on the main stress axes orientations ($\sigma_1 > \sigma_2 > \sigma_3$) and the axial ratios ($R = (\sigma_2 - \sigma_3)/(\sigma_1 - \sigma_3)$). The method allows us to distinguish different overprinted stresses. It considers the striae to run parallel to the maximum shear stress (Bott, 1959) and the stress field to be homogeneous at the outcrop scale. In prolate ellipsoids (axial ratios: 0-0.33), the σ_2 and σ_3 axes have similar values, the σ_1 axis being the most significant one. In oblate ellipsoids (axial ratios: 0.66-1), meanwhile, σ_1 and σ_2 have similar magnitudes, and the extensional axis is well defined.

3.2. Geophysical Methods

An important aspect of the development of this thesis was the acquisition of new geophysical data, and their subsequent processing and modeling considering the geological framework.

3.2.1. Gravity

If the Earth is conceived as a perfect sphere, homogeneous and without rotation, the gravitational acceleration (g) at the surface would be constant. However, the Earth rotates, is slightly flat at the poles, and has lateral density irregularities. Therefore, gravity depends on several factors such as latitude, elevation, topography, tidal effects, instrumental drift or lateral density variations. In order to isolate the effect of density contrast caused by the geologic structures, it seems necessary to apply several corrections. These corrections will be described in the section on processing.

Instruments

A gravimeter denotes any instrument designed to measure spatial variations in gravitational acceleration. The most common type used in exploration surveys is based on a mass-spring system such as the LaCoste & Romberg, Scintrex and Worden instruments. A Master Worden gravimeter, with a maximum accuracy of 0.01 mGal, was used to acquire the data of the detailed survey of the Ronda Depression (Fig. 3-2a). Data acquisition was carried out in cycles of less than three hours in order to accurately correct the instrumental drift, tide variations and barometric changes. For the two general transects of San Pedro de Alcántara-Castilblanco de los Arroyos and Coin-Fuente Obejuna, we used a CG-5 Scintrex Autograv gravimeter with a maximum accuracy of 0.001 mGal that features tidal correction, allowing one to measure long time cycles, generally of a complete working day (Fig. 3-2b). Measurements were referenced to the base stations of the I.G.N. national gravimetric network of Málaga and Sevilla in order to calculate the absolute gravity value.

The relative positioning of the gravity stations was performed using a global positioning system (GPS) receiver, and the altitude of the stations was determined

Figure 3-2. *Equipment used to acquire the gravity data;* **a)** *Gravity measurement using a Master Worden gravimeter;* **b)** *Gravity measurement using a CG-05 Scintrex Autograv gravimeter;* **c)** *barometric altimeter and Garmin e-trex GPS.*

with a barometric altimeter with an accuracy of 0.5 m (Fig. 3-2c). So as to accurately correct for diurnal variations in elevation due to the atmosphere pressure evolution, a barograph was located near the base station during the measurement cycles. The accurate elevation of the sites was determined through the measurements at different geodetic reference points of the I.G.N. during the field data acquisition.

Processing and modeling

The Bouguer anomaly was obtained by means of the programs CICLOS and ANOMALIA developed by J. Galindo-Zaldívar. The instrumental drift and tides were linearly corrected through the CICLOS program to obtain the Observed Gravity (gobs) at each field station. After that, the theoretical value of the gravity at sea level (gl), obtained by the Geodetic Reference System formulae (GRS, 1967), must be subtracted from the gobs to correct for the earth's elliptical shape and rotation,

$$g_l = 978031.849\ (1+0.005278895\ \sin^2\varphi + 0.000023462\ \sin^4\varphi)\ (\text{mGal})$$

(φ is the latitude in degrees)

In addition, the Free Air correction (0.3086 mGal/m) may solve the elevation differences at the gravity locations with respect to the datum itself, and is considered to obtain the Free Air anomaly (g_{fa}).

$$g_{fa} = go_{bs} - g_l + 0.3086\ h\ (\text{mGal})$$

(h is the elevation above sea level)

The Bouguer correction accounts for the excess/deficit of mass underlying observation points placed at higher/lower locations than the elevation datum. The

Bouguer gravity anomaly (BG) is given by:

$$BG = go_{bs} – (g_l + 0.3086\ h) - (0.04193\ \rho\ h)\ (mGal)$$

(ρ is the average density of the rocks underlying the survey area in g/cm³)

Finally, the Terrain or Topographic correction (TC) accounts for variations in the observed gravitational acceleration caused by topography near each station. The Terrain-corrected Bouguer gravity anomaly (gt) is given by:

$$g_t = go_{bs} – (g_l + 0.3086\ h) – (0.04193\ \rho\ h) + TC\ (mGal)$$

The Free Air and the Bouguer corrections were calculated using the ANOMALIA program. The Terrain correction was determined with the GRAVMASTER program, by applying the Hammer circle (Hammer, 1939 and 1982). In the Ronda sector, topographic correction was calculated using a digital terrain elevation model with a grid of 10 meters of cell size for the first 1.600 meters (B-G Zones), and 200 meters thereafter, to a total distance of 22 kilometres (H-M Zones). For the transects, it was enough to apply a digital terrain elevation model with a grid of 90 meters of cell size for the first 22 kilometres (B-M Zones).

In a profile orthogonal to the anomaly elongation, the wavelength of the anomaly is indicative of the depth of the anomalous body. Deep and far geologic structures generate variations of the gravity field, showing large wavelengths and low gradients (regional anomaly). On the other hand, local shallow bodies give rise to small anomalies with high horizontal gradients (noise). In between these two extremes, there are bodies of real interest for researchers, located at an intermediate range of depths, that produce the residual anomaly. The Bouguer anomaly is the sum of all the effects.

Bouguer Anomaly = Regional Anomaly + Noise + Residual Anomaly

The first step to be taken when modeling the geologic structure of interest is to separate the effect of the shallow bodies by deleting the anomalous values related to noise. If the study is focalized in the regional structure, the regional anomaly is taken into account; whereas in local studies, the residual anomaly related to local bodies is isolated. It is difficult to accurately separate the two influences, although one option is to determine the regional gravity anomaly calculated from an independent data set such as the general information provided by 1:500.000 Bouguer anomaly map of the Spanish Instituto Geográfico Nacional (I.G.N, 1976), or else to construct a highly smoothed profile or map from the Bouguer Anomaly data. After that, the observed anomalies were modeled using the GRAVMAG V.1.7. program of the British Geological Survey (Pedley et al., 1993), which makes it possible to perform 2D and 2.5D models.

3.2.2. Magnetotelluric

The time-variations of the Earth's magnetic field are caused by the interaction of the solar wind with the Earth's magnetosphere. These oscillations of the magnetic field induce an electric current that generates an electric field at the Earth´s surface. The MT method is a passive electromagnetic technique based on simultaneous measurement of the natural magnetic and electric fields in orthogonal directions at the Earth´s surface (Vozoff, 1972) and on the determination of their ratios (impedance tensor) at different frequencies (related to research depths). Temperature, pressure, porosity and physical and chemical state could be important factors determining the electrical resistivity of the rocks.

Instruments

The magnetotelluric equipment includes sensors to measure the magnetic and electric fields and to store the data. The sensors used to measure the three components of the magnetic field (H_x, H_y, H_z) are designed for different period ranges. Induction coils are the most common sensor for shallow targets. The number of loops in the coil would depend on the period measured; yet nowadays, the same coil could be used for a broad range of periods considering calibration factors (Fig. 3-3a). For long-period surveys, the magnetic field is registered with a flux-gate magnetometer (Fig. 3-3b).

The two horizontal components of the electric field (Ex, Ey) are determined measuring the potential difference between two pairs of non-polarizable electrodes placed in orthogonal directions, generally N-S and E-W, and spaced at a sufficient distance (50-100 meters) to guarantee that voltage could be registered by the data logger. The electrodes must be in contact with the soil and buried 30-70 cm deep in order to avoid temperature and humidity changes. At dry places and for long time measurements it is common to put wet kaolin and copper sulphate at the base of the electrode to preserve humidity and provide a good contact.

The electric and magnetic sensors are connected to a central unit or data logger (ADU-06 for broadband equipment or LEMI-417 for long-period equipment) that allows for acquiring, filtering and amplifying the electric and magnetic field signals. It stores the data and converts them from analogical to digital format in order to be later processed on a PC. The system is connected to a GPS antenna to locate the measurement site and synchronize the signal received by the different recording stations, in order to apply remote reference methods to improve the results in noisy stations.

Processing

As pointed out earlier, the magnetotelluric method is based in the simultaneous measurement of the five components of the magnetic (H_x, H_y, H_z) and electric fields

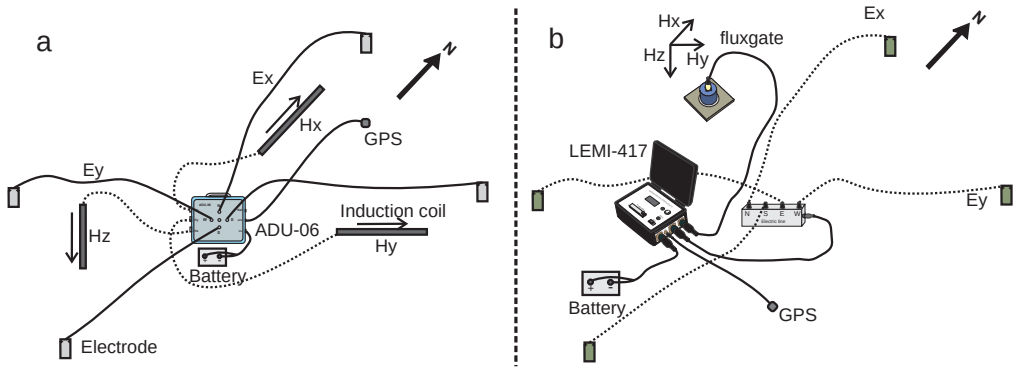

Fig. 3-3. *Field installation sketch of the different components of the;* **a)***broad-band metronix ADU-06; and* **b)** *the long-period LEMI-417 equipment.*

(E_x, E_y). They are recorded as time series that represent wave amplitude versus time. These time series could be converted, using a Fourier transform, from the time domain through the frequency domain. Finally, we could obtain the impedance tensor (Z), also called transfer functions. This tensor linearly represents the electric and magnetic field components for each frequency (Vozoff, 1972):

$$E_x = Z_{xx} H_x + Z_{xy} H_y$$
$$E_y = Z_{yx} H_x + Z_{yy} H_y$$

Through the impedance tensor, we obtain eight unknown elements of the equation (4 real: ρ_{axy}, ρ_{axx}, ρ_{ayx}, ρ_{ayy}; and 4 imaginary ones: φ_{xy}, φ_{xx}, φ_{yx}, φ_{yy}) and four equations to solve for each studied frequency. This system could be determined using statistical methods, because the same frequency is repeatedly measured for the time series record. Estimates of the complex elements of Z were obtained using robust processing techniques (Huber, 1981).

Through estimation of the impedance tensor, we were able to obtain the apparent resistivity values (ρ_a) and phase (φ) for each frequency analyzed:

$$\rho_{a,xy}(T)=T/(2\pi\mu)[Z_{xy}(T)]2$$
$$\varphi_{xy}(T)=\arctan\{Im(Z_{xy}(T))/Re(Z_{xy}(T))\}$$

Im and Re being the imaginary and real parts of the impedance tensor, respectively; μ is the magnetic permeability in the free-space and T is the period measured.

The penetration of an electromagnetic wave in a MT sounding (ρ(T), skin depth) depends on the oscillation frequency (or period) and the average resistivity of the overlying rocks (ρ_a, apparent resistivity),

$$\rho(\mathrm{T}) \approx 500\sqrt{\rho_a T} \quad \text{(m)}$$

The tipper is a useful parameter for determining the lateral resistivity variations of the studied zone. It is a vector that relates the magnetic field vertical component with the magnetic field horizontal components at each point. If we project the tipper vector in the horizontal plane, it could be decomposed into a real and an imaginary part that are orthogonal to the geological strike. These vectors are called induction arrows (Schmucker, 1970) and constitute a robust indicator of the contrast and strike of the electrical structures on a regional scale. Their graphic representation could be reversed (Parkinson convention; the arrow pointing to the conductive zones) or non-reversed (Schmucker or Weise convention; the arrow pointing away from the conductive zone).

The processing of the broadband magnetotelluric data presented here was performed using the Winglink program. Time series of the long-period magnetotelluric data were processed with a modern robust data code (Varentsov, 2007) to obtain transfer function apparent resistivities, phases and tipper.

Modeling

If we already know the components of the impedance tensor, we could perform dimensionality analysis in order to determine the geolectric strike. The dimensionality is defined as 1D if the conductivity depends only on depth. If it also depends on one horizontal direction (x,z), the study area is considered as 2D. In this case, the horizontal direction that mainly conditions the conductivity structure is called strike; and it may be related to the presence of mineralized or water saturated faults and joints, or other conductive structures as dikes. In 3D cases, the conductivity changes in two horizontal directions and with depth (x,y,z).

The study of dimensionality and the determination of the geoelectrical strike of data included in this study were based on analysis of the induction arrows and Bahr decomposition (Bahr, 1988 and 1991). The strike exhibits 90º ambiguity, which can be solved through the information provided by the induction arrows and the geological structures. After strike is determined, it is possible to develop resistivity models based on the inversion of the resistivity and phase curves. Modeling of the data was accomplished in our case using the Winglink program, which allows 1D, 2D and 3D models to be created by means of complex algorithms. In two-dimensional models, the equations describing the electromagnetic fields can be uncoupled in two independent modes: TE mode (or E-polarization), in which the electrical currents flow orthogonal to the strike; and TM mode (or H-polarization), in which the currents flow parallel to the strike. The

2D inversion of the San Pedro de Alcántara-Castilblanco de los Arroyos transect was accomplish using the RLM2DI code (Mackie et al., 1997) for both TE and TM modes. This method solves the inversion through the finite differences iterative adjustment of the resistivity and phase curves in the TE mode and the TM mode, assuming that the profile modeled is orthogonal to the electric field. For this reason, it is necessary to determine the regional strike and rotate the impedance tensor to the reference system defined by the main structures.

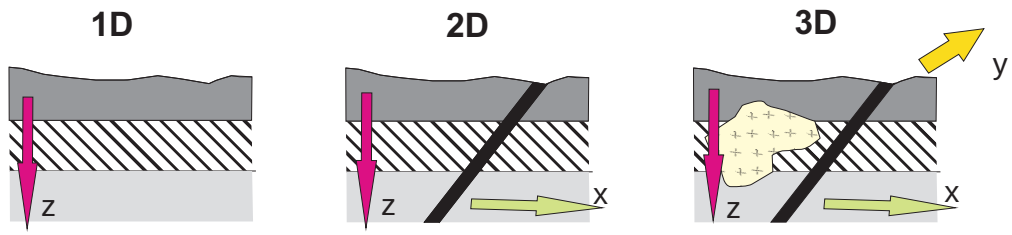

Figure 3-4. *Sketches interpreting the dimensionality of geological structures.*

3.2.3. Seismicity

A) Seismicity distribution

Earthquake distribution analysis is a tool required for locating the geological structures that may possibly be active in a region. Although faults can have a seismic or a creeping activity, large faults generally have segments of different seismic activity made evident by the seismicity distribution. It is also useful to determine the existence of deep detachment levels that could accommodate crustal deformation. In the Betic Cordillera, the existence of a layered crust with major detachment levels has been probed through several geophysical methods. Projection of the earthquake hypocenter distribution over images obtained by means of other geophysical methods, such as tomographic or magnetotelluric models, could help to clarify the main features of these active structures.

In the context of this Ph.D. Thesis, earthquake data from the Instituto Geográfico Nacional seismicity database (Fig.3-4; I.G.N., 2007), acquired by the National Seismic Network, were analyzed. The temporal window selected for this study covers the period 1990-2006. The database was filtered in order to eliminate earthquakes located more than 20 kilometres away from the transect described in chapter 5, as well as events with magnitudes under 2.5 or that could be related to quarry explosions. In determining earthquake location, the IGN uses a velocity model constituted by flat layers (Mezcua and Martínez Solares, 1983; IASPEI-91 model). The first layer is 12 kilometre thick and the P waves propagate at 6.1 km/s. In the second layer, till a depth of 25 kilometres, the P waves propagate at 6.4 km/s. From 25 to 32 kilometres the velocity is 6.9 km/s, and for 32 km or more an infinite layer with a velocity of 8 km/s is assumed.

B) Earthquake focal mechanisms and present-day stresses

The right dihedra method (Angelier and Mechler, 1977) was applied along with Gephart's stress inversion method (Gephart, 1990) to a catalogue of earthquake focal mechanisms determined by previous authors in the San Pedro de Alcántara-Castilblanco de los Arroyos area between 1968 and 2007 (Bezzeghoud et al., 1999; Buforn et al., 1997, 2004; Coca, 1999; Coca and Buforn, 1994; I.A.G. website 2007; I.G.N. website 2007; Mezcua and Rueda, 1997; Morales et al., 1999; Stich et al., 2006). In addition, new focal mechanisms located at the Morón de la Frontera and Cañete la Real areas (Ruiz-Constán et al., 2009) were considered in order to accurately establish the stress distribution in the western transect of the Betic Cordillera. The new focal mechanisms were calculated using time-domain, least squares inversion to obtain the deviatoric seismic moment tensor following the procedure described in Stich et al. (2003).

The right dihedra method determines graphically, by means of stereographic projection, common zones of compression and tension for a given set of focal mechanisms. This method does not provide information about the stress ratio. However, Gephart's method allows one to determine the directions of main stress axes σ_1, σ_2, σ_3 and the axial ratio ($R = (\sigma_2 - \sigma_1) / (\sigma_3 - \sigma_1)$). The axial ratio is an indicator of the

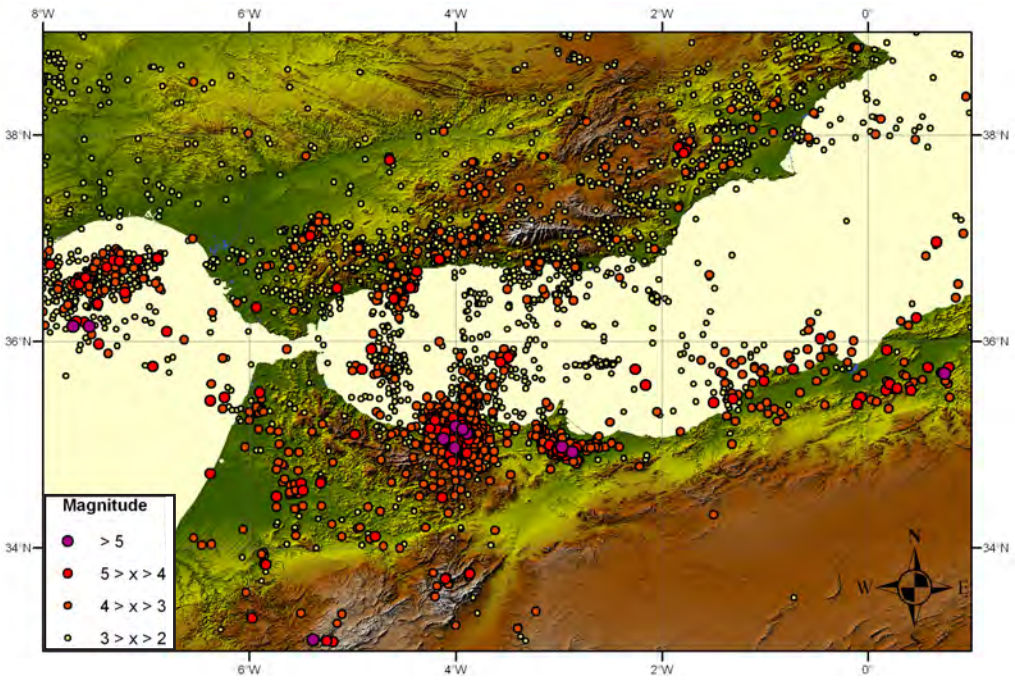

Figure 3-5. *Seismicity distribution in the Betic-Rif Cordillera and surrounding areas during the period 1990-2006 (I.G.N. 2007).*

dominating stress regime because it relates the magnitude of the intermediate principal stress to both the maximum principal stress and the minimum principal stress. The method is based on a robust inversion scheme that places less emphasis on erratic data and does not require knowledge of the true fault plane, since the nodal plane with the smaller misfit is chosen as the fracture plane.

PART II

4. Deep deformation pattern from electrical anisotropy in an active arched orogen (Betic Cordillera, western Mediterranean)

5. Crustal structure, recent and active deformation and stress in the frontal part of a continental collision: a northwestern Betic Cordillera transect

6. Is the northwestern Betic Cordillera mountain front active in the context of the convergent Eurasia-Africa plate boundary?

7. Gravity anomalies and orthogonal box fold development on heterogeneous basement in the Neogene Ronda Depression (western Betic Cordillera)

Outline

The present section tries to briefly describe the structure of the Ph.D. Thesis to favour a better understanding of the text. In the Part I, it was summarized some introductory data relevant to focused the studied area and previous geological and geophysical researches (Chapter 1). In chapters 2 and 3, respectively, I settled the aims of this study and described the different geological and geophysical methods applied.

The main body of the text (Part II) comprise four articles that describe new geological and geophysical data in the western Betic Cordillera and their implications in the recent evolution of the area.

Chapter 4, "*Deep deformation pattern from electrical anisotropy in an active arched orogen (Betic Cordillera, western Mediterranean)*" presents long period magnetotelluric data acquired in the SW Iberian Massif and the western Betic Cordillera that provide first evidence of electrical anisotropy in the upper mantle of the Mediterranean region. This contribution attempts to integrate the electrical anisotropy data with seismic anisotropy data to discuss the mantle deformation patterns that may be produced by the different geodynamic models proposed.

Chapter 5, "*Crustal structure, recent and active deformation and stress in the frontal part of a continental collision: a northwestern Betic Cordillera transect*" presents the first broad-band magnetotelluric data in western Betics and reveals the existence of a deep conductive southward dipping body. MT data are combined with new gravity data and seismicity distribution to corroborate the deep structure along a transect from the Iberian Massif foreland towards the Málaga coast. In addition, the present day stress analysis is established through the analysis of earthquake focal mechanims.

Chapter 6, "*Is the northwestern Betic Cordillera mountain front active in the context of the convergent Eurasia-Africa plate boundary?*" describes new morphologic, seismologic and neotectonic evidence of recent and present-day deformation in the northwestern front of the Betic Cordillera through the analysis of microfaults (Morón de la Frontera- Puebla de Cazalla sector) and new earthquake focal mechanisms.

Chapter 7, "*Gravity anomalies and orthogonal box fold development on heterogeneous basement in the Neogene Ronda Depression (western Betic Cordillera)*" provides a description of the main tectonic structures that deform the Neogene sedimentary infill of the Ronda Basin. New gravity data allows to determine the distribution of evaporitic rocks below the sedimentary infill and to discuss the role of their distribution on the reactivation of basement antiforms that affect the Neogene infill.

The Part III jointly discuss (Chapter 8) and summarize the main conclusions (Chapter 9) of the Thesis in the frame of the Gibraltar Arc evolution. Finally, Chapter 10 tries to schematize the future perspectives of the geological and geophysical researches in this area.

4

Deep deformation pattern from electrical anisotropy in an active arched orogen (Betic Cordillera, western Mediterranean)

A. Ruiz-Constán [1], J. Galindo-Zaldívar [1,2], A. Pedrera [1], J. A. Arzate [3], J. Pous [4], F. Anahnah [1], E. Asensio [4], C. Marín-Lechado [5], W. Heise [6], F. A. Monteiro Santos [6]

Submitted for publication

Long period magnetotelluric data acquired in the Iberian Massif and the Betic Cordillera arched orogen provide first evidence of electrical anisotropy in the upper mantle of the Mediterranean region. Strike analysis at different periods reveals preferred structure orientation related to olivine elongation in the mantle, and points to a heterogeneous anisotropy pattern. At deep levels (periods $\geq 10^4$ s), all the sites show a common N-S geoelectrical strike (~N170ºE), which may represent a low intensity deformation, possibly related to 'frozen' pre-alpine plate tectonics. For periods between 10-10^3 s, a N-S constant strike (~N180ºE) at the Betic Cordillera sites contrasts with the E-W strike (~N85ºE) in the Iberian Massif. An increase in the module of the induction arrows from the Iberian Massif to the inner part of the Betic Cordillera probably reflects higher deformation towards the axis of the Eurasian-African plate boundary. The integration of electrical anisotropy data with seismic anisotropy allows us to discuss mantle deformation patterns produced by delamination and subduction, suggesting that the latter mechanism may be more suitable for the alpine evolution of the western Gibraltar Arc.

Key words: Eurasian-African plate boundary, Gibraltar Arc, magnetotelluric, mantle deformation.

1. Departamento de Geodinámica. Universidad de Granada.
Campus Fuentenueva, 18071-Granada, Spain.
2. Instituto Andaluz de Ciencias de la Tierra. Facultad de Ciencias.
3. Centro de Geosciencias. Universidad Nacional Autónoma de México
4. Departament de Geodinámica i Geofísica. Universitat de Barcelona.
5. Instituto Geológico y Minero de España
6. Departamento de Física y Centro de Geofísica. Universidade de Lisboa

4.1. Introduction

Our knowledge of lithospheric mantle deformation is poor, due to the lack of accurate deep geophysical techniques and the scarcity of peridotite outcrops. The magnetotelluric (MT) method allows for characterization of the electrical conductivity of the lithosphere, proving a sensitive tool for determining its structure and strain. The electrical anisotropy is interpreted to be associated with preferred interconnection of conductive minerals at crustal levels or with hydrogen diffusion along the olivine a-axis in the mantle (Mareschal et al., 1995). In recent years, long period magnetotelluric (LMT) research has started to shed light on the structure of the lithospheric mantle, which was traditionally deduced from seismic anisotropy, related to the strain-induced alignment of the olivine at mantle depths (Silver and Chan, 1988). The comparison between electrical and seismic techniques provides an exciting prospect to envisage the deep evolution of orogens, although there is no consensus regarding the correlation between both results (Ji et al., 1996; Eaton et al., 2004; Hamilton et al., 2006).

New LMT data from the western Betic Cordillera provide the first electrical anisotropy results of the upper mantle of the western Mediterranean. They are integrated with previous seismic anisotropy studies of Pn and SKS shear wave splitting. The aim of this study is to discuss the recent geodynamic evolution of the western Mediterranean, where a number of controversial models have been proposed to explain the development of the Gibraltar Arc in the context of the NW-SE Eurasian-African convergent plate boundary.

4.2. Geodynamic Setting

The Betic Cordillera, together with the Rif Cordillera, forms the western end of the Alpine orogen in Europe and northern Africa (Fig. 4-1). The Alborán Sea extensional basin is located in the inner part of this arcuate orogenic belt, which formed during the Neogene in a general setting of Eurasian-African plate convergence (Dewey et al., 1989). The position and kinematics of the plate boundary are clearly established from the Mid Atlantic Ridge up to the Gorringe Bank (Fig. 4-1a). However, the plate boundary blurs to the east, where it turns into a wide area of oblique convergence with distributed deformation and where several traces of the plate boundary have been proposed without consensus (Fadil et al., 2006, and references therein).

The Betic Cordillera constitutes the northern branch of the Gibraltar Arc and has been divided into two main tectonic domains: the Internal and the External Zones, separated by the Flysch units (Fig. 4-1b). The Internal Zones are made up of thrust stack of metamorphic complexes involving mainly Palaeozoic and Triassic rocks. The Ronda peridotites, conforming the largest orogenic lherzolite in the world, constitute a mantle-lithosphere slab emplaced within the western Internal Zones. The External Zones are a fold-and-thrust belt composed of Mesozoic and Cenozoic carbonatic-evaporite rocks. During the early Miocene, the Internal Zones were displaced towards

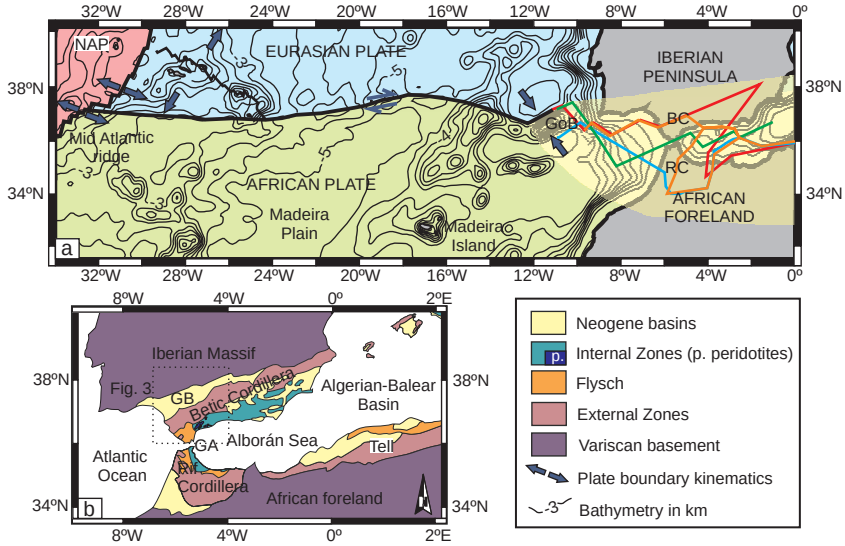

Figure 4-1. *General setting of the study area;* **a)** *Eurasian-African plate boundary sketch. Several proposed plate boundaries at the Gibraltar Arc are drawn (colored lines; Fadil et al., 2006);* **b)** *Geological sketch of the western Mediterranean. GoB: Gorringe Bank; BC: Betic Cordillera; RC: Rif Cordillera; GA: Gibraltar Arc; GB: Guadalquivir Basin; NAP: North American plate.*

the west (Andrieux et al., 1971), deforming the External Zones. At this stage, the Algerian-Balear and the Alborán basin opened simultaneously. From Burdigalian to the end of the middle Miocene, an extensional stage contributes to the exhumation of the metamorphic complexes. Since late Tortonian, the displacement of the Internal Zones towards the west was largely blocked (Sanz de Galdeano, 1990) and a N-S to NW-SE compression due to the convergence of the African and Eurasian plates occurred simultaneously with a major ENE-WSW extension. This new geodynamic setting was accompanied, from the late Tortonian up to the present, by evident vertical movements due to the NW-SE compression and to isostatic readjustments.

The Iberian Massif (Fig. 4-1b), the foreland of the Betic Cordillera, crops out to the north and forms part of the Variscan belt of central Europe. Refraction seismic profiles (ILIHA DSS Group, 1993) suggest a layered lower lithosphere down to a depth of at least 90 km. Velocities derived from reflection data indicate that the lithospheric mantle is anisotropic or that the layers underwent a slight regional dip. A N80ºE seismic anisotropic trend was determined in the southern Iberian Massif (Diaz et al., 1998).

Recent evolution of the western Mediterranean is a matter of great controversy among Earth sciences researchers. Several hypotheses have been proposed: (1) models associated with detachment and/or delamination of subcontinental lithosphere beneath the Alborán Sea (Platt and Vissers, 1989; Seber et al., 1996), and (2) models involving

subduction associated with slab roll-back and/or detachment of the slab (Blanco and Spakman, 1993; Lonergan and White, 1997; Morales et al., 1999; Gutscher et al., 2002). In more recent years a new hypothesis combining both mechanisms has been proposed (Duggen et al., 2005).

4.3. Previous deep seismic anisotropy studies

Teleseismic events recorded in the Iberian Massif and the Betic Cordillera have been inverted using Pn (Calvert et al., 2000a; Serrano et al., 2005) and SKS splitting results (Buontempo et al., 2008) to image mantle velocity and anisotropy structure (Fig. 4-2). In the eastern Alborán Sea and N Morocco, the direction of the fastest Pn velocity is roughly parallel to the Eurasia-Africa NW-SE plate convergence; whereas SKS results show an E-W trend. To the north and west, both directions are similar and run almost parallel to the main trend of the Betic Cordillera (E-W in its central part and N-S in the curvature of the Gibraltar Arc). In the Iberian Massif, however, the relationship between the direction of the fastest Pn velocity (NE-SW, Serrano et al., 2005) and major variscan tectonic trends (NW-SE to E-W) cannot be directly established. While the anisotropy pattern obtained is very similar using the two methods, evidence supporting either a subduction (Buontempo et al., 2008) or a delamination (Calvert et al., 2000b) model has been invoked.

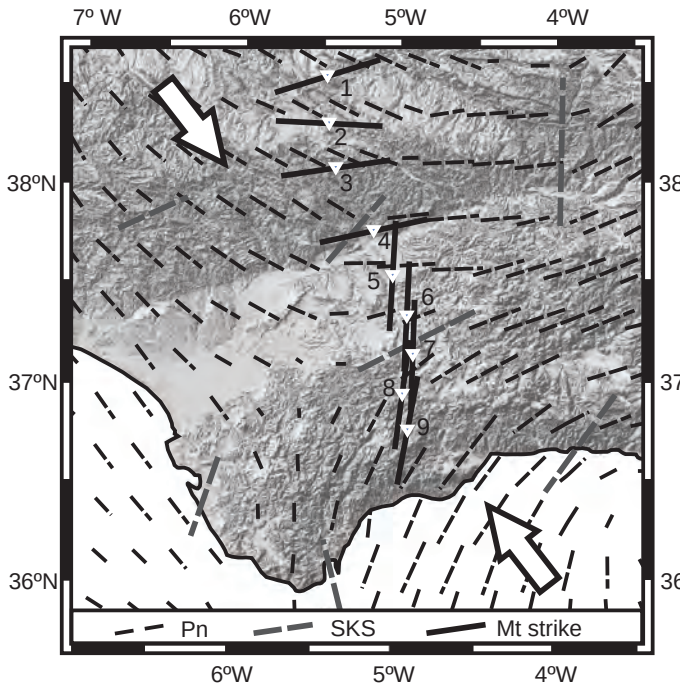

Figure 4-2. *SKS, Pn fast directions (redrawn from Buontempo et al., 2008 and Calvert et al., 2000b) and geoelectrical strike determined using LMT data (range 10^2-10^3 s). Large arrows indicate the trend of plate convergence.*

4.4. New MT data

MT data were collected along a 180-km-long profile that runs approximately NNW-SSE, orthogonal to the major geological structures (Fig. 4-3). The profile consists of nine LMT sites acquired using LEMI-417 instruments in a period range of 10–20000 s. Time series were processed with a modern robust data code (Varentsov, 2007) and transfer functions apparent resistivities, phases and tipper were obtained. A site located at 250 km distance in Portugal was used for a single remote reference analysis. The data are of good quality with the exception of site 4, where a railway produced EM noise, and so it has been discarded for interpretation.

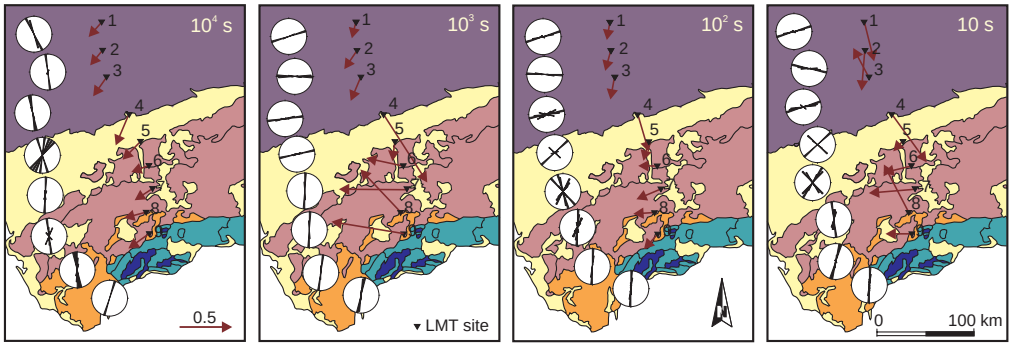

Figure 4-3. *Real induction arrows for 4 selected periods (10-10⁴ s) and circular histograms of phase-sensitive strike. Geological legend same as in fig. 4-1.*

Electrical anisotropy is represented by the direction of maximum conductivity (geoelectrical strike) and it was determined using the Bahr´s method (Bahr, 1988). The phase tensor (Cadwell et al., 2004) was also calculated to corroborate that the data are unaffected by the galvanic distortion produced by near-surface heterogeneities (Appendix A). The ambiguity of 90º inhererent to strike determination was resolved by considering the directions of the induction arrows. They are orthogonal to the geoelectrical strike, point to high-conductivity zones (Parkinson convention), and their magnitudes are directly proportional to the lateral resistivity gradients. Results indicate that strike varies with period (Fig. 4-3). For the longest periods ($\geq 10^4$ s), corresponding to deep levels, all the sites show a common N-S (~N170ºE) pattern. For periods between 10^3-10 s, strike variations could be observed: in the southern part of the profile (sites 6-9) the strike shows a consistent N-S trend (~N180ºE), whereas in the northern part (sites 1-4) the strike turns into E-W (~N85ºE). At site 5, placed in the Guadalquivir Basin, an intermediate NE-SW trend was observed.

The largest magnitudes of the induction arrows (Fig. 4-4) could be observed in the Betic Cordillera sites (6-9), at periods comprised between 10 and 10^3 s, increasing toward the Internal Zones of the cordillera with a constant W sense. Sites in the Iberian

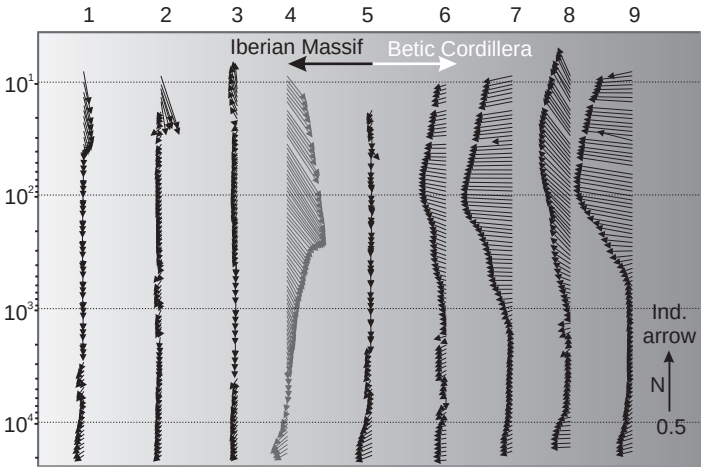

Figure 4-4. *Real induction arrows along the profile for periods comprised between 10-20000 s.*

Massif show lower magnitudes and the trend of the induction arrows undergoing rotation to the south (sites 1-3). A slight increase in the magnitude is also detected at periods greater than 10^4 s in the whole profile, and all the induction arrows also show a homogeneous trend pointing to the W-SW.

4.5. Discussion and conclusions

The first lithospheric electrical anisotropy results from LMT data obtained in the northern branch of the Gibraltar Arc (western sector of the Eurasian-African plate boundary) may constitute key data to validate and discuss the different geodynamical models proposed for the region. A rough estimate reveals that the researched zone attains a depth of approximately 120 km (~10^4s), corresponding to the upper mantle, and may extends up to the lower crust, crossing the Moho discontinuity (periods ~10-10^2s).

The geoelectrical strikes determined in the Betic Cordillera and in the Iberian Massif are consistent in the two geological domains and reveal a layered structure (Fig. 4-5). N-S strikes occur at depth (~10^4 s), in the lithospheric mantle of the whole region (Zone C). At shallow levels (~10^3 s to ~10 s), in the lower crust and uppermost mantle, the geoelectric strikes tend to align with a N-S direction in the Betic Cordillera (Zone A), and roughly along an orthogonal E-W direction in the Iberian Massif (Zone B). A sharp transition zone reveals a NE-SW strike in the region between the two domains (Zone E). At ~10-10^2 s, the induction arrows show high magnitude, but at ~10^3-10^4 s their magnitude dramatically decreases (bar module of Zones D and C). This change in magnitude is especially noticeable below the Betic domain (sites 5 to 9).

The presence of a lateral heterogeneity could also produce an induction arrow pattern pointing to a local conductor body (Wanamaker, 2005), that in this case would be located to the west of the profile (Apendix B). However, in the study area the induction arrows show a homogeneous pattern in each geological domain, with a sharp transition, that is in better agreement with mantle anisotropy due to regional processes. In addition, it has not been reported the presence of wide high conductive bodies to the west of the profile.

The MT method provides better vertical resolution than seismic shear-wave splitting studies because the measured period determines the target depth. Nevertheless, the latter have a very good lateral resolution that provides valuable complementary information. In the western Betic Cordillera, the seismic anisotropies give N-S trends, roughly parallel to the major geological structures in this part of the arc, and similar to the electrical anisotropy results (Fig. 4-2). To the North, both methods provide oblique trends. Obliquity between both anisotropy directions have been described in regions that have undergone low shear strains, meanwhile in high shear strain situations the anisotropy directions parallelize the shear zone (Tommasi et al., 1999). However, obliquity could not be discarded to correspond to the different depth ranges studied (Frederiksen et al. 2006).

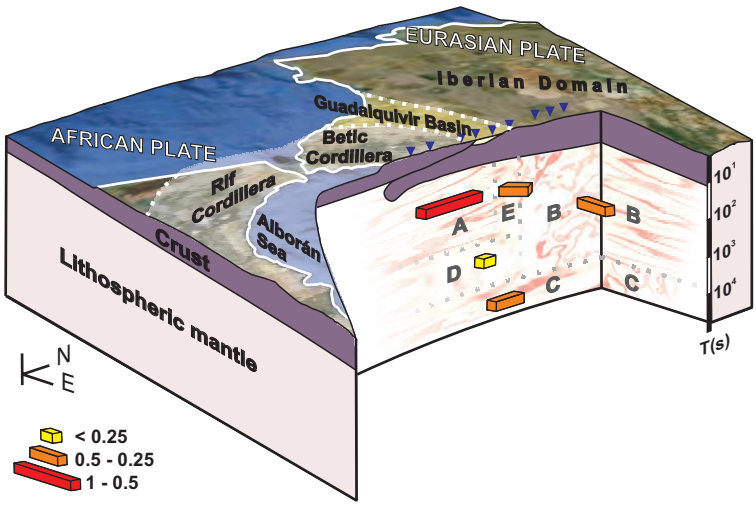

Figure 4-5. *Mantle anisotropy sketch of the northern part of the Eurasian-African plate boundary; bar orientations represent the geoelectric strike and their module is related to the induction arrows magnitude.*

Magnitudes of the induction arrows undergo a remarkable southward increase from the Iberian Massif, with a more stable geological structure, to the inner part of the Betic Cordillera. If this setting can be attributed to the major conductive crustal

thickness of the Betic Cordillera, the induction arrows in the Iberian Massif should point to the SE, but instead they point W-SW. Thus, its most probable origin may be the increase of deformation towards the Internal Zones.

Delamination and subduction, proposed as the main mechanisms responsible for the alpine evolution of the Gibraltar Arc, produce different mantle deformation patterns. Delamination reflect irregular or radial anisotropy directions at different depths below the affected region due to the flow of asthenosphere replacing the removed mantle (West et al., 2009). The regular N-S strike pattern observed along the profile at $\sim 10^4$ s, from the Iberian Massif to the Internal Zones of the Betic Cordillera, does not support delamination mechanism, at least not below this sector of the Cordillera. The origin of the regional N-S deep constant strike could be a consequence of different processes, one of the most probable being an inherited 'frozen' feature from the pre-alpine plate kinematics or the opening of the northern Atlantic.

In transpression zones located along plate boundaries, as the Betic-Rif Cordillera, lateral displacement (simple shear) and compression at right angles to the plate boundary (pure shear) could occur (Morel and Meghraoui, 1996). Deformation related to the westward emplacement of the Internal Zones of the Betics may produce N-S strikes at shallow levels, along the front of the tectonic arc, through dominant pure shear due to the E-W shortening. The Ronda peridotites crop out at the Internal Zones of the Betic Cordillera and show mainly NE-SW high temperature stretching lineations (Tubía, 1994), with opposite shear senses that also suggest an important pure shear component. Finally, E-W strikes determined in the Iberian Massif foreland may be a consequence of the combination of pure and simple shear deformation. A sharp transition occurs below the mountain front, without affecting the deep lithospheric mantle.

The anisotropy pattern evidenced in this research is better supported by an eastward dipping subduction zone-rollback model occurring during the alpine evolution of the region. In such a setting, the lithospheric mantle would only be intensely affected towards the east, at the anomalous Alborán Sea mantle (Hatzfeld, 1976), with the vertical of the western Betic Cordillera remaining as a 'frozen' deep mantle below $\sim 10^4$ s, and having a relatively more isotropic intermediate domain between 10^3 and 10^4 s.

Acknowledgements:

This study was supported by a PhD grant to the first author from Spain's Ministerio de Educación y Ciencia, projects CSD2006-00041 and CGL 2006-06001 (MEC), and Junta de Andalucía.

Appendix A

Near-surface conductivity heterogeneities could distort long period MT data and difficult their interpretation at deep levels. However, the phase tensor analysis, proposed by Cadwell et al. (2004), is unaffected by galvanic distortion. The phase tensor is determined by the amplitude and phase relationships between the horizontal components of the electric and magnetic fields. The major axes of the phase tensor ellipse indicate the preferred flow direction of the induction current in a similar way to the induction arrows. If the regional structure is 2-D, the direction of the principal axes will be the same as the strike direction given by the Bahr (1988, 1991) and Groom and Bailey (1989, 1991) methods. The colour of the ellipses represent the geometric mean of the maximum and minimum phase and is indicative of the increasing (>50º) or decreasing (<50º) of conductivity with depth.

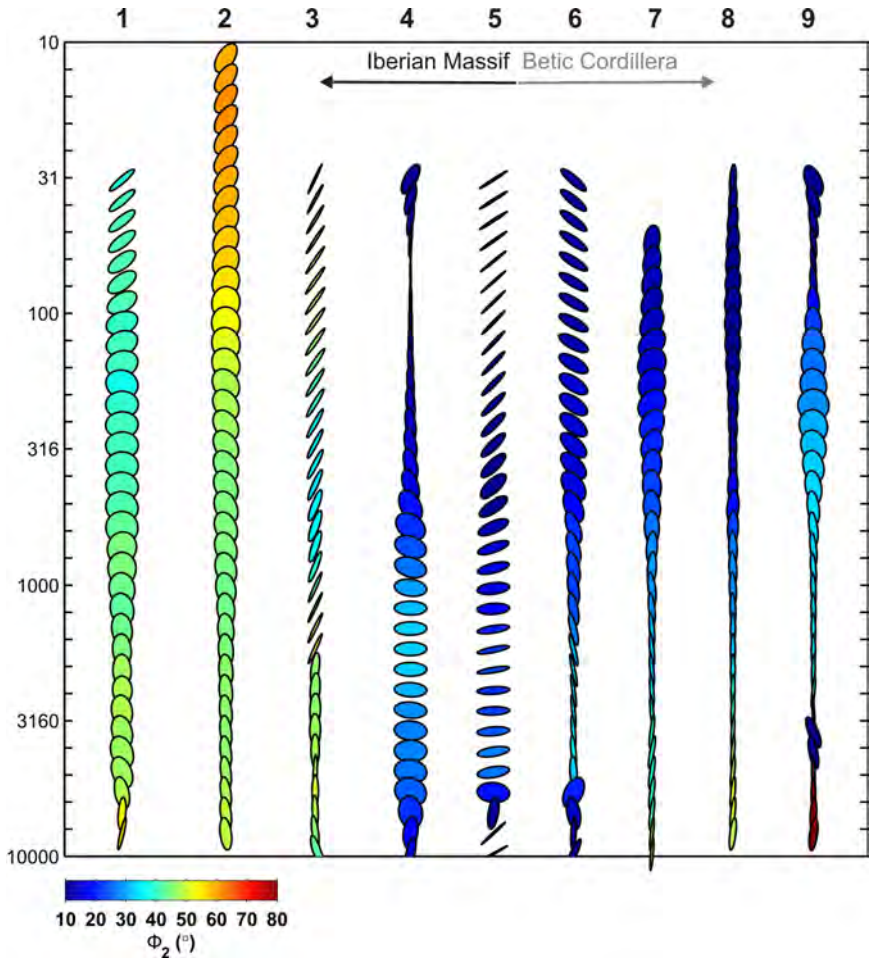

Fig. 4-6. Phase tensor ellipses along the profile for periods comprised between 10-10000 s.

Appendix B

3D forward magnetotelluric model of the studied transect obtained from the long period magnetotelluric data between 10 and 10000 s. The model try to reproduce the induction arrows pattern, through the presence of a conductive body placed westwards of the profile, to contrast the anisotropy hypothesis with the existence of a lateral heterogeneity. The model that better fit the real vectors is unrealistic through geological criteria and shows gradual transitions between the Betic Cordillera and the Iberian Massif, in contrast with the marked transition between these geological domains in the real data.

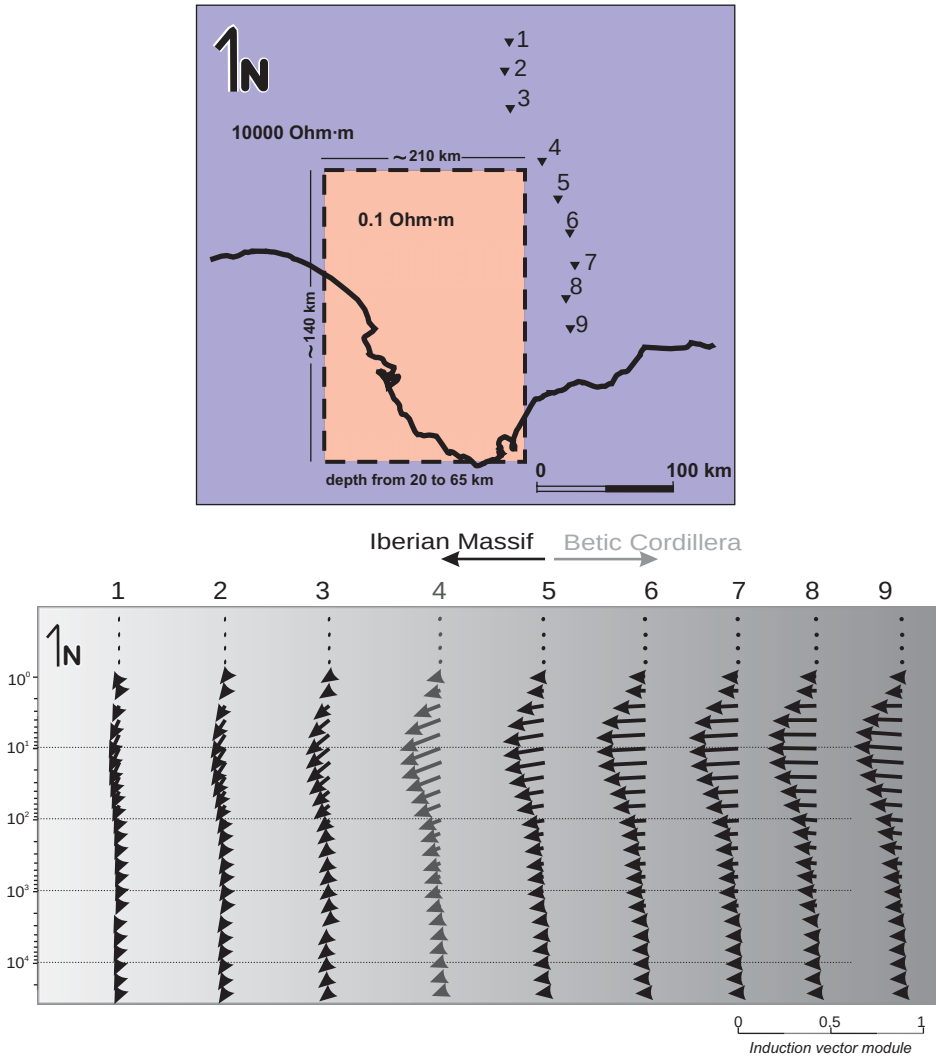

Figure. 4-7. *3D forward magnetotelluric model of the studied transect obtained from the long period magnetotelluric data between 10 and 10000 s.*

5

Crustal structure, recent and active deformation and stress in the frontal part of a continental collision: a northwestern Betic Cordillera transect

Ruiz-Constán, A. [1], Galindo-Zaldívar, J. [1, 2], Pedrera, A.[1] and Anahnah, F.[1]

Submitted for publication

Distribution of recent and present-day deformation in the Betic-Rif Cordillera, located in the western Eurasian-African NW-SE slow convergence (~ 5 mm/a) area, shows an heterogeneous pattern. New deep resistivity data in a NW-SE transect of the western Betics point to the presence of a kilometric SE-wards dipping conductive body at middle crustal levels. These data support that the Iberian Massif crust, including basic rocks, extends southward below the Betics and the Alborán Sea. Shallow seismicity is preferably located at the Betic Cordillera mountain front, indicating its present-day activity. The earthquakes are progressively deeper toward the SE, with intermediate depths near the coast that would support the present activity of continental subduction. The main relief features of the region likewise agree with this tectonic setting; and while in the NW mountain front relief uplift is related to active shallow faulting, towards the SE there is no such evidence, though recent rising is underlined by non-deformed marine terraces and uplifted marine Tortonian calcarenites. Overall, the northwestern Betic Cordillera offers a good example of the heterogeneous deformation of continental crust within a region of convergence, clearly evidencing that at shallow levels the shortening is mainly solved by the relief uplift and extension, whereas in deep levels it is accommodated by reverse faulting and subduction.

Key words: continental subduction, 2D resistivity model, gravity model, intermediate seismicity, stress field

1. Departamento de Geodinámica. Universidad de Granada.
Campus Fuentenueva, 18071 Granada, Spain.
2. Instituto Andaluz de Ciencias de la Tierra CSIC-UGR. Facultad de Ciencias.
Universidad de Granada. 18071 Granada, Spain.

5.1. Introduction

In convergent plate boundaries, deformation is accommodated by the development of collision or subduction zones. In oceanic-continental plate boundaries, subduction of oceanic crust generally occurs (Song et al., 2006). Over time, consumption of the subducting slab leads to closure of the oceanic basin as well as continental collision, thereby producing crustal thickening and the development of an orogen, like the Himalayas (O´Brien, 2001). Although continental crust may be considered resistent to subduction due to its relatively low density (McKenzie, 1969), in certain convergence settings it may occur. High-pressure metamorphic rocks described in widespread examples around the world (Chemenda et al., 1996; Faure et al., 2003; Goffé et al., 1989), and thermo-mechanical models (Negredo et al., 2007; Ranalli et al., 2000) indicate that continental crust may be at least partly subducted.

Stress distribution along subducting slabs, effected through the inversion of earthquake focal mechanisms, has been widely addressed in oceanic subduction zones (Lemoine et al., 2002; Seno and Yoshida, 2004; Xu and Kono, 2002) and to a lesser extent in continental subduction zones (Singh, 2000; Khan, 2003). Stress field distribution is largely conditioned by two variables: the slab pull and the mantle´s resistance to the slab sinking. These factors, in turn, are determined by the geometry and nature of the slab and other features of the tectonic setting, including the age of the slab, rate of convergence (Fugita and Kanamori, 1981), bending of the slab (Christova and Tsapanos, 2000) or slab detachment (Sperner et al., 2001). The establishment of the deep stress regime along the slab may serve to better understand the geodynamic evolution of the area.

Seismic tomography models performed in the Mediterranean region (Amato et al., 1998; Wortel and Spakman, 2000) shed light on the deep geometry of most of the belts that surround the Mediterranean Sea (Fig. 5-1a; Apennines, Dinarides, Maghrebides) confirming the presence of subduction slabs. In the western Mediterranean, considerable research has aimed to explain the development of the Gibraltar Arc. Subduction has also been invoked as a developmental mechanism of the Betic-Rif Cordillera (Blanco and Spakman, 1993; Lonergan and White, 1997; Morales et al., 1999; Thiebot and Gutscher, 2006; Torres-Roldán, 1979), although its geometry, polarity, recent evolution and relationships with other mechanisms are not as well established as in other Alpine Mediterranean chains. Alternative mechanisms based on the delamination of a lithospheric mantle (Calvert et al., 2000b; Platt and Vissers, 1989; Seber et al., 1996) have also been proposed. In any case, the deep structural data are key in the discussion of the geodynamic evolution of this controversial region.

Although recent research has focused on the shallow seismicity in the Betic-Rif Cordillera (Fernández-Ibáñez and Soto, 2008), the western Alborán Sea is likewise affected by intermediate earthquakes, deeper than 70 kilometres, that are connected

with the shallow seismicity of the western Betic Cordillera (de Vicente et al., 2007). The seismicity pattern in the western Betic Cordillera-Alborán Sea transect involves shallow earthquake hypocenters near the mountain front and a progressive deepening of seismicity towards the Alborán Sea, reaching depths of around 120 km. In the area of Málaga, seismic tomography images (Morales et al., 1999) allow them to associate a low-velocity body with the intermediate seismicity, probably representing an active continental subduction. Until now the influence of this lithospheric structure, with limited lateral continuity, has not been taken into account in the establishment of the recent and current stress pattern and tectonic activity of the western Betic Cordillera.

The aim of the present contribution, then, is to determine the crustal structure and present day stress field in a transect of the western Betic Cordillera in order to improve the knowledge of the recent evolution of the Betic mountain range, the formation of the Gibraltar Arc and the origin of the seismogenic zones. To this end we have performed a NW-SE cross section using several geological and geophysical techniques (magnetotelluric, gravity and seismotectonics). Transpressive contexts, like the present-day Eurasia-Africa plate boundary, share features of transcurrent and convergent plate boundaries, and prove interesting for detailed study.

5.2. Geological and Geophysical setting

The Betic-Rif Cordillera (Fig. 5-1a), located at the western end of the Mediterranean Sea, forms an arc-shaped mountain belt that surrounds the Alborán Sea. Since the Cretaceous, N-S to NW-SE convergence between the Eurasian and African plates (Dewey et al., 1989) has produced shortening contributing to the recent and present-day relief uplift (Braga et al., 2003). The Betic Cordillera comprises three main domains with different lithological and structural features (Fig. 5-1b): the External Zones, mostly composed of Triassic to Miocene sedimentary rocks deposited on the South-Iberian palaeomargin (García-Hernández et al., 1980); the Internal Zones, structured in three main stacked metamorphic complexes which are, in ascending order, the Nevado-Filábride, the Alpujárride and the Maláguide (Galindo-Zaldívar et al., 1989); and the Flysch Units (Martin-Algarra, 1987) constituted by Cretaceous to Miocene sediments that crop out between the Internal and the External Zones. Cropping out to the north is the Guadalquivir Basin, an asymmetric Neogene foreland basin whose sedimentary infill (Sierro et al., 1996) increases southwards due to the load of the Betic Cordillera over the Iberian Massif foreland. This basin is mainly filled by autochthonous sediments, although its southern edge is constituted by Mesozoic and Cenozoic chaotic olistostromes that came from the External Zones in relation with the Gibraltar Arc development. The present-day active front of the Betic Cordillera is located south of the olistostromic front (Ruano et al., 2004). Other sedimentary basins, like the Ronda Basin (Fig. 5-1b), were formed since the Neogene, simultaneously to the relief development.

The Iberian Massif foreland is a part of the variscan belt formed by igneous and metamorphic rocks, with a WNW-ESE main structural trend. Both large granitic bodies and metabasites are intruded in metapelitic host rocks (Simancas, 1983). Seismic tomography and magnetic anomaly studies in the central Betic Cordillera (Serrano et al., 2002) and deep seismic reflection profiles in the eastern Betics (Galindo-Zaldívar et al., 1997) evidence the continuity of the variscan basement below the Betic Cordillera tectonic units.

Recent volcanism in the Betic-Rif Cordillera shows a widespread pattern and geochemical affinities both from active subduction zones (Gill et al., 2004) and intraplate-related magmatism (Duggen et al., 2005). The first type entails Late Miocene to Early Pliocene (8.2–4.8 Ma) calc-alkaline and shoshonitic rocks, whereas the second involves Late Miocene to Pleistocene (6.3–0.65 Ma), Si-poor, Na-rich magmatic rocks. Volcanism, however, was apparently not as extensive in the Alborán Sea as in normal subduction zones, and ceased altogether in the Late Miocene when the oceanic lithosphere subduction stopped (Duggen et al., 2008).

A large variety of geophysical data have been used to constrain the crustal structure of the eastern and central parts of the cordillera, including ESCIBETICAS deep reflection seismic profiles (Galindo-Zaldívar et al., 1997), magnetotelluric data (Martí et al., 2004; Pedrera et al., 2008; Pous et al., 1999) and several shallow seismic tomographies (Carbonell et al., 1998; Dañobeitia et al., 1998; Serrano et al., 2002). In the Alborán Sea, deep seismic tomographies provide the most detailed available data on deep structure, and therefore have been largely used to support the delamination or subduction models (Blanco and Spakman, 1993; Morales et al., 1999; Spakman, 1990). Yet knowledge of the present-day deep crustal structure of the western part of the Betic Cordillera is poorer than in the eastern sector. Gravity studies (Bonini et al., 1973; Casas and Carbó, 1990) support the crustal thickening from the Alborán Sea to the Betic Cordillera. Refraction seismic profiles performed in this area (Medialdea et al., 1986) established the Moho depth around 32-34 km below the Iberian Massif, and about 30 km below the Gibraltar Strait, decreasing to the east till 20 km. New MT data provide further insight as to the crustal structure of the western Betics on the basis of a different physical property, the electrical resistivity of the rocks.

The aim of this contribution is to constrain the major crustal structures and the seismotectonic pattern in a Betic Cordillera transect, between Sevilla and Marbella, from new 2D MT and gravity models combined with seismicity analysis and surface geological observations. This cross section was selected taking into account its orthogonal direction with respect to the NE-SW Betic Cordillera trend and the fact that it lies parallel to the NW-SE present-day convergence between the Eurasian and African plates.

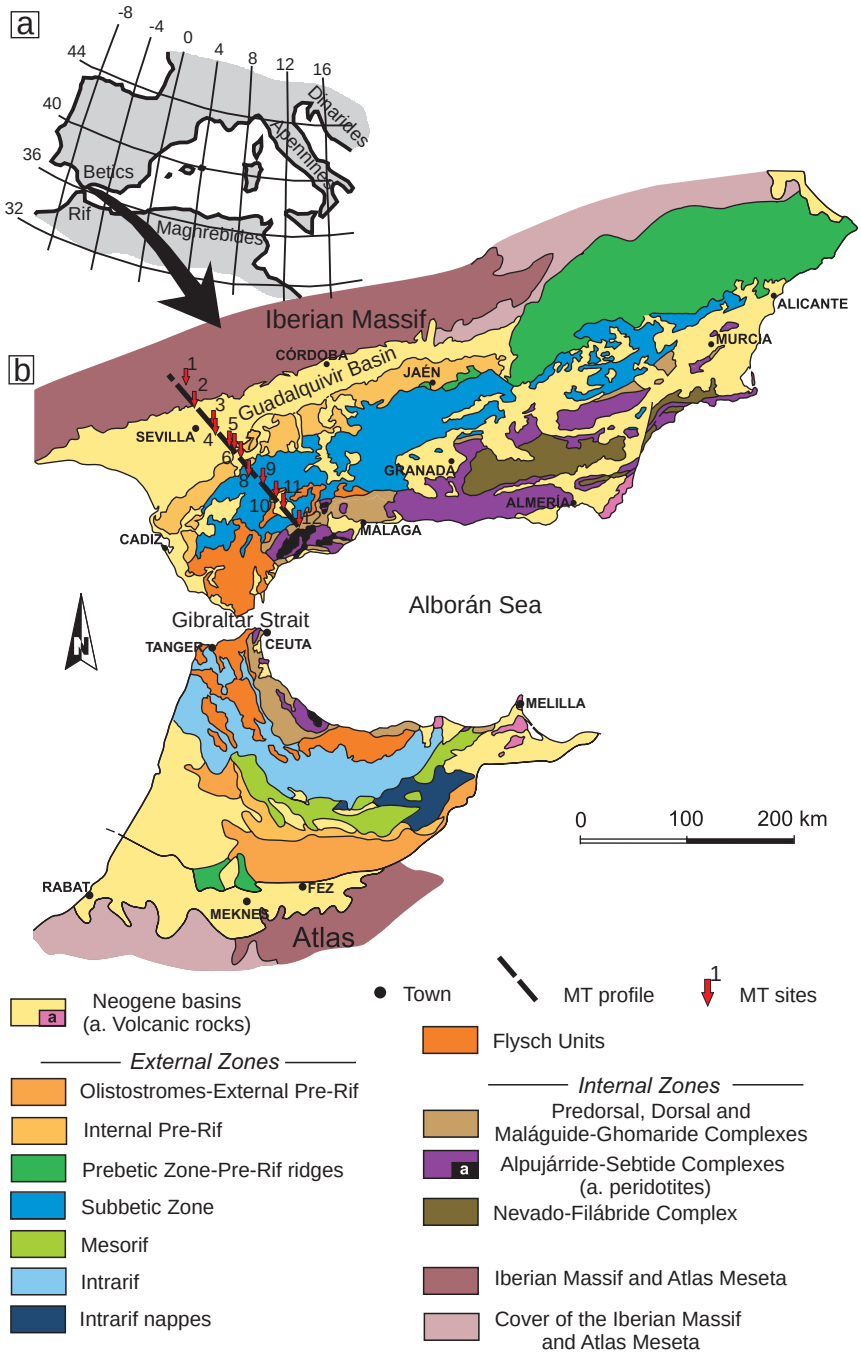

Figure 5-1. a) *General location of the Betic Cordillera in the framework of the Mediterranean Alpine chains;* **b)** *Geological map of the Betic Cordillera; arrows are the MT sites projected along the interpreted profile in a NW–SE direction.*

5.3. Resisitivity data

5.3.1. Magnetotelluric sounding methodology and data acquisition

The magnetotelluric technique (MT) is an electromagnetic method used to constrain spatial variations of the Earth's resistivity by measuring the natural electric and magnetic fields at the Earth's surface (Vozoff, 1972). Twelve new MT soundings (Fig. 5-1b; Appendix A) were acquired using Metronix ADU06 equipment.

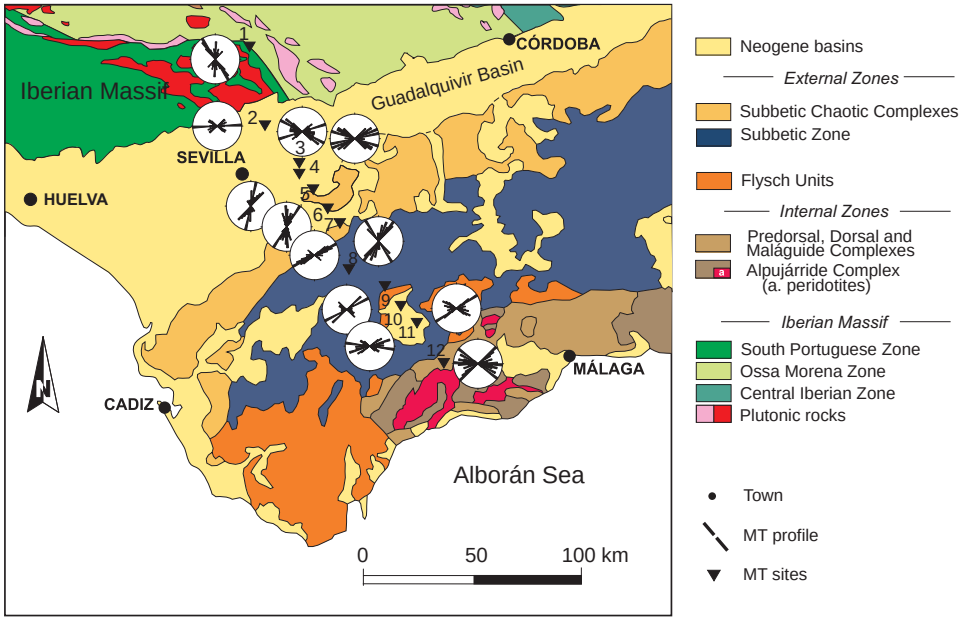

Figure 5-2. *Circular histograms of phase-sensitive strike.*

Dimensionality of the measured impedances was determined by using the Bahr (1988,1991) decomposition for each site (Fig. 5-2). The ambiguity of 90º inhererent to strike determination was resolved by considering the directions of the induction arrows and the regional structures. The strike obtained is mainly NE-SW in the Betic Cordillera, although differences in the strike (E-W, NE-SW) were found at the two northern stations of the profile located at the Iberian Massif. However, the most consistent orientation for the purpose of 2D imaging of the whole profile (Fig. 5-1) is a NW-SE direction, orthogonal to the main regional geological structures of the Betic Cordillera. Magnetotelluric data with periods of up to 100 s were inverted in this profile. The 2D inversion was performed using the RLM2DI code (Mackie et al., 1997) for TM (Transversal Magnetic Model) and TE (Transversal Electric Model)

resistivities and phases. Static-shift problems were detected as displacements between TE and TM mode at the shortest periods of the curves 4 and 11. All the corrections were smaller than one decade. The smoothing factor (τ) used during inversion was 3; the floor standard deviation errors considered for TM and TE, resistivity and phases, were 5.0 %. The RMS misfit between the measured data and the model response is 3.3.

The deep magnetotelluric profile (Fig. 5-3) provides the first resistivity image of the western region and constitutes a complete transect of the western Betic Cordillera. The sites are located from the Iberian Massif, crossing the Guadalquivir Foreland Basin, to the External Zones and up to the Internal Zones. The presence in the area of several important cities with a widespread network of electric power lines (Sevilla, Marbella and Ronda), made it difficult to find adequate places for MT sites. Consequently, it was not possible to include additional sites to improve the quality. This effect is particularly relevant in the northern and southern edges of the profile, determining the poor quality of low frequencies. Not well constrained deep areas are indicated in grey (Fig. 5-3).

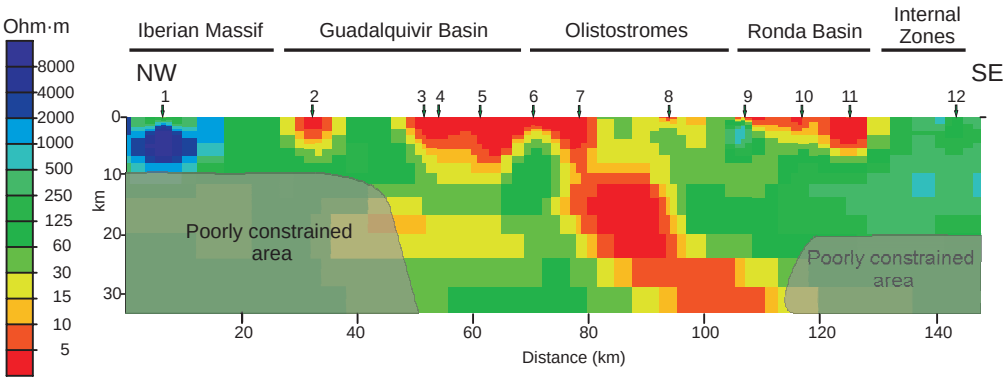

Figure 5-3. *Two-dimensional electrical resistivity model.*

5.3.2. Geological interpretation of resistivity data

Surface geological data are in consonance with the heterogeneous resistivity values revealed by the 2D resistivity model at the upper crust. Conductive bodies located at shallow levels are related with the sedimentary infill of the Ronda and Guadalquivir basins. In contrast, large resistivity bodies can be found in the northern and southern boundaries of the profile. The northern one (Site 1, Fig. 5-3) may be related to granitic bodies cropping out in the Iberian Massif foreland, while the southern one (Site 12, Fig. 5-3) may be associated with limestones of the Internal Zones frontal units.

At middle levels of the crust, beneath sites 7 and 9 (Fig. 5-3), a kilometric conductive body dipping south-eastward could be observed. It may correspond to basic

igneous rocks intruded in the Iberian Massif crust, located below the Betic Cordillera, similar to those that have been recognized in the eastern Betic Cordillera (Bohoyo et al., 2000). These rocks, placed at a depth of around 15-30 kilometres, have no associated magnetic anomalies, as at such depths temperature must be near or above the Curie point, implying a loss of magnetic properties. The southward extension of this main conductive body could not be confirmed due to the electrical anthropic interferences near the southern end of the profile impeding MT research. Another possibility is that the lateral end of the body lies to the SE, enclosed in the Iberian Massif crust. In any case, the presence of this elongated body suggests a southeastward dip of the crustal structure.

5.4. Gravity data

5.4.1. Methodology and acquisition of new gravity data

The study of Bouguer gravity anomaly in complex tectonic areas, where so many bodies influence the anomaly, implies that often gravity models are not unique and need to be constrained by other available data. Such is the case of the western Betic Cordillera, where several gravity models have been proposed to date (Bonini et al., 1973; Casas and Carbó, 1990). A new gravity survey (Fig. 5-4a) was performed along the transect reaching southward up to the coastline. This profile helps check and improve the crustal structure established in the resistivity image, and propose its southward continuity. The gravity survey comprised 348 gravity stations with a mean spacing of 500 meters. The data were acquired using a CG-5 Scintrex gravimeter with a maximum accuracy of 0.001 mGal. The instrumental drift and tide variations were automatically corrected by this gravimeter. The measurement stations were positioned with an e-trex Garmin GPS and a barometric altimeter with 0.5 meter altitude precision. The absolute altitude of the stations was established through measurements in several geodetic vertexes near the profile. In order to determine the absolute gravity value, data were referenced to the Málaga and Sevilla base stations of the I.G.N. national gravimetric network (I.G.N., 2007). Topographic correction was performed up to a distance of 20 kilometres using a digital terrain model with a grid of 90 m cell size due to the limited effect of the farthest reliefs. The Bouguer anomaly was calculated taking into account a standard density of 2.67 g/cm^3.

5.4.2. Gravity modeling and crustal structure

We propose a new 2D NW-SE gravity model (Fig. 5-4b) taking into account the surface geological data, the 2D resistivity image and seismic tomography research (Morales et al., 1999) based on seismicity distribution. The model was developed using the GRAVMAG V.1.7. program of the British Geological Survey (Pedley et al., 1993). The average density assigned to each geological unit is related to its main lithology according to standard values (Telford et al., 1990) and is indicated in Fig. 5-4b.

The gravity profile shows the transition from the stable continental crust of the Iberian Massif through the cross section of the Betic Cordillera, up to the thinned continental crust of the Alborán Sea margin. The positive Bouguer anomaly values toward the northwestern end of the profile point to the presence of a high density body, possibly basic rocks, that extends northwards beyond the profile, and is probably located at middle levels of the Iberian crust. These high anomaly values, reaching 80 mGal, are conditioned by the presence of this body and are not observed to the east or west of this profile (I.G.N., 1976). To the south, the Iberian Massif continues below the Betic Cordillera, and a decrease in the Bouguer anomaly is produced by the low density Neogene sediments of the Guadalquivir and Ronda Basins and the Mesozoic-Cenozoic sedimentary rocks of the External Zones of the Betic Cordillera.

From the stable Iberian Massif, the Moho increases its depth southwards. First, there is a progressive deepening below the External Zones due to the load of the Betic Cordillera. Southwards, the Iberian continental crust sinks into the mantle towards the Alborán Sea, as corroborated by the southward dipping of deep structures obtained by MT data and the seismicity distribution. A basic rock body is included at middle and deep crustal levels, emplaced in the crust of the Iberian Massif, as evidenced by MT researches. The overprinting of several bodies makes it difficult to accurately determine the deep structure of each one, like the sinking continental crust into a dense mantle, but they would support the proposed deep structural model for this transect of the Cordillera.

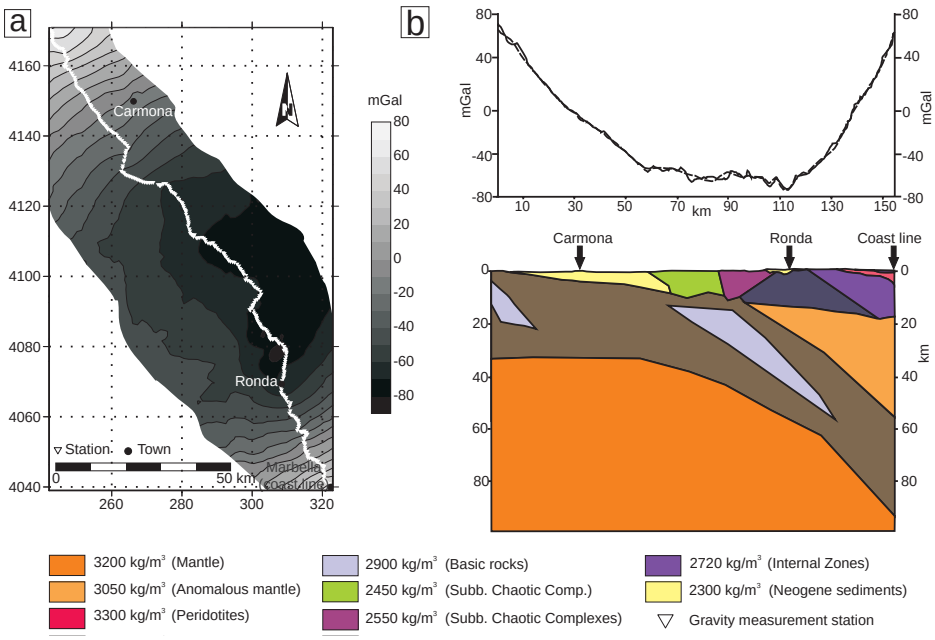

Figure 5-4. a) *Bouguer gravity anomaly map;* **b)** *NW-SE 2D model performed taking into account the main tectonic structures that crop out in the area.*

5.5. Seismicity distribution

Seismicity in the Betic-Rif Cordillera (Fig. 5-5a) is characterized by continuous activity of moderate earthquakes (Buforn et al., 1991). Earthquakes in this region are associated with the Eurasia-Africa plate boundary and extend over a wide area, suggesting that this is a diffuse deformation zone. Analysis of the Instituto Geográfico Nacional seismicity database (I.G.N., 2007) (Fig. 5-5a, b and c), underlines several features of the active deep structures of the region. In the Betic Cordillera and Alborán Sea, one of the most striking features is the intermediate seismicity that occurs only in the area south of Málaga, reaching 120 km (Fig. 5-5c). In this region, hypocenter depth increases progressively to the SE.

At shallow levels (Fig. 5-5c), seismicity is preferably concentrated in the Betic Cordillera mountain front and may be indicative of its present-day activity in this profile. It is also important to note the seismic gap ocurring between 25 and 60 kilometres beneath the Alborán Sea.

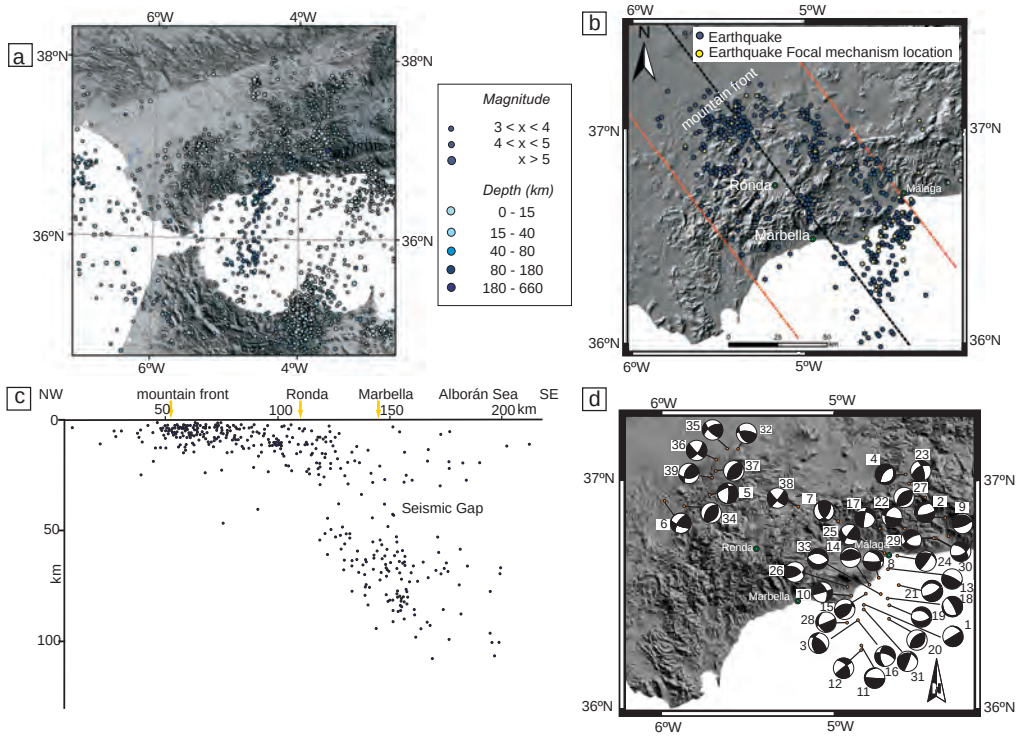

Figure 5-5. a) *Seismicity distribution of the Eurasian-African plate boundary in the western Mediterranean;* **b)** *Earthquake projected in the NW-SE transect;* **c)** *NW-SE profile of the seismicity in western Betics;* **d)** *Earthquake focal mechanism solutions obtained by several authors (see text for details); solutions are in equal area, lower hemisphere projection with white parts representing compressional quadrant.*

5.6. Earthquake focal mechanisms

The earthquake focal mechanisms are highly variable throughout the region (Fig. 5-6). While at shallow levels P axes are split into two main populations, with NW-SE and NE-SW orientations, T axis orientations range from subvertical to E-NE-N-ward plunging. The deep earthquake focal mechanism orientations are more disperse, with some predominant NW-SE to subvertical trends of P axes, and subvertical to southward plunging T axes.

In order to accurately establish the stress distribution in the western transect of the Betic Cordillera, we applied the right dihedra method (Angelier and Mechler, 1977) and Gephart's stress inversion method (Gephart, 1990) to a set of earthquake focal mechanisms (Table 5-1 and Fig. 5-5d) calculated in the area by previous authors (Bezzeghoud et al., 1999; Buforn et al., 1997, 2004; Coca, 1999; Coca and Buforn, 1994; I.A.G. website 2007; I.G.N. website 2007; Mezcua and Rueda, 1997; Morales et al., 1999; Stich et al., 2006).

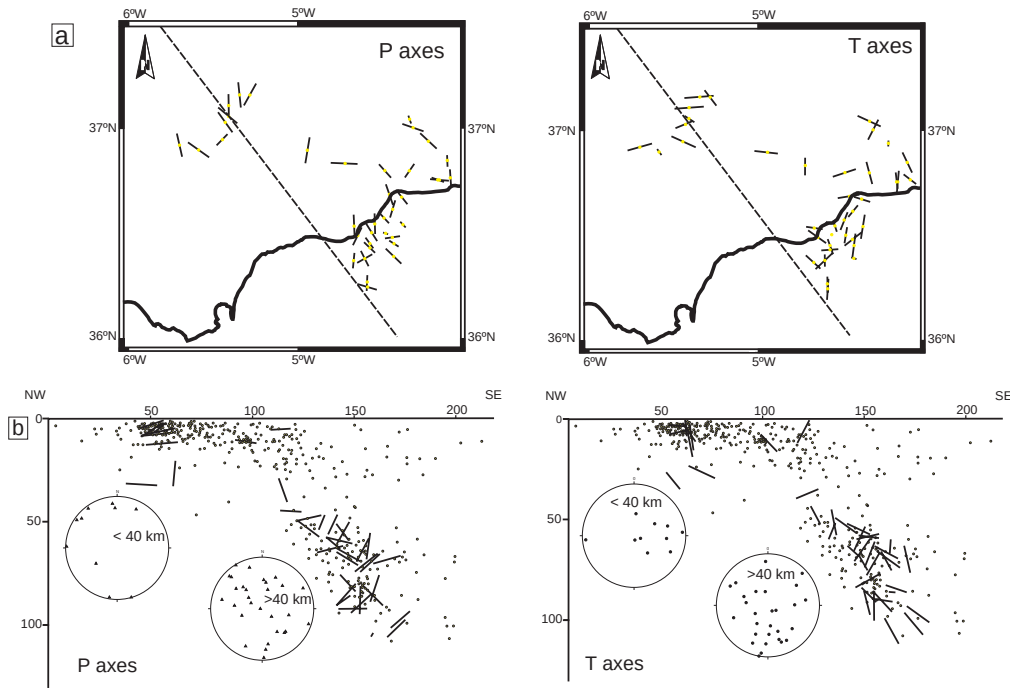

Figure 5-6. a) *Horizontal and* **b)** *NW-SE vertical projection of the pressure and tensional axes calculated using the focal mechanism solutions (different lengths of axes are due to projection into profile line). Stereographic projection of P and T axes (equal area projection, lower hemisphere) are included in Fig 5-5b.*

ID	*Date*	*Lat*	*Long*	*Z*	*Strike*	*Dip*	*Rake*	*Mag*	*Ref.*	*Group*
1	680213	36.48	-4.56	91	334	10	5	4.3	1	3
2	740613	36.87	-4.12	60	78	72	-69	4.1	1	3
3	750807	36.41	-4.59	105	186	42	138	5.2	1	3
4	791222	37.06	-4.34	40	*210	64	-86	4	2	4
5	790501	36.95	-5.42	24	*249	35	-24	4	2	
6	801203	36.92	-5.67	27	*114	68	155	4.3	2	1
7	810121	36.85	-4.71	5	*153	56	46	4	2	
8	860513	36.6	-4.48	90	*87	74	-123	4.3	3	3
9	870327	36.79	-4.1	79	*69	72	76	3.5	3	4
10	880530	36.52	-4.63	80	75	88	35	3.6	4	4
11	881128	36.3	-4.57	100	*93	88	-85	3.5	3	3
12	881212	36.28	-4.57	95	*232	87	146	4.5	3	3
13	890719	36.64	-4.43	95	*296	79	94	3	3	3
14	900206	36.57	-4.53	68	*270	23	96	3.4	3	4
15	900502	36.53	-4.55	95	*36	49	57	4.2	3	3
16	901118	36.41	-4.59	85	*175	51	-30	3.4	3	3
17	910825	36.82	-4.48	58	*286	39	-173	3.8	3	4
18	920314	36.51	-4.43	64	*118	14	-123	3.6	5	3
19	920903	36.48	-4.42	86	298	41	-61	3.5	4	3
20	931109	36.42	-4.42	70	223	60	86	3.5	4	3
21	940101	36.57	-4.37	68	60	71	-103	3.5	6	3
22	950317	36.82	-4.34	56	100	85	-56	4	6	3
23	951118	37.02	-4.32	52	238	59	154	3.6	6	3
24	951128	36.7	-4.38	68	35	84	76	3.5	6	4
25	960622	36.71	-4.45	68	120	58	172	3.9	6	3
26	961227	36.56	-4.65	59	60	60	49	3.8	6	4
27	970318	36.96	-4.23	56	43	34	87	3.7	6	3
28	970820	36.4	-4.65	68	67	86	-63	4.2	6	3
29	20703	36.78	-4.18	63	*128	46	-26	3.4	8	4
30	20704	36.78	-4.17	63	*311	58	-34	3.4	8	3
31	20824	36.46	-4.56	70	96	21	165	4.2	9	3
32	20915	37.16	-5.27	4	273	68	58	4.1	10	2
33	21121	36.53	-4.47	92	*97	45	-94	4.3	8	3
34	30725	36.9	-5.56	6	29	40	82	3.5	10	1
35	60311	36.91	-4.93	10.7	136	68	149	4.4	11	2
36	70102	37.11	-5.39	5.1	133	79	-159	3.6	11	2
37	70918	37.06	-5.39	5.6	217	56	86	3.9	11	1
38	70102	37.16	-5.33	2.3	39	85	-15	3.6	11	2
39	70630	37.03	-5.41	10.8	204	60	45	4.4	11	1

Table 5-1. *Solutions for focal mechanisms represented in Figure 5-5. From left to right, columns give: 1 identity number in figure 5-5; 2 date in format year/month/day; 2 latitude and 3 longitude (degrees of the epicentre); 4 depth, km; 5,6,7 fault angle parameters of one of the two nodal planes, given as strike/dip/rake in Aki and Richards (2002 coordinate system); 8 magnitude and 9 article reference (1, Coca and Buforn, 1994; 2, Bezzeghoud and Buforn,1999; 3, Buforn et al., 1997;4, Morales et al., 1999; 5, Coca, 1999; 6, Buforn et al., 2004; 7, Mezcua and Rueda, 1997; 8, del Fresno, 2004; 9, I.A.G. website; 10, Stich et al., 2006; 11, I.G.N. website). * wave-form inversion.*

The right dihedra method (Angelier and Mechler, 1977) determines graphically, by means of stereographic projection, common zones of compression and tension for a given set of focal mechanisms. This method does not provide information about the stress ratio. However, Gephart's method allows one to determine the directions of main stress axes σ_1, σ_2, σ_3 and the axial ratio ($R = \sigma_2 - \sigma_1 / \sigma_3 - \sigma_1$). The axial ratio is an indicator of the dominating stress regime because it relates the magnitude of the intermediate principal stress to both the maximum principal stress and the minimum principal stress. The method is based on a robust inversion scheme that places less emphasis on erratic data and does not require knowledge of the true fault plane, since the nodal plane with the smaller misfit is chosen as the fracture plane.

Shallow focal mechanisms in the western Betics (<30 km; Fig. 5-5d), mostly located at the front of the mountain range (Ruiz-Constán et al., 2009), are predominantly reverse and strike-slip faults. In view of the roughly orthogonal orientation of P axes, we divided the shallow seismicity into two subsets (Fig. 5-7). The focal mechanism solutions mainly show NW-SE horizontal compression (Group 1, Table 5-2), slightly dipping toward the NW and parallel to the Africa-Eurasia convergence (Figs. 5-6a and 5-7). Although this is the main pattern, local perturbations due to interaction between blocks, or due to the change of principal stress axes after relaxation in a setting of close values between the maximum and intermediate principal stress (R=0.15; Table 5-2), also produce shortening in NE-SW and N-S directions (Group 2, Table 5-2).

Depth		*Group*	*N*	σ_1	σ_2	σ_3	*R*	ε
Shallow	1	NW-SE	4	346/4	79/34	251/56	0.15	0.478
(0-40 km)	2	N-S	4	18/7	273/64	111/25	0.85	0.371
Intermediate	3	Lower side	8	113/45	6/17	261/40	0.55	1.886
(40-105 km)	4	Upper side	21	306/37	96/49	204/15	0.3	6.388

Table 5-2. *Stress ellipsoids determined by Gephart's method. N—number of earthquake focal mechanisms used in the inversion; σ_1—maximum compressive stress; σ_2—intermediate compressive stress; σ_3—minimum compressive stress; $R=(\sigma_2-\sigma_1/(\sigma_3-\sigma_1))$ magnitude ratio of principal stresses (see text); ε—average misfit angle.*

Focal mechanism solutions of deeper seismicity, limited to the southern edge of the profile (Fig. 5-5d), are quite variable, fundamentally involving reverse and strike-slip faults, although normal faults and focal mechanisms showing subvertical and subhorizontal nodal planes are also important. There is a more complex stress pattern at these depths. Although P and T-axes do not coincide with σ_1 and σ_3 when there is fracture reactivation, their orientations suggest general NE-SW strike extension along the more external and upper side of the slab (Fig. 5-6b). In a cross section, P-axis plunge evolves from almost horizontal at shallow and frontal positions of the Cordillera, to down-dip compression in the inner part of the slab, and roughly orthogonal to the seismogenic body in its outer part. Thus, for stress analysis we distinguished two subsets of focal

mechanisms, taking into account the location inside the seismogenic body and the orientation of the tensional and compressional axes. Gephart's method indicates a 45º ESE oriented maximum compression and a 40º WSW well defined maximum extension in the lower and inner side of the slab. However, in the outer part of the seismogenic body Gephart's method provided a well constrained slab extension roughly along strike, with the minimum stress axis plunging toward the SW and a NW-SE maximum compression. The right dihedra diagram (Fig. 5-7) shows orientations with a 100% pressure dihedra or with 100% tension dihedra in all the subsets, in approximate agreement with the main axes orientation as determined using Gephart's method. Hence, the active stress ellipsoids are well defined. Another important feature of the intermediate seismicity is the lack of earthquakes at 25-55 km (Fig. 5-6b), which would indicate an apparent cutoff between the shallow and the intermediate seismicity.

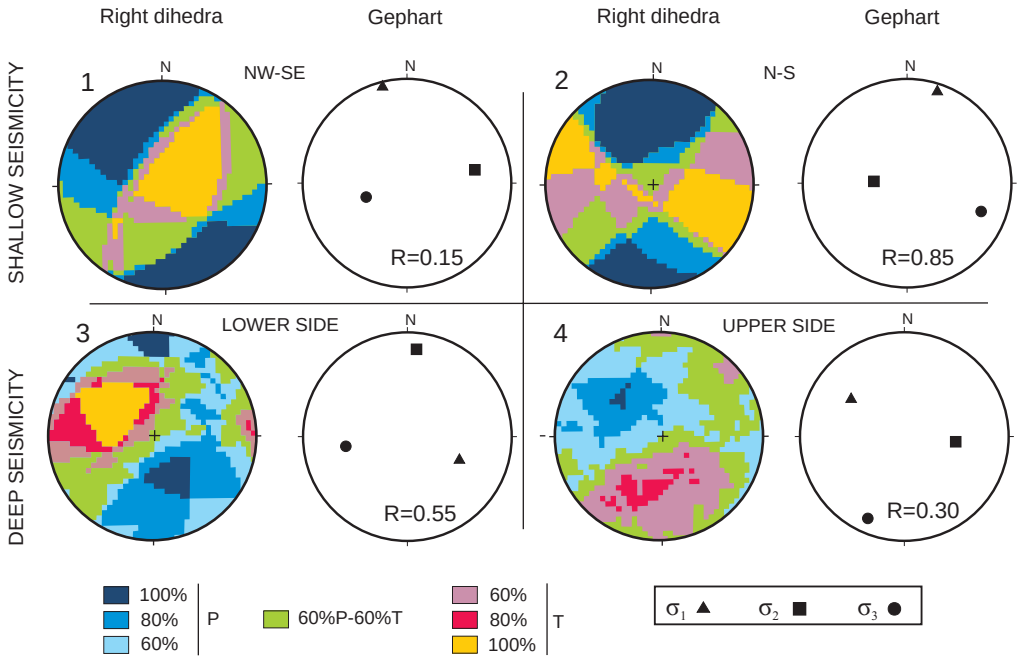

Figure 5-7. *Results from the analysis of the 4 groups of earthquake focal mechanisms using the right dihedra method (Angelier and Mechler, 1977) and Gephart's method (Gephart, 1990) in left and right columns, respectively.*

5.7. Geological and geomorphological evidence of recent deformations

The actual relief that surrounds the Alborán Sea formed since Tortonian times due to the uplift of the Betic-Rif Cordillera, and as a consequence of shortening related to the Eurasia-Africa plate convergence (De Mets et al., 1994) and perhaps to other

interacting mantle processes that are largely discussed in the literature as delamination processes (Calvert et al., 2000b; Platt and Vissers, 1989; Seber et al., 1996) or subduction roll-back (Blanco and Spakman, 1993; Gueguen et al., 1997; Gutscher et al., 2002; Lonergan and White, 1997; Morales et al., 1999; Thiebot and Gutscher, 2006; Torres-Roldán, 1979). Geomorphologic data indicate that major relief in the southern edge of the studied transect. This zone holds clear evidence of recent and possibly actual uplift, although most took place before the early Pliocene (Braga et al., 2003). Nonetheless, the elevated marine terraces of the Malaga coast line (Zazo et al., 1999) and the marine Tortonian calcarenites that crop out widely in the region (Sanz de Galdeano and Alfaro, 2004) are very scarcely affected by faults, and only in some sectors —like the Ronda Depression— are they deformed by large open folds (Ruiz-Constán et al., 2008). While marine Tortonian calcarenites are uplifted up to few hundred meters above the present-day sea level in the Betic Cordillera, northwards, in the Guadalquivir foreland Basin, Tortonian calcarenites have undergone subsidence due to the lithospheric flexure of the Iberian Massif (García-Castellanos et al., 2002) and as a consequence of the cordillera load. This subsidence produced a large trough and, in conjunction with the advance of the Betic mountain range, led to the large Subbetic Olistostrome emplacement through tectonic and gravitational mechanisms. At present, the only shallow tectonic activity in this section is recognized near the northwestern edge of the cordillera, with shallow seismicity and evidence of relief uplift that include sharp mountain front and river incision.

5.8. Discussion

The development of the Gibraltar Arc, formed by the Betic-Rif Cordillera surrounding the Alborán Sea, has spawned long and controversial discussions. Geodynamic models supporting delamination, roll-back or even mantle diapirism (Blanco and Spakman, 1993; Lonergan and White, 1997; Platt and Vissers, 1989; Seber et al., 1996) have been proposed to explain the development of a Alborán Sea Neogene basin in a setting of NW-SE plate convergence (De Mets et al., 1994). Yet we lack accurate data on the deep structure of this region that would help constrain the discussion. On the basis of marine research, an active east-dipping subduction zone constrained in a E-W section (Gutscher et al., 2002; Thiebot and Gutscher, 2006) can be invoked to explain some observed features, such as the west vergent thrusting in the Gulf of Cádiz, the high p-wave velocity slab detected by seismic tomography, or the presence of active mud volcanoes and destructive historical earthquakes. The above authors point to an oceanic nature of the crust. To the east, in the Malaga area, Morales et al. (1999) analyzed a N-S cross section point to the presence of a low seismic velocity body that they relate to the subduction of the Iberian Massif continental crust below the Alborán Sea. The area analyzed in the present contribution lies between the two aforementioned realms, in the Betic Cordillera, in a NW-SE cross section that runs parallel to the Eurasian-African present-day plate convergence (De Mets et al., 1994) and orthogonal to the Betic Cordillera structure due to its arcuate character. The new

geophysical data (magnetotelluric, gravity and seismicity) serve to better constrain the character of subduction in the northern edge of the Gibraltar Arc.

Subduction related volcanism in the Alborán Sea ceased in the Late Miocene when new hydrated oceanic lithosphere stopped subducting (Duggen et al., 2008). These authors evoke delamination of subcontinental lithosphere beneath the edges of southern Iberia and northwestern Africa to explain the end of the volcanism. However, the transition between oceanic-subduction and continental-subduction could also trigger the same pattern in the volcanic record of the Alborán Basin due to the refractory nature of the continental crust and the reduced present-day lateral continuity of the subduction zone as a relict of the Miocene one.

A minimum depth of 90 km, as well as rapid exhumation, is required for ultrahigh-pressure (HP) metamorphic rocks to crop out in continental collision zones (Brun and Facenna, 2008; Chemenda et al., 1996). In this context, exhumation is related to the subduction of small continental lithosphere blocks that trigger slab rollback (Brun and Faccenna, 2008). The space created by the rollback favors the ascent of the buoyant continental crust previously subducted. This process is recurrently evident in the Alpine Mediterranean belt (Goffé et al., 1989; Jolivet et al., 2003; Monié et al., 1991), where HP metamorphic rocks of continental crust sequences are widely exposed. In the Internal Zones of the Betic Cordillera, both the Nevado-Filábride Complex and the overlying Alpujárride Complex, with different ages and exhumation rates, underwent similar metamorphic evolutions at different times, reaching up to 10-13 kBar (Azañón et al. 1998), corresponding to minimum depths of 40 km. The Nevado-Filábride high pressure-low temperature metamorphism gives an age of 25 Ma (Monié et al., 1991) as the end of the high-pressure evolution. Other authors (López Sánchez-Vizcaíno et al., 2001), however, point to an exhumation age of 15 Ma for this metamorphic complex. The Alpujárride Complex exhumation occurs between 22 and 18 Ma (Monié et al., 1994; Platt et al., 1996). Thus, metamorphic evolution would support continental subduction as a mechanism occurring in the past and being repeated in the recent evolution of the Betic Cordillera.

Seismicity distribution in the Betic Cordillera indicates that active structures are progressively shallow to the N-NW, until reaching the cordillera mountain front, where very shallow seismicity (3-4 km) has been registered (Ruiz-Constán et al., 2009). In addition, intermediate seismicity shows this area to have a SE-dipping pattern, reaching depths of 120 km, though with a seismic gap between 25 and 60 km. This aseismic zone could be related with a low seismic velocity wedge corresponding to the anomalous mantle with low seismic velocities, low densities and high temperature, described in early research (Hatzfeld, 1976) and still supported today (Gutscher et al. 2002). Seismic distribution may indicate that the mountain front in this transect is active and that the regional uplift is caused by the propagation to the NW of crustal detachments producing the elevation of hanging wall without deforming the surface. This deformation pattern entails a typical piggyback thrust sequence, with recent

deformation mainly concentrated in the External Zones of the orogenic wedge, while the Internal Zones remain inactive. Therefore, the shortening in deeper levels of the crust may result from the sinking of the Iberian Massif continental crust beneath the Betic Cordillera and the Alborán Sea, as suggested by the 2D resistivity image (Fig. 5-8) and corroborated by the gravity model.

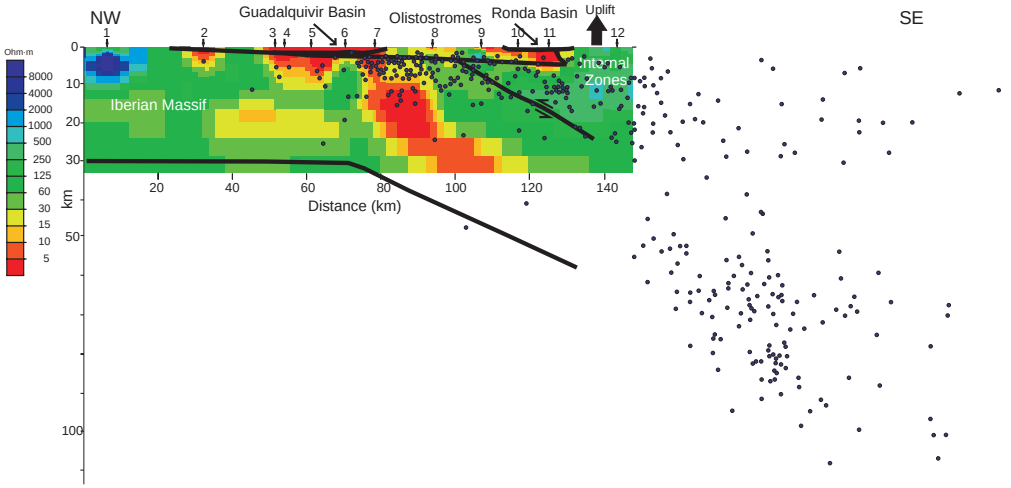

Figure 5-8. *Geological interpretation of the 2D resistivity model superposed on the seismicity in a 20 km wide transect. The solid lines of the model outline the main tectonic complexes.*

Generally, the stress field in subducting slabs is of down-dip compression or down-dip extension, conditioned by the prevalence of the slab pull or the mantle resistance to the edge of the slab. However, several studies have demonstrated that these general rules do not match with the stress behavior in natural examples. Other features of subducting slabs, such as bending, age or length, could condition a variable stress field (Christova and Tsapanos, 2000; Fugita and Kanamori, 1981). The stress tensor analysis of 39 earthquake focal mechanisms located in the western Betics shows differences between the shallow and the intermediate seismicity as well as between the external and internal part of the slab. The results obtained are similar for both the Gephart method (Gephart, 1990) and the right dihedra method (Angelier and Mechler, 1977) (Fig. 5-7). At shallow depths the stress is compressive, due to the NW-SE Eurasia-Africa plate convergence, although orientation varies between a mainly NW-SE and a local N-S major stress axis, probably due to stress release permutations or block interaction. At intermediate depths, also in general, a NW-SE inclined major axis orientation is determined, but two different stress regimes are observed in the external and the internal parts of the slab. The outer part is under extension along the NE-SW strike, whereas the inner part is in down-dip compression. Along-strike horizontal extension was first observed in the Aleutian arc (Stauder, 1968) and was related to

the arc curvature. In the Betic Cordillera area, the arcuate character of the Gibraltar strait and the limited lateral continuity of the subduction zone are causes that may also condition the along-strike extension.

5.9. Conclusions

The first MT profile of the northwestern transect of the Betic Cordillera is seen to be in agreement with the surface geological data, and reveals a deep conductive southward dipping body in the southern edge. Further geophysical data, including gravity and seismicity, support the geometry and present day activity of a southeastward dipping subduction zone, compatible with the NW-SE plate convergence. The continental Iberian crust continues below the Betic Cordillera and the northern Alborán Sea. New data can be viewed in the framework of previous research that analyzed a N-S section located to the east (Morales et al., 1999) and an E-W marine section located west of the transect (Gutscher et al., 2002), confirming the arcuate nature of the subducting slab along the northwestern branch of the Gibraltar Arc. In the NW-SE transect, the subducting slab is probably folded and broken into two segments separated by a seismic gap. Continental subduction also took place in the past, as demonstrated by the HP/LT metamorphism that affected several tectonic units of the Internal Zones.

Stresses vary along this subduction zone and suggest that the Iberian continental crust is forced to sink into the mantle. Although there are local perturbations, maximum stress is generally NW-SE subparallel to plate convergence. It is subhorizontal at shallow levels near the mountain front, and plunges at depth, modified by the folding of the slab. In the external and upper part, NE-SW along-strike extension prevails, probably due to the short lateral continuity of the subducting slab. In the internal arch, meanwhile, the parallelism of the major compressive axis with the slab dip support its forced subduction into the mantle, as a consequence of the stress propagation along this rigid continental body.

The relief uplift of the western Betic Cordillera is the surface expression of the active crustal subduction described here. Active tectonic structures with related seismicity located at shallow levels in the mountain front become deep to the southeast, thereby suggesting a typical piggyback sequence of deformation of an orogenic wedge. These data would support the fact that one of the main mechanism active at present in the Betic Cordillera is the NW-SE African Eurasian plate convergence, although other mechanisms (delamination, roll-back, among others) have been proposed and may be more relevant for the Miocene evolution.

Acknowledgements:

This study was supported by a PhD grant to the first author from Spain's Ministerio de Educación y Ciencia and the projects CSD2006-00041 and CGL 2006-06001 (MEC) and Junta de Andalucía.

Appendix A

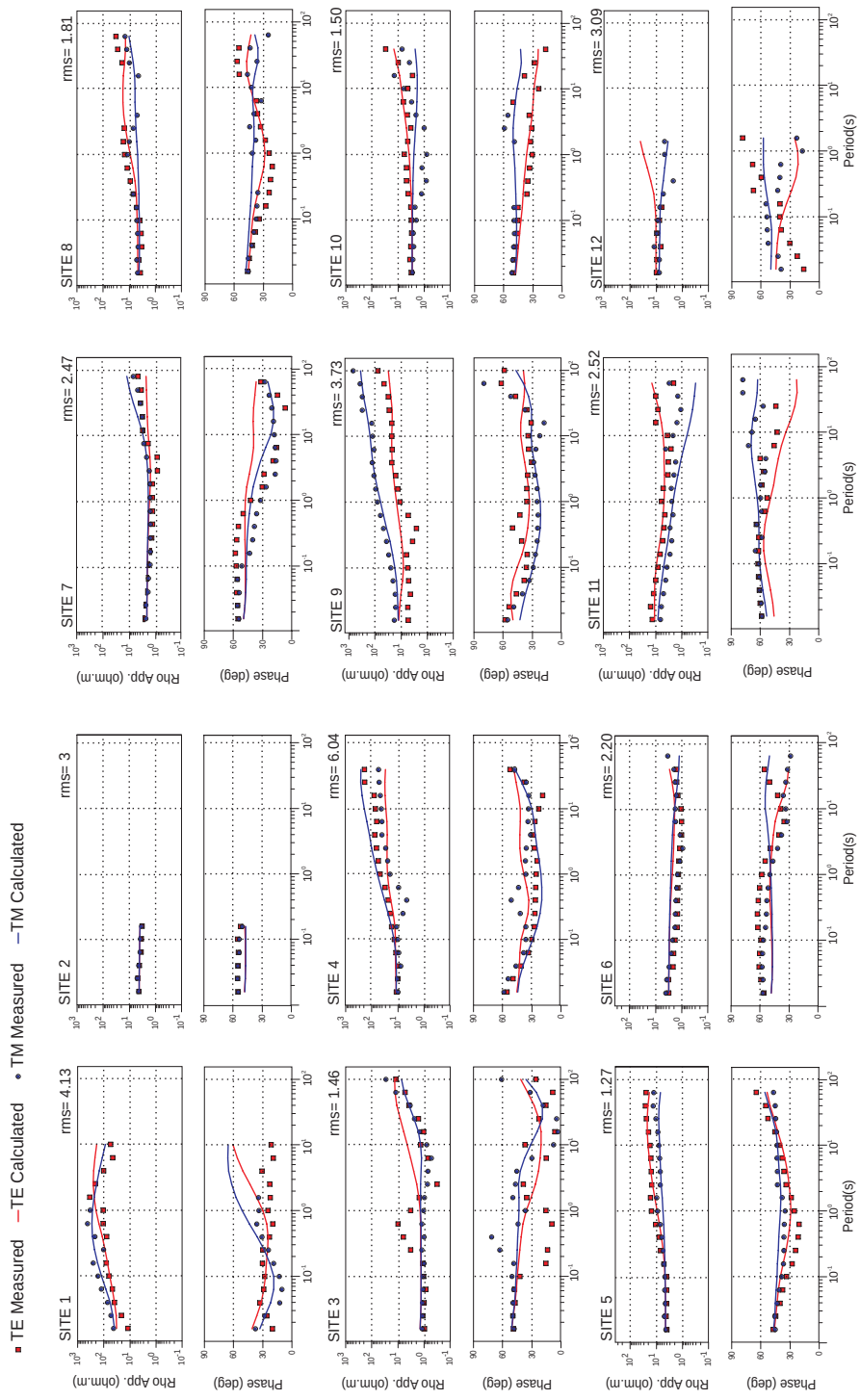
TE Measured
TE Calculated
TM Measured
TM Calculated
SITE 1
rms= 4.13
SITE 2
rms= 3
SITE 3
rms= 1.46
SITE 4
rms= 6.04
SITE 5
rms= 1.27
SITE 6
rms= 2.20
SITE 7
rms= 2.47
SITE 8
rms= 1.81
SITE 9
rms= 3.73
SITE 10
rms= 1.50
SITE 11
rms= 2.52
SITE 12
rms= 3.09
Rho App. (ohm.m)
Phase (deg)
Period(s)

6

Is the northwestern Betic Cordillera mountain front active in the context of the convergent Eurasia-Africa plate boundary?

A. Ruiz-Constán[1], D. Stich[2], J. Galindo-Zaldívar[1,3] and J. Morales[2]

TERRA NOVA, 2009 (Received 10 June 2008/ Accepted 13 May 2009)

The present relief of the Betic-Rif Cordillera has been mainly developed since the Late Miocene in the context of the Eurasia-Africa NW-SE oblique convergence and other interacting processes like slab roll-back or delamination. However, seismicity distribution and field observations reveal that most of the external mountain front of the Betics is not clearly active at Present, and tectonic activity is generally concentrated towards the innermost zones (Alborán Domain). New seismological data and recent faulting evidence from the northwesternmost front —the one best oriented with respect to the plate convergence— allow to discuss the present behaviour. Surface observations mainly indicate a N-S extensional tectonic regime, contrasting with the shallow reverse NW-SE compressive and the strike-slip earthquake focal mechanisms. Altogether these data suggest the activity of a tectonic wedge with top-to-the-NW tectonic transport, bounded by a NW-SE transfer fault that separates the active western from the inactive eastern segments of the mountain front.

Key words: earthquake focal mechanisms, thrust, transfer fault, extensional tectonics, stress and paleostress, western Alpine Mediterranean Belt.

1. Departamento de Geodinámica. Universidad de Granada.
Campus Fuentenueva, 18071-Granada, Spain.
2. Instituto Andaluz de Ciencias de la Tierra CSIC-UGR. Facultad de Ciencias.
Universidad de Granada. 18071-Granada, Spain.
3. Instituto Andaluz de Ciencias de la Tierra, CSIC- Universidad de Granada,
18071- Granada, Spain

6.1. Introduction

The main deformation pattern developed in the frontal part of orogenic wedges is a thin-skinned fold and thrust belt with a piggy-back thrust sequence (Bally et al., 1970; Davis et al., 1983). Accordingly to this model, recent deformation in active cordilleras is mainly concentrated in the external zones of the orogen (Becker, 2000), with the internal zones remaining mainly inactive. In these compressional settings, piggy back basins are formed on top of the thrust sheets and may help to constrain the timing of deformation (Lawton and Trexler, 1991; Wagreich, 2001; Martín-Martín and Martín-Algarra, 2002).

In regions with scattered seismicity of moderate magnitude, it is difficult to associate earthquakes with the individual active faults recognized at surface (Sanz de Galdeano et al., 1995). Yet the combined use of geological data and different stress analysis methods, such as focal mechanisms or borehole breakouts, is useful for obtaining present-day stress field maps (Zoback et al., 1989; Negredo et al., 2002; Fernández-Ibáñez et al., 2007). Focal mechanism analysis in the Betic-Rif Cordillera have generally taken into account the whole region (Buforn et al., 1995; Henares et al., 2003) or subdivided it into broad areas with similar tectonic features (Stich et al., 2003, 2006; Buforn et al., 2004). Such studies have underlined the significant complexity of tectonic deformation in the Eurasia-Africa plate boundary, as well as the heterogeneity of tectonic stresses in a short period of time (De Vicente et al., 2007). Generally, while focal mechanisms with NW-SE compression and less than 20 km depth prevail in the External Zones of the Betics, predominant in the Internal Zones are NE-SW tensional contexts that mainly give rise to NW-SE normal, E-W normal and dextral and NE-SW sinistral faults (Galindo-Zaldívar et al., 1993). Although the general stress pattern of the Betic Cordillera is relatively well established, detailed studies of reduced areas are needed to more clearly identify their seismogenic sources and geodynamic implications.

Despite plate convergence (McClusky et al., 2003; Serpelloni et al., 2007), previous studies of the central and eastern Betic Cordillera indicate that the external mountain front is inactive, with deformation and seismicity concentrated towards the Internal Zones (Ruano et al., 2004; Marín-Lechado et al., 2007). Seismicity in the western region exhibits a particular pattern, with shallow earthquake hypocenters (less than 15 km depth) near the mountain front and a progressive deepening of seismicity towards the Alborán Sea, where earthquakes reach depths of around 120 km (Figs. 6-1b and 1d).

The aim of this contribution is to describe new morphologic, seismologic and neotectonic evidence of recent and present-day deformation in the northwestern front of the Betic Cordillera in order to assess its activity. This study may contribute to establish the different behaviour of the mountain fronts formed in this arched orogen.

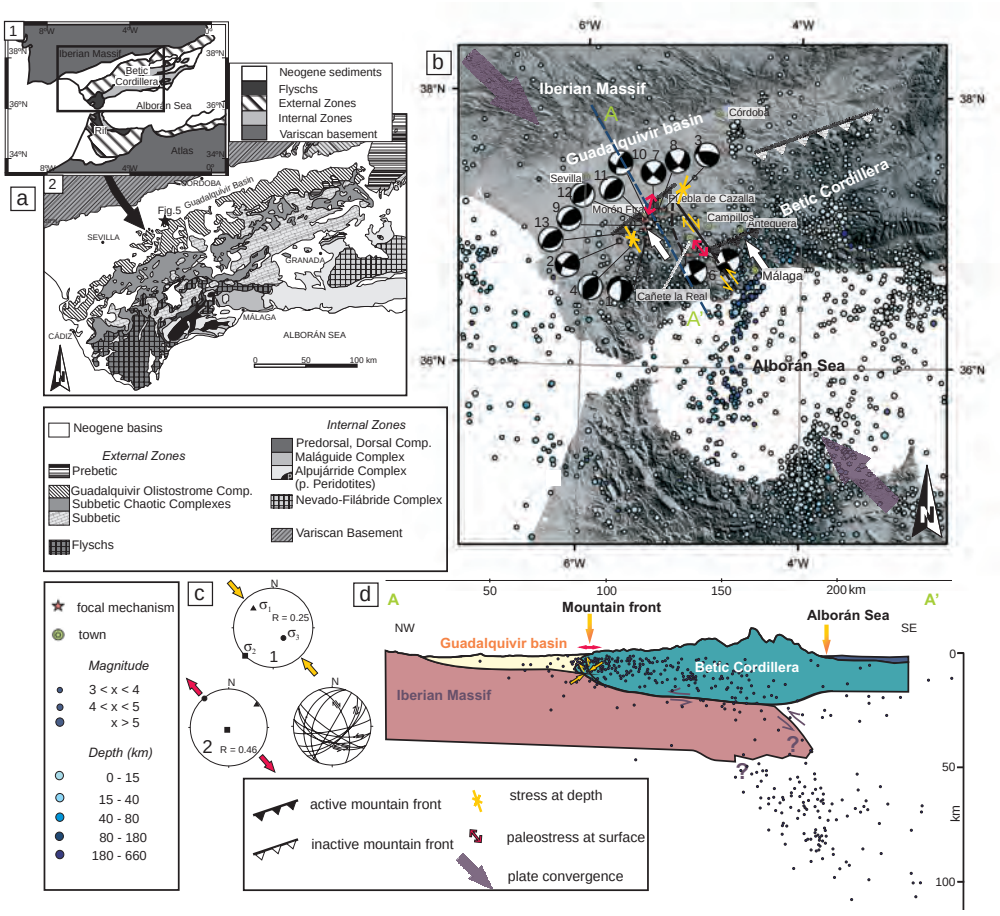

Figure 6-1. *Tectonic sketch and seismicity of the western Betic Cordillera* **a)** *Geological map of the Betic Cordillera showing the different domains (1) and enlarged detail of the western and central sectors (2). The location of Figure 6-5 is marked.* **b)** *Earthquake distribution in the western Mediterranean region taken from IGN database (data from 2000 to 2007); colour coded with respect to depth, and size coded with respect to magnitude. Focal mechanism solutions for the northwestern Betics are given in equal area, lower hemisphere projection. Numbers for focal mechanisms are according to Table 1.* **c)** *Average stress tensor using a grid search approach for stress magnitude ratio* $R = ((\sigma_2 - \sigma_1)/(\sigma_3 - \sigma_1))$ *and principal stress axis orientations: (1) Stress tensor analysis using Gephart´s method, (2) Paleostress solution for the Cañete la Real faults.* **d)** *Seismicity cross-section and tectonic sketch of the northwestern transect of the Betic Cordillera.*

6.2. Geological setting

The Betic-Rif Cordillera (Fig. 6-1a), the westernmost end of the circum-Mediterranean Alpine Chain, is an arc-shaped mountain belt that surrounds the Alborán Sea. Eurasian-African oblique NW-SE relative plate convergence, ongoing from the Cretaceous to present (De Mets et al., 1994; Dewey et al., 1989; Rosenbaum et al.,

2002; Sanz de Galdeano and Alfaro, 2004) together with subduction and roll-back models with different geometry (Torres-Roldán, 1979; Blanco and Spakman, 1993; Doglioni et al., 1997; Lonergan and White, 1997; Morales et al., 1999; Bijwaard and Spakman, 2000; Gutscher et al., 2002; Thiebot and Gutscher, 2006) have been proposed as mechanisms responsible for the Betic-Rif Cordillera development. Alternative models based on the delamination of lithospheric mantle have also been proposed (Platt and Vissers, 1989; García-Dueñas et al., 1992; Calvert et al., 2000b; Platt et al., 2003). Thus, debate surrounding the driving mechanism is still lively. The deep structures, including the geometry and polarity of the subduction zone, plus the recent tectonic evolution, stand as key features that are not well elucidated and that may evidence the importance of each process.

The Betic Cordillera is divided into three major domains: the External Zones (South Iberian Domain), the Internal Zones (Alborán Domain) and the Flysch Units. The External Zones constituted the Mesozoic and Tertiary margin of the Iberian Massif and comprise Mesozoic and Cenozoic carbonate series with local intercalations of igneous rocks. These rocks were strongly shortened by thin-skinned thrusting and folding during the Miocene (García-Hernández et al., 1980). The Flysch Units, formed by Mesozoic and Cenozoic turbiditic clays and marls, crop out in the western Betics along the contact between the Internal and External Zones. The Internal Zones are constituted by three main superposed metamorphic complexes separated by detachment faults (Galindo-Zaldívar et al., 1989, Jabaloy et al., 1992).

The Guadalquivir Basin is an asymmetric, southward deepening Neogene foreland basin, formed by the load of the Betic Cordillera over the Iberian Massif foreland (García-Castellanos et al., 2002). The northern part of the basin is mainly filled by autochthonous sediments, while the southern part is formed by Mesozoic and Cenozoic chaotic olistostromes coming from the External Zones. These sediments of Middle Miocene age, generally referred to as the Olistostrome Complex (Roldán and García-Cortés, 1988), formed the mobile front of the Betic Cordillera active boundary during the Early-Middle Miocene. The combined development of thrusts, slides, transcurrent faults and diapirism (Pérez-López and Pérez-Valera, 2003) configured its chaotic structure.

6.3. Seismicity distribution, earthquake focal mechanisms and stress field

Earthquakes in the surroundings of the Gibraltar Arc (Fig. 6-1b) show generally diffuse geographical distribution, although several clusters and possible alignments may be distinguished, and low to moderate magnitudes ($m \leq 5.5$; Buforn et al., 1995; Serrano, 1999). Most earthquakes are located at shallow depths ($h < 40$ km; Buforn et al., 2004), although in the Malaga region intermediate seismicity reaches down to 120 km (Fig. 6-1d) (Morales et al., 1999). In western Betics (Fig. 6-1b), earthquakes are located in the frontal part of the Olistostrome Complex, at the contact with the sedimentary infill of the Guadalquivir Basin. In the central and eastern Betics (East of Malaga meridian, Fig 6-1b), however, seismicity is located in a more internal part of the orogen.

Only four seismic source estimates were available previously in the northwestern Betics (Buforn et al., 2004, Stich et al., 2006). The recent improvement of the seismic broadband network —providing good azimuthal coverage of the study area from 18 stations within a distance of 200 km— and the significant seismic activity in the western Betics in 2006 (near the village of Cañete La Real) and 2007 (near Morón de la Frontera) allow us to extend this data set substantially.

We performed time-domain, least squares inversion for the deviatoric seismic moment tensor following the procedure described in Stich et al. (2003). Full three-component displacement waveforms were used in order to integrate body wave and surface wave information (Fig. 6-2). Waveforms were filtered between 15 and 35 s periods. A layered earth model with 32 km thick continental crust was used to calculate synthetic Greens functions (Stich et al., 2003), and a set of trial hypocenter depths with an increase of 2 km was tested in inversion. This allowed us to obtain appropriate waveform matches and stable estimates for seismic moment and faulting orientation for another nine earthquakes taking place in 2006 and 2007 (moment magnitude from 3.6 to 4.4, Table 6-1). The faulting style ranges from pure reverse to pure strike slip. Reverse solutions show ~NW-SE P-axis orientation, subparallel to plate convergence, and hypocenter depths of 8 km for the best-resolved solutions. Depths of strike slip solutions, with ~NW-SE and ~SW-NE striking nodal planes, are not as well resolved. The depth resolution for most of the events is around 4 km.

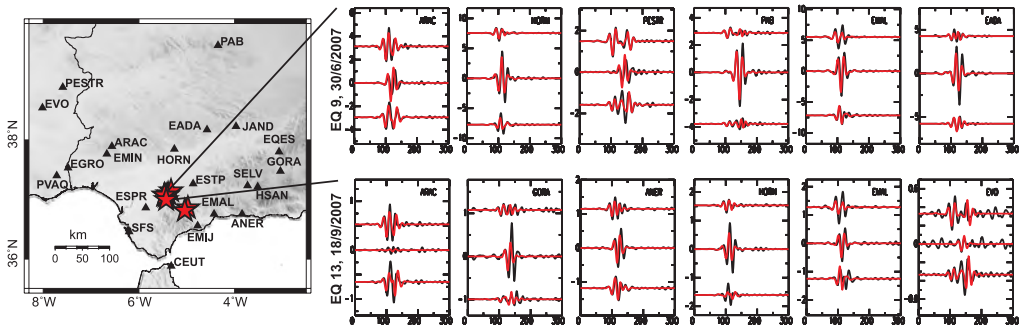

Figure 6-2. *Distribution of near-regional broadband seismic stations (triangles) used for moment tensor inversion, and examples for waveform fits for the 30/6/2007, 3:53:45 earthquake (top) and the 18/9/2007, 23:20:42 earthquake (bottom). Station panels give radial, transverse and vertical displacement (from top to bottom), observed seismograms in black, and predicted waveforms in red (units in s and μm).*

In order to quantify the pattern of seismic deformation, we estimate the average stress tensor from the focal mechanisms shown in Table 1 using a grid search approach for stress magnitude ratio $R = ((\sigma_2 - \sigma_1)/(\sigma_3 - \sigma_1))$ and principal stress axis orientations (Gephart, 1990). Maximum principal stress was obtained at direction N315ºE and plunge 30º (Fig. 6-1c), parallel to the plate convergence. A low R value of 0.25 was

likewise obtained, which may favour stress permutations between σ_2 and σ_1 and permit NE-SW compression locally (indeed, observed for event 3 in Table 1, with P-axes at N26ºE).

Nr.	Date	time	lat [°]	lon [°]	z [km]	M	Nodal planes (strike/ dip/ rake)	clvd	ref
1	01/05/1979	13:49:54	36.95	-5.42	24	4.0	249/ 35/ -24; 359/ 77/ -123	-	1
2	03/12/1980	22:16:28	36.92	-5.67	27	4.3	114/ 68/ 155; 214/ 67/ 24	-	1
3	15/09/2002	20:54:19	37.16	-5.27	4	4.1	273/ 68/ 58; 152/ 38/ 143	5%	2
4	25/07/2003	03:37:55	36.90	-5.56	6	3.5	29/ 40/ 82; 219/ 50/ 97	6%	2
5	11/03/2006	13:43:07	36.87	-5.00	22	3.9	152/ 80/ -2; 242/ 88/ -170	1%	3
6	26/03/2006	18:15:40	36.83	-5.04	14	3.7	151/ 70/ 5; 59/ 85/ 160	10%	3
7	02/01/2007	12:19:26	37.11	-5.39	10	3.6	44/ 84/ -10; 135/ 80/ -174	19%	3
8	02/01/2007	15:00:47	37.16	-5.33	14	3.6	37/ 64/ -21; 137/ 71/ -152	22%	3
9	30/06/2007	03:53:45	37.07	-5.45	8	4.4	218/ 53/ 61; 81/ 46/ 123	6%	3
10	30/06/2007	11:29:35	37.08	-5.42	8	3.6	205/ 71/ 34; 103/ 58/ 157	13%	3
11	14/09/2007	03:45:06	37.06	-5.40	12	3.6	224/ 56/ 78; 65/ 36/ 107	15%	3
12	14/09/2007	03:45:49	37.05	-5.41	8	3.6	220/ 36/ 81; 51/ 55/ 96	3%	3
13	18/09/2007	23:20:42	37.01	-5.43	8	3.9	217/ 57/ 82; 51/ 34/ 102	3%	3

Table 6-1. *Earthquake mechanisms in the context of the northwestern Betic mountain front. From left to right, columns give: 1) Reference number (Fig. 6-1B); 2) date; 3) origin time (UTC); 4) latitude and 5) longitude of the epicentre (IGN and IAG catalogue); 6) depth from moment tensor inversion (except 1 and 2); 7) moment magnitude MW (except 1 and 2, local magnitude mb); 8) fault angle parameters of nodal planes (strike/ dip/ rake); 9) percentage of non-double couple (CLVD) remainder for moment tensor solutions; and 10) reference (1: Buforn et al., 2004; 2: Stich et al., 2006; 3: this study).*

6.4. Recent deformation and paleostresses in the NW mountain front

Traditionally, geological studies involving the mountain front of the Betics have focused on sedimentological aspects of the Guadalquivir Foreland Basin (Sanz de Galdeano and Vera, 1992; Roldán, 1995; Riaza and Martínez del Olmo, 1996; Sierro et al., 1996) and on the rocks cropping out in the mountain front (Roldán and García-Cortés, 1988). The northwestern mountain front of the Betic Cordillera, that may be determined from the hillshade images (Figs. 6-1b and 6-3), has a roughly NE-SW trend. However, it is sinuous in detail, indicating a context of slow recent tectonic deformation. The northwesternmost front is advanced over the Guadalquivir foreland Basin with respect to the surrounding areas (Figs. 6-1b and 6-3). Although this setting may be a consequence of erosion, the sector is mostly affected by shallow seismicity (in contrast to the neighbouring sectors), suggesting the presence of active tectonic structures.

The generalized flat topography of the Guadalquivir Basin, the chaotic structure of the Guadalquivir Olistostrome Complex cropping out at the mountain front and its slow tectonic activity all determine the scarcity of outcrops recording present-day deformations. Brittle deformation in Middle-Late Miocene marls and marly limestones,

lying unconformably over the boundary region between the autochthonous Guadalquivir sediments and the Olistostrome Complex and related to the sedimentary infill of piggy-back basins (Roldán and Rodríguez-Fernández, 1991), is very intense.

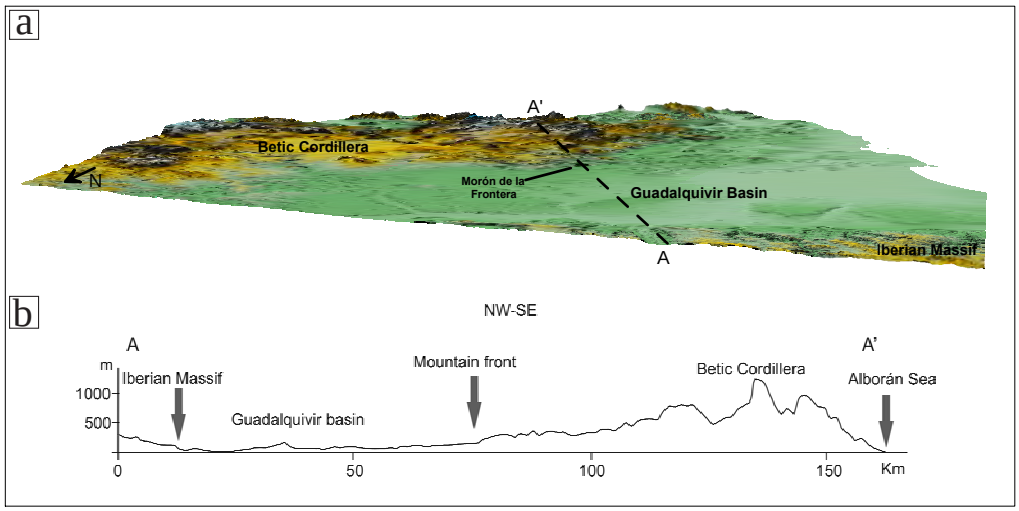

Figure 6-3. a) *3-D perspective view of the Betic Cordillera mountain front and,* **b)** *NW-SE topographic profile of the northwestern mountain front.*

The faults (Figs. 6-4a and 6-4b) have NNE-SSW main orientations, although NW-SE faults are also very common. Fault planes are generally subvertical, with a main strike-slip component and striae plunging 0-20º (Fig. 6-4c). In addition, recent faults have been identified in the boundaries of large limestone blocks of the Olistostrome Complex in the Cañete La Real area (Figs. 6-1c and 6-4d), indicating transtensional right-lateral and left-lateral kinematics that vary depending on the fault plane orientations, and would suggest NW-SE extension above areas of concentrated seismicity.

The paleostress field was determined using the Search Grid Method (Galindo-Zaldívar and González-Lodeiro, 1988) (Fig. 6-5; Table 6-2). We selected seven sites for a local analysis of microfaults and mesofaults, four of them providing enough data for the calculation of paleostress. Data from Middle-Late Miocene sediments reveal a well constrained nearly horizontal NNE-SSW tension (phase I). Anyway, additional local paleostress has been identified in station 1 (Fig. 6-5) that reveals another N-S tension stage (phase II). Radial extension was obtained from the analysis in Cretaceous rocks.

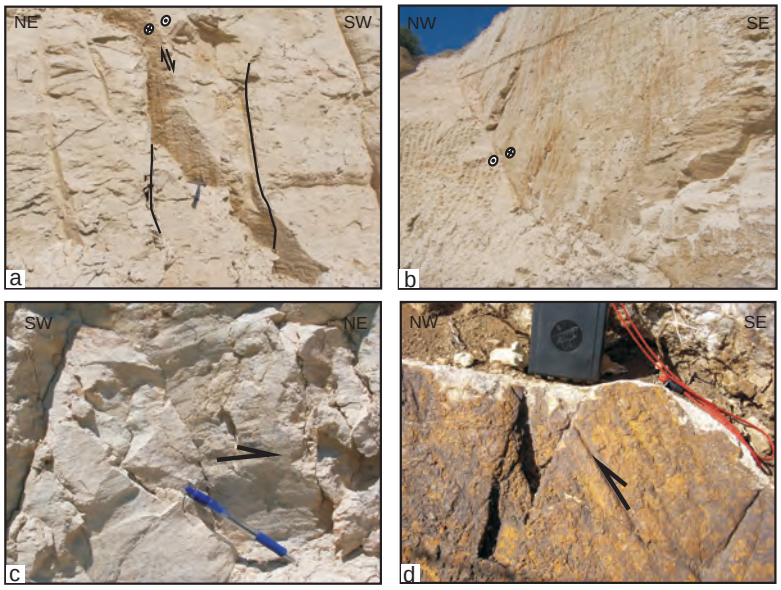

Figure 6-4. *Field examples of different structures that deform the Middle-Late Miocene marls and marly limestones cropping out at the northwestern mountain front (a, b, and c) and the limestones that crop out in the Cañete la Real area (d).* **a)** *NE-SW dextral strike-slip fault displacing another strike-slip fault of higher dip,* **b)** *N-S sinistral strike-slip fault,* **c)** *and* **d)** *examples of strike-slip striae.*

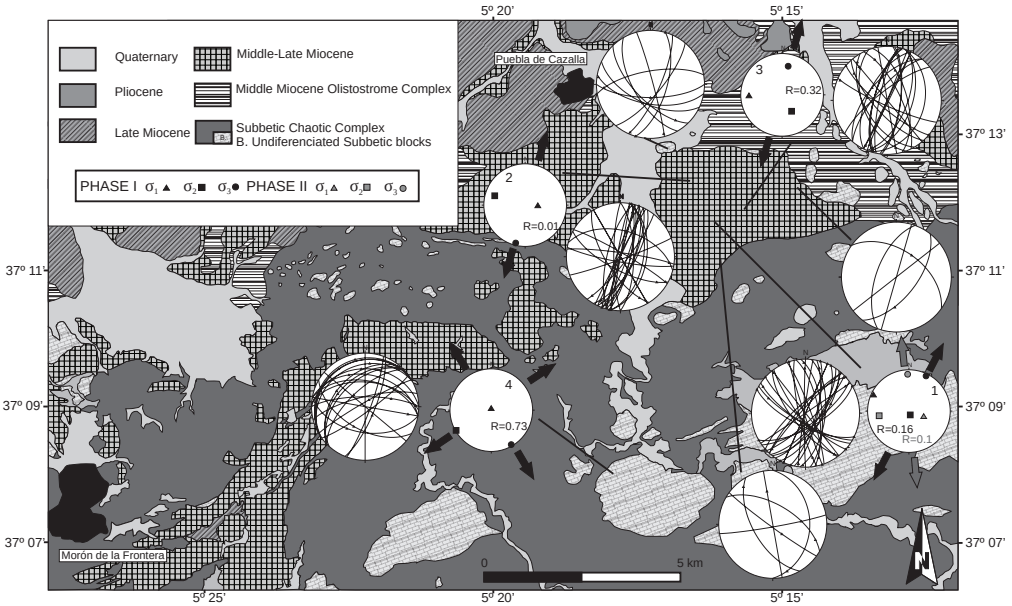

Figure 6-5. *Stereoplots of stress axes obtained from palaeostress analysis (equal area, lower hemisphere projection). The arrows indicate the trend of extension axes. R indicate the stress magnitude ratio* $R = ((\sigma_2 - \sigma_1)/(\sigma_3 - \sigma_1))$.

Ref	*Rock age*	*N*	σ_1	σ_2	σ_3	*R*
1	Late Serravallian-Early Tortonian	30	295/6	161/82	26/6	0.16
			109/59	261/28	358/12	0.1
2	Late Serravallian-Early Tortonian	20	91/65	287/24	194/6	0.01
3	Late Serravallian-Early Tortonian	22	269/21	150/52	12/30	0.32
4	Cretaceous	22	357/86	150/4	240/2	0.73
B Fig. 6-3	Jurassic	13	50/6	212/84	320/2	0.46

Table 6-2. *Paleostress ellipsoids determined from the Search Grid Method (Galindo-Zaldívar and González-Lodeiro, 1988). Ref., reference number in the figures; N, total number of measurements; σ_1, σ_2, σ_3, trend and plunge of the main axes of stress ellipsoid; R, axial ratio.*

6.5. Discussion and conclusions

In active convergent plate boundaries we expect to observe piggy back sequences and active deformation in the external mountain front. However, the arched Betic Cordillera mountain front is only active in certain segments (Fig. 6-1b). Most studies on recent tectonics developed in the eastern and central Betics show that active deformation and seismicity mainly affect the Internal Zones, while the topographic mountain front may represent a relict structure developed during Early and Middle Miocene (Ruano et al., 2004). However, new data from the northwestern Betic Cordillera mountain front —including shallow seismicity, recent deformations and geomorphological features— evidence the presence of an active tectonic wedge with top-to-the-NW tectonic transport bounded to the northeast by a NW-SE transfer fault (Fig. 6-1b).

Most focal mechanisms calculated in the frontal zone point to the existence of NE-SW striking thrust faults, at a depth of 8-12 kilometers, that may have top-to-the-NW tectonic transport. The Gephart's method (1990) indicates a northwestward inclination of maximum stress, compatible with the activity of low-angle thrust faults (Figs. 6-1b and 1d). Estimates for focal depth are not accurate enough for discerning whether the seismogenic active thrust is located in the more brittle upper part of the Variscan basement or just at the main contact with the Betic Cordillera. The active thrusts do not reach the surface, but may be related to NE-SW folds associated with blind thrusts at the mountain front.

Seismicity distribution in the western sector of the mountain front is clearly clustered around Morón-Puebla de Cazalla (Fig. 6-1b). One of the most significant features is an unusual seismic gap in the Campillos-Antequera area, east of the Moron seismic maximum, with a very straight NW-SE western boundary. This gap coincides with the presence of huge masses of ductile sediments belonging to the Subbetic Chaotic Complexes. East of this border the seismicity front is displaced southwards.

The eastern boundary of the seismogenic orogenic wedge is characterised by strike slip focal mechanisms showing opposite kinematics, which may be related to

transfer faults. They are oriented parallel to the plate convergence direction (NW-SE) and accommodate differential shortening between individual sectors without contributing to the regional strain. This orientation would also be compatible with the trend of the eastern limit of the seismogenetic orogenic wedge, suggesting that transfer faults restrict the continuity of seismicity in the frontal part of the orogen at depth. In the most External Zones, they correspond to NW-SE dextral faulting focal mechanisms (the January 2007 Morón earthquakes), whereas southeastwards they correspond to sinistral faulting (the 2006 Cañete events), the latter apparently located slightly deeper.

Towards the NE of the orogenic wedge, locally NE-SW compression is observed near the mountain front. This orientation of the maximum compression axis may be a consequence of the permutation of the regional NW-SE orientation, favoured by the close magnitudes of maximum and intermediate stress axes, as revealed by the low R values of the stress ellipsoid (Fig. 6-1c). Moreover, this situation may be also due to local stress disturbances at the corner of the indenting orogenic wedge (Fig. 6-1b) that could possibly reorient the principal stress directions (Schedl and Wiltschko, 1987).

In active mountain fronts, the apparent inconsistency between seismic deformation and geological field data is a common observation (Berberian, 1995; Costa et al., 2000). In the area of our study, field data suggest a roughly N-S to NW-SE extension since the Middle Miocene. To reconcile these observations we propose that, while the orogenic wedge thickens and undergoes shortening at depth, extensional collapse affects the uppermost levels in roughly the same direction (Fig. 6-1b and 1d).

The variable tectonic activity of each sector of the Betic-Rif mountain front may be a consequence of its arched character with respect to the NW-SE 5 mm/year plate convergence (McClusky et al., 2003; Serpelloni et al., 2007). The western Betic mountain front has a more appropriate orientation to be active, orthogonal with regard to present-day NW-SE to WNW-ESE convergence. In the Rif Cordillera mountain front, southern branch of the Gibraltar Arc, antiforms of SW and S vergence associated with blind thrusts deform up to the Neogene foreland basins of Saïss and Gharb (Bargach et al., 2004). In contrast to the Betic Cordillera, here thrusts in some places reach the surface and deformation propagates as far as the foreland.

In sum, the northwesternmost mountain front is the only one that remains active in the arched Betic Cordillera, owing to its favourable orientation with respect to the present-day convergence of the Eurasian-African plates, and the moderate lower topography of the orogenic wedge as compared to the central and eastern Betics. The active tectonic structures are partitioned, thus indicating a NW-SE oriented compression and thrusting at depth, extension at surface, and the presence of transfer faults with opposite kinematics in its northeastern boundary.

Acknowledgements:

The projects CSD2006-00041, CGL2006-06001, CGL2005-04541-03-01-BTE, RNM-149 RNM-104, CGL2008-01830/BTE, and a MEC PhD grant given to the first author are acknowledged. We thank Dr. C. Doglioni, Dr. F. de Lamotte, and four anonymous reviewers, experts in alpine geology but supporting different models, for helping improve the quality of this contribution through their comments.

7

Gravity anomalies and orthogonal box fold development on heterogeneous basement in the Neogene Ronda Depression (western Betic Cordillera)

A. Ruiz-Constán[1], J. Galindo-Zaldívar[1, 2], A. Pedrera[1] and C. Sanz de Galdeano[2]

JOURNAL OF GEODINAMICS, 2009 (Received 25 April 2008/ Accepted 15 September 2008)

The Ronda Depression constitutes a Neogene intramontane basin located in the External Zones of the western Betic Cordillera. Main deformation structures affect only the southwestern part of its sedimentary infill and consist of NNE-SSW and WNW-ESE box folds that developed simultaneously. New gravity data reveal two negative NNE-SSW elongated Bouguer anomalies, unrelated to basin depocenters, but corresponding to the accumulation of low-density plastic Triassic basement rocks in the core of antiforms or directly under the northwestern undeformed sedimentary infill. The Subbetic basement is also deformed by Early Burdigalian to Serravallian NNE-SSW folds and thrusts, although there is no clear continuity with those affecting the Late Miocene sedimentary infill. The aim of this contribution is to describe in detail the Late Miocene folds that deform the Ronda Depression, as well as to discuss the role of the basement nature on their reactivation. The reactivation of the pre-Tortonian folds, due to the heterogeneous distribution of evaporitic Triassic rocks in the basement as well as the presence of rigid limestones in the southwestern basin boundary, determined the simultaneous orthogonal fold development that only evidence local deformation

Key words: neogene basin, gravity models, low density basement, fold reactivation.

1. Departamento de Geodinámica. Universidad de Granada.
Campus Fuentenueva, 18071-Granada, Spain.
2. Instituto Andaluz de Ciencias de la Tierra CSIC-UGR. Facultad de Ciencias.
Universidad de Granada. 18071-Granada, Spain.

7.1. Introduction

The behaviour of plastic rocks facilitates the presence of detachment levels determining the style of deformation. Analogue modelling studies have focused on the effects of different rheological rock properties in detachment features (Nilforoushan and Koyi, 2007). Anomalous evaporitic rock accumulations located in these detachments greatly condition antiform nucleation (Bonini, 2003; Marques, 2006) and may favour the simultaneous development of oblique compressive structures, sometimes even orthogonal to the main structural trend (Callot et al., 2007; Crespo-Blanc, 2008). Such oblique folds and thrusts have usually been interpreted as a consequence of overprinted deformation stages (Caritg et al., 2003; Mon et al., 2005). Moreover, the accumulation of low-density evaporitic rocks at depth determines the development of vertical movements related to salt tectonics producing diapiric structures. They may be isometric or elongated, depending on the origin, evolution and initial distribution of low density rocks. Establishing the position of these low density evaporitic rocks accumulations is essential to understand the superficial folded structures. Gravity studies are key in elucidating the position and geometry of such structures because they commonly give rise to a negative Bouguer gravity anomaly (Jallouli et al., 2005; Pinto et al., 2005).

Gravity studies in sedimentary basins also allow to determine the thickness of the sedimentary infill, related to the irregularities of the basal unconformity and the presence of recent deformation structures. In sedimentary basins, Bouguer anomaly minima are generally interpreted as depocenters, considering that basement rocks are denser than the sedimentary infill. However, in basins with heterogeneous basements, the superposed effect of basement and infill rocks may give rise to a complex Bouguer anomaly pattern that needs to be analyzed in order to isolate each contribution.

The External Zones of the Betic Cordillera (Fig. 7-1) are constituted by Mesozoic sediments with Triassic evaporitic rocks at the lower part of the sequence. In the westernmost sectors, these Mesozoic rocks are deformed mainly by NE-SW to NNE-SSW folds and thrusts rooted in the evaporitic rocks. However, fold and thrust trends change frequently along the Cordillera; and interference structures have been recognized, as in the eastern Betics (Sanz de Galdeano et al., 2006; García-Tortosa et al., 2007) or in the central Betics (Crespo-Blanc, 2008). In any case, their coetaneous development is still under debate because in areas like the External Zones of the Central Betics, paleomagnetic studies (Platzman, 1992; Platt et al., 1995) have demonstrated a late rotation, suggesting a constant initial fold orientation. In many cases, establishing the age of deformation is complicated by the absence of a young sedimentary cover that could be used as a marker.

The study of folds in Neogene-Quaternary basins allows us to characterize the recent tectonic evolution simultaneous to relief uplift. Therefore, many research efforts have been undertaken in the eastern (Groupe de Recherche Neotectonique de l'Arc de Gibraltar, 1977; Marín-Lechado et al., 2007; Pedrera et al., 2007) and central (Ruano et al. 2004) part of the Cordillera. In addition, gravimetry has been widely used in the

Eastern Betic Cordillera (Granada Depression, Morales et al., 1990; Campo de Dalías, Marín-Lechado et al., 2007), or in the Guadix-Baza Depression (Sanz de Galdeano et al., 2007) in order to determine sediment thickness distribution in Neogene-Quaternary basins. However, no detailed tectonic or gravimetric research has been reported to date on the intramontane sedimentary basins of western Betics.

The Tortonian–Messinian Ronda depression, located in the External Zone of the Betic Cordillera, constitutes a good example of intramontane depression that can provide new insights into the development of recent deformations consisting mainly of medium to large scale folds, and very scarce meso and microfaults. The aim of this contribution is to describe in detail the Late Miocene folds that deform its sedimentary infill, as well as its relationships with the heterogeneous pre-Miocene basement structure. New gravity data acquired during this study determine the distribution of evaporitic rocks below the sedimentary infill, and allow us to discuss the role of their concentrations on the reactivation of basement antiforms that affect the Neogene infill.

7.2. Geological setting

The Betic-Rif Cordillera (Fig. 7-1) is an arc-shaped orogen that constitutes the western end of the Mediterranean Alpine chain. The outer arc of this orogen consists of a fold-and-thrust belt (External Zones), while the inner arc is composed of an allochthonous pile of tectonic complexes including metamorphic rocks (Internal Zones). The External Zones comprise the Subbetic and Prebetic zones, the latter outcropping only in the eastern Betic Cordillera. The Internal Zones are formed by three main complexes that are, from bottom to top: the Nevado-Filábride (outcropping only in the Eastern and Central Betics), the Alpujárride and the Maláguide complexes. In addition, the Dorsal and Predorsal complexes may be located in an intermediate position, in-between the Flysch Units and other units of the Internal Zones.

The Betic-Rif arc geometry developed during the latest Oligocene and Early to Middle Miocene as a result of the Eurasian-African plate convergence and the westward drift of the Internal Zones. In the western Betic Cordillera, this setting caused the northwestward thrusting and folding of the Mesozoic–Cenozoic rocks of the Subbetic Units in front of the migrating Internal Zones.

Since Miocene, sedimentary basins were individualised and record the transition from marine to continental sedimentation as a consequence of relief uplift. Deposition in the External Zones mainly took place in the Guadalquivir foreland Basin (Sanz de Galdeano and Vera, 1992; Viseras et al., 2004), and was conditioned by huge olistostromic masses from the frontal part of the External Zones. At the beginning of the Late Miocene, several piggy-back basins were individualized from the Guadalquivir foreland Basin (Sanz de Galdeano and Vera, 1992) during the development of the Subbetic fold and thrust belt (Roldán-García, 1995; Ruano et al., 2004; Crespo-Blanc, 2007) with different sedimentary and tectonic signatures, due to the northwestward progression of their mobile basement.

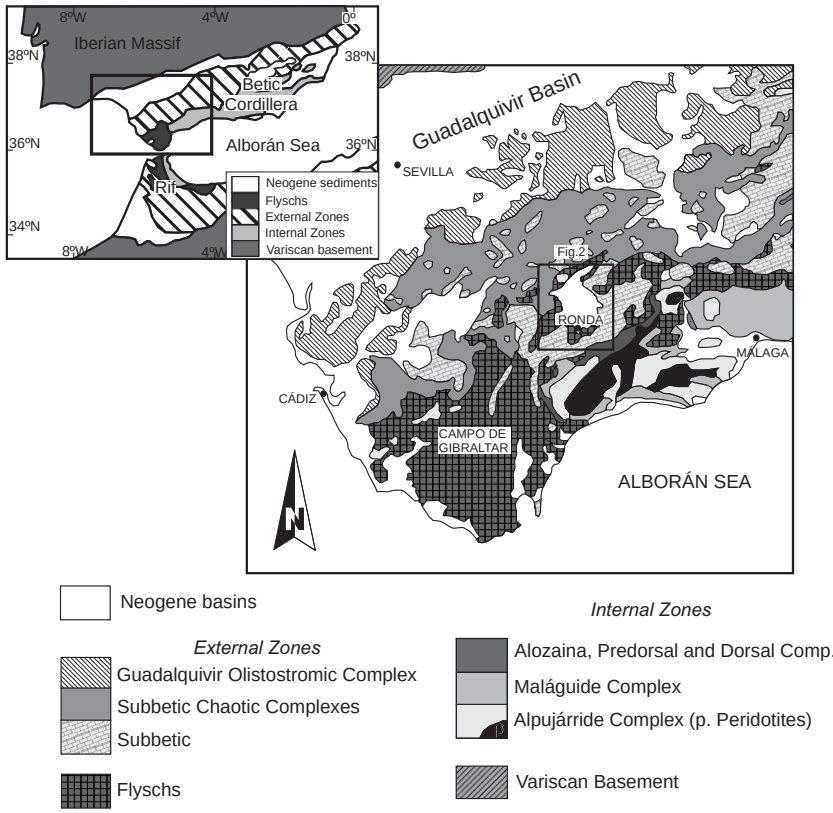

Figure 7-1. *Geological setting of the Ronda Depression in the framework of the Betic and Rif.*

The Ronda Depression (Fig. 7-1) constitutes one of the largest piggy-back basins in the western Betics. It is located over the northwesternmost Subbetic Units with continuous structure, the Subbetic Chaotic Complexes and the Flysch Units. Subbetic Units are formed by Triassic to Middle Miocene sedimentary rocks with local intercalations of igneous rocks. The Subbetic structure in this region is described by Crespo-Blanc and Campos (2001) as a NW-vergent fold-and-thrust belt, post-Early Burdigalian in age. Within the Betic External Zones, Keuper Triassic levels have been traditionally considered as detachment levels where the main thrust structures are generally rooted.

Towards the northwestern mountain front of the cordillera, Subbetic Units are widely deformed and show a chaotic structure (Pérez-López and Sanz de Galdeano, 1994). These Subbetic Chaotic Complexes are mainly composed by a Keuper Triassic matrix including post-Triassic blocks, some of them of Middle Miocene age, deformed by the combined development of thrusts, slides, transcurrent faults and diapirism (López-Garrido and Vera, 1974; Calaforra and Pulido-Bosch, 1999; Pérez-López and

Pérez-Valera, 2003). Flysch Units crop out in the Betic Cordillera lengthwise along the contact between the Internal and External Zones, mainly in the broad area of the Campo de Gibraltar, and between the different Subbetic Units. The Mesozoic and Cenozoic sediments that constitute these units are turbiditic clays and marls.

The sedimentary infill of the Ronda Depression (Fig. 7-2), Late Miocene in age, is divided into four formations (Serrano, 1979; Rodríguez-Fernández, 1982). From bottom to top these are: I) Gastor Formation, made up of sands, silts and heterogeneous conglomerates of Tortonian age that lie unconformably over the Triassic basement rocks in the northwestern border of the depression. II) Tajo Formation, formed by heterogeneous conglomerates of pre-Late Tortonian age with clasts proceeding from the Subbetic and Flysch southern units. This formation lies unconformably over the Flysch Units. III) Mina Formation, located conformably over the Gastor Formation and composed by marls and sandy silts of Early Tortonian-Late Messinian age. It crops out in the western half of the depression. IV) Setenil Formation, Late Tortonian-Late Messinian in age, crops out throughout the depression, except in the northwestern part. It lies over basement rocks or Mina Formation sediments, although it could also be In facies transition with this formation. Rodríguez-Fernández (1982) differentiated two members in this formation: a Limestone Member and a Calcarenite one.

The Neogene sedimentary infill of the Ronda Depression lies unconformably upon the External Zones and Flysch basement. The boundaries of the depression are not conditioned by high angle faults as occur in many points of other basins of the Betic Cordillera like the Granada Basin (Rodriguez-Fernández and Sanz de Galdeano, 2006). Only locally inside the basin can we find NE-SW and NNW-SSE minor normal faults, which do not reach cartographic scale and cannot be represented. These brittle structures mainly deform the Tortonian calcarenites of the Setenil formation and are concentrated in the southern part of the basin.

7.3. Orthogonal folds in the Ronda Depression

The Neogene sediments of the Ronda Depression are mainly deformed by two sets of NNE-SSW and WNW-ESE kilometric folds (Fig. 7-2). These structures have a heterogeneous pattern of distribution and are essentially located in the southern and southwestern parts of the depression. In the eastern sector, outcrops are scarce because the zone is extensively cultivated, and there is not significant relief due to the low dip of the layers and the outcropping marls. In the northern part, however, fluvial incision allows us to observe tilted Tortonian-Messinian calcarenites (Fig. 7-3a). Thus, folds probably do not propagate through these regions and affect only the southwestern part of the Depression.

The Salinas Fold is the major structure observed in the whole Depression. It is a NNE-SSW box shaped antiform with a two-kilometre-wide crest. The dip of the flanks (Figs. 7-2, 7-3 and 7-4) increases sharply, from 20º to 70º. This feature produces straight

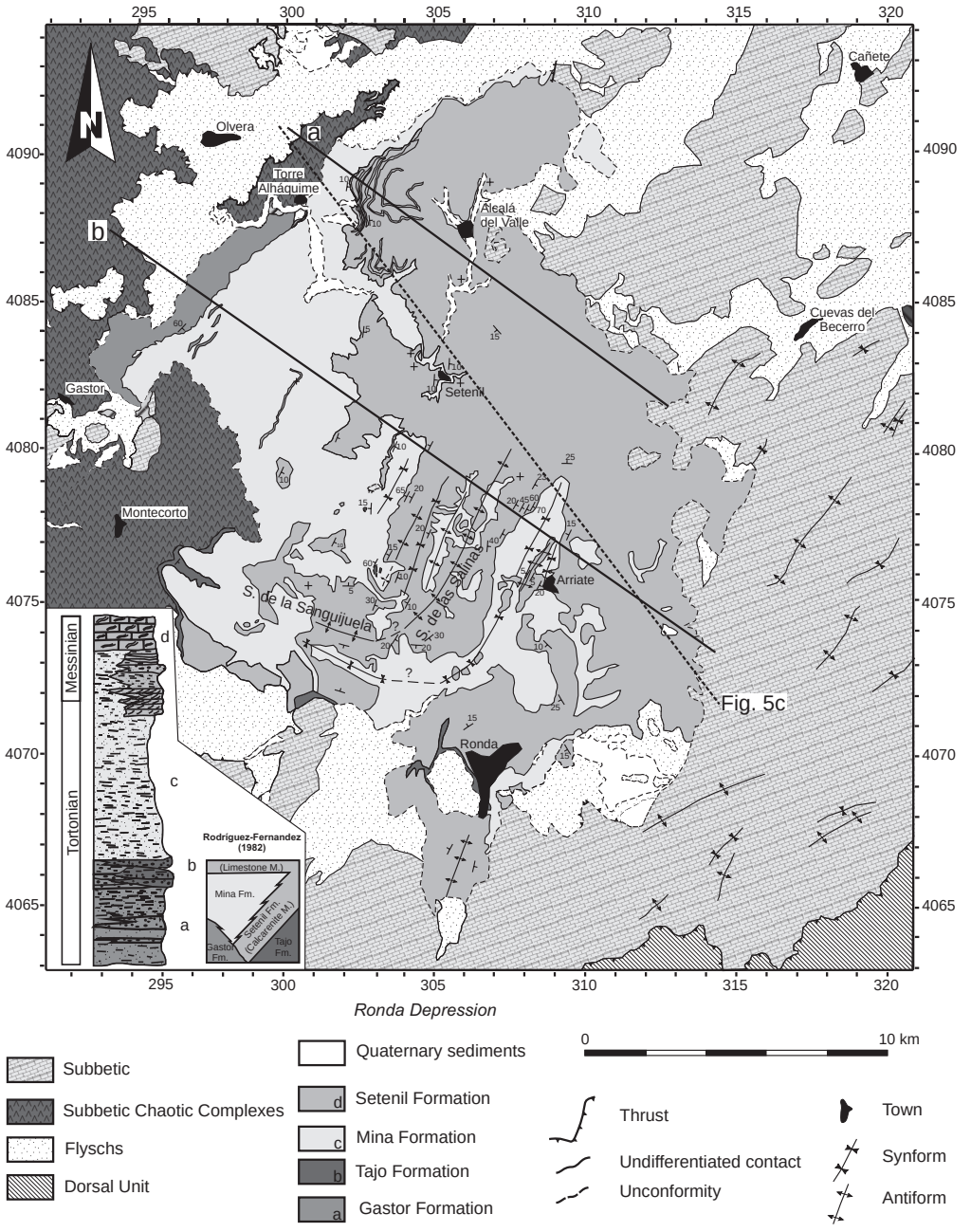

Figure 7-2. *Tectonic sketch of the Ronda Depression. Cross sections of Fig. 7-3 and gravity profile of Fig. 7-5c are indicated. UTM coordinates are in kilometres.*

boundaries in the topographic intersection that are not related to large NE-SW normal faults, as suggested by previous authors (Serrano, 1979). The antiform culmination is essentially flat, with dips lower than 20º. Therefore, the geometry of the fold could be described as a box-fold without vergence (Fig. 7-3b). Although previous authors (Rodríguez-Fernández 1982) point to the local presence of some patches of Triassic rocks cropping out in the core of the antiform, only Tortonian-Messinian calcarenites from Setenil Formation and some patches of Messinian marls have been distinguished in this study. Six cartographic folds could be described running parallel to the Salinas Fold, constituting a fold set that deforms an area 6 km long and 8 km wide (Figs. 7-2 and 7-3b). In addition, it is possible to identify minor folds with metric wave length and the same orientation as the Salinas antiform, approximately N30ºE. Their geometry is open, with flanks dipping around 15-20º. These minor folds are fundamentally located in the crest zone of the Salinas Fold and deform the calcarenites of Setenil Formation. It is not possible to determine if they also deform the Late Messinian Limestone Member of the Setenil Formation, because there are scarce outcrops of these rocks, and in all of them a 10º southeastward dipping is observed.

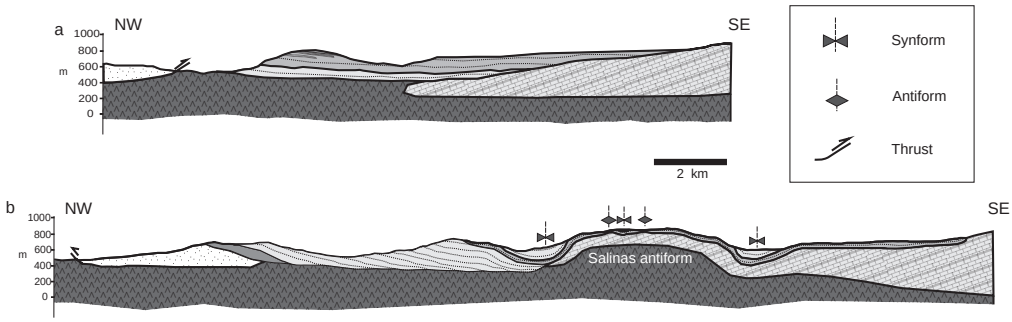

Figure 7-3. *Geological NW-SE cross-sections of the Ronda Depression. The position of the cross-sections is marked in Fig. 7-2. Gravity data have been qualitatively taken into account to constraint the deep structure. The legend is the same as in Fig. 7-2*

The WNW-ESE Sierra de la Sanguijuela antiform (Fig. 7-2), situated SW of the Salinas Fold, is parallel to the southwestern border of the depression. Its shape resembles that of the Salinas antiform and could be considered as the prolongation of this fold, given that there are not interference structures between the two, although there is a sharp change in fold axis orientation. There are no minor antiforms parallel to the Sanguijuela antiform, in contrast to the Salinas one. Both sides of these folds there are two synforms with the same orientation, NE-SW in the Salinas sector and WNW-ESE in the Sanguijuela sector (Fig. 7-2 and 7-3b). Marls pertaining to the Mina Formation crop out in the core of these synforms.

The most recent rocks deformed by the kilometric box-folds are Tortonian-Messinian calcarenites. The depression has no Pliocene deposits and the Quaternary

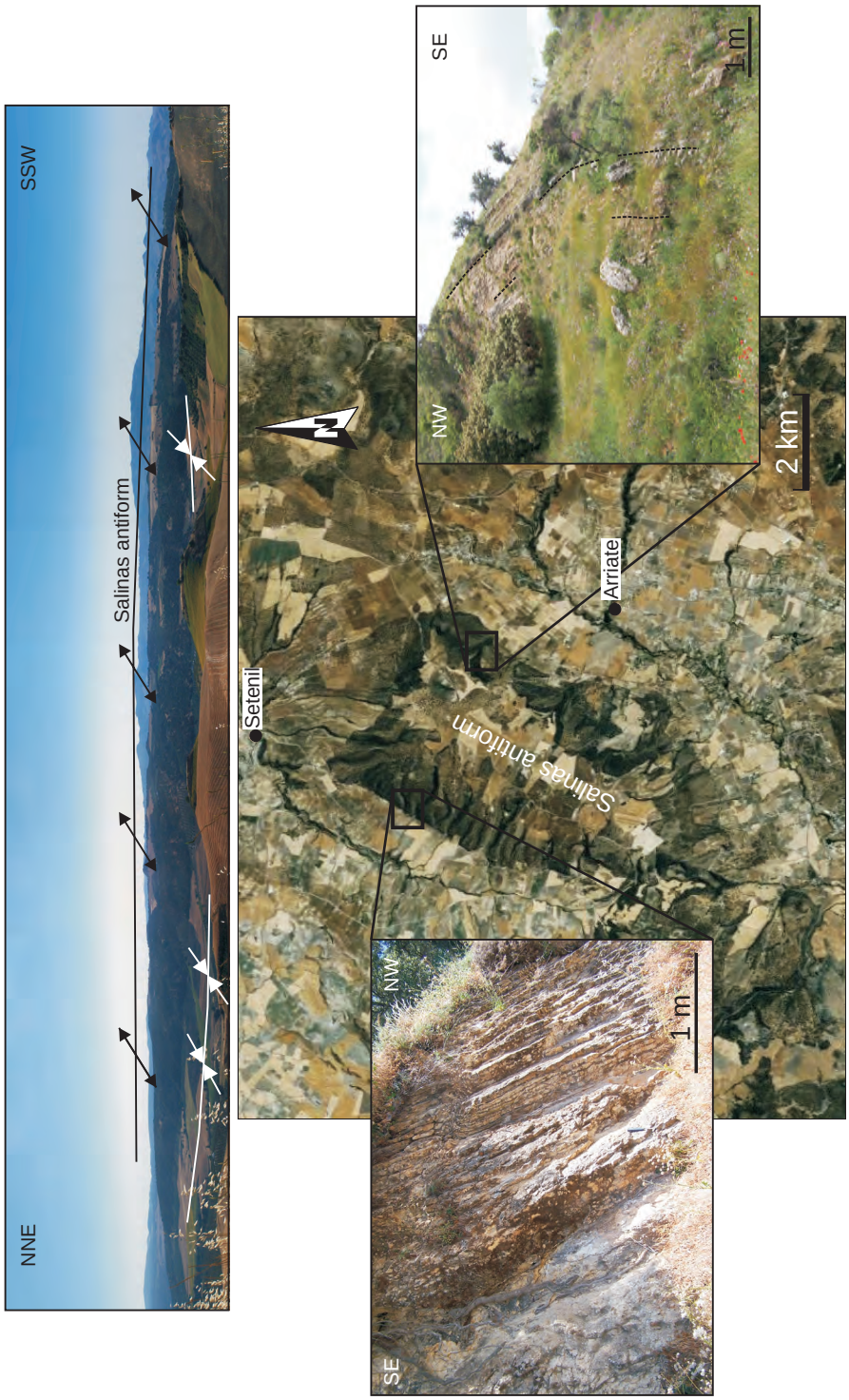

Figure 7-4. *Panoramic view and orthophoto image of the Salinas Antiform. Photographs show the high dip of the flanks in this box fold.*

sediments are reduced to the non-deformed river channels. Although it is not possible to determine the end of the activity of these folds, field observations indicate that both types of folds were simultaneously active in Late Tortonian to Late Messinian times.

7.4. Gravity anomaly and deep structure

A new gravity survey was performed in the Ronda Depression in order to determine the sedimentary thickness and the deep geometry and nature of its basement. Data were acquired in several profiles covering all the sedimentary infill and the Depression boundaries. Measurement stations along profiles were spaced at an average of 250 metres. Gravity data were acquired using a Master Worden gravimeter, with a maximum accuracy of 0.01 mGal. The measurement sites were located with an e-trex Garmin GPS and a barometric altimeter with 0.5 meter altitude precision. The measurements were referenced to a base station of the I.G.N. national gravimetric network, located in Málaga, in order to calculate the absolute gravity value. Data acquisition was carried out in cycles of less than three hours in order to accurately correct the instrumental drift, tide variations and barometric changes. Topographic correction was done using a digital terrain model with a grid of 10 meters of cell size for the first 1600 meters, and 200 meters thereafter, to a total distance of 22 kilometres. The Bouguer anomaly was calculated taking into account a standard density (d= 2670 kg/m^3) similar to the density of the Subbetic rocks forming the basement.

The heterogeneous basement lithology (and therefore density) of the region made it impossible to isolate the residual anomaly associated with the Neogene sedimentary infill of the Ronda Depression, and therefore delimit its thickness. Whereas at the southern boundary the basement is formed by Subbetic limestones with a high density contrast, the northern basement is constituted by Triassic rocks and Flysch units with density values that are similar to or lower than the sedimentary infill.

In the Bouguer anomaly map 1:1.000.000 (I.G.N., 1976) (Fig. 7-5a), values in the southern part of the Ronda Depression increase progressively to the SE. However, in the western and northern parts, the isolines have a N-S direction, and anomaly values increase gradually to the W. Changes in the direction of the regional anomaly signalled by this Bouguer anomaly map are probably related to the deep crustal structure and make it impossible to distinguish the anomaly related to the basement heterogeneities and the variations in thickness of sedimentary infill. Therefore, a 2D model that considers both sedimentary infill and shallow basement structures was made using the Bouguer anomaly, with the GRAVMAG V.1.7. program of the British Geological Survey (Pedley et al., 1993). A constant regional anomaly value due to the deep crustal structures was taken into account.

The main features of the detailed Bouguer anomaly map of the Ronda Depression (Fig. 7-5b) are two marked gravity minima observed in the middle and northwestern parts of the depression. The southernmost one is elongated in NE-SW orientation and

reaches values of -88 mGal, while the minimum placed to the north reaches -78 mGal. These minima are not detected in the regional gravity map of Spain 1:1.000.000 (I.G.N., 1976; Fig. 7-5a) due to its scale and to the large distance between measurements. There is a good correlation between the southernmost minima and the main structures of the Depression.

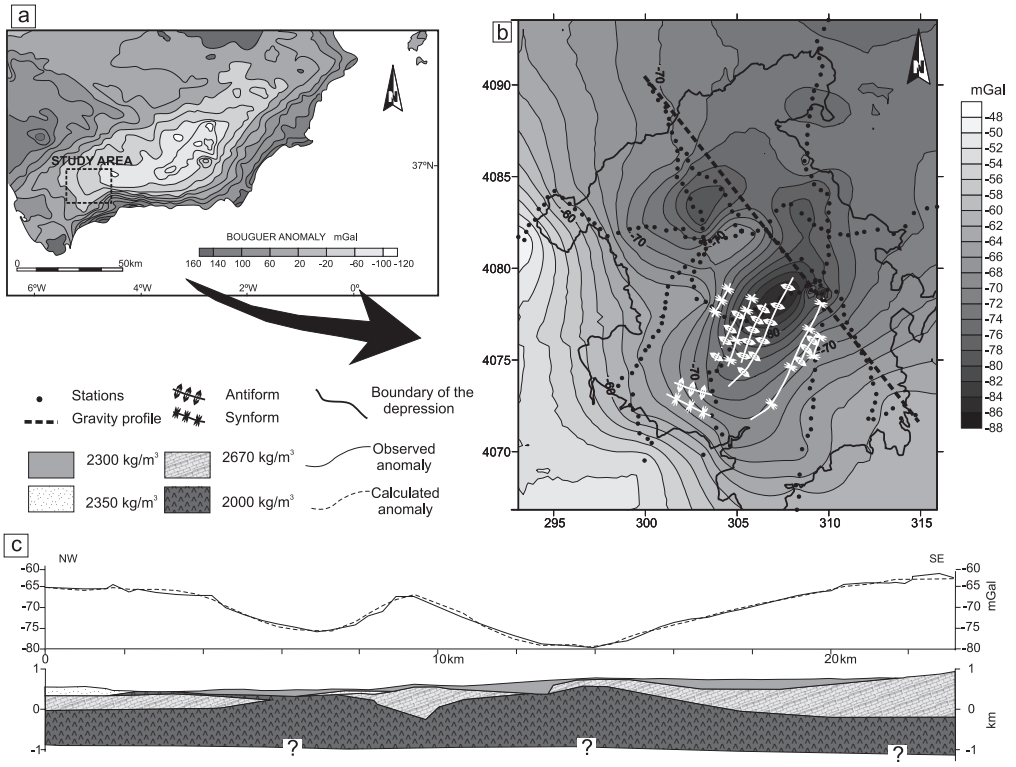

Figure 7-5. *Bouguer anomalies and gravity model:* **a)** *Bouguer anomaly map of Betic Cordillera 1:1.000.000 (I.G.N. 1976);* **b)** *Bouguer anomaly map of Ronda Depression. The modelled profile and the axial traces of the folds are drawn (in grey: minor open folds; in white: Salinas and Sanguijuela folds);* **c)** *2D NW-SE gravity model.*

In sedimentary basins, minima are generally related to depocenters located on synformal structures. Yet the correlation of the Bouguer gravity minima with the depression's major structures evidences that the southernmost minimum is over the Salinas antiform, which is the main antiform of the depression (Fig. 7-5b). In some cases gravity minimum could be also related to ancient depocentres inverted. However, this is not the situation in the Ronda Depression, where the lower parts of the sedimentary sequence are located in the core of the antiform. In other words, the gravity anomaly in this region allows us to determine the basement structure of the depression, but does not enable us to accurately estimate the sedimentary infill geometry.

In order to integrate the surface geological data, a NW-SE gravity model orthogonal to the main NE-SW folds was developed (Fig. 7-5c). The average density assigned to each geological unit is related to the main lithology observed in the field according to Telford et al. (1990): 2300 kg/m^3 for the sedimentary infill, 2670 kg/m^3 for the Subbetic limestones, 2350 kg/m^3 for the Flysch sandstones, and 2000 kg/m^3 for the Triassic marls with gypsum. The anomaly values change gradually, with no sharp variations at the boundaries of the sedimentary infilling. This fact, together with the surface geological data, suggests that the borders of the depression are unconformities and are not related with high angle faults. In the southern part of the Depression, the Neogene sediments are placed over Subbetic units with a continuous NE-SW structure. However, northwest of the Salinas fold, the basement has a chaotic structure and there are kilometric limestone blocks included in a Triassic matrix.

The thickness of the Neogene sedimentary infill is irregular and may attain 300 m according to the geological data and the gravity modelling, although this cannot be ascertained because there are no clearly related residual anomalies. Moreover, the thickness of Triassic rocks located at the base of the model cannot be established accurately due to the lack of other geophysical data as wells or seismic profiles. However, it is possible to determine the areas where these rocks are nearby the surface and their geometry. Gravity method can provide evidence of lateral contrasts in density, but not the vertical contrast, as horizontal layers whose effect is a constant regional level may be overprinted upon regional anomalies.

7.5. Discussion

In neotectonic studies, the precise dating of structures is essential for elucidating the tectonic evolution of a region. The study of deformed intramontane sedimentary basins is especially interesting, because it allows for precise estimations of the age of recent tectonic structures. However, it is necessary to establish the mechanisms of deformation in order to distinguish regional tectonic structures from local reactivations that may lead to erroneous interpretations. In this way, the development of orthogonal oriented structures, such as folds, should be analyzed in detail in order to determine their simultaneous development in a deformation stage, or the overprinting that would evidence two regional deformation stages. The presence of low density rocks at depth is the main mechanism responsible for reactivation of earlier structures through salt tectonics involving only local deformations. The Ronda Depression, affected by irregularly distributed orthogonal folds, provides a good opportunity to investigate the late development of folds and to discuss the implications thereof.

In the western Betics, a main part of the brittle and ductile deformation of the outcropping tectonic units took place before Tortonian, as rocks of Late Miocene age lie unconformably over the deformed External Zones and Flysch Units. In addition, deformation in these Late Miocene rocks is local and generally of low intensity, consisting of tilting, smooth folds and very scarce faults with short slip. The NE-

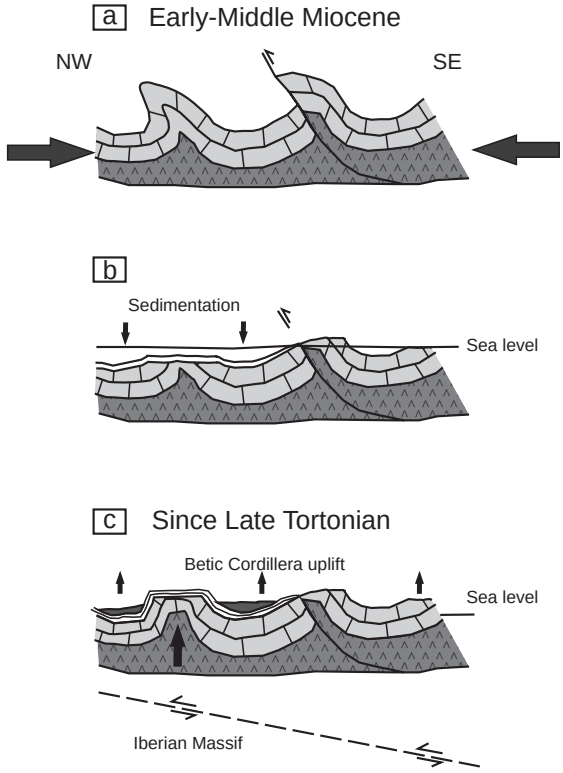

Figure 7-6. *Tectonic evolution sketch of fold reactivation in the Ronda Depression.* **a)** *Post-Early Burdigalian deformation event that determines the structure of the Subbetic due to the NW-SE Eurasian-African plate convergence;* **b)** *During Late Tortonian-Late Messinian, marine sediments of the Ronda Depression were deposited in a progressive unconformity;* **c)** *Since Late Tortonian, removilization and uplift of previous thick Triassic rock accumulations simultaneous to the uplift of the Betic Cordillera.*

SW fold-and-thrust belt that determines the structure of the Subbetic basement (Fig. 7-6a) was developed in a post-Early Burdigalian deformation event (Crespo-Blanc and Campos, 2001; Pérez-López and Pérez Valera, 2007; Crespo-Blanc, 2008). In this stage, accompanied by regional NW-SE compression due to the Eurasian-African plate convergence, low density rocks were differentially accumulated at the core of the antiformal structures.

Gravity data acquired in the depression allow us to discern the different nature of the basement placed beneath the current outcrop of Neogene sediments. This fact conditions the heterogeneous distribution of the folds deforming the Late Miocene infill. Subbetic limestones are identified continuously from the southern border of the depression up to the central part. In addition, northwards of the Salinas antiform, large kilometric blocks of high density (Fig. 7-5c) are attributed to Jurassic limestones of the Subbetic units, which may represent the Subbetic Chaotic Complexes. Bouguer gravity

minima point to areas of accumulation and shallow position of the low density Triassic rocks. These minima have NE-SW elongated shapes (Fig. 7-5b), similar to the trend of the folds that deform the surrounding basement and the southern part of the Depression. In the northwestern minimum, the gravity model suggests that Triassic rocks are located directly under the undeformed sedimentary infill. However, the southeastern minimum coincides with the core of the Las Salinas antiform (Fig. 7-5b and c), suggesting that low density rocks were related to the fold development.

During Late Tortonian-Late Messinian, marine sediments of the Ronda Depression were deposited in a progressive unconformity (Rodríguez-Fernández, 1982) over the Salinas antiform due to the interference of sedimentation, erosion, and tectonic processes (Fig. 7-6b). The development of box-fold geometries could be consequence of removilization and uplift of previous thick Triassic rock accumulations (Fig. 7-6c) simultaneous to the uplift of the Betic Cordillera and the transition from marine to continental sedimentation. Other factors are needed to develop this type of fold in compressional settings, as has been establish using analogue models (Bonini, 2003): load due to the overlying sedimentary sequence, the presence of fluids and, indeed, a sharp inversion of density in the sedimentary sequence. The combination of these factors may condition the fold type: from type 1 (Bonini, 2003) localized above a thrust up to type 2, formed in the front of the most external thrust. The development of box fold geometries, as the Salinas-Sanguijuela antiform, is a transitional situation between both cases.

Previous studies (Serrano 1979) have proposed a strictly diapiric origin of the Salinas fold conditioned by the presence of ductile Triassic rocks in its core. In any case, the previous tectonic setting would have conditioned an early NE-SW elongated accumulation of low-density rocks that determined the late reactivation of the fold. This setting, where the fold orientation is inherited, may then be analyzed to understand the local deformations, but cannot be used to determine recent regional deformation stages.

The salt tectonics that occurred during the reactivation of the Salinas antiform may be responsible for its geometry and location, featuring sharp boundaries, box-fold shape without predominant vergence, and restricted deformation in the southeastern part of the depression. The orthogonal development of the Sanguijuela fold was produced roughly simultaneously to the formation of the Salinas fold. Both folds are connected along an area of highly curved crest line showing none of the typical dome-and-basin interference structures that are generally seen in orthogonal trending folds. The sharp change in orientation in the southern part of the Depression may be due to the WNW-ESE thick, rigid limestones of the southwestern boundary of the depression. The late folds do not propagate outside the depression. The competent folded upper layer, made up of the Jurassic limestones and Neogene sedimentary infill, accommodates the southward pushing of the Las Salinas antiform by the development of the La Sanguijuela antiform. Similar examples of fold development related to a high accumulation of ductile Triassic rocks have been described by other authors in the Betic Cordillera (López-Garrido and Vera, 1974).

The slightly deformed and unconformable Neogene sedimentary infill in the western Betic Cordillera suggests that the deformation is concentrated largely in correspondence of deep rooted structures that only affect the frontal part. Piggy-back basins like the Ronda Depression mainly underwent northwestward transport and uplift. Crespo-Blanc and Campos (2001) considered the late folds to be open, deforming the thrust planes that affect the basement of the depression. However, the continuity of the folds affecting the surrounding basement with the folds observed in the Late Miocene infill is not well constrained, and probably does not occur because field observations give no evidence that the basal unconformity has been affected by these structures in the basin boundaries. Thus, folds of the Late Miocene sedimentary infill are local, restricted to the Ronda Basin and may not be used to date the regional deformation stages.

7.6. Conclusions

The detailed study of the Ronda Depression, including field geological and gravity observations, provides some insights for analysis of fold reactivation in a framework of heterogeneity of the basement and sedimentary infill. An early deformation stage during NW-SE African and Eurasian plate convergence affected the basement during Early and Middle Miocene times and produced a NE-SW oriented fold-and-thrust belt. During this stage, the accumulation of plastic low density Triassic rocks, belonging to the Subbetic sequence, took place in the core of NW vergent folds. Since the Late Miocene, the Ronda Depression may be considered a northward-moving piggy-back basin, having undergone uplifting, evidenced by the elevation of the unconformable Tortonian-Messinian marine sediments, but scarce tectonic deformation. The removilization of this inherited and heterogeneous distribution of Triassic rocks is evidenced by Bouguer gravity minima. The accumulation of low density basement rocks conditioned the development of the Salinas box-shaped antiform, while the simultaneously developed orthogonal Sanguijuela fold is determined by the competent southern border of the basin.

Reactivation of basement folds by diapirism is one of the main mechanisms of deformation of the sedimentary infill placed above low density basement rocks. Although reactivated folds are generally elongated and may be interpreted as a consequence of a new regional tectonic compressive deformation stage, several features may be considered as evidence of the different mechanisms at work during their origin: heterogeneous fold distribution; no dominant vergence and mostly box geometries. Furthermore, this setting can give rise to the simultaneous development of folds with orthogonal axes. These recent folds are formed by salt tectonics and should be analyzed with caution, as has been done in the Ronda Depression, because they only evidence local deformation stages.

Acknowledgements:

This study was supported by a PhD grant to the first author from Spain's Ministerio de Educación y Ciencia and the projects CSD2006-00041 and CGL 2006-06001 (MEC) and Junta de Andalucía.

PART III

8. Implications of the lithospheric structure and recent deformations of the western Betic Cordilleras in geodynamic models

9. Conclusions

10. Future perspectives

8

Implications of the lithospheric structure and recent deformations of the western Betic Cordillera in geodynamic models

New data presented in Part II of this Ph.D. Thesis aim to improve our regional knowledge of the lithospheric structures of western Betic Cordillera. They are focused, moreover, on two key areas –the mountain front and the intramontane Ronda Basin– to reveal the main features of the recentmost deformations. This chapter intends first to discuss the suitability of applied methodologies, underlining their major advantages and disadvantages, the novelty of their use in the study area, and their main contributions. Thereafter, new data are discussed in the framework of the general body of knowledge about the area, so that we might analyze the most significant recent geological events proposed to date for the Betic-Rif-Alborán region. The new data relevance is highlighted in the discussion of the geodynamics models suggested for the Neogene and Present evolution of the zone.

8.1 Methodological aspects

Structural and recent tectonic research studies in the western Betic Cordillera tend to be scarcer than in the eastern and central parts, probably due to comparatively poor quality of the outcrops, which are highly conditioned by a flat topography, the covering vegetation, and the low intensity of recent deformation. The lack of recent detailed geophysical research can also be attributed to its complex geological setting, where correlation of surface and depth structures is complicated. As underlined in the Introduction, geophysical studies based on the seismic properties of the rocks have prevailed for this region, giving rise to seismologic, seismic tomography and seismic anisotropy studies.

The fact that magnetotelluric research was recently applied for the first time in this region to obtain resistivity images and geoelectrical anisotropy data, the findings described here will contribute to the better understanding of deep structures. However, the magnetotelluric method is a passive technique involving the measurement of natural fields that make it sensitive to anthropic interferences. This feature conditioned the final location of the MT sites, from the Internal Zones of the Betic Cordillera up to its foreland, owing to the existence of several important cities with a widespread network of electric power lines (Sevilla, Marbella, Ronda, Palma del Río). Consequently, the southern end of both profiles was restricted to approximately 30 kilometers from the

coast, to avoid the influence of the sprawling towns near the shoreline. The effect of the railway power lines along the northern border of the Guadalquivir Basin is particularly relevant toward the northern edge of the transects, where many records are not included in the profile due to its huge lateral influence. At the edges of the transects, it was impossible to improve the quality of the low frequencies to better constrain deep regions because possible additional sites were located in very noisy areas.

Overall, the MT method provides good vertical resolution, as the different periods analyzed determine the target depth. This feature allows us to clearly establish the transition between different geoelectric strikes with depth. Yet it is not easy to arrive at an accurate correlation between periods and depths due to the geological complexity of the studied area. A tentative approach was undertaken here, although a more detailed study would be needed to fully integrate results.

Gravity studies have proven to be key for elucidating the sedimentary infill geometry and location of depocentres in basins with a homogeneous basement in view of the density contrast (Marín-Lechado et al., 2007; Pedrera et al., 2006; Sanz de Galdeano et al., 2007). In basins with heterogeneous basements, the superposed effect of sedimentary infill may give rise to a complex Bouguer anomaly pattern that must be analyzed in order to isolate each contribution. The results obtained in the Ronda Depression show an interesting and unusual relationship between the gravity minimum and the main antiform in the area. Analysis of the data acquired during this study points to distribution of evaporitic rocks below the sedimentary infill, and allows us to discuss the role of their concentrations in the context of posterior reactivation of basement antiforms. Although the gravity study sheds light on the basement structure of the depression, it does not enable us to accurately estimate the sedimentary infill thickness, which might be better constrained through the data obtained by wells and other geophysical techniques.

As mentioned above, in regionally complex areas where so many bodies influence the anomaly, gravity models are not unique and need to be constrained by other available data. Such is the case of the western Betic Cordillera, where several gravity models have been proposed up to date (Bonini et al., 1973; Casas and Carbó, 1990). It would therefore prove beneficial to include new geological and geophysical data to solve the limitations of each method and to improve the models. Magnetic data are traditionally related to gravity data, as both constitute potential fields. Magnetic data were acquired simultaneously to the gravity measurements along the transects, but they were affected by interferences of anthropic origin. The magnetic anomalies considered in this Ph.D. Thesis were derived from the aeromagnetic map (Ardizone et al., 1989) because they considered deep targets, so they are not affected by the shallow magnetic noise.

Seismotectonic studies in the Betic-Rif Cordillera have generally analyzed the region as a whole (Buforn et al., 1995; Henares et al., 2003) or clustered the region into

broad areas with similar tectonic features (Buforn et al., 2004; Stich et al., 2003, 2006). Such research efforts have underlined the complex tectonic deformation of the Eurasia-Africa plate boundary, in addition to the heterogeneity of tectonic stresses in a short period of time (De Vicente et al., 2008). While the general stress pattern of the Betic Cordillera is relatively well established, detailed studies of reduced areas are essential to elucidate the seismogenic sources and geodynamic implications.

8.2. Main features of the Neogene-Quaternary geodynamic evolution of the Betic Cordillera

During the Early-Middle Miocene, N-S overprinted by NE-SW extension and thinning of the continental crust took place at the Internal Zones (Crespo-Blanc et al. 1994; Simancas and Campos, 1993) simultaneous with NW-SE shortening in the surrounding External Zones of the Betic Cordillera (Comas et al., 1999; Jolivet and Faccenna, 2000; Lonergan and White, 1997; Platt and Vissers, 1989). From the Late Tortonian onwards, the westward drift of the Internal Zones stopped, and the Alboran Sea was progressively restricted. The Neogene basins in southern Spain become continental, in a regional setting of N-S to NNW-SSE convergence between Eurasia and Africa, together with nearly perpendicular extension (Dewey et al., 1989; Ott d'Estevou and Montenat, 1985; Sanz de Galdeano and Vera, 1992). NW-SE compression continued to be active in the northwestern mountain front of the Betic Cordillera, as revealed by the earthquake focal mechanism described in Chapter 5. This sector advances over the Guadalquivir foreland Basin with respect to the surrounding areas, although its sinuous boundary suggests a context of slow recent tectonic deformation. Even though this feature could also be the consequence of erosion, shallow seismicity with thrust fault focal mechanisms (in contrast to the neighbouring sectors) are detected at shallow levels. The active blind thrusts do not reach the surface, but may be related to NE-SW folds located by the mountain front. Notwithstanding, field data of the same area suggest roughly N-S to NW-SE extension since the Middle Miocene. To reconcile these observations we propose that, while the orogenic wedge thickens and undergoes shortening at depth, extensional collapse affects the uppermost levels in roughly the same direction.

East of the Morón de la Frontera seismic maximum, an unusual seismic gap in the Campillos-Antequera area, featuring a very straight NW-SE western boundary, determines the southward displacement of the seismicity front. NW-SE transfer faults showing opposite kinematics accommodate the differential shortening between individual sectors without contributing to the regional strain. The different tectonic activity of each sector of the Betic-Rif mountain front may be due to the arched character of the cordillera with respect to the NW-SE 5 mm/year plate convergence (McClusky et al., 2003; Serpelloni et al., 2007). The Morón de la Frontera mountain front has a more appropriate orientation to be active, orthogonal with regard to present-day convergence. In contrast to the Betic Cordillera, in the Rif mountain front, antiforms

of SW and S vergence associated with blind thrusts deform up to the Neogene foreland basins of Saïss and Gharb (Bargach et al., 2004) reaching the surface at some places, and propagating deformation as far as the foreland.

Late Miocene rocks that lie unconformably upon southern parts of the studied transects (Ronda Basin and other outcrops in Álora and Pizarra; Fig. 1-2) show local and generally low intensity deformation, consisting of tilting, smooth folds and very scarce faults with short slip. These features suggest that the deformation is concentrated at shallow crustal levels northwards, to the frontal part, while southwards it is basically restricted to deeply rooted structures. Piggy-back basins located above these structures, like the Ronda Depression, mainly underwent northwestward transport and uplift.

Resistivity data from the San Pedro de Alcántara-Castilblanco de los Arroyos transect reveal a deep conductive southward dipping body at the middle crust of the southern edge, which may correspond to basic igneous rocks. The shape of the body suggests southward continuation of the continental Iberian Massif crust below the western Betic Cordillera and the northern Alborán Sea. Further geophysical data, including gravity and seismicity distribution, also support this geometry. One of the main problems with the proposed subduction zone in the Gibraltar Arc area would be the limited lateral extension of such a zone. If the intermediate seismicity distribution (>40 km depth) is correlated with the horizontal extension of the subduction zone, it is noteworthy that it occurs from the Málaga coast and continues westward, roughly retracing the arc curvature. The restricted extension of the subduction may have to do with paleogeographic irregularities of the southern Iberia continental crust before subduction started.

Distinct dipping and crustal natures of the subduction have been evoked to explain this reduced seismogenic area. Gutscher et al. (2002) put forth the presence of an active east-dipping subduction of oceanic crust along an E-W section crossing the Gibraltar strait. Onshore in the Málaga area, Morales et al. (1999) analyzed an orthogonal N-S cross-section pointing to the subduction of continental crust belonging to the Iberian Massif below the Alborán Sea. Both contributions are fundamentally based on seismic tomography images, and attempt to integrate other data such as tectonic transport directions, stress analysis, presence of mud volcanoes, and seismicity distribution. Results presented in this Ph.D. Thesis correspond to an area in an intermediate position between the two cited studies and suggest the lateral continuity of both subduction zones. Assuming an Early-Middle Miocene westward subduction zone, with or without delamination in the edges, the rollback mechanism should continue until the system completely sinks into the dense oceanic lithosphere (Lonergan and White, 1997; Royden, 1993); these authors estimate that rollback occurred in the Alboran Sea between 23 and 10 Ma. There are two main ways to stop the rollback: 1) by the collision of the retreating subduction zone with a mid-oceanic ridge or, 2) when dense oceanic lithosphere is completely consumed and the arc collides with continental lithosphere. The latter mechanism would be more plausible in the Betic-Rif Cordillera setting, in

light of previous seismic tomography studies (Morales et al., 1999) and the resistivity image presented in this Ph.D. Thesis, which propose a continental nature for the subduction body. In such a setting, the subduction zone geometry would be observed as an inheritance of its Miocene evolution. The olistostromic complexes of the Betic-Rif Cordillera (Berastegui et al., 1998; Flinch, 1993; Roldán, 1988), together with the accretionary wedge located west of Gibraltar (Gutscher et al. 2002) may be analogous to the arc-associated imbricated trench sediments formed in subduction zones. These sediments would reveal the last position of the finally arched subduction zone, though present-day thrust fault shallow seismicity remains only at the northwestern front of the Betics, by virtue of its suitable orientation, as pointed out before.

Assuming the above geodynamic setting, the intermediate earthquake focal mechanisms were analyzed in order to clarify the stress field in this restricted region. Stresses vary throughout the area and suggest that the Iberian continental crust is forced to sink into the mantle. Despite local perturbations, the regional maximum stress is generally NW-SE and subparallel to plate convergence. It is subhorizontal at shallow levels near the mountain front, and plunges at depth, modified by the curvature of the slab. In the external and upper part, NE-SW along-strike extension prevails, orthogonal to the compression trend and probably favored by the short lateral continuity of the subducting slab. In the internal arch, meanwhile, the parallelism of the major compressive axis with the slab dip would support its forced subduction into the mantle, as a consequence of the stress propagation along this rigid continental body.

The geoelectrical strike determined by means of magnetotelluric data could provide some useful information about the structural trend of a region. At the crust, it is highly conditioned by the structural directions of geological structures such as faults or dykes. NE-SW to NNE-SSW strikes for the crust of the Betic Cordillera roughly draw its arcuate structural geometry. In the Iberian Massif foreland, the relatively limited data are also congruent with surface geological structures, showing E-W trend for the site placed over the South Portuguese Zone, and NE-SW for the Ossa Morena Zone. In the uppermost mantle, nearly orthogonal strikes have been determined between the Betic Cordillera and the Iberian Massif. At deeper levels however, the strike remains constant in a N-S direction for all the stations in both geological domains.

Indeed, the mantle anisotropy trends may be conditioned by mantle deformation induced by the recent geodynamic evolution. If we try to evoke the deformation pattern caused by a delamination model, it would probably reflect irregular or radial anisotropy directions with respect to the arc curvature, due to asthenospheric flow replacing the removed mantle. This pattern should be detected in the whole column below the affected region. Yet the deep regular N-S strike pattern observed from the Iberian Massif to the Internal Zones of the Betic Cordillera does not support the action of such a mechanism, at least not below this sector of the Cordillera. Deformation related to the westward emplacement of the Internal Zones of the Betics may produce N-S strikes at shallow levels, along the front of the tectonic arc, through dominant pure shear due to the E-W

shortening. Finally, E-W strikes determined in the Iberian massif foreland may be a consequence of the combination of pure and simple shear deformation.

Therefore, although it is not possible to totally discard other geodynamic models, the anisotropy pattern and the resistivity structure evidenced in this research are better supported by an eastward dipping subduction zone-rollback model occurring during the Early-Middle Miocene evolution of the region. In such a setting, the lithospheric mantle would only be intensely affected towards the east, at the anomalous Alborán Sea mantle (Hatzfeld, 1976), while the deep mantle below the western Betic Cordillera would maintain its older 'frozen' structure, similar to that observed below the Iberian Massif. Since the Late Miocene, only the adequately oriented northwestern front of the Cordillera, and the related subduction of continental crust towards the Alborán Sea, would remain active in the framework of NW-SE plate convergence.

9

Conclusions

This chapter summarizes the main findings obtained through the geophysical and geological research accomplished in this Ph.D. Thesis, starting with the results related to deep mantle structures, followed by crustal structures, to finally deal with the recent and active deformations, and so offer a full view of the recentmost tectonic evolution of the western Betic Cordillera.

9.1. Lithospheric mantle structure

Results from long-period magnetotelluric soundings in the western Betic Cordillera and SW Iberian Massif provide the first lithospheric electrical anisotropy data in the northern branch of the Gibraltar Arc and reveal the main trends of mantle deformation structures. These geoelectric anisotropy data are probably related to the olivine elongations produced during mantle deformations. The geoelectrical strike determined is consistent in each geological domain and reveals a roughly layered structure. The strikes obtained are, in short:

▪ The deep lithospheric mantle of the whole region is characterized by a N-S strike revealed by low magnitude induction arrows pointing to the west (~10^4 s period).

▪ In the lower crust and uppermost lithospheric mantle, the strike is N-S in the Betic Cordillera, as reflected by westward induction arrows that are very large in magnitude. Meanwhile, in the Iberian Massif the strike is E-W, roughly orthogonal to the Betic Cordillera results, with the induction arrows pointing to the S (~10^3 s to ~10 s periods).

▪ Below the Guadalquivir Basin, a NE-SW strike reveals a sharp transition zone between the two domains.

▪ Between ~10^3 and ~10^4 s the magnitude of the induction arrows dramatically decreases, especially below the Betic Cordillera.

The homogeneous N-S strike revealed at deeper lithospheric mantle levels below both geological domains may be a ‘frozen’ tectonic feature. It could be related to Pre-alpine plate kinematics, or to the opening of the northern Atlantic Ocean.

Electrical anisotropy trends in the uppermost mantle of western Betics (~10-10^3s periods) may be related to the westward emplacement of the Internal Zones during the Oligocene and Early-Middle Miocene. Dominant pure shear mechanisms along the front of the tectonic arc, related to the E-W shortening, could produce N-S strikes in the uppermost lithospheric mantle. At the Iberian Massif foreland, the combination of pure and simple shear deformation, related to the westward lateral displacement of the Internal Zones, would condition the E-W electrical anisotropy strikes. A sharp transition between both geological domains is revealed by the NE-SW strike obtained below the Guadalquivir foreland Basin.

The induction arrows show a southward increase in their magnitude from the Iberian Massif foreland up to the Internal Zones of the Betic Cordillera. In such a setting, the most probable origin of this pattern would be conditioned by the increase of deformation towards the inner part of the orogen.

Disagreement between mantle seismic and electrical anisotropy directions could, furthermore, be conditioned by the different depth ranges studied under the two methods, which take into consideration different physical properties.

The anisotropy pattern evidenced is better supported by an eastward dipping subduction zone-rollback model occurring during the Early-Middle Miocene evolution of the region. If delamination occurred, irregular or radial anisotropy directions with respect to the arc curvature due to the flow of asthenosphere replacing the removed mantle can be expected. This feature was not indicated by resistivity data, at least not below the studied sector, where regular N-S strike patterns are detected at deeper levels. In a subduction setting, on the other hand, the lithospheric mantle would only be intensely affected towards the east, where the anomalous Alborán Sea mantle is located. However, the deep mantle below western Betic Cordillera preserves its older 'frozen' structure, showing an anisotropy trend similar to the Iberian Massif mantle.

9.2. Crustal structure, seismicity distribution and present day stress at the San Pedro de Alcántara-Castilblanco de los Arroyos transect

The broadband magnetotelluric profile running from San Pedro de Alcántara (Málaga Coast) to Castilblanco de los Arroyos (Sierra Morena) reveals a heterogeneous resistivity structure in the upper crust. Conductive bodies located at shallow levels are related with the sedimentary infill of the Ronda and Guadalquivir basins. In contrast, large resistivity bodies at the northern and southern boundaries of the profile are respectively related to granitic bodies cropping out in the Iberian Massif foreland and limestones of the Internal Zones frontal units.

At middle crustal levels, a deep conductive southward dipping body in the southern edge of the profile may correspond to basic igneous rocks intruded in the

Iberian Massif crust. This geometry could point to the southward continuation of the continental Iberian Massif crust below the western Betic Cordillera and the northern Alborán Sea. Further geophysical data, including gravity and seismicity distribution, come to support this geometry.

Intermediate seismicity below the Málaga coast and the northern margin of the Alborán Sea shows a SE-dipping pattern, reaching depths of 120 km, with a seismic gap between 25 and 60 km that could be related with a low seismic velocity wedge corresponding to the Alborán Sea anomalous mantle.

The stress tensors determined from earthquake focal mechanisms might be clustered in several seismotectonic domains to arrive at a better understanding of the area:

▪ At shallow depths, maximum stress has a generally NW-SE horizontal trend subparallel to plate convergence. There are also local perturbations revealing N-S compression, probably due to stress release permutations or block interaction.

▪ A general NW-SE inclined compressional axis orientation is determined at intermediate depths, but with differences between the external and the internal part of the seismogenic zone. The inner part is in down-dip compression, whereas the outer part is under extension along the NE-SW strike. The parallelism of the major compressive axis with the slab dip supports its forced subduction into the mantle, as a consequence of the stress propagation along this rigid continental body. On the other hand, the arcuate character of the Betic-Rif Cordillera and the limited lateral continuity of the subduction zone may favor the along-strike extension.

9.3. Seismicity distribution and present day stress in the northwestern mountain front

Very shallow seismicity has been registered at the Morón de la Frontera-Puebla de Cazalla area, indicating a N-NW progressive shallowing of the active structures from the Internal Zones until reaching the mountain front. The active thrusts do not reach the surface, but may be related to NE-SW folds associated with blind thrusts at the mountain front. Unusual NE-SW compression is locally observed near the mountain front, at the NE edge of the orogenic wedge. This stress is most likely a consequence of the permutation of the regional NW-SE compression, favored by the close magnitudes of maximum and intermediate stress axes. Moreover, this situation could be influenced by local stress disturbances at the corner of the indenting orogenic wedge that would possibly reorient the principal stress directions.

A remarkable seismic gap east of the Moron seismic maximum, with a very straight NW-SE boundary, coincides with the presence of huge masses of ductile sediments belonging to the Subbetic Chaotic Complexes. This boundary is characterised

by strike-slip earthquake focal mechanisms showing opposite kinematics, which may be related to NW-SE transfer faults parallel to the plate convergence. These faults could accommodate differential shortening between individual sectors.

Brittle deformation in Middle-Late Miocene sediments of the southern border of the Guadalquivir basin is very intense. NNE-SSW subvertical fault planes with a main strike-slip component are predominant, although NW-SE faults are also very common. Paleostress analysis of the field data suggests a roughly N-S to NW-SE extension since the Middle Miocene. The apparent inconsistency between seismic deformation and geological field data may be explained by wedge thickening that produces shortening at depth coeval with extensional collapse at the uppermost levels, in roughly the same direction.

In sum, the northwesternmost mountain front is the only one that remains active in the arched Betic Cordillera, owing to its favorable orientation with respect to the present-day convergence of the Eurasian-African plates. The active tectonic structures are partitioned, thus indicating a NW-SE oriented compression and thrusting at depth, extension at surface, and the presence of transfer faults with opposite kinematics in its northeastern boundary. In the eastern and central Betics, active deformation and seismicity mainly affect the Internal Zones, and the topographic mountain front may represent a relict structure developed during Early and Middle Miocene.

9.4. Surface and shallow crustal structure of the Neogene Ronda Basin

The Neogene sediments of the Ronda Depression are mainly deformed by folds with nearly orthogonal axes, no dominant vergence, and featuring box geometries, essentially located in the southern and southwestern parts of the depression. In addition, it is possible to identify minor open folds with metric wave length and the same orientation as the Salinas antiform, and very scarce faults with short slip. These minor folds are fundamentally located in the crest zone of the Salinas Fold and deform the calcarenites of Setenil Formation.

The Ronda depression is slightly deformed, suggesting that it mainly underwent uplift and northwestward transport since the Late Miocene, as a piggy-back basin. Most of the folds affecting the Late Miocene infill are not in continuity with the basement folds, because basal unconformity is undeformed at the boundaries. Thus, folds deforming the sedimentary infill can be considered local, restricted to the Ronda Basin, and may not be used to date the regional deformation stages.

Gravity data acquired in the depression reveal the distinctive nature of the basement. Subbetic limestones are identified continuously from the southern border of the depression up to its central part. Northwards of the Salinas antiform, high-density kilometric blocks attributed to limestones of the Subbetic units are involved in a low-density matrix. Two gravity minima with NE-SW elongated shapes show

trends similar to those of the basement folds of the southern part of the basin. The northwestern minimum may be conditioned by the location of the Triassic rocks under the undeformed sedimentary infill, whereas the southeastern minimum coincides with the core of the Las Salinas antiform.

In order to better understand the unusual location of the gravity minima over the higher reliefs of the basin, the following tectonic evolution is proposed:

▪ During a post-Early Burdigalian deformation event, a compressional deformation stage affected the basement of the Ronda Basin and produced a NE-SW oriented fold-and-thrust belt as a consequence of the NW-SE Eurasian-African plate convergence. During this stage, in the core of the NW vergent folds, an accumulation of plastic low-density Triassic rocks takes place.

▪ During a Late Tortonian-Late Messinian stage, marine sediments of the Ronda Depression were deposited in a progressive unconformity over the Salinas antiform.

▪ Since the Late Miocene, the Ronda Depression may be considered a northward-moving piggy-back basin, having undergone uplifting, evidenced by the elevation of the unconformable Tortonian-Messinian marine sediments, but scarce tectonic deformation. The removilization and uplift of previous thick Triassic rock accumulations could produce the development of box-fold geometries without predominant vergence, while the coetaneous development of the orthogonal Sanguijuela fold was determined by the competent southern border of the basin, which acted as a backstop. Both folds are connected along an area of highly curved crest line showing none of the typical dome-and-basin interference structures that are generally seen in orthogonal trending folds.

9.5. Contribution to geodynamic models

Geological and geophysical data presented in this Ph.D. Thesis are better supported by an eastward dipping subduction zone-rollback model occurring during the Early-Middle Miocene evolution of the Betic-Rif-Alborán area. Other geodynamic mechanisms in eastern regions may also have occurred, such as delamination, although they are not evidenced in this research.

Since the Late Miocene, a typical piggy-back deformation takes place in the northwestern transect of the Betic Cordillera. Recent and active structures, underlined by seismicity, are mainly concentrated at shallow crustal levels in the mountain front and the External Zones of the orogenic wedge. The compressional deformation progressively affects deeper crustal levels towards the Internal Zones, while shallow structures become inactive and the Cordillera undergoes uplift. This deep crustal thrust zone is finally in continuity with the continental subduction associated with intermediate seismicity in the Alborán Sea, the last active segment that remains active from inherited Miocene subduction.

9

Conclusiones

En este capítulo se resumen los principales resultados de esta Tesis Doctoral obtenidos a partir de diferentes datos geológicos de campo y geofísicos. En primer lugar, se describirán los resultados relacionados con la estructura tanto del manto como de la corteza. Finalmente, se destallarán las deformaciones recientes y activas, para poder obtener una visión completa de la evolución mas reciente de la Cordillera Bética occidental.

9.1. Estructura del manto litosférico

Los resultados obtenidos mediante sondeos magnetotelúricos de largo periodo en la Cordillera Bética occidental y la región suroccidental del Macizo Ibérico, proporcionan los primeros datos de anisotropía eléctrica de la rama norte del Arco de Gibraltar y revelan las principales orientaciones de las estructuras de deformación. La anisotropía eléctrica está relacionada con la elongación de minerales como el olivino producida durante los procesos de deformación en el manto. La dirección geoeléctrica determinada (strike) es congruente en cada dominio geológico y revela una estructura estratificada en algunos sectores. A continuación se describen sus principales características:

▪ El manto litosférico más profundo investigado está caracterizado por un strike N-S en toda la región, determinado por vectores de inducción de pequeña magnitud que apuntan hacia el oeste (periodos ~10^4 s).

▪ En la corteza inferior y la parte superior del manto litosférico, el strike de la Cordillera Bética es N-S, remarcado por la existencia de vectores de inducción de gran magnitud que apuntan hacia el oeste. En el Macizo Ibérico, sin embargo, el strike es de dirección E-O, con flechas de inducción que apuntan hacia el S (periodos entre ~10^3-10 s).

▪ Bajo la Cuenca del Guadalquivir se produce la transición entre ambos dominios, con una orientación NE-SO de la anisotropía eléctrica.

▪ Entre ~10^3 y ~10^4 s la magnitud de los vectores de inducción decrece sustancialmente, en especial bajo la Cordillera Bética.

El strike N-S determinado para los niveles más profundos del manto litosférico bajo ambos dominios geológicos debe ser una característica tectónica relicta,

probablemente relacionada con movimientos pre-alpinos de las placas tectónicas o con la apertura del Atlántico Norte.

Las direcciones de anisotropía en el manto superior de la Cordillera Bética occidental (periodos comprendidos entre ~10-10^3s) deben estar relacionadas con el desplazamiento hacia el oeste de las Zonas internas durante el Oligoceno y Mioceno inferior y medio. Mecanismos de cizalla pura a lo largo del frente del arco tectónico, relacionados con el acortamiento E-O, podrían producir strikes N-S la parte superior del manto litosférico. En el Macizo Ibérico, la combinación de mecanismos de cizalla simple y cizalla pura, relacionados con el emplazamiento hacia el oeste de las Zonas Internas, condicionaría la existencia de direcciones E-O de anisotropía. Entre ambos dominios geológicos existe una transición brusca, determinada por la existencia de strikes NE-SO bajo la Cuenca de antepaís del Guadalquivir.

La magnitud de los vectores de inducción se incrementa desde el Macizo Ibérico hasta las Zonas Internas de la Cordillera Bética. En este contexto, el origen más probable de este incremento debe estar relacionado con la mayor deformación observada en las zonas mas internas del orógeno.

Las incongruencias entre las direcciones de anisotropía eléctrica y sísmica deben estar condicionadas por los diferentes rangos de profundidades estudiadas por ambos métodos, que consideran diferentes propiedades físicas.

Las diferentes direcciones de anisotropía eléctrica determinadas para la región etán bien sustentadas por el modelo de subducción y *rollback* hacia el oeste propuesto para la evolución de la cordillera durante el Mioceno inferior y medio. En el caso de que hubieran ocurrido procesos de delaminación, la pauta que se esperaría observar sería irregular o radial con respecto a la curvatura del arco, en relación con el flujo astenosférico que reemplazaría el manto previamente desplazado. Sin embargo, estas características no se han advertido en el sector, ya que en los niveles más profundos se observan direcciones de anisotropía N-S muy regulares. Por otro lado, en un contexto de subducción, el manto litosférico sólo sería afectado intensamente hacia el este, donde se encuentra el manto anómalo del Mar de Alborán.

9.2. Estructura cortical, distribución de la sismicidad y campo de esfuerzos actual a lo largo de la transversal de San Pedro de Alcántara-Castilblanco de los Arroyos

El perfil magnetotelúrico de banda ancha realizado entre San Pedro de Alcántara (costa de Málaga) hasta Castilblanco de los Arroyos (Sierra Morena) muestra la estructura heterogénea de la corteza superior. Los cuerpos conductores observados en superficie reflejan la continuidad en profundidad de las cuencas Neógenas del Guadalquivir y de Ronda. Por otra parte, los grandes cuerpos resistivos, localizados en

los bordes del perfil, muestran la presencia de cuerpos graníticos en el Macizo Ibérico y de calizas de las unidades frontales de las Zonas Internas, respectivamente.

En el borde sur del perfil, a niveles medios de la corteza, se observa un cuerpo conductor que buza al SE y que puede corresponderse con rocas ígneas básicas intruidas en la corteza del Macizo Ibérico. Esta geometría podría estar relacionada con la subducción hacia el SE de la corteza continental del Macizo Ibérico bajo la Cordillera Bética occidental y el borde norte del Mar de Alborán. Otros datos geofísicos, tales como anomalías gravimétricas y distribución de la sismicidad, también avalan esta geometría.

La zona con sismicidad intermedia es más profunda hacia el SE, bajo la costa de Málaga y el margen norte del Mar de Alborán, donde alcanza profundidades de 120 kilómetros. Entre 25 y 60 km se localiza una zona asísmica que podría estar relacionada con la zona de baja velocidad sísmica del manto anómalo del Mar de Alborán.

Los tensores de esfuerzos determinados a partir de mecanismos focales de terremotos pueden ser agrupados en varios dominios sismotectónicos:

▪ En la parte alta de la corteza, el máximo esfuerzo compresivo es generalmente horizontal y de dirección NO-SE, subparalelo a la convergencia de placas. Se detectan también algunas perturbaciones locales que indican compresión N-S, probablemente debido a permutaciones de los esfuerzos o interacción entre bloques.

▪ A profundidades intermedias se ha determinado una compresión NO-SE inclinada, pero con diferencias entre la parte externa e interna de la zona sismogénica. En la parte interior el eje es subparalelo a la inclinación de la laja, mientras que en la parte exterior la extensión esta orientada NE-SO paralela a la dirección. El paralelismo del máximo esfuerzo con el buzamiento de la laja marcaría su subducción forzada en el manto, como consecuencia de la propagación de los esfuerzos a lo largo del bloque de corteza continental. Por otro lado, el carácter arqueado de la Cordillera Bético-Rifeña y la limitada continuidad lateral de la zona de subducción favorecerían la extensión en la dirección de la laja.

9.3. Distribución de la sismicidad y estado de esfuerzos actual en el frente NO de la Cordillera Bética.

En el área de Morón de la Frontera-Puebla de Cazalla se registra sismicidad muy superficial que indicaría la progresiva somerización de las estructuras activas hacia el N-NO desde las Zonas Internas hasta alcanzar el frente montañoso. Los cabalgamientos activos no cortan la superficie, pero su expresión superficial debe corresponder a los pliegues NE-SO que deforman hasta la topografía. En el borde NE de la cuña orogénica se observa una dirección de compresión NE-SO inusual en la región, que puede ser

consecuencia de la permutación de la dirección de compresión NO-SE, favorecida por la similar magnitud de los ejes de esfuerzo máximo e intermedio. Además, esta situación podría deberse a perturbaciones locales en el borde de la cuña orogénica indentada que produjera la reorientación de las principales direcciones de esfuerzo.

Al este del máximo sísmico localizado en Morón de la Frontera existe una región con una inusual ausencia de terremotos que coincide con el afloramiento de grandes masas de sedimentos con un comportamiento plástico de los Complejos Caóticos Subbéticos. Este límite está caracterizado por mecanismos focales de terremotos de falla de salto en dirección con cinemática opuesta, que deben estar relacionados con fallas transfers paralelas a la convergencia de placas. Estas fallas acomodarían el acortamiento diferencial entre sectores individuales.

La deformación frágil de los sedimentos del Mioceno medio-superior que afloran en el borde sur de la Cuenca del Guadalquivir es muy intensa. Las fallas predominantes son subverticales de orientación NNE-SSO y con una componente principal de salto en dirección dextra, aunque también son muy comunes las fallas de dirección NW-SE sinistras. El análisis de paleosfuerzos a partir de los datos de campo sugiere una dirección de extensión N-S a NO-SE desde el Mioceno medio. La aparente inconsistencia entre los datos sísmicos y geológicos se explicaría mediante el engrosamiento cortical de la cuña orogénica que produciría acortamiento en profundidad, coetáneo y en la misma dirección que el colapso extensional de los niveles superiores.

En resumen, el frente montañoso noroccidental es el único que continua activo en la Cordillera Bética, debido a su orientación favorable debido a la curvatura del arco con respecto a la actual dirección de convergencia entre las placas Euroasiática y Africana. Existe una partición de las estructuras activas, que indicaría la existencia de cabalgamientos con una dirección de compresión NO-SE en profundidad, extensión en superficie y la existencia de fallas transfer con cinemática opuesta en su borde nororiental. En la Cordillera Bética central y oriental, la deformación activa y la sismicidad afectan principalmente a las Zonas Internas y el frente montañoso topográfico representaría una estructura relicta desarrollada durante el Mioceno inferior y medio.

9.4. Estructura cortical superficial de la Cuenca Neógena de Ronda

Los sedimentos de la Cuenca Neógena de Ronda están deformados fundamentalmente por pliegues con ejes casi perpendiculares, sin vergencia predominante y geometrías en caja, esencialmente localizados en la parte sur y suroccidental de la depresión. Además, es posible identificar escasas fallas con saltos pequeños y pliegues menores con longitud de onda métrica y la misma orientación que el pliegue de las Salinas. Estos pliegues menores se localizan en la zona de cresta del pliegue de las Salinas y deforman las calcarenitas de la Formación Setenil.

La escasa deformación de la Depresión de Ronda sugiere que desde el Mioceno superior ha sido elevada y transportada hacia el NW como una cuenca *piggy-back*. La mayoría de los pliegues que deforman los sedimentos del Mioceno superior no están en continuidad con los que afectan al basamento, ya que la discordancia basal no está deformada en los bordes. Por tanto, los pliegues que afectan al relleno sedimentario tienen un carácter local, restringido a la Cuenca de Ronda y no pueden ser usados para datar etapas de deformación regional.

Los datos gravimétricos adquiridos en la depresión revelan la diferente naturaleza de su basamento. Las calizas subbéticas se reconocen de forma continua desde el borde meridional de la depresión hasta su parte central. Hacia el N del antiforme de las Salinas se detecta la existencia de bloques de alta densidad atribuidos a calizas del Subbético englobadas en una matriz de baja densidad. Dos mínimos gravimétricos elongados NE-SO muestran similar orientación que los pliegues del basamento de la parte meridional de la cuenca. El mínimo situado al NO debe estar generado por la presencia de rocas triásicas de baja densidad bajo el relleno sedimentario, mientras que el mínimo situado al SE coincide con el núcleo de la antiforma de las Salinas.

Los resultados obtenidos sugieren la siguiente evolución tectónica:

▪ Durante una etapa de deformación post-Burdigaliense inferior, un evento compresivo afectó al basamento de la Cuenca de Ronda y generó los pliegues de orientación NE-SO del cinturón de pliegues y cabalgamientos como consecuencia de la convergencia de placas de dirección NO-SE. Durante esta etapa, en el núcleo de los pliegues vergentes al NO se produjo la acumulación de rocas Triásicas de baja densidad y comportamiento plástico.

▪ Durante el Tortoniense superior- Messiniense superior, los sedimentos marinos de la Depresión de Ronda fueron depositados en una discordancia progresiva sobre el antiforme de las Salinas.

▪ Desde el Mioceno superior, la Depresión de Ronda puede ser considerada una cuenca de tipo *piggy-back* elevada y transportada hacia el NO, debido a que los sedimentos marinos de edad Tortoniense-Messiniense de la cuenca están topográficamente elevados pero comparativamente poco deformados. La removilización y levantamiento de las rocas triásicas previamente acumuladas podría producir el desarrollo de un pliegue con geometría en caja, sin vergencia predominante, de forma simultanea al desarrollo del pliegue ortogonal de la Sanguijuela, determinado por la presencia de un borde sur competente que actúa como contrafuerte. Ambos pliegues están conectados a lo largo de una zona de cresta curva que no muestra ninguna de las típicas interferencias en domos y cubetas que se observan generalmente en regiones con pliegues perpendiculares superpuestos.

9.5 Contribución a los modelos geodinámicos

Los datos geológicos y geofísicos que se presentan en esta Tesis Doctoral favorecen un modelo de subducción con *rollback* hacia el oeste durante la evolución de la Cordillera Bético-Rifeña y el Mar de Alborán en el Mioceno inferior y medio. No obstante, otros modelos geodinámicos que incluyan delaminación podrían producirse en áreas más orientales pero no se evidencian en este estudio.

Desde el Mioceno superior, la secuencia de deformación en la transversal NO de la Cordillera Bética es de tipo *piggy-back*. Las estructuras recientes y activas, resaltadas por la sismicidad, están principalmente concentradas en niveles corticales superficiales del frente montañoso y de las Zonas Externas de la cuña orogénica. Hacia las Zonas Internas, la deformación compresiva afecta progresivamente niveles mas profundos de la corteza mientras que las estructuras superficiales son inactivas y la cordillera es elevada. Esta zona de cabalgamientos corticales está en continuidad con la subducción continental asociada a la sismicidad intermedia del Mar de Alborán, último segmento activo heredado de la subducción Miocena.

10

Future perspectives

Advancement in knowledge of the Betic Cordillera calls for multidisciplinary research involving more detailed geological, geomorphological, geophysical and geodetic studies, and the application of techniques to date insufficiently used in this region or others, that might provide still more valuable information.

Based on the recent development of the Digital Elevation Models (DEM), geomorphological studies have experienced very considerable development. Their application to the analysis of drainage networks through the determination of different geomorphologic indexes, and the facility in qualitatively/quantitatively determining the most significant features of the relief, make such models an attractive emerging tool for applications in recent and active tectonic studies. At any rate, the most remarkable results should be harvested when used in combination with detailed field work and geochronological data.

In addition, the quantification of the active structures motion, folds and faults, necessarily involves measurement of the geodetical networks already deployed and the installation of new regional and local networks. Accurate results will take a long time to in coming, due to the low deformation rate of these structures. The importance to accomplish this scientific target is unquestionable, however.

A more profuse development of deep seismic reflection and refraction studies will also provide valuable information of the crustal structure in future research efforts. Detailed field magnetic data can likewise be of great interest due to the presence of important magnetic anomalies in the region that have not been studied until now. The measurement of new broadband and long-period magnetotelluric data with a closer distribution will help us to better define the resistivity structure of the crust and upper mantle. An E-W transect crossing the cordillera from the Atlantic to the Mediterranean coast could provide great worth data toward a better understanding of the geodynamic evolution of the Betics. Up to now, the MT data have been acquired at the most interesting transects of the cordillera. However, the increasing database will allow us to create 3D models that will provide more complete and accurate information about the deep structures.

Integrative efforts taking into account the growing number of field and geophysical surveys in the Rif Cordillera, together with marine studies underway in the Alborán Sea, will provide complementary information that is certain to enhance an understanding of the area as a whole. The development of such combined research endeavors in the next few years will finally constrain the Miocene to Present geodynamic models, now under discussion, in this complex region of plate tectonic convergence.

References

Aki, K. and Richards, P.G., 2002. Quantitative Seismology, 2nd edition. University Science Books, New York.

Aldaya, F., Campos, J., García-Dueñas, V., González-Lodeiro, F., Orozco, M., 1984. El contacto Alpujárrides/Nevado-Filábrides en la vertiente meridional de Sierra Nevada. Implicaciones tectónicas. In: El borde mediterráneo español: evolución del orógeno bético y geodinámica de las depresiones neógenas. Departamento de Investigaciones Geológicas, C.S.I.C. and Universidad de Granada, Granada, ISBN 00-05776-7, 18-20.

Aldaya, F., García-Dueñas, V. and Navarro-Vilá, F., 1979. Los mantos alpujárrides del tercio central de las Cordilleras Béticas. Ensayo de correlación tectónica de los Alpujárrides. Acta Geol. Hisp., 14, 154-166.

Alfaro, P., Delgado, J., Sanz de Galdeano, C., Galindo-Zaldívar, J., García-Tortosa, F.J., López-Garrido, A.C., López-Casado, C., Marín, C., Gil, A. and Borque, M.J., 2007. The Baza Fault: a major active extensional fault in the Central Betic Cordillera (south Spain). Int. J. Earth Sci. (Geol Rundsch). doi: 10.1007/s00531-007-0213-z.

Almeida, E., Monteiro Santos, F., Mateus, A., Heise, W. and Pous, J., 2005. Magnetotelluric measurements in SW Iberia: New data for the Variscan crustal structures analyses. Geophys. Res. Lett., 32, L08312. doi:10.1029/2005GL022596.

Almeida, E., Pous, J., Monteiro Santos, F., Fonseca, P., Marcuello, A., Queralt, P., Nolasco, R., and Mendes Victor, L., 2001. Electromagnetic imaging of a transpressional tectonics in SW Iberia. Geophys. Res. Lett., 28, 439– 442.

Amato, A., Margheriti,, L., Azzara, R., Basili, A., Chiarabba, C., Ciaccio, M.G., Cimini, G.B., Di Bona, M., Frepoli, A., Lucente, F.P., Nostro, C. and Selvaggi, G., 1998. Passive Seismology and Deep Structure in Central Italy. Pure Appl. Geophys., 151, 479–493.

Andrieux, J. and Mattauer, M., 1973. Précisions sur un modèle explicatif de l'Arc de Gibraltar. Bull. Soc. Géol. France, 15, 115-118.

Andrieux, J., Fontboté, J. M., and Mattauer, M., 1971. Sur un modelè explicatif de l'Arc de Gibraltar. Earth Planet. Sci. Lett., 12, 191-198.

Angelier, J. and Mechler, P., 1977. Sur une méthode graphique de recherche des contraintes principales également utilisable en tectonique et sismologie: la méthode des dièdres droits. Bulletin de la Société Géologique de la France, 7, 1309–1318.

Araña, V. and Vegas R., 1974. Plate tectonics and volcanism in the strait of Gibraltar. Tectonophysics, 24, 197-212.

Ardizone J., Mezcua J. and Socias I., 1989. Mapa aeromagnético de España Peninsular, IGN, 1:1.000.000.

Azañón, J.M., Crespo-Blanc, A. and García Dueñas, V., 1997. Continental collision, crustal thinning and nappe forming during the pre-Miocene evolution of the Alpujarride Complex (Alboran Domain, Betic). Journal of Structural Geology, 19, 1055–1071.

Azañón, J.M., Galindo-Zaldívar, J., García-Dueñas, V. and Jabaloy, A., 2002. Alpine tectonics II, Betic Cordillera and Balearic Islands. In: The geology of Spain. (Gibbons, W., Moreno, T., Eds.). Geol. Soc. London, 401-416.

Azañón, J.M., García Dueñas, V., Martínez Martínez, J.M. and Crespo-Blanc, A., 1994. Alpujarride tectonic sheets in the central Betics and similar eastern allochthonous units (SE Spain). Comptes Rendues Academie Sciences Paris, 318, 667–674.

Azañón, J.M., García-Dueñas V. and Goffé, B., 1998. Exhumation of high-pressure metapelites and coeval crustal extension in the Alpujarride complex (Betic Cordillera). Tectonophysics, 285, 231-252.

Azor, A., González Lodeiro, F. and Simancas, J.F., 1994. Tectonic evolution of the boundary between the Central Iberian and Ossa-Morena Zones (Variscan Belt, SW Spain). Tectonics, 13, 45–61.

Bahr, K., 1988. Interpretation of the magnetotelluric impedance tensor: Regional induction and local telluric distortion. J. Geophys., 62, 119–127.

Bahr, K., 1991. Geological noise in magnetotelluric data: a classification of distortion types. Physics of the Earth and Planetary Interiors, 66, 24-38.

Bakker, H.E., De Jong, K., Helmers, H. and Bierman, C., 1989. The geodynamic evolution of the Internal Zone of the Betic Cordilleras (South-East Spain): a model based on structural analysis and geothermobarometry. Journal of Metamorphic Geology, 7, 359–381.

Balanyá, J. C. and García-Dueñas, V., 1987. Les directions structurales dans le Domaine d'Alborán de part et d'autre du Détroit de Gibraltar. Comptes Rendus de l'Académie des Sciences de Paris, 304, 929-932.

Balanyá, J.C. and García-Dueñas, V., 1986. Grandes fallas de contracción y de extension implicadas en el contacto entre los dominios de Alborán y Sudibérico en el Arco de Gibraltar. Geogaceta, 1, 19-21.

Balanyá, J.C. and García-Dueñas, V., 1991. Estructuración de los mantos Alpujárrides al W de Málaga (Béticas, Andalucía). Geogaceta, 9, 30-33.

Balanya, J.C., Garcia-Dueña, V., Azañón, J.M. and Sanchez-Gomez, M., 1997. Alternating contractional and extensional events in the Alpujarride nappes of the Alboran Domain (Betics, Gibraltar Arc). Tectonics, 16, 226-238.

Bally, A.W., Gordy, P.L., Stewart, G.A. and Keating, L.F., 1970. Structure, Seismic Data, and Orogenic Evolution of Southern Canadian Rocky Mountains. Bulletin of Canadian Petroleum Geology, 14, 337-381.

Banda, E. and Ansorge, J., 1980. Crustal structure under the central and eastern part of the Betic Cordillera. Geophys. J. Roy. Astr. Soc., 63, 515-532.

Banda, E., Gallart, J., García Dueñas, V., Dañobeitia, J. J. and Makris, J., 1993. Lateral variation of the crust in the Iberian Peninsula: new evidence from the Betic Cordillera. Tectonophysics, 221, 53-66.

Bard, J.P., 1977. Signification tectonique des métatholéïtes d´affinité abyssale de la ceinture métamorphique de basse presión d´aracena (Huelva, Espagne). Bull. Soc. Géol. France, 19, 385–393.

Bargach, K., Ruano, P., Chabli, A., Galindo-Zaldívar, J., Chalouan, A., Jabaloy, A., Akil, M., Ahmamou, M., Sanz de Galdeano, C., and Benmakhlouf, M., 2004. Recent Tectonic Deformations and Stresses in the Frontal Part of the Rif Cordillera and the Saïss Basin (Fes and Rabat Regions, Morocco). Pure Appl. Geophys., 161, 521–540.

Barranco, L., Ansorge, J. and Banda, E., 1990. Seismic refraction constraints on the geometry of the Ronda peridotitic massif (Betic Cordillera, Spain). Tectonophysics, 184, 379-392.

Becker, A., 2000. The Jura Mountains —an active foreland fold-and-thrust belt? Tectonophysics, 321, 381–406.

Berástegui, X., Banks, C., Puig, C., Taberner, C., Waltham, D., and Fernàndez, M., 1998. Lateral diapiric emplacement of Triassic evaporites at the southern margin of the Guadalquivir Basin, Spain. In: A. Mascle, C. Puigdefàbregas, H.P. Luterbacher and M. Fernàndez, Editors, Cenozoic Foreland Basins of Western Europe, Geological society Special Publications, London, 49–68.

Berberian, M., 1995. Master “blind” thrust faults hidden under the Zagros folds: active basement tectonics and surface morphotectonics. Tectonophysics, 241, 193-195.

Bezzeghoud, M. and Buforn, E., 1999. Source Parameters of the 1992 Melilla Spain, (Mw=4.8), 1994 Alhoceima (Morocco, Mw=5.8) and 1994 Mascara (Algeria, Mw=5.7). Earthquakes and seismotectonic implications. Bull. Seismol. Soc. Am., 89, 359–372.

Bijwaard, H., and Spakman, W., 2000. Non-linear global P-wave tomography by iterated linearized inversion. Geophysical Journal International, 141, 71–82.

Bijwaard, H., Spakman, W. and Engdahl, E. R., 1998. Closing the gap between regional and global travel time tomography. J. Geophys. Res., 103, 30055-30078.

Bird, P., 2003. An updated digital model of plate boundaries. Geochemistry, Geophysics, Geosystems, 4. doi: 10.1029/2001GC000252.

Blanco, M.J. and Spakman, W., 1993. The P-wave velocity structure of the mantle below the Iberian Peninsula: evidence for subducted lithosphere below southern Spain. Tectonophysics, 221, 13-34.

Blumenthal, M., 1927. Versuch einer tektonischen Gliederung der Betischen Kordilleren von Central and Südwest Andalusien. Eclog. Geol. Helv., 21, 358-365.

Bohoyo, F., Galindo-Zaldívar J. and Serrano, I., 2000. Main features of the basic rock bodies of the Archidona Region derived from geophysical data External Zones, Betic Cordillera. Earth and Planetary Sciences, 330, 667–674.

Bonini, M., 2003. Detachment folding, fold amplification, and diapirism in thrust wedge experiments. Tectonics, 22.

Bonini, W.E., Loomis T.P. and Robertson, J.D., 1973. Gravity anomalies, ultramafic intrusions and the tectonics of the region around the Strait of Gibraltar. Journal of Geophysical Research, 8, 1372-1382.

Booth-Rea, G., Ranero, C.R., Martínez-Martínez J.M. and Grevemeyer, I., 2007. Crustal types and Tertiary tectonic evolution of the Alborán sea, western Mediterranean. Geochem. Geophys. Geosyst., 8, 1-25.

Bott, M.H.P., 1959. The mechanics of oblique slip faulting. Geol. Mag., XCVI (2), 109-117.

Bouillin, J.P., Durand-Delga, M. and Olivier, P., 1986. Betic-Rifian and Tyrhenian Arcs: distinctive features, genesis, and development stages. In: The origin of Arcs. (Wezel, F. C., Ed.). Elsevier Science Publishers, Amsterdam., 21, 281-304.

Bourgois, J., 1978. La transversale de Ronda (Cordillères bétiques, Espagne). Dones géologiques pour un modéle d'évolution de l'arc de Gibraltar. Ph.D. Thesis, Univ. Besançon, 445 pp.

Braga, J.C., Martín J.M. and Quesada, C., 2003. Patterns and average rates of late Neogene-Recent uplift of the Betic Cordillera, SE Spain. Geomorphology, 50, 13-26.

Brun, J.P. and Faccenna, C., 2008. Exhumation of high-pressure rocks driven by slab rollback. Earth and Planetary Science Letters, 272, 1–7.

Buforn, E. and Coca, P., 2002. Seismic moment tensor for intermediate depth earthquakes at regional distances in Southern Spain. Tectonophysics, 356, 49–63.

Buforn, E., Bezzeghoud, M., Udías, A. and Pro, C., 2004. Seismic sources on the Iberia–African plate boundary and their tectonic implications. Pure Appl. Geophys., 161, 623–646.

Buforn, E., Coca, P., Udias, A. and Lasa, C., 1997. Source mechanism of intermediate and deep earthquakes in southern Spain. J. Seismol., 1, 113–130.

Buforn, E., Sanz de Galdeano, C. and Udías A., 1995. Seismotectonics of the Ibero-Maghrebian region. Tectonophysics, 248, 247-261.

Buforn, E., Udias, A. and Madariaga, R., 1991. Intermediate and deep earthquakes in Spain. Pure and Applied Geophysics, 136, 375–393.

Buontempo, L., Bokelmann, G.H.R., Barruol and G., Morales, J., 2008. Seismic anisotropy beneath southern Iberia from SKS splitting. Earth and Planetary Science Letters, 273, 237–250. doi: 10.1016/j.epsl.2008.06.024

Burg, J.P., Iglesias, M., Laurent, Ph., Matte, Ph. and Ribeiro, A., 1981. Variscan intracontinental deformation: the Coimbra–Córdoba Shear Zone (SW Iberian Peninsula). Tectonophysics, 78, 161– 177.

Calaforra, J.M. and Pulido-Bosch, A., 1999. Gypsum karst features as evidence of diapiric processes in the Betic Cordillera, Southern Spain. Geomorphology, 29, 251–264.

Calais, E., DeMets, C. and Nocquet, J. M., 2003. Evidence for a post 3.16 Ma change in Nubia-Eurasia-North America plate motions? Earth. Plan. Sci. Lett., 216, 8–92.

Calderón y Arana, 1890. Edad geológica de los terrenos de Morón de la Frontera. Bol. Inst. Geol. Min. De España., XVII, 235-239.

Caldwell, T.G, Bibby, H.M. and Brow, C., 2004. The magnetotelluric phase tensor. Geophys. J. Int., 158, 457–469.

Callot, J.P., Jahani, S. and Letouzey, J., 2006. The Role of Pre-Existing Diapirs in Fold and Thrust Belt Development. In: Lacombe, O., Roure, F., Lavé, J., Vergés, J. (ed.). Thrust Belts and Foreland Basins, 309-325.

Calvert, A., Sandvol, E., Seber, D., Barazangi, M., Roecker, S., Mourabit, T., Vidal, F., Alguacil, G. and Jabour, N., 2000a. Geodynamic evolution of the lithosphere and upper mantle beneath the Alboran region of the western Mediterranean: Constraints from travel time tomography. Journal of Geophysical Research, 105, 10871–10898.

Calvert, A., Sandvol, E., Seber, D., Barazangi, M., Vidal, F., Alguacil, G. and Jabour, N., 2000b. Propagation of regional seismic phases (Lg and Sn) and Pn velocity structure along the Africa–Iberia plate boundary zone: tectonic implications. Geophysical Journal International, 142, 384–408.

Cano Medina, F., 1990. Hoja 1036, Olvera. Mapa Geologico de España. Escala 1:50.000.

Carbonell, R., Sallaresa, V., Pous, J., Dañobeitia, J.J., Queralt, P., Ledo, J.J. and García Dueñas, V., 1998. A multidisciplinary geophysical study in the Betic chain southern Iberia Peninsula. Tectonophysics, 288, 137-152.

Carbonell, R., Simancas, F., Juhlin, C., Pous, J., Pérez-Estaún, A., González-Lodeiro, F., Muñoz, G., Heise, W., Ayarza, P., 2004. Geophysical evidence of a mantle derived intrusion in SW Iberia. Geophys. Res. Lett., 31, L11601.

Caritg, S., Burkhard, M., Ducommun, R., Helg, U., Kopp, L. and Sue, C., 2003. Fold interference patterns in the Late Palaeozoic Anti-Atlas belt of Morocco. Terra Nova, 16, 27–37.

Casas, A. and Carbó, A., 1990. Deep Structure of the Betic Cordillera Derived from the Interpretation of a complete Bouguer Anomaly Map. Journal of Geodynamics, 12, 137-147.

Casquet, C., Galindo, C., Tornos, F. and Velasco, F., 2001. The Aguablanca Cu–Ni ore deposit (Extremadura, Spain), a case of synorogenic orthomagmatic mineralization: isotope composition of magmas (Sr, Nd) and ore (S). Ore Geology Reviews, 18, 237–250.

Chalouan, A. and Michard, A., 1990. The Ghomarides nappes, Rif coastal range, Morocco: a variscan chip in the Alpine belt. Tectonics, 9, 1565–1583.

Chalouan, A. and Michard, A., 2004. The Alpine Rif Belt (Morocco): a case of Mountain building in a Subduction-subduction-transform fault triple junction. Pure and applied Geophysics, 161, 489–519.

Chalouan, A., Michard, A., Feinberg, H., Montigny, R. and Saddiqui, O., 2001. The Rif moutain building (Morocco): a new tectonic scenario. Bulletin de la Société Géologique de France, 172, 603-616.

Chauve, P., 1963. Etude géologique du Nord de la province de Cadix. Mem. Inst. Geol. y Minero de España, LXIX, 377.

Chemenda A.I., Mattauer, M. and Bokun, A.N., 1996. Continental subduction and a mechanism for exhumation of high-pressure metamorphic rocks: new modelling and field data from Oman. Earth and Planetary Science Letters, 143, 73-182.

Christova, C. and Tsapanos, T., 2000. Depth distribution of stresses in the Hokkaido Wadati– Benioff zone as deduced by inversion of earthquake focal mechanisms. J. Geodyn., 30, 557–573.

Cloetingh, S. and Niewland, F., 1984. On the mechanisms of lithospheric stretching and doming: a finite element analysis. Geol. Mijnbouw, 63, 315-322.

Coca, P. and Buforn, E., 1994. Mecanismos focales en el sur de España: periodo 1965–1985. Estudios Geológicos, 50, 33–45.

Coca, P., 1999. Métodos para la inversión del tensor momento sísmico. Terremotos del Sur de España. Ph.D. Thesis, Universidad Complutense, Madrid, 300 pp.

Comas, M.C., Platt, J.P., Soto, J.I. and Watts, A.B., 1999. The origin and tectonic history of the Alborán Basin: Insights from Leg 161. In: R. Zahn, M.C. Comas and A. Klaus, Editors, Proc. ODP, Scientific Results, 161, 555–579.

Córdoba, D., Banda, E., and Ansorge, J., 1988. P-wave velocity–depth distribution in the Hercynian crust of Northwest Spain, Phys. Earth Planet. Inter., 51, 235–248.

Costa, C.H., Diederix, H., Gardini, C. and Cortés, J., 2000. The Andean orogenic front at Sierra de Las Peñas-Las Higueras, Mendoza, Argentina. Journal of South American Earth Sciences, 13, 287-292.

Crespo-Blanc A. and Orozco, M., 1991. The boundary between the Ossa–Morena and South Portuguese Zones (Southern Iberian Massif): a major suture in the European Hercynian Chain. Geologische Rundschau, 80, 691–702.

Crespo-Blanc, A. and Campos, J. 2001. Structure and Kinematics of the South Iberian paleomargin and its relationship with the Flysch Trough units; extensional tectonics within the Gibraltar Arc fold-and thrust belt (western Betics). Journal of Structural Geology, 23, 1615-1630.

Crespo-Blanc, A., 2007. Superimposed folding and oblique structures in the palaeomargin-derived units of the Central Betics (SW Spain). Journal of the Geological Society London, 164, 621–636.

Crespo-Blanc, A., 2008. Recess drawn by the internal zone outer boundary and oblique structures in the paleomargin-derived units (Subbetic Domain, central Betics): An analogue modelling approach. Journal of Structural Geology, 30, 65-80.

Crespo-Blanc, A., Orozco, M. and García-Dueñas, V., 1994. Extension versus compression during the Miocene tectonic evolution of the Betic Chain. Late folding of normal fault systems. Tectonics, 13, 78–88.

Cruz San Julian, J.J., 1990. Hoja 1037, Teba. Mapa Geólogico de España. Escala 1:50.000.

Cuevas, J., 1990. Microtectónica y metamorfismo de los Mantos Alpujárrides del tercio central de las Cordilleras Béticas. Publicaciones especiales del Boletín Geológico y Minero de España, Madrid, 129 pp.

Dañobeitia, J.J., Sallarès, V. and Gallart, J., 1998. Local earthquakes seismic tomography in the Betic Cordillera southern Spain. Earth and Planetary Science Letters, 160, 225-239.

Davis, D., Suppe, J. and Dahlen, F.A., 1983. Mechanics of fold-and-thrust belts and accretionary wedges. Journal of Geophysical Research, 88, 1153-1172.

De Jong, K., 1991. Tectono-metamorphic studies and radiometric dating in the Betic Cordilleras (SE Spain) with implications for the dynamics of extension and compression in the Western Mediterranean area. Ph. D. Thesis, Vrije Univ. Amsterdam, Netherlands, 204 pp.

De Jong, K., 1993. The Tectono-Metamorphic and Chronological Development of the Betic Zone (Se Spain) with Implications for the Geodynamic Evolution of the Western Mediterranean Area. Proc. Kon. Ned. Akad. Wet., 96 , 295-333.

De Mets, C., Gordon, R.G, Argus, D.F. and Stein, S., 1994. Effect of recent revisions to the geomagnetic reversal time scale on estimate of current plate motions. Geophys. Res. Lett., 21, 2191-2194.

de Vicente, G., Cloetingh, S., Muñoz-Martín, A., Olaiz, A., Stich, D., Vegas, R., Galindo-Zaldívar, J. and Fernández-Lozano, J., 2008. Inversion of moment tensor focal mechanisms for active stresses around the microcontinent Iberia: Tectonic implications. Tectonics, 27, TC1009. doi:10.1029/2006TC002093.

del Fresno, C., 2004. Sismotectónica de regiones activas: Terremotos de profundidad intermedia en el Sur de España. Master Thesis, Universidad Complutense de Madrid, España, 108 pp.

del Olmo Sanz, A., Moreno-Serrano, F., Campos-Fernandez, J., Estevez, A., García-Dueñas, V., García-Rosell, L., Martin-Algarra, A., Orozco, M. and Sanz de Galdeano, C. (1990). Hoja 1051, Ronda. Mapa Geologico de España. Escala 1:50.000.

Delgado, F., Estevez, A., Martin, J.M. and Martin-Algarra, A., 1981. Observaciones sobre la estratigrafía de la Formación Carbonatada de los Mantos Alpujárrides (Cordillera Betica). Estudios Geológicos (Madrid), 37, 45-57.

Delgado, J., Alfaro, P., Galindo-Zaldívar, J., Jabaloy, A., López Garrido, A. C., Sanz de Galdeano, C., 2002. Structure of the Padul-Nigüelas Basin (S Spain) from H/V Ratios of Ambient Noise: Application of the Method to Study Peat and Coarse Sediments. Pure and Applied Geophysics, 159, 2733-2749. doi: 10.1007/s00024-002-8756-1.

DeMets, C., Gordon, R.G., Argus, D.F., Stein, S., 1994. Effect of recent revisions to the geomagnetic reversal time scale on estimates of current plate motions. Geophys. Res. Lett., 21, 2191-2194.

Dewey, J.F., Helman, M.L., Turco, E., Hutton, D.H.W. and Knott, S.D., 1989. Kinematics of the western Mediterranean. In: Alpine Tectonics (edited by Coward, M. P., Dietrich, D. and Park, R.G.). Geological Society Special Publication, 45, 265-283.

Díaz, J. and Gallart, J., 2009. Crustal structure beneath the Iberian Peninsula and surrounding waters: A new compilation of deep seismic sounding results. Physics of the Earth and Planetary Interiors, 173, 181–190. doi:10.1016/j.pepi.2008.11.008

Díaz, J., Gallart, J., Hirn, A. and Paulssen, H., 1998. Anisotropy beneath the Iberian Peninsula: the contribution of the ILIHANARS Broad-band Experiment. Pure and Applied Geophysics, 151, 395–405.

Díaz, J., Hirn, A., Gallart, J., and Senos, L., 1993. Evidence for azimuthal anisotropy in southwest Iberia from deep seismic sounding data. Phys. Earth Planet. Interiors, 78, 193–206.

Didon, J., Durand-Delga, M. and Kornporbst, J., 1973. Homologies géologiques entre les deux rives du Détroit de Gibraltar. Bulletin de la Société géologique de France, 7/15, 77–105.

Docherty, C. and Banda, E., 1995. Evidence for the eastward migration of the Alboran Sea based on regional subsidence analysis: A case for basin formation by delamination of the subcrustal lithosphere? Tectonics, 14, 804-818.

Doglioni, C., Gueguen, E., Sabat, F. and Fernández, M., 1997. The western Mediterranean extensional basins and the Alpine orogen. Terra Nova, 9, 109-112.

Duggen, S., Hoernle, K., Bogaard, Pvd and Garbe-Schönberg, D., 2005. Post-collisional transition from subduction- to intraplate-type magmatism in the westernmost Mediterranean: evidence for continental-edge delamination of subcontinental lithosphere. Journal of Petrology, 46, 1155–1201.

Duggen, S., Hoernle, K., Klügel, A., Geldmacher, J., Thirlwall, M., Hauff, F., Lowry, D., Oates, N., 2008. Geochemical zonation of the Miocene Alborán Basin volcanism (westernmost Mediterranean): geodynamic implications. Contrib. Mineral. Petrol. doi: 10.1007/s00410-008-0302-4.

Duggen, S., Hoernle, K., van den Bogaard, P. and Garbe-Schönberg, D., 2004a. Post-Collisional Transition from Subduction to Intraplate-type Magmatism in the Westernmost Mediterranean: Evidence for Continental-Edge Delamination of Subcontinental Lithosphere. Journal of Petrology, 46, 1155-1201. doi:10.1093/petrology/egi013.

Duggen, S., Hoernle, K., van den Bogaard, P., Harris, C., 2004b. Magmatic evolution of the Alboran Region: the role of subduction in forming the western Mediterranean and causing the Messinian Salinity Crisis. Earth and Planetary Science Letters, 218, 91-108.

Dupuy, C., Dostal, J. and Bard, J.P., 1979. Trace elements geochemistry of Paleozoic amphibolites of SW Spain. Tschermaks Min. Ptr. Mitt., 26, 87–93.

Durand-Delga, M. and Olivier, P., 1988. Evolution of the Alboran block margin from Early Mesozoic to Early Miocene time. In: The Atlas System of Morocco (Jacobshagen, V.H., Ed.). Springer Verlag, Berlin, 15, 465-480.

Durand-Delga, M., 1972. La courbure de Gibraltar, extremité occidentale des chaînes alpines, unit l´Europe et l´Afrique. Eclog. Geol. Helv., 65, 267-278.

Durand-Delga, M., Rossi, P., Olivier, P. and Puglisi, D., 2000. Situation structurale et nature ophiolitique de roches basiques jurassiques associe´es aux flyschs maghrébins du Rif (Maroc) et de Sicile (Italie). Comptes-Rendus de l'Académie des Sciences de Paris, 331, 29-38.

Eaton, D. W., Jones, A.G., Ferguson, I.J., 2004, Lithospheric anisotropy structure inferred from collocated teleseismic and magnetotelluric observations: Great Slave Lake shear zone, northern Canada. Geophysical Research Letters, 31, L19614. doi:10.1029/2004GL020939.

Egeler, C. G. and Simon, O. J., 1969. Orogenic evolution of the Betic Zone (Betic Cordilleras, Spain) with emphasis on the nappe structures. Geol. Mijnbouw, 48, 296-305.

Fadil, A., Vernant, P., McClusky, S., Reilinger, R., Gomez, F., Sari, D. B., Mourabit, T., Feigl, K., and Barazangi, M., 2006. Active tectonics of the western Mediterranean: Geodetic evidence for rollback of a delaminated subcontinental lithospheric slab beneath the Rif Mountains, Morocco. Geology, 34, 529-532.

Fallot, P., 1948. Les cordilleras Bètiques. Estudios Geol., 4, 259-279.

Farias, P., Gallastegui, G., González Lodeiro, F., Marquínez, J., Martín- Parra, L.M., Martínez Catalán, J.R., de Pablo Maciá, J.G. and Rodríguez Fernández, L.R., 1987. Aportaciones al conocimiento de la litoestratigrafía y estructura de Galicia Central. Mem. Museo e Lab. Miner. Geol. Fac. Ciências, Univ. Oporto, 1, 411-431.

Faure, M., Lin, W., Schärer, U., Shu, L., Sun Y., and Arnaud, N., 2003. Continental subduction and exhumation of UHP rocks. Structural and geochronological insights from the Dabieshan East China, Lithos, 70, 213– 241.

Fernàndez, M., Marzán, I., and Torne, M., 2004. Lithospheric transition from the Variscan Iberian Massif to the Jurassic oceanic crust of the Central Atlantic. Tectonophysics, 386, 97–115.

Fernàndez, M., Marzán, I., Correia, A., and Ramalho, E., 1998. Heat flow, heat production, and lithospheric thermal regime in the Iberian Peninsula. Tectonophysics, 291, 29–53. doi:10.1016/S0040-1951(98)00029-8.

Fernández-Ibáñez, F. and Soto, J.I., 2008. Crustal rheology and seismicity in the Gibraltar Arc western Mediterranean. Tectonics, 27, TC2007. doi:10.1029/2007TC002192.

Fernández-Ibáñez, F., Soto, J.I., Zoback, M.D. and Morales., J, 2007. Present-day stress field in the Gibraltar Arc (western Mediterranean). J. Geophys. Res., 112.

Flecha, I., Palomeras, I., Carbonell, R., Simancas, F., Ayarza, P., Matas, J., González-Lodeiro and F., Pérez-Estaún, A., 2009. Seismic imaging and modelling of the lithosphere of SW-Iberia. Tectonophysics, doi:10.1016/j.tecto.2008.05.033

Flinch, J.F., Bally, A.W. and Wu, S., 1996. Emplacement of a passive-margin evaporitic allochthon in the Betic Cordillera of Spain Geology, 24, 67–70.

Fontbote, J.M., 1964. Itinerario geológico Granada-Jaén. Pub. Lab. Geol. Univ. Granada., 45bis.

Frederiksen, A.W., Ferguson, I.J., Eaton, D., Miong, S.-K. and Gowan, E., 2006. Mantle fabric at multiple scales across an Archean–Proterozoic boundary, Grenville Front, Canada. Physics of the Earth and Planetary Interiors, 58, 240–263.

Fugita, K. and Kanamori, H., 1981. Double seismic zones and stresses of intermediate depth earthquakes. Geophys. J. R. Astron. Soc., 66, 131–156.

Gaibar-Puertas, C., 1973. El campo de pesantez y la estructura geológica del Estrecho de Gibraltar. Instituto Geográfico y Catastral (Madrid).

Galindo-Zaldívar, J. and González-Lodeiro, F., 1988. Faulting phase differentiation by means of computer search on grid pattern. Annales Tectonicae, 2, 90– 97.

Galindo-Zaldívar, J., 1986. Etapas de fallamiento neógenas en la mitad occidental de la depresión de Ugíjar (Cordilleras Béticas). Estudios Geológicos, 42, 1–10.

Galindo-Zaldívar, J., González Lodeiro and F., Jabaloy, A., 1989. Progressive extensional shear structures in a detachment contact in the western Sierra Nevada (Betic Cordilleras, Spain). Geodinámica Acta, 3, 73-85.

Galindo-Zaldívar, J., González-Lodeiro, F. and Jabaloy A., 1993. Stress and palaeostress in the Betic-Rif cordilleras (Miocene to the present). Tectonophysics, 227, 105-126.

Galindo-Zaldívar, J., González-Lodeiro, F., Jabaloy, A., Maldonado, A. and Schreider, A.A., 1998. Models of magnetic and Bouguer gravity anomalies for the deep structure of the central Alborán Sea basin. Geo. Mar. Lett., 18, 10-18.

Galindo-Zaldívar, J., Jabaloy, A., González Lodeiro, F. and Aldaya, F., 1997. Crustal structure of the central sector of the Betic Cordillera SE Spain. Tectonics, 16, 18-37.

Galindo-Zaldívar, J., Jabaloy, A., Serrano, I., Morales, J., González-Lodeiro, F. and Torcal, F., 1999. Recent and present-day stresses in the Granada Basin (Betic Cordilleras): example of a late Miocene present-day extensional basin in a convergent plate boundary. Tectonics, 18, 686–702.

García-Casco, A. and Torres-Roldán, R.L., 1996. Disequilibrium induced by fast decompression in St-Bt-Grt-Ky-Sil-And metapelites from the Betic Belt (southern Spain). J. Petrol., 37, 1207– 1239.

García-Castellanos, D., Fernández, M. and Torne, M., 2002. Modelling the evolution of the Guadalquivir foreland basin southern Spain. Tectonics, 21, 1018. doi:10.1029/2001TC001339.

García-Dueñas, V. and Balanyá, J.C., 1986. Estructura y naturaleza del arco de Gibraltar. Maleo, Bol. Inf. Soc. Geol. Portugal, 2, 23.

García-Dueñas, V., Balanyá, J.C. and Martínez-Martínez, J.M., 1992. Miocene extensional detachments in the outcropping basement of the Northern Alboran Basin (Betics) and their tectonic implications. Geo-Marine Letters, 12, 88–95.

García-Dueñas, V., Banda, E., Torné, M., Córdoba, D., E.-B. group, 1994. A deep seismic reflection survey across the Betic Chain (southern Spain): First results. Tectonophysics, 232, 77-89.

García-Hernández, M., López-Garrido, A.C., Rivas, P., Sanz de Galdeano, C. and Vera, J.A., 1980. Mesozoic palaeogeographic evolution of the external zones of the Betic Cordillera. Geologie en Mijnbouw, 59, 155-168.

García-Tortosa, F.J., Sanz de Galdeano, C., Alfaro, P., Galindo Zaldívar, J., Peláez, J.A., 2007. La falla y los pliegues de Galera. In: Sanz de Galdeano, C., Peláez, J.A. (ed.). La cuenca de Guadix Baza. Estructura, tectónica activa, sismicidad, geomorfología y dataciones existentes, 141-153.

Gephart, J.W., 1990. FMSI: A Fortran program for inverting fault/slickenside and earthquake focal mechanism data to obtain the regional stress tensor. Comput. Geosci., 16, 953–989.

Gill, R.C.O., Aparicio, A., El Azzouzi, M., Hernandez, J., Thirlwall, M.F., Bourgois, J. and Marriner, G.F., 2004. Depleted arc volcanism in the Alboran Sea and shoshonitic volcanism in Morocco: geochemical and isotopic constraints on Neogene tectonic processes. Lithos, 78, 363– 388.

Gill, R.C.O., El Aparicio, A., El Azzouzi, M., Hernandez, J., Thirlwall, M.F., Bourgois, J. and Marriner, G. F., 2004. Depleted arc volcanism in the Alborán Sea and shoshonitic volcanism in Morocco: geochemical and isotopic constraints on Neogene tectonic processes. Lithos, 78, 363-388.

Goffe, B., Michard, A., García-Dueñas, V., González-Lodeiro, F., Monie, P., Campos, J., Galindo-Zaldívar, J., Jabaloy, A. Martinez-Martinez, J.M. and Simancas, J.F., 1989. First evidence of high-pressure, low-temperature metamorphism in the Alpujarride nappes, Betic Cordilleras SE Spain. European Journal of Mineralogy, 1, 139-142.

Gómez-Pugnaire, M.T. and Fernández-Soler, J.M., 1987. High-pressure metamorphism in metabasites from the Betic Cordilleras (SE Spain). Contrib. Mineral. Petrol., 95, 231–244.

Grevemeyer, I., Kaul, N. and Kopf, A., 2009. Heat flow anomalies in the Gulf of Cadiz and off Cape San Vincente, Portugal. Marine and Petroleum Geology, 26, 795–804. doi:10.1016/j.marpetgeo.2008.08.006.

Grimison, N.L. and Chen, W., 1986. The Azores–Gibraltar plate boundary; focal mechanisms, depth of earthquakes and their tectonic implications. J. Geophys. Res., 91, 2029–2047.

Groom, R.W. & Bailey, R.C., 1991. Analytical investigations of the effects of near surface three-dimensional galvanic scatterers on MT tensor decomposition, Geophysics, 56, 496–518.

Groom, R.W. and Bailey, R.C., 1989. Some effects of multiple lateral inhomogeneities in magnetotellurics. Geophys. Prospect., 37, 697–712.

Groupe de Recherche Néotectonique de l´Arc de Gibraltar, 1977. L'histoire tectonique récente (Tortonien a Quaternaire) de l'Arc de Gibraltar et des bordures de la mer d'Alboran. Bull. Soc. Géol. Fr., 7, t. XIX.

Gueguen, E., Doglioni, C. and Fernández, M., 1997. Lithospheric boudinage in the Western Mediterranean back-arc basin. Terra Nova, 9, 184-187.

Gurría, E. and Mezcua, J., 2000. Seismic tomography of the crust and lithospheric mantle in the Betic Cordillera an Alborán Sea. Tectonophysics, 329, 99-119.

Gutscher, M.-A., 2004. What caused the Great Lisbon Earthquake?, Science, 305, 1247-1248.

Gutscher, M.-A., Malod, J., Rehault, J.P., Contrucci, I., Klingelhoefer, F., Mendes, L. and Spackman, W., 2002. Evidence for active subduction beneath Gibraltar. Geology, 30, 1071–1074.

Hamilton, M. P., Jones, A. G., Evans, R. L., Evans, S., Fourie, C.J.S., Garcia, X., Mountford, A., Spratt, J.E. and the SAMTEX MT Team, 2006. Electrical anisotropy of South African lithosphere compared with seismic anisotropy from shear-wave splitting analyses. Physics of the Earth and Planetary Interiors, 158, 226–239

Hammer, S., 1939. Terrain corrections for Gravimeters Stations. Geophysics, 4, 184-194.

Hammer, S., 1982. Critique of Terrain Corrections for Gravity Stations. Geophysics, 47, 839-840.

Hatzfeld, D. and Ben Sari, D., 1977. Grands profils sismiques dans la région de l'Arc de Gibraltar. Bull. Soc. Géol. Fr., 7, 749–756.

Hatzfeld, D., 1976. Etude sismologique et gravimetrique de la estructure profonde de la mer d´Alborán: Mise n évidence d´un manteau anormal. Comptes Rendus de la Academie des Sciences de Paris, 283, 1021-1024

Henares, J., López Casado C., Sanz de Galdeano, C., Delgado J. and Peláez J.A., 2003. Stress fields in the Iberian-Maghrebi region. Journal of Seismology, 7, 65–78.

Hoernle, K., Van den Bogaard, P., Duggen, S., Mocek, B. and Garbe Schönberg, D., 1999. Evidence for Miocene subduction beneath the Alborán Sea: 40Ar/39Ar dating and geochemistry of volcanic rocks from Holes 977A and 978A. In: Proc. ODP. Sci. Results. (Zahn, R., Comas, M. C. y Klaus, A., Eds.). College Station, TX (Ocean Drilling Program), 161, 357-373.

Houseman, G.A., McKenzie, D.P. and Molnar, P., 1981. Convective instability of a thickened boundary layer and its relevance for the thermal evolution of the continental crust. J. Geophys. Res., 86, 6115-6132.

Huber, P. J., 1981. Robust statistics, Wiley, New Cork.

I.A.G., 2007. http://www.ugr.es/~iag/tensor/mtc.html.

I.G.N., 1976. Mapa de anomalías de Bouguer. Escala 1:1.000.000. I.G.N., Madrid.

I.G.N., 2007. http://www.ign.es/ign/es/IGN/Sismologia10Espana/jsp.

ILIHA DSS Group, 1993. A deep seismic sounding investigation of lithospheric heterogeneity and anisotropy beneath the Iberian Peninsula. Tectonophysics, 221, 35–51.

Jabaloy, A., Galindo-Zaldívar, J. and González-Lodeiro, F., 1992. The Mecina extensional system: its relation with the post-Aquitanian piggy-back basins and the paleostresses evolution (Betic Cordilleras, Spain). Geo-Mar. Lett., 12, 96-103.

Jallouli, C., Chikhaoui, M., Braham, A., Moncef Turk, M., Mickus, K., Benassi, R., 2005. Evidence for Triassic salt domes in the Tunisian Atlasfrom gravity and geological data. Tectonophysics, 396, 209– 225.

Ji, S., Rondenay, S., Mareschal, M. and Senechal, G., 1996, Obliquity between seismic and electrical anisotropies as a potential indicator of movement sense for ductile shear zones in the upper mantle. Geology, 24, 1033–1036.

Jiménez-Pintor, J., Galindo-Zaldívar, J. Ruano, P. and Morales, J., 2002. Anomalías gravimétricas y magnéticas en la depresión de Granada (Cordilleras Béticas): tratamiento e interpretación. Geogaceta, 31, 143–146.

Jolivet, L. and Facenna C., 2000. Mediterranean extension and the Africa-Eurasia collision. Tectonics, 19, 1095-1107.

Jolivet, L., Faccenna, C., Goffé, B., Burov, E. and Agard, P., 2003. Subduction tectonics and exhumation of high-pressure metamorphic rocks in the Mediterranean orogens. American Journal of Science, 303, 353–409.

Julivert, M., Fontboté, J.M., Ribeiro, A. and Nabais Conde, L.E., 1974. Mapa tectónico de la Península Ibérica y Baleares, escala 1:1.000.000. Instituto Geológico y Minero de España, Madrid.

Khan, P.K., 2003. Stress State, Seismicity and Subduction Geometries of the Descending Lithosphere Below the Hindukush and Pamir. Gondwana Research, 6, 867-877.

Klitgord, K.D., and Schouten, H., 1986. Plate kinematics of the central Atlantic. In Vogt, P.R., and Tucholke, B.E., (eds.), The western North Atlantic region, Geology of North America. M., Boulder, Colorado, Geological Society of America, 351–378.

Lawton, T.F. and Trexler, J.H., 1991. Piggyback basin in the Sevier orogenic belt, Utah: Implications for development of the thrust wedge. Geology, 19, 827–830 .

Leblanc, D. and Olivier, P., 1984. Role of strike-slip faults in the Betic-Rifian orogeny. Tectonophysics, 101, 345-355.

Lemoine, A., Madariaga, R. and Campos, J., 2002. Slab-pull and slab-push earthquakes in the Mexican, Chilean and Peruvian subduction zones. Physics of the Earth and Planetary Interiors, 132, 157–175.

Lonergan, L. and White, N., 1997. Origin of the Betic-Rif mountain belt. Tectonics, 16, 504–522.

Lonergan, L., 1993. Timing and kinematics of deformation in the Malaguide Complex, Internal Zone of the Betic Cordillera, Southeast Spain. Tectonics, 12, 460–476.

Loomis, T.P., 1975. Tertiary mantle diapirism, orogeny and plate tectonics east of the Strait of Gibraltar. Am. J. Sci., 275, 1-33.

López Sánchez-Vizcaíno, V., M. T. Gómez Pugnaire, A. Azor, and J. M. Fernández-Soler, 2003. Phase diagram sections applied to amphibolites: A case study from the Ossa-Morena/Central Iberian Variscan suture (Southwestern Iberian Massif). Lithos, 68, 1–21.

López Sánchez-Vizcaíno, V., Rubatto, D., Gómez-Pugnaire, M.T., Trommsdorff, V. and Müntener, O., 2001. Middle Miocene high-pressure metamorphism and fast exhumation of the Nevado-Filábride Complex, SE Spain. Terra Nova, 13, 327-332.

López-Garrido, A.C. and Vera, J.A., 1974. Diapirismo reciente en la depresión de Guadix-Baza (Sector del Negretín). Estudios Geológicos, 30, 611-618.

Lotze, F., 1945. Zur Gliederung der Varisziden der Iberischen Meseta. Geotekt. Forsch., 6, 78-92.

Luján, M., Storti, F., Balanyá, J.C., Crespo-Blanc, A. and Rossetti, F., 2003. Role of décollement material with different rheological properties in the structure of the Aljibe unit thrust imbricate (Flysch Trough, Gibraltar Arc): an analogue modelling approach. J. Struct. Geol., 25, 867–881.

Mackie, R.L., Rieven, S. and Rodi, W., 1997. User's manual and software documentation for two-dimensional inversion of magnetotelluric data. Earth Resources Laboratory Rpt., Massachusetts Institute of Technology, Cambridge, MA.

Mareschal, M., Kellett, R.L., Kurtz, R.D., Ludden, J.N. and Bailey, R.C., 1995. Archean cratonic roots, mantle shear zones and deep electrical anisotropy. Nature, 375, 134–137.

Marín-Lechado, C., Galindo-Zaldívar, J., Rodríguez-Fernández, L.R. and Pedrera A., 2007. Mountain front development by folding and crustal thickening in the Internal Zone of the Betic Cordillera-Alboran Sea Boundary. Pure Appl. Geophys., 164, 1-21. doi :10.1007/s00024-006-0157-4.

Marques, F.O. and Cobbold, P.R., 2006. Effects of topography on the curvature of fold-and-thrust belts during shortening of a 2-layer model of continental lithosphere. Tectonophysics, 415, 65–80.

Martí, A., Queralt, P. and Roca, E., 2004. Geoelectric dimensionality in complex geologic areas: application to the Spanish Betic Chain. Geophys. J. Int., 157, 961-974.

Martí, D. and the ALCUDIA Team, 2009. The crustal structure of the Central Iberian Zone from the ALCUDIA deep seismic reflection transect. EGU General Assembly. Viena. Geophysical Research Abstracts.

Martí. A., 2006. A magnetotelluric investigation of geoelectrica dimensionality and study of the Central Betic crustral structure. Ph. D. Thesis. University of Barcelona, 307 pp.

Martín Serrano, A., 1986. Hoja 1021, Morón de la Frontera. Mapa Geologico de España. Escala 1:50.000.

Martín, J.M. and Braga, J.C., 1987. Alpujárride carbonate deposits (southern Spain)—marine sedimentation in a Triassic Atlantic. Palaeogeogr., Palaeoclimat., Palaeoecol., 59, 243–260.

Martín-Algarra, A. 1987. Evolución geológica alpina del contacto entre las Zonas Internas y las Zonas Externas de las Cordilleras Béticas. Tesis Doctoral, Universidad de Granada, Granada, 1171 pp.

Martinez del Olmo, W., García Mallo, J., Leret, G., Serrano Oñate, A.; Suarez Alba, J., 1984. Modelo tectosedimentario del bajo Guadalquivir. I Congreso Español de Geología, 1, 199-213

Martínez-Martínez, J.M., Booth-Rea, G., Azañón, J.M. and Torcal, F., 2006. Active transfer fault zone linking a segmented extensional system (Betics, southern Spain): Insight into heterogeneous extension driven by edge delamination. Tectonophysics, 422, 159–173.

Martín-Martín, M. and Martín-Algarra, A., 2002. Thrust sequence and syntectonic sedimentation in a piggy-back basin: the Oligo-Aquitanian Mula–Pliego Basin (Internal Betic Zone, SE Spain). Comptes Rendus Geosciences, 334, 363-370.

Martín-Martín, M., Sanz de Galdeano, C., García-Tortosa, F.J., Martín-Rojas, I., 2006. Tectonic units from the Sierra Espuña-Mula area (SE Spain): implication on the triassic paleogeography and the geodynamic evolution for the Betic-Rif Internal Zone. Geodinamica Acta, 19, 1-15.

Matte, P., 1986. Tectonics and plate tectonics model for the Variscan Belt of Europe. Tectonophysics, 126, 329–374.

McClusky, S., Reilinger, R., Mahmoud, S., Ben Sari, D., and Tealeb, A., 2003. GPS constraints on Africa (Nubia) and Arabia plate motions. Geophysical Journal International, 155, 126–138.

McKenzie, D.P., 1969. Speculations on the consequences and causes of plate motions. Geophys. J. R. Astron. Soc., 18, 1-32.

Medialdea, T., Suriñach, E., Vegas, R., Banda, E. and Ansorge, J., 1986. Crustal structure under the western end of the Betic Cordillera Spain. Annales Geophysicae, Series B: Terrestrial and Planetary Physics, 4, 457-464.

Mezcua, J. and Martínez Solares, J. M., 1983. Sismicidad del Área Ibero-Mogrebí. Instituto Geográfico Nacional, Madrid, Publ. técnica, 203.

Mézcua, J. and Rueda, J., 1997. Seismological evidence for a delamination process in the lithosphere under Alborán Sea. Geophys. J. Int., 129, F1–F8.

Mon, R., Monaldi, C.R. and Salfity, J.A., 2005. Curved structures and interference fold patterns associated with lateral ramps in the Eastern Cordillera, Central Andes of Argentina. Tectonophysics, 399, 173-179.

Monié, P., Galindo-Zaldívar, J., González-Lodeiro, F., Goffe, B. and Jabaloy, A., 1991. 40Ar/39Ar geochronology of Alpine tectonism in the Betic Cordilleras southern Spain. Journal of the Geological Society, 148, 289-297.

Monié, P., Torres-Roldán, R. L. and García-Casco, A., 1994. Cooling and exhumation of the Wertern Betic Cordilleras, 40Ar/39Ar thermochronological constraints on a collapsed terranes. Tectonophysics, 238, 353–379.

Monteiro Santos, F. A., A. Mateus, E. P. Almeida, J. Pous, and L. A. Mendes-Victor, 2002. Are some of the deep crustal conductive features found in SW Iberia caused by graphite? Earth Planet. Sci. Lett., 201, 353–367.

Monteiro Santos, F. A., J. Pous, E. P. Almeida, P. Queralt, A. Marcuello, H. Matías, and L. A. Mendes V., 1999. Magnetotelluric survey of the electrical conductivity of the crust across the Ossa Morena Zone and South Portuguese Zone suture. Tectonophysics, 313, 449– 462.

Morales, J., Serrano, I., Jabaloy, A., Galindo-Zaldívar, J., Zhao, D., Torcal, F., Vidal, F. and Gonzalez-Lodeiro, F., 1999. Active continental subduction beneath the Betic Cordillera and Alboran Sea. Geology, 27, 735–738.

Morales, J., Serrano, I., Vidal, F. and Torcal, F., 1997. The depth of the earthquake activity in the Central Betics (southern Spain). Geophys. Res. Lett., 24, 3289–3292.

Morales, J., Vidal, F., De Miguel, F., Alguacil, G., Posadas, A.M., Ibáñez, J.M., Guzmán, A. and Guirao, J.M., 1990. Basement structure of the Granada basin, Betic Cordilleras, Southern Spain. Tectonophysics, 171, 337-348.

Morel, J.L. and Meghraoui, M., 1996. Goringe-Alboran-Tell tectonic zone: A transpression system along the Africa-Eurasia plate boundary. Geology, 24, 755–758.

Moreno Serrano, F., García-Dueñas, V., Campos Fernández, J., Garcia-Rossell, L., Orozco Fernández, M. and Sanz de Galdeano, C., 1990. Hoja 1050, Ubrique. Mapa Geologico de Espana. Escala 1:50.000.

Morley, C.K., 1993. Discussion of Origins of Hinterland Basins to the Rif-Betic Cordillera and Carpathians. Tectonophysics, 226, 359-376.

Munhá, J., 1983. Hercynian magmatism in the Iberian Pyrite Belt in The Carboniferous of Portugal, edited by M. J. Lemos de Sousa and J. T. Oliveira. Mem. Serv. Geol. Port., 29, 38 – 81.

Munhá, J., Oliveira J.T., Ribeiro, A., Oliveira, V., Quesada, C., and Kerrich, R., 1986. Beja-Acebuches ophiolite, characterization and geodynamic significance. Maleo, 2, 31.

Muñoz, D., Cisternas, A., Udías, A., Mezcua, J., Sanz de Galdeano, C., Morales, J., Sánchez-Venero, M., Haessler, H., Ibañez, J., Buforn, E., Pascual, G. and Rivera, L., 2002. Microseismicity and tectonics in the Granada Basin (Spain). Tectonophysics, 356, 233–252.

Muñoz, G., A. Mateus, J. Pous, W. Heise, F. Monteiro Santos, and E. Almeida, 2008. Unraveling middle-crust conductive layers in Paleozoic Orogens through 3D modeling of magnetotelluric data: The Ossa-Morena Zone case study (SW Iberian Variscides). J. Geophys. Res., 113, B06106, doi: 10.1029/2007JB004987.

Muñoz, G., W. Heise, C. Paz, E. Almeida, F. Monteiro Santos, and J. Pous, 2005. New magnetotelluric data trough the boundary between the Ossa Morena and Centroiberian Zones. Geol. Acta, 3, 215– 223.

Negredo, A. M., Bird, P., Sanz de Galdeano, C. and Buforn, E., 2002. Neotectonic modeling of the Ibero-Maghrebian region. Journal of Geophysical Research, 107.

Negredo, A.M., Replumaz, A., Villaseñor, A. and Guillot, S., 2007. Modeling the evolution of continental subduction processes in the Pamir–Hindu Kush region. Earth and Planetary Science Letters, 259, 212–225.

Nilforoushan, F. and Koyi, H.A., 2007. Displacement fields and finite strains in a sandbox model simulating a fold-thrust-belt. Geophys. J. Int., 169, 1341–1355.

O'Brien, P. J., 2001. Subduction followed by collision: Alpine and Himalayan examples. Physics of the Earth and Planetary Interiors, 127, 277–291.

O'Dogherty, L., Rodríguez-Cañero, R., Gursky, H.J., Martín-Algarra, A.and Caridroit, M., 2000. New data on Lower Carboniferous stratigraphy and palaeogeography of the Malaguide Complex (Betic Cordillera, Southern Spain). Earth and Planetary Sciences, 331, 533–541

Oliveira, J.T., 1990. Stratigraphy and syn-sedimentary tectonism in the South Portuguese Zone. - In: Pre-Mesozoic Geology of Iberia. Eds: D. Dallmeyer and E. Martinez. 334–347. Springer Verlag.

Ott d'Estevou, P. and Montenat, C., 1985. Evolution structurale de la zone bétique orientale (Espagne) du Tortonien a l'Holocène. C. R. Acad. Sci. Paris, 300, 363–368.

Palomeras, I., Carbonell, R., Flecha, I., Simancas, F., Ayarza, P., Matas, J., Martínez Poyatos, D., Azor, A., González Lodeiro, F. and Pérez-Estaún, A., 2009. Nature of the lithosphere across the Variscan Orogen of SW Iberia: Dense wide-angle seismic reflection data. J. Geophys. Res., 114, B02302.

Pedley, R.C., Busby, J.P. and Dabeck, Z.K., 1993. GRAVMAG User Manual- Interactive 2.5D gravity and magnetic modelling. British Geological Survey, Technical Report WK/93/26/R.

Pedrera, A., Galindo-Zaldívar , J., Ruiz-Constán, A., Duque, C., Marín-Lechado, C. and Serrano, I., 2009. Recent large fold nucleation in the upper crust: Insight from gravity, magnetic, magnetotelluric and seismicity data (Sierra de Los Filabres-Sierra de Las Estancias, Internal Zones, Betic Cordillera). Tectonophysics, 463, 145–160. doi:10.1016/j.tecto2008.09.037.

Pedrera, A., Galindo-Zaldívar, J., Sanz de Galdeano, C., and López Garrido, A.C., 2007. Fold and fault interactions during the development of an elongated narrow basin, the Almanzora Neogene-Quaternary Corridor (SE Betic Cordillera, Spain). Tectonics, 26.

Pedrera, A., Marín-Lechado, C., Galindo-Zaldívar, J., Rodríguez-Fernández, L.R. and Ruiz-Constán, A., 2006. Fault and fold interaction during the development of the

Neogene-Quaternary Almería-Níjar basin (SE Betic Cordilleras). In: G. Moratti, and A. Chalouan (Eds), Tectonic of the Western Mediterranean, Geological Society of London. Special Publications, 262, 217-230.

Perconig, E., 1960-1962. Sur le constitution géologique de LÁndalousie occidental en particulier du bassin du Guadalquivir. (Espagne méridionale). In: livre a le memoire du Prof. P. Fallot. mem. H-série S.G.F. 1, 229-256.

Pérez-López, A. and Pérez-Valera, F., 2003. El diapirismo como factor principal de la resedimentación de las rocas del Triásico durante el Terciario en las Zonas Externas de la Cordillera Bética. Geotemas, 5, 189-193.

Pérez-López, A. and Pérez-Valera, F., 2007. Palaeogeography, facies and nomenclature of the Triassic units in the different domains of the Betic Cordillera (S Spain). Palaeogeography Palaeoclimatology Palaeocology, 254, 606-627.

Pérez-López, A. and Sanz de Galdeano, C., 1994. Tectónica de los materiales triásicos en el sector central de la Zona Subbética (Cordillera Bética). Rev. Soc. Geol. Esp., 7, 141-153.

Pignatelli García, R., and Crespo Zamorano, A., 1977. Hoja 1004, Marchena. Mapa Geológico de España. Escala 1:50.000.

Pinto, V., Casas, A., Rivero, L. and Torné, M., 2005. 3D gravity modeling of the Triassic salt diapirs of the Cubeta Alavesa (northern Spain). Tectonophysics, 405, 65–75.

Platt J.P., Whitehouse, M.J., Kelley, S.P., Carter, A. and Hollick, L., 2003. Simultaneous extensional exhumation across the Alboran Basin: implications for the causes of late orogenic extension. Geology, 31, 251–254.

Platt, J., Allerton, S., Kirker, A. and Platzman, E., 1995. Origin of the western Subbetic arc (South Spain), palaeomagnetic and structural evidence. Journal of Structural Geology, 12, 765-775.

Platt, J.P. and Vissers, R.L.M., 1989. Extensional collapse of thickened continental lithosphere: A working hypothesis for the Alboran Sea Gibraltar Arc. Geology, 17, 540-543.

Platt, J.P., Soto, J.I. and Comas, M.C., 1996. Decompression and high-temperature–low-pressure metamorphism in the exhumed floor of an extensional basin, Alboran Sea, western Mediterranean. Geology, 24, 447–450.

Platzman, E.S., 1992. Paleomagnetic rotations and the kinematics of the Gibraltar Arc. Geology, 20, 311-314.

Pollack, H. N., Hurter, S. J. and Johnson, J. R., 1993. Heat Flow from the Earth's Interior: Analysis of the Global Data Set. Reviews of Geophysics, 31, 267–280.

Polyak, B.G., Fernández, M., Khutorskoy, M.D., Soto, J.I., Basov, I.A., Comas, M.C.,

Khain, V.E., Alonso, B., Agapova, G.V., Mazurova, I.S., Negredo, A., Tochitsky, V.O., de la Linde, J., Bogdanov, N.A. and Banda, E., 1996. Heat flow in the Alboran Sea, western Mediterranean. Tectonophysics, 263, 191-218. doi:10.1016/0040-1951(95)00178-6.

Pous, J., G. Muñoz, W. Heise, J. C. Melgarejo, and C. Quesada, 2004. Electromagnetic imaging of Variscan crustal structures in SW Iberia: The role of interconnected graphite. Earth Planet. Sci. Lett., 217, 435– 450.

Pous, J., Galindo, J., Ruiz-Constán, A., Heise, W., Asensio, E., Ibarra, P., Monteiro Santos, F., Pedrera, A., Anahnah, F., Arzate, J., 2009. MT TopoIberia: Long period measurements in the Iberian Massif (Central Spain). IAGA 11th Scientific Assembly, Abstract book.

Pous, J., Queralt, P., Ledo, J. and Roca, E., 1999. A high electrical conductive zone at lower crustal depth beneath the Betic Chain Spain. Earth and Planetary Science Letters, 167, 35–45.

Ranalli G., Pellegrini, R. and D'Offizi, S., 2000. Time dependence of negative buoyancy and the subduction of continental lithosphere. Journal of Geodynamics, 30, 539-555.

Riaza, C. and Martínez del Olmo, W., 1996. Depositional model of the Guadalquivir Gulf of Cádiz Tertiary basin, En: Tertiary Basins of Spain (P.F. Friend and C.J. Dabrio Eds.). Cambridge Univ. Press, 330-338.

Ribeiro, A., Cabral, J., Baptista, R. and Matias, L., 1996. Stress pattern in Portugal mainland and the adjacent Atlantic region, West Iberia. Tectonics, 15, 641–659.

Rimi, A., Chalouan, A. and Bahi, L., 1998. Heat flow in the westernmost part of the Alpine Mediterranean system (the Rif, Morocco). Tectonophysics, 285, 135–146. doi:10.1016/S0040-1951(97)00185-6.

Rimi. A. and Lucazeau, F., 1987. Heat flow density measurements in northern Morocco. Journal of African Earth Sciences, 6, 835-843.

Robardet, M. and Gutiérrez Marco, J.C., 1990. Sedimentary and Faunal Domains in the Iberian Peninsula during Lower Paleozoic Times. In: Dallmeyer, R.D., Martínez García, E. (Eds.), Pre-Mesozoic Geology of Iberia. Springer, Berlin, 383– 395.

Robardet, M., 1976. L'originalité du segment hercynien sud-ibérique au Paléozoïque inférieur: Ordovicien, Silurien et Dévonien dans le Nord de la Province de Séville (Espagne). C. R. Acad. Sci. Paris, Sér. D, 283, 999– 1002.

Rodríguez-Fernández, J. and Sanz de Galdeano, C., 2006. Late orogenic intramontane basin development: the Granada basin. Betics (southern Spain).. Basin Research 18, 85-102.

Rodríguez-Fernández, J., 1982. El Mioceno del sector central de las Cordilleras Béticas. Ph.D. Thesis. Universidad de Granada, 224 pp.

Roldán, F.J. and García-Cortés, A., 1988. Implicaciones de materiales triásicos en la Depresión del Guadalquivir, Cordilleras Béticas (Provincias de Córdoba y Jaén). II Congr. Geol. España, 1, 189-192.

Roldán, F.J. and Rodríguez Fernández, J., 1991. Un ejemplo de cuenca piggy-back asociada a la evolución neógena del frente de las Zonas Externas Béticas. Comunicaciones. I Congreso del Grupo Español del Terciario. Vic., 297-300.

Roldán, F.J., 1988. Estudio geológico de las Unidades Neógenas comprendidas entre Espejo y Porcuna (provincias de Córdoba y Jaén). Depresión del Guadalquivir. Tesis de Licenciatura. Universidad de Granada. 107 pp.

Roldán, F.J., 1995. Evolución neógena de la Cuenca del Guadalquivir. Unpubl. Ph.D. Thesis, Univ. Granada, 259 pp.

Rosenbaum, G., Lister, G.S. and Duboz, C., 2002. Relative motions of Africa, Iberia and Europe during Alpine orogeny. Tectonophysics, 359, 117-129.

Royden, L.H., 1993. Evolution of retreating subduction boundaries formed during continental collision. Tectonics, 12, 629-638.

Ruano, P., 2003. Estructuras tectónicas recientes en la transversal central de las Cordilleras Béticas. Ph. D. Thesis. Universidad de Granada. 446 pp.

Ruano, P., Galindo-Zaldívar, J. and Jabaloy, A., 2004. Recent Tectonic Structures in a Transect of the Central Betic Cordillera. Pure Appl. Geophys. 161, 541–563.

Ruiz-Constán, A., Galindo-Zaldívar, J., Pedrera, A. and Sanz de Galdeano, C., 2008. Gravity anomalies and orthogonal box fold development on heterogeneous basement in the Neogene Ronda Depression Western Betic Cordillera. Journal of Geodynamics doi:10.1016/j.jog.2008.09.004.

Ruiz-Constán, A., Galindo-Zaldívar, J., Sanz de Galdeano, C., 2005. Gravity anomalies and structure of the La Zubia alluvial fan (western Sierra Nevada, Betic Cordilleras). Geogaceta 38, 67-70.

Ruiz-Constán, A., Stich, D., Galindo-Zaldívar, J., Morales, J., 2009. Is the northwestern Betic Cordillera mountain front active in the context of the convergent EurasiaAfrica plate boundary?, Terra Nova, 21, 352-359.

Sánchez Jiménez, N., (2004). Estructura gravimétrica y magnética de la corteza del suroeste peninsular (zona surportuguesa y zona de Ossa-Morena). Ph.D. Thesis. Universidad Complutense de Madrid.

Sanz de Galdeano, C. and Alfaro, P., 2004. Tectonic significance of the present relief of the Betic Cordillera. Geomorphology, 63, 175-190.

Sanz de Galdeano, C. and Andreo, B., 1995. Structure of Sierra Blanca (Alpujarride Complex, west of the Betic Cordillera). Estudios Geológicos (Madrid), 51, 43-55.

Sanz de Galdeano, C. and Vera, J.A., 1992. Stratigraphic record and palaeogeographical context of the Neogene basins in the Betic Cordillera, Spain. Basin Research, 4, 21–36.

Sanz de Galdeano, C., 1983. Los accidentes y fracturas principales de las Cordilleras Béticas. Estudios Geol., 39, 157-165.

Sanz de Galdeano, C., 1990. Geologic evolution of the Betic Cordilleras in the Western Mediterranean, Miocene to the present. Tectonophysics, 172, 107– 119.

Sanz de Galdeano, C., Delgado, J., Galindo-Zaldívar, J., Marín-Lechado, C., Alfaro, P. and García Tortosa, F.J., 2007. Principales rasgos geológicos deducidos a partir de los mapas gravimétricos de la cuenca de Guadix-Baza. In: Sanz de Galdeano C., Peláez J.A. (ed.). La cuenca de Guadix Baza. Estructura, tectónica activa, sismicidad, geomorfología y dataciones existentes, 101-110.

Sanz de Galdeano, C., Galindo-Zaldívar, J., López Garrido, A.C., Alfaro, P., Pérez-Valera, F., Pérez-López, A. and García Tortosa, F.J., 2006. La falla de Tíscar: Su significado en la terminación sudoeste del arco Prebético. Rev. Soc. Geol. España, 19, 271-280.

Sanz de Galdeano, C., López Casado, C., Delgado, J. Peinado, M.A., 1995. Shallow seismicity and active faults in the Betic Cordillera. A preliminary approach to seismic sources associated with specific faults. Tectonophysics, 248, 293-302.

Schedl, A. and Wiltschko D.V., 1987. Possible effects of pre-existing basement topography on thrust fault ramping. Journal of Structural Geology, 9, 1029-1037.

Schmucker, U., 1970. Anomalies of Geomagnetic Variations in the Southwestern United States. University of California Press, Berkeley, 165 pp.

Seber, D., Barazangi, M., Ibenbrahim, A. and Demnati, A., 1996a. Geophysical evidence for lithospheric delamination beneath the Alboran Sea and Rif-Betics mountains. Nature, 379, 785-790.

Sella, G. F., Dixon, T. H. and Mao, A., 2002. REVEL: a model for recent plate velocities from space geodesy. J. Geophys. Res., 107. doi:10.1029/2000JB000033.

Seno, T. and Yoshida, M., 2004. Where and why do large shallow intraslab earthquakes occur?, Physics of the Earth and Planetary Interiors, 141, 183–206.

Serpelloni, E. Vannucci, G., Pondrelli, S., Argnani, A., Casula, G., Anzidei, M., Baldi P. and Gasperini, P., 2007. Kinematics of theWestern Africa-Eurasia plate boundary from focal mechanisms and GPS data, Geophys. J. Int., 169, 1180-1200.

Serrano, F., 1979. Los foraminíferos planctónicos del Mioceno superior de la cuenca de Ronda y su comparación con los de otras áreas de la Cordilleras Béticas. Ph.D. Thesis. Facultad de Ciencias. Universidad de Málaga, 272 pp.

Serrano, I., 1999. Distribución espacial de la sismicidad en las Cordilleras Béticas-Mar de Alborán. Unpubl. Ph.D. Thesis, Universidad de Granada, 231 pp.

Serrano, I., Bohoyo, F., Galindo-Zaldívar, J., Morales, J. and Zhao, D., 2002. Geophysical signatures of a basic-body rock placed in the upper crust of the External Zones of the Betic Cordillera Southern Spain. Geophysical Research Letters, 29, doi:10.1029/2001GL013487.

Serrano, I., Hearn, T.M., Morales, J. and Torcal, F., 2005. Seismic anisotropy and velocity structure beneath the southern half of the Iberian Peninsula: Physics of the Earth and Planetary Interiors, 150, 317–330. doi:10.1016/j.pepi.2004.12.003.

Serrano, J., Morales, J., Zhao, D., Torcal, F. and Vidal, F., 1998. P wave tomographic images in the Central Betics- Alboran Sea (Southern Spain) using local earthquakes: contribution for a continental collision. Geophy. Res. Lett., 25, 4031-4034.

Sierro, F.J., González Delgado, J.A., Dabrio, C.J., Flores, J.A. and Civis, J., 1996. Late Neogene depositional sequences in the Foreland basin of Guadalquivir (SW Spain). In: Tertiary basins of Spain (P.F. Friend and C.J. Dabrio, Eds.). Cambridge Univ. Press, 329-334.

Silver, P.G. and Chan, W.W., 1988. Implications for continental structure and evolution from seismic anisotropy. Nature, 335, 34–39.

Simancas, J. F., 1983. Geología de la extremidad oriental de la zona Sudportuguesa. Thesis Doctoral, Univ. Granada, 439 pp.

Simancas, J.F. and Campos, J., 1993. Compresión NNW-SSE tardi a postmetamórfica y extensión subordinada en el Complejo Alpujárride (Dominio de Alborán, Orógeno bético). Revista Soc. Geol. España, 6, 23–26.

Simancas, J.F., Carbonell, R., González-Lodeiro, F., Pérez-Estaún, A., Juhlin, C., Ayarza, P., Kashubin, A., Azor, A., Martínez-Poyatos, D., Almodóvar, G.R., Pascual, E., Sáez, R. and Expósito, I., 2003. Crustal structure of the transpressional Variscan orogen of SW Iberia: SW Iberia deep seismic reflection profile (IBERSEIS). Tectonics, 22, 1-20.

Simancas, J.F., González Lodeiro, F., Expósito Ramos, I., Azor, A. and Martínez Poyatos, D., 2002. Opposite subduction polarities connected by transform faults in the Iberian Massif and west-European Variscides. In: Martı´nez Catalán, J.R., Hatcher, R.D., Arenas, R., Díaz García, F. (Eds.), Variscan –Appalachian Dynamics: the Building of the Late Paleozoic Basement. Spec. Pap. - Geol. Soc. Am., 364, 253– 262.

Simancas, J.F., Martínez Poyatos, D., Expósito, I., Azor, A. and González Lodeiro, F., 2001. The structure of a major suture zone in the SW Iberian Massif: the Ossa-Morena/Central Iberian contact. Tectonophysics, 332, 295– 308.

Singh, D.D., 2000. Seismotectonics of the Himalaya and its vicinity from centroid-moment tensor CMT solution of earthquakes. Journal of Geodynamics, 30, 507-537.

Socías, I., Mezcua, J., Lynam, J. and Del potro, R., 1991. Interpretation o fan aeromagnetic survey of the spanis mainland. Earth and Planetary Science Letters, 105, 55-64.

Song, S., Zhang, L., Niu, Y., SU, L., Song, B. and Liu, D., 2006. Evolution from Oceanic Subduction to Continental Collision: a Case Study from the Northern Tibetan Plateau Based on Geochemical and Geochronological Data. Journal of Petrology, 47, 435-455.

Spakman, W. and Wortel, R., 2004. A tomographic view on Western Mediterranean geodynamics. In: W. Cavazza, F.M. Roure, W. Spakman, G.M. Stampfli and P.A.Z. (eds.), The TRANSMED Atlas - The Mediterranean region from crust to Mantle. Springer, Berlin, Heidelberg.

Spakman, W., 1990. Tomographic images of the upper mantle below central Europe and the Mediterranean. Terra Nova, 2, 542 – 553.

Sperner, B., Lorenz, F., Bonjer, K., Hettel, S., Müller, B. and Wenzel, F., 2001. Slab break-off, abrupt cut or gradual detachment? New insights from the Vrancea Region SE Carpathians, Romania. Terra Nova, 13, 172-179.

Staub, R., 1926. Gedarker zun Taktonik Spaniens. Vierterjahrset d. Natura. Ges. Zurich, 71, 196-261.

Stauder, W., 1968. Tensional character of earthquake foci beneath the Aleutian trench with relation to sea-floor spreading. J. Geophys. Res., 73, 7693–7701.

Stich, D., Ammon C.J. and Morales, J., 2003. Moment tensor solutions for small and moderate earthquakes in the Ibero-Maghreb region. Journal of Geophysical Research, 108, doi:10.1029/2002JB002057..

Stich, D., Serpelloni, E., Mancilla, F.L. and Morales, J., 2006. Kinematics of the Iberia–Maghreb plate contact from seismic moment tensors and GPS observations. Tectonophysics 426, 295–317.

Suriñach and R. Vegas, 1988. Lateral inhomogeneities of the Hercyninan crust in central Spain, Phys. Earth Planet. Int., 51, 226–234.

Suriñach E. and Vegas R., 1993. Estructura general de la corteza en una transversal del Mar de Alborán a partir de datos de sísmica de refracción-reflexión de gran ángulo. Interpretación geodinámica. Geogaceta, 14, 126-128.

Suriñach, E. and Udías, A.,1978. Derminación de la raiz de Sierra Nevada-Filábrides a partir de medidas de refracción sísmica y gravimetría. In: Reunión sobre la Geodinámica de la Cordillera Bética y Mar de Alborán, Serv. Publ. Univ. Granada, 25–35.

Tapponnier, P., 1977. Évolution tectonique du système alpin en Méditerranée: poinçonnement et écrasement rigide-plastique. Bull. Soc. Géol. Fr., 7, 437-460.

Telford, W.M., Geldart, L.P. and Sheriff, R.E., 1990. Applied Geophysics, Cambridge University press, 770 pp.

Thiebot, E. and Gutscher, M.A., 2006. The Gibraltar Arc seismogenic zone (part 1): Constraints on a shallow east dipping fault plane source for the 1755 Lisbon earthquake provided by seismic data, gravity and thermal modeling. Tectonophysics, 426, 135–152.

Tommasi, A., Tikoff, B. and Vauchez, A., 1999. Upper mantle tectonics: three-dimensional deformation, olivine crystallographic fabrics and seismic properties. Earth and Planetary Science Letters, 168, 173–186.

Torné, M. and Banda, E., 1992. Crustal thinning from the Betic cordillera to the Alborán Sea. Geo-Marine Letters, 2, 76-81.

Torné, M., Banda, E., García-Dueñas, V. and Balanyá J.C., 1992. Mantle-lithosphere bodies in the Alboran crustal domain (Ronda peridotites, Betic-Rif orogenic belt). Earth and Planetary Science Letters, 110, 163-171.

Torné, M., Fernández, M., Comas, M.C. and Soto J.I., 2000. Lithospheric structure beneath the Alboran Basin: Results from 3D gravity modeling and tectonic relevance. J. Geophys. Res., 105, 3209-3228. doi:10.1029/1999JB900281.

Tornos, F., Casquet, C., Galindo, C., Velasco, F. and Canales, A., 2001. A new style of Ni-Cu mineralization related to magmatic breccia pipes in a transpressional magmatic arc, Aguablanca, Spain. Miner. Depos., 36, 700–706.

Torres-Roldán R.L., Polli G. and Peccerillo A., 1986. An Early Miocene arc-tholeitic magmatic dyke event from the Alboran sea. Evidence for precollisional subduction and back arc-crustal extension in the westernmost Mediterranean. Geol. Rundschau, 75, 219–234.

Torres-Roldan, R. L, 1979. The tectonic subdivision of the Betic Zone (Betic Cordilleras, southern Spain); its significance and one possible geotectonic scenario for the westernmost Alpine Belt. American Journal of Science, 279, 19-51.

Tubía, J.M., 1985. Sucesiones metamórficas asociadas a rocas ultramáficas en los Alpujárrides occidentales (Cordilleras Béticas, Málaga). Ph.D. Thesis, Univ. Pais Vasco, 300 pp.

Tubía, J.M., 1988. Estructura de los Alpujarrides occidentales; Cinematica y condiciones de emplazamiento de las peridotitas de Ronda. Publ. Esp. Bol. Geol. Miner., 99. 1-124.

Tubía, J.M., 1994. The Ronda peridotites (Los Reales nappe): an example of the relationship between lithospheric thickening by oblique tectonics and late extensional deformation within the Betic Cordillera (Spain). Tectonophysics, 238, 381-398.

Tubía, J.M., Cuevas, J., Navarro-Vila, F., Alvarez, F. and Aldaya, F., 1992. Tectonic evolution of the Alpujarride Complex (Betic Cordillera, southern Spain). Journal of Structural Geology, 14, 2, 193-203.

Varentsov Iv.M., 2007. Arrays of simultaneous EM soundings: design, data processing and analysis. In Spichak, V. V. Eds., Electromagnetic sounding of the Earths interior: Methods in geochemistry and geophysics. Elsevier, 40, 263-277.

Vera, J.A., 1988. Evolución de los sistemas de depósito en el margen Ibérico de las Cordilleras Béticas. Rev. Soc. Geol. España, 1, 373-391.

Vera, J.A., 2004. Zonas externas Béticas. In: Vera, J.A. (Ed.), Geología de España. Sociedad Geológica de España-Instituto Geológico y Minero de España, 354-389.

Villasante-Marcos, V.; Osete, M.L.; Gervilla, F. and García-Dueñas, V., 2003, Paleomagnetic study of the Ronda peridotites (Betic Cordillera, sotuhern Spain). Tectonophysics, 377, 119-141.

Viseras, C., Soria, J.M. and Fernández, J., 2004. Cuencas neógenas postorogénicas de la Cordillera Bética. In: Vera (ed.) Geología de España. SGE – IGME, 576-581.

Vissers, R.L.M., 1981. A structural study of the central Sierra de los Filabres (Betic Zone, SE Spain). GUA Papers of Geol. Ser. I 15, 1 –154.

Vozoff, K., 1972. The magnetotelluric method in the exploration of sedimentary basins. Geophysics 37, 1, 98-141.

Wagreich, M., 2001. A 400-km-long piggyback basin (Upper Aptian-Lower Cenomanian) in the Eastern Alps. Terra Nova, 13, 401- 406.

Wannamaker, P.E., 2005. Anisotropy versus heterogeneity in Continental solid Earth electromagnetic studies: fundamental response characteristics and implications for physicochemical state. Surv. Geophys., 26, 733–765.

Watts, A.B., Platt, J. and Buhl, P., 1993. Tectonic evolution of the Alboran Sea Basin. Basin Res., 5, 153-177.

Weijermars, R., Roep, T. B., Van den Eeckhout, B., Postma, G., Kleverlaan, K., 1985. Uplift history of a Betic fold nappe inferred from Neogene-Quaternary sedimentation and tectonics (in the Sierrra Alhamilla and Almeria, Sorbas and Tabernas Basins of the Betic Cordilleras, SE Spain). Geol. Mijnbouw, 64, 397-411.

West, J.D., Fouch, M.J., Roth, J.B., and Elkins-Tanton, L.T., 2009. Vertical mantle flow associated with a lithospheric drip beneath the Great Basin. Nature Geoscience, 2, 439-444. doi:10.1038/NGEO526.

Working Group for Deep Seismic Sounding in the Alboran Sea 1974-1975 (WGDSSAS-1974-1975, 1978). Crustal seismic profiles in the Alborán Sea preliminary results. Pure and Applied Geophysics, 116, 167-180

Wortel, M.J. and Spakman, R.W., 2000. Subduction and Slab detachment in the Mediterranean-Carpathian Region. Science, 290, 1910-1917. doi: 10.1126/science.290.5498.1910

Wortel, M.J.R. and Spakman, W., 1992. Structure and Dynamics of subducted lithosphere in the Mediterranean region. Proc. Kon. Ned. Akad. Wet., 95, 325-347.

Xu, J. and Kono, Y., 2002. Geometry of slab, intraslab stress field and its tectonic implication in the Nankai trough, Japan. Earth Planets Space, 54, 733–742.

Zazo, C., Silva, P.G., Goy, J.L., Hillaire-Marcel, C., Ghaleb, B., Lario, J., Bardají, T. and González, A., 1999. Coastal uplift in continental collision plate boundaries: data from the Last Interglacial marine terraces of the Gibraltar Strait area S Spain. Tectonophysics, 301, 95-109.

Zeck, H.P., 1996. Betic-Rif orogeny: subduction of Mesozoic Tethys lithosphere under eastward drifting Iberia, slab detachment shortly before 22 Ma, and subsequent uplift and extensional tectonics. Tectonophysics, 254, 1-16.

Zeck, H.P., Monié, P., Villa, I.M. and Hansen, B.T., 1992. Very high rates of cooling and uplift in the Alpine belt of the Betic Cordilleras, southern Spain. Geology, 20, 79-82.

Zoback, M. L., Zoback, M. D., Adams, J. et al., 1989. Global patterns of intraplate stresses: A status report on the World Stress Map Project of the International Lithosphere Program. Nature, 341, 291– 298.